Dissertation

submitted to the
Combined Faculty of Natural Sciences and Mathematics
of the Ruperto Carola University Heidelberg, Germany
for the degree of
Doctor of Natural Sciences

Presented by
M.Sc. Yasmin Demerdash
Born in Cairo, Egypt
Oral examination on 22.06.2023

The Transcriptional Landscape of Hematopoietic Stem and Progenitor Cells during Acute Inflammatory Stress

Referees:

Prof. Dr. Nina Papavasiliou

Dr. Michael Milsom

"I dedicate this thesis to my beloved father, Essam Demerdash, and my beloved mother, Abeer Azouz whose unwavering love for me knows no bounds. This thesis stands as a testament to your faith in me and the countless sacrifices you have made to provide me with the opportunities and resources needed to succeed. You have instilled in me the values of resilience, perseverance, and determination, inspiring me to never give up and always strive for my best. Your unconditional love and belief in my abilities have been the cornerstone of my achievements, and I am forever grateful for your presence in my life.

I owe my success to you…

I love you!"

I also want to dedicate this work to my brother Ahmed Essam as a testament to the idea that where there is determination, there is always a path forward.

Abstract

Hematopoietic stem cells (HSCs) are critical components of the hematopoietic system and are responsible for renewing all blood cell lineages throughout life. These cells are quiescent and reside in niches in the bone marrow (BM). Over the past decade, our group and others have discovered that inflammatory stress impacts quiescent HSCs *in vivo*, leading to their activation. However, the dynamics, heterogeneity, and mechanisms underlying stress-induced activation of HSCs remain unclear.

In this thesis, I unraveled the mechanisms regulating HSCs proliferation and recovery in response to acute treatment with the proinflammatory cytokine interferon alpha (IFNα) by initially determining three-time points representing the sensing, proliferation, and recovery phases of HSCs' proliferative response to acute IFNα treatment. Using time series bulk RNA sequencing (RNAseq), I identified distinct molecular patterns and changes in the activation and repression of various biological categories in HSCs. Surprisingly, even after returning to a quiescent state 72 hours (h) post-treatment, HSCs remained metabolically active and underwent a significant metabolic shift towards oxidative phosphorylation (OXPHOS). In addition, the tricarboxylic acid cycle (TCA), pentose phosphate pathway (PPP), fatty acid, and purine metabolism were reduced, and HSCs showed decreased myeloid priming and bias.

Thus far, little is known about the dynamics and heterogeneity of these stress responses in the whole hematopoietic stem and progenitor (HSPC) cells. Inflammation-induced marker changes in the HSPCs compartment make it challenging to investigate the heterogeneity in the inflammatory response in HSPCs. Thus, I employed a single-cell (Sc) time series RNAseq experiment to study the heterogeneous and dynamic impacts of IFNα on HSPCs. The results showed heterogeneity in the response of HSPCs to IFNα, with HSCs being the strongest responders based on their gene expression changes. In collaboration with Brigitte Bouman and Dr. Laleh Haghverdi at the MDC in Berlin, we developed and used a response-pseudotime inference approach to analyze the scRNAseq data and identified global and cell type-specific inflammation signatures, revealing unique molecular patterns of gene expression and biological processes in response to IFNα.

Interestingly, we were able to associate reduced myeloid differentiation programs in HSPCs with a reduced abundance of myeloid progenitors and differentiated cells following IFNα treatment. Taken together, the single-cell time series analyses have allowed us to unbiasedly study the heterogeneous and dynamic impact of IFNα on the HSPCs.

In addition to investigating the dynamics and heterogeneity of the response of HSCs to IFNα, I compared the immediate transcriptional response of HSCs to various other proinflammatory cytokines. This analysis showed that IFNs, TNFα, ILs, and mimetics of viral and bacterial infections induced unique gene alterations in HSCs, underscoring the diversity of cytokine responses in these cells.

Finally, I investigated how the baseline levels of these proinflammatory cytokines regulate hematopoiesis. Analysis of the hematopoietic system in *Ifnar*$^{-/-}$*Ifngr*$^{-/-}$ (2KO) and *Ifnar*$^{-/-}$*Ifngr*$^{-/-}$*Tnfrsf1dKOIl1r*$^{-/-}$ (5KO) mice under homeostatic conditions revealed a decrease in HSCs and LSKs compared with wild-type (WT) mice. Furthermore, HSCs from these cytokine receptors knockout (KO) mice showed impaired colony-forming capacity and early competitive advantage. Interestingly, 5KO mice also showed a delayed recovery of HSCs cycling following 5-FU treatment. In addition, bulk RNA sequencing of 5KO HSCs revealed altered cell cycle pathways. Overall, these results underscore the essential role of proinflammatory cytokines in regulating HSC function during homeostasis.

In conclusion, this thesis comprehensively explains the transcriptional changes within the HSPCs population in response to proinflammatory cytokines, focusing on IFNα

Zusammenfassung

Hämatopoetische Stammzellen (HSC) sind entscheidende Komponenten des blutbildenden Systems und für die lebenslange Erneuerung aller Blutzelllinien verantwortlich. Diese Zellen sind inaktiv und besiedeln die Nischen im Knochenmark (BM). In den letzten zehn Jahren haben unsere Gruppe und andere Forscher entdeckt, dass Entzündungsstress die inaktiven HSZ in vivo beeinflusst und zu ihrer Aktivierung führt. Die Dynamik, Heterogenität und die Mechanismen, die der stressinduzierten Aktivierung von HSZ zugrunde liegen, sind jedoch nach wie vor unklar.

In dieser Arbeit habe ich die Mechanismen entschlüsselt, die die Proliferation und Regenerierung von HSZs als Reaktion auf eine akute Behandlung mit dem proinflammatorischen Zytokin Interferon alpha (IFNα) regulieren, indem ich zunächst drei Zeitpunkte ermittelt habe, die die Wahrnehmungs-, Proliferations- und Erholungsphasen der proliferativen Reaktion von HSCs auf eine akute IFNα-Behandlung darstellen. Mithilfe von Zeitreihen-RNA-Sequenzierung (RNAseq) identifizierte ich unterschiedliche molekulare Muster und Veränderungen bei der Aktivierung und Unterdrückung verschiedener biologischer Kategorien der HSZ. Überraschenderweise blieben die HSZ auch nach der Rückkehr in einen Ruhezustand 72 Stunden (h) nach der Behandlung metabolisch aktiv und unterzogen sich einer signifikanten metabolischen Verschiebung in Richtung oxidativer Phosphorylierung (OXPHOS). Darüber hinaus waren der Tricarbonsäurezyklus (TCA), der Pentosephosphatweg (PPP), der Fettsäure- und der Purinstoffwechsel reduziert, und die HSZ zeigten eine verringerte myeloisches Muster und Ausrichtung.

Bislang ist wenig über die Dynamik und Heterogenität dieser Stressreaktionen in den gesamten hämatopoetischen Stamm- und Vorläuferzellen (HSPZ) bekannt. Entzündungsbedingte Markerveränderungen in den HSPZ machen es schwierig, die Heterogenität der Entzündungsreaktion in HSPZs zu untersuchen. Daher habe ich ein Einzelzell-(Sc)-Zeitreihen-RNAseq-Experiment durchgeführt, um die heterogenen und dynamischen Auswirkungen von IFNα auf HSPZs zu untersuchen. Die Ergebnisse zeigten eine Heterogenität in der Reaktion der HSPZs auf IFNα, wobei die HSZs am

stärksten auf die Veränderungen in ihrer Genexpression reagierten. In Zusammenarbeit mit Brigitte Bouman und Laleh Haghverdi am MDC in Berlin haben wir einen Response-Pseudotime-Inference-Ansatz entwickelt und verwendet, um die scRNAseq-Daten zu analysieren und globale und zelltypspezifische Entzündungssignaturen zu identifizieren, die einzigartige molekulare Muster der Genexpression und biologische Prozesse als Reaktion auf IFNα aufzeigen. Interessanterweise konnten wir reduzierte myeloische Differenzierungsprogramme in HSPZs mit reduzierten myeloischen Progenitoren und differenzierten Zellen nach IFNα-Behandlung in Verbindung bringen. Insgesamt haben uns die Einzelzell-Zeitreihenanalysen ermöglicht, die heterogenen und dynamischen Auswirkungen von IFNα auf die HSPZs unvoreingenommen zu untersuchen.

Neben der Untersuchung der Dynamik und Heterogenität der Reaktion von HSZ auf IFNα habe ich die unmittelbare transkriptionelle Reaktion von HSZ auf verschiedene andere proinflammatorische Zytokine verglichen. Diese Analyse zeigte, dass IFNs, TNFα, ILs und Mimetika viraler und bakterieller Infektionen einzigartige Genveränderungen in HSCs induzieren, was die Vielfalt der Zytokinreaktionen in diesen Zellen unterstreicht.

Schließlich habe ich untersucht, wie die Ausgangswerte dieser proinflammatorischen Zytokine die Hämatopoese regulieren. Die Analyse des hämatopoetischen Systems von *Ifnar*$^{-/-}$*Ifngr*$^{-/-}$ (2KO) und *Ifnar*$^{-/-}$*Ifngr*$^{-/-}$*Tnfrsf1dKOIl1r*$^{-/-}$ (5KO) Mäusen unter homöostatischen Bedingungen ergab eine Abnahme der HSZ und LSKs im Vergleich zu Wildtyp (WT)-Mäusen. Darüber hinaus zeigten die HSZ dieser Mäuse mit Zytokinrezeptor-Knockout (KO) eine verminderte Fähigkeit zur Koloniebildung und einen frühen Wettbewerbsvorteil. Interessanterweise zeigte sich bei 5KO-Mäusen auch eine verzögerte Erholung der HSZ- Zyklen nach einer 5-FU-Behandlung. Die Sequenzierung der gesamten RNA von 5KO-HSZ zeigte veränderte Zellzykluswege. Insgesamt unterstreichen diese Ergebnisse die wesentliche Rolle der proinflammatorischen Zytokine bei der Regulierung der HSZ-Funktion während der Homöostase.

Zusammenfassend erklärt diese Arbeit umfassend die transkriptionellen Veränderungen innerhalb der Population der hämatopoetischen Stamm- und Vorläuferzellen (HSPCs) als Reaktion auf proinflammatorische Zytokine, wobei der Schwerpunkt auf IFNα liegt.

Table of Contents

1 Introduction

1.1 Hematopoietic Stem Cells: The Foundation of Blood

1.1.1 Stem Cells concepts

In adulthood, the continuous generation of new cells is essential for tissue maintenance and regeneration, especially in cases where many terminally differentiated cells, such as those of the gastrointestinal tract, skin, and blood, have a limited lifespan. Stem cells play a critical role in this process, as they can differentiate into various mature cell types (Zakrzewski et al. 2019). They are known not only for their ability to produce a variety of mature cells but also for their ability to self-renew. Self-renewal refers to the formation of daughter cells that are phenotypically identical to the parent cell and allow the production of stem cells with the same potential to generate cellular components. Stem cells contribute to the construction of organs and the maintenance of healthy tissues in adults through their unique properties (Clevers et al. 2015). During development, a single stem cell has the potential to give rise to an entire organism (Murry and Keller et al. 2008). Even in adulthood, stem cells play a critical role in maintaining tissue homeostasis by generating functional mature cells, including those involved in the regular renewal of the intestinal epithelium. In addition, they aid in tissue repair after damage, such as scar formation in the skin, and respond to noxious stimuli by producing immune cells to fight infection (Clevers et al. 2015; Post and Clevers et al. 2019). As a result, stem cell research has become an increasingly important field in medicine with potential implications for understanding diseases, developing treatments, and regenerative therapies.

1.1.2 The discovery and significance of HSCs

Hematopoietic stem cells (HSCs), one of the best-studied somatic stem cells, form the basis of the hematopoietic system and are among the most well-characterized tissues of the human body (Ng and Alexander et al. 2017). The hematopoietic system is composed of various types of blood cells that are crucial for the maintenance and immune protection of the body. The blood is an exceptionally regenerative tissue due to the relatively short lifespan of its effector cells. For example, fully developed red blood cells only last about 120 days (Shemin and Rittenberg et al. 1946). To sustain the blood system, self-renewing HSCs play a vital role. These cells possess the unique

ability to provide lifelong repopulation of all blood cell lineages.

The discovery of HSCs was pioneered after the bombings of Hiroshima and Nagasaki in 1945 (Douple et al. 2011). Physicians observed that those who died from lower doses of radiation over a long period of time had an impaired hematopoietic system. Several years later, it was discovered that when mice were exposed to total body irradiation, they died for the same reason. However, they could be saved by receiving bone marrow (BM) transplants from mice that hadn't been exposed to radiation. This was possible because the transplanted cells repopulated the recipient's body (Jacobson et al. 1951). The first experimental evidence for HSCs was provided when it was shown that a single BM cell could regenerate all myeloid and lymphoid blood cell types (Abramson, Miller, and Phillips et al. 1977). To date, transplantation of BM cells or HSCs is the most common curative treatment for hematopoietic failure and many patients with hematologic malignancies (Czechowicz and Weissman et al. 2011).

1.1.3 Hematopoesis

The ontogeny of the hematopoietic system is characterized by a transient wave of hematopoiesis that starts early during embryonic development. This wave initiates blood circulation before HSCs develop by generating transitory hematopoietic cell populations (Palis and Yoder et al. 2001). This is followed by HSCs emergence at around embryonic day 10.5 (E10.5) in the Aorta-Gonad-Mesonephros (AGM) region, umbilical and vitalline arteries (de Bruijn et al. 2000; Taoudi et al. 2008). The HSCs then spread through the circulation and undergo a transient developmental phase in the fetal liver. Around the time of birth, they migrate to the BM, where they reside, and start permanent definitive hematopoiesis (Ciriza et al. 2013). HSCs then generate progenitor cells that differentiate into specialized cell types with distinct functions. These include myeloid cells such as monocytes and macrophages, lymphoid cells like B and T cells, and erythrocytes (red blood cells) and platelets (Seita and Weissman et al. 2010). Each type of blood cell serves a specific purpose in maintaining body physiology or protecting the body from harmful agents. For instance, red blood cells transport oxygen throughout the body and play a role in regulating the pH of bodily fluids. White blood cells act as a first line of defense by trapping and destroying foreign invaders such as bacteria, while platelets are responsible for clotting to stop bleeding after an injury or surgery (Nicholson et al. 2016). Together, these diverse cell types work cooperatively to keep the body healthy.

This introduction is primarily centered on murine hematopoiesis unless stated otherwise.

1.1.4 Hematopoietic hierarchy

Functional assays and the discovery of surface markers have contributed to developing hierarchical models for hematopoiesis (Woolthuis and Park et al. 2016). This hierarchy is characterized by stepwise differentiation (Figure 1.1A), with HSCs residing at the apex. HSCs exhibit the highest self-renewal and multipotency and are predominantly in a quiescent state under homeostasis, with approximately 70-80% of cells in the G0 cell cycle phase. They can be further classified based on their cell cycle activity into active (aHSC) and dormant (dHSC) subpopulations. dHSCs are in a deeply quiescent state and have greater long-term self-renewal capacity than aHSCs (van der Wath et al. 2009; Wilson et al. 2008). They are only activated under stress or injury conditions (Wilson et al. 2008). Mathematical modeling showed that dHSCs divide much less frequently than aHSCs, dHSCs have a slower division rate of around 150 days (van der Wath et al. 2009; Wilson et al. 2008). It is proposed that dHSCs function as a backup population protected from exhaustion and mutations. Transcriptional analysis shows that dHSCs are in a state of biosynthetic shutdown and have lower metabolic activity than aHSCs, and express GPRC5C as a surface marker (Cabezas-Wallscheid et al. 2017).

HSCs then differentiate into multipotent progenitors (MPPs) that retain full lineage potential but have limited self-renewal capacity. MPPs then give rise to oligopotent progenitors, common myeloid progenitors (CMP), or common lymphoid progenitors (CLP), with CMPs producing myeloid cells such as granulocytes, erythrocytes, platelets, and monocytes, and CLPs producing lymphoid cells such as NK cells, B- and T-cells (Woolthuis and Park et al. 2016; Bryder, Rossi, and Weissman et al. 2006) (Figure 1.1A). This classical tree-like model of hematopoiesis, which posits distinct stable populations of progenitors with varying potencies, was deciphered from experiments on bulk samples that mask heterogeneity between individual cells. Limiting-dilution and single-cell transplantation assays have revealed inherent lineage biases among murine and human HSCs, with only a small subset of HSCs exhibiting unbiased multilineage engraftment upon transplantation (Dykstra et al. 2007; Morita, Ema, and Nakauchi et al. 2010).

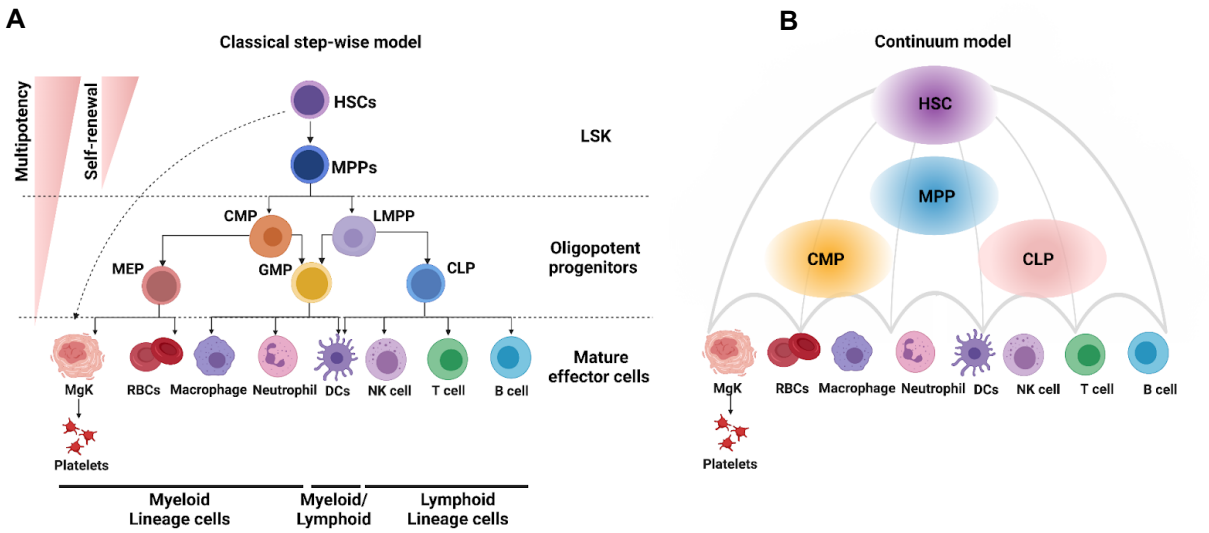

Figure 1.1 Hematopoietic differentiation hierarchy

(A) The conventional classical model of hematopoiesis suggests that HSCs go through a stepwise progression of discrete intermediate progenitor stages to undergo lineage commitment. This model is characterized by a tree-like structure where lineage decisions are made at binary branching points. The first decision point results in a separation between common myeloid and lymphoid progenitors. Additionally, there is a proposed shortcut to the megakaryocytic lineage, represented by curved dashed lines. Redrawn and modified based on (Bryder et al., 2006) **(B)** In a Continuous Waddington model, HSCs do not transition through discrete intermediate states but instead undergo a gradual acquisition of lineage-committed transcriptomic states. According to this model, cell types downstream of HSCs, including MPPs and CMPs, should not be viewed as distinct entities, but rather as transient states within the continuum of HSPCs. Redrawn and modified based on (Haas et al., 2018) LSK, Lin^-, $Sca1^+$, $ckit^+$; HSC, hematopoietic stem cell; MPP, multipotent progenitor; CLP, common lymphoid progenitor; CMP, common myeloid progenitor; GMP, granulocyte–macrophage progenitor; MEP, megakaryocyte–erythrocyte progenitor; LMPP, lymphoid primed multipotent progenitors; MkP, megakaryocytic progenitor; Mgk,Megakaryocyte. Created with BioRender.com.

The majority of HSCs displayed lineage-biased engraftment, which was characterized by differences in reconstitution kinetics and lineage contribution. Recent advances in single-cell technologies have revealed heterogeneity among individual cells, challenging this classical model (Haas, Trumpp, and Milsom et al. 2018) (Figure 1.1B). The discovery of lymphoid-primed multipotent progenitors (LMPPs), a progenitor population with lymphoid and granulocytic-monocytic (GM) potential but lacking significant megakaryocytic-erythroid (MegE) potential, suggests an early step of lineage commitment before the CMP-CLP bifurcation (Adolfsson et al. 2005). Single-cell transcriptional profiling has revealed transcriptional lineage priming, further

supporting the presence of a highly heterogeneous HSCs and progenitor compartment in humans and mice (Velten et al. 2017; Moignard et al. 2013; Grover et al. 2016). Moreover, in-depth analysis of oligopotent progenitor populations, such as CMPs, has shown that these populations are heterogeneous and appear to consist of multiple lineage-committed progenitor populations (Paul et al. 2016). Lineage-committed HSCs have also been identified, with megakaryocytic (Mk) restricted cells exhibiting high self-renewal capacity (Haas et al. 2015; Yamamoto et al. 2013). These recent experimental findings have led to a change in our understanding of the hematopoietic hierarchy, with lineage commitment occurring continuously rather than in a stepwise binary fashion (Figure 1.1B). Although phenotypically identified HSCs and progenitor populations can still be used as a model for functional and transcriptional analysis, the intrinsic heterogeneity within these defined populations must always be considered when interpreting results (Haas, Trumpp, and Milsom et al. 2018).

1.1.5 Characterization of HSCs by surface marker expression patterns

With advancements in flow cytometry technology and the availability of monoclonal antibodies, we have been able to study HSCs biology by utilizing fluorophore-coupled antibodies targeted toward cell-specific surface markers (Hulett et al. 1969). Each stage of HSCs differentiation is identified, isolated, and characterized using distinctive cell surface markers. HSCs are typically found within a cell population that lacks lineage (Lin) markers of mature hematopoietic cells, such as B220, CD4, CD8, CD11b, Gr1, and Ter119, but are positive for stem cell antigen-1 (Sca-1) and stem cell factor receptor (cKit). This marker combination, known as LSK (Lin^- $Sca1^+$ $c\text{-}Kit^+$), enriches for HSCs and various types of progenitor cells (Challen et al. 2009). However, only 10% of this LSK compartment represents HSCs (Challen et al. 2009), so additional markers like CD34 and CD135 (Flt-3) are used to purify stem cells further. CD34 helps distinguish between cells with long-term ($CD34^-$) and short-term ($CD34^+$) repopulation capacity within the LSK population (Matsuoka et al. 2001). Moreover, combining this marker set with the signaling lymphocyte activation molecule (SLAM) (Kiel et al. 2005) protein family, such as CD150 and CD48, facilitates the identification of hematopoietic stem and progenitor cells and correlates progenitor primitiveness. The LSK $CD34^-$ $CD150^+$ $CD48^-$ population phenotype includes HSCs and is the most widely used gating scheme (Kiel et al. 2005; Oguro, Ding, and Morrison 2013).

Despite the great effort to enrich for HSCs, the continual reporting of new markers for HSCs purification makes it challenging to know which purification strategies yield the highest proportion of long-term multi-lineage HSCs. Moreover, many of these markers differ between mice and humans, and their expression changes dramatically during ontogeny and inflammation. This highlights the countless challenges scientists face when working on the hematopoietic system (Challen et al. 2009).

1.1.6 Functional analysis for stem cells and progenitors

The inability to maintain and expand HSCs *in vitro* is a major challenge in HSCs research (Clark, Jamieson, and Keating 1997). To address this issue and assess HSCs self-renewal, potency, and function, various *in vitro* and *in vivo* methods have been developed, as flow cytometry analysis of hematopoietic stem and progenitors (HSPCs) alone is not enough to evaluate HSCs capacity. The most widely used *in vitro* technique today is the colony-forming unit (CFU) assay (Purton and Scadden et al. 2007). This assay involves culturing total BM cells or sorted BM subsets in a semi-solid methyl-cellulose culture medium containing appropriate cytokines. Single cells are dispersed in the medium, and colonies grow over a period of 7 to 14 days based on the initial potency of the given cell. The progenitor cells proliferate and differentiate, forming colonies restricted to the myeloid lineage. Lymphoid potential cannot be assessed because additional extrinsic factors required for lymphoid development are not present in this culture condition (Purton and Scadden et al. 2007). The colonies can be characterized and quantified by their unique morphology, with different lineages being generated depending on the cell type. Mixed colonies (CFU-GEMM) are formed by immature stem and progenitor cells, while restricted cell subsets produce myeloid (CFU-G/M/GM) or erythroid (CFU-E, BFU-E) colonies. Primary platings of total BM cells mainly assess the capacity of lineage-restricted progenitor cells. To evaluate HSC capacity, serial CFU assays are necessary as HSCs primarily form colonies in the second and third rounds of the CFU assay (Purton and Scadden et al. 2007). This assay has become the benchmark in vitro functional assay to determine progenitor's potential and short-term stem cell potential.

In vivo long-term repopulation assays, such as limiting dilution assays, competitive assays, and serial transplantation assays, have emerged as the gold standard for functional analysis of HSCs (Purton and Scadden et al. 2007). To successfully carry

out transplantation approaches, it is necessary to deplete recipient HSCs in the BM via irradiation or high-dose cytotoxic drug treatment, creating vacant HSCs niches that can be occupied by the transplanted HSCs (Weissman and Shizuru et al. 2008). As only HSCs are capable of indefinitely restoring the entire hematopoietic system of irradiated recipient mice, this assay provides a reliable test of HSCs reconstitution capacity. To measure the donor transplant performance over a period of several months, transplantation assays typically require the identification of transplanted cells and their progeny in the recipients, which can be achieved using congenic mice that express different allelic variants of the Ly5 antigen (CD45). CD45.1, CD45.2, and CD45.1/.2 mice are commonly used for this purpose, as they enable the identification of HSCs, progenitors, and mature cells in both the BM and peripheral blood (PB) based on surface antigen expression (Purton and Scadden et al. 2007). In serial transplantation assays, cells are serially transplanted into secondary and tertiary recipients to assess the long-term repopulation capacity of a given HSC pool (Ramkumar, Gerstein, and Zhang et al. 2013). Competitive transplantation assays compare the HSCs potential of two different populations after an equal number of cells are transplanted into a common recipient (Harrison et al. 1980; Kwarteng and Heinonen et al. 2016). In limiting dilution assays, serially diluted HSCs are transplanted with a fixed number of supporting cells to measure HSCs frequency (Taswell et al. 1981; Sieburg, Cho, and Müller-Sieburg et al. 2002). This is the standard method for assessing functional HSCs content.

Recently, single-cell transplantation assays have become more popular for studying HSCs potency, lineage-skewing, and priming, thereby revealing clonal heterogeneity at the stem cell level (Dykstra et al. 2007; Yamamoto et al. 2013). In this approach, single HSCs are isolated and transplanted into recipient mice that have been lethally irradiated. However, co-transplantation of supportive BM cells is necessary to ensure the survival of the recipient mice. By analyzing the efficiency of engraftment and the lineage output of a clonal hematopoietic system in the recipients over time, the transplanted HSCs can be retrospectively characterized.

1.2 Response of Hematopoietic Stem Cells to Inflammatory stress

Infections pose a significant threat to the hematopoietic system throughout our lives, as our bodies are constantly exposed to microbial threats. In addition, factors such as severe blood loss or chemotherapy can result in a considerable loss of hematopoietic cells, which requires an increased demand for hematopoiesis (Trumpp, Essers, and

Wilson et al. 2010; Baldridge, King, and Goodell et al. 2011; Takizawa, Boettcher, and Manz et al. 2012). Despite being quiescent during homeostasis, HSCs rapidly activate in response to stress conditions to replenish the cellular progeny lost due to cell death. Although the exact mechanism by which quiescent HSCs are induced to exit G0 phase in the face of proliferative stress is not fully understood, HSCs return to a quiescent state after homeostasis is restored, as this is critical for maintaining genome stability, reducing the risk of leukemia, and protecting HSCs from exhaustion (Wilson et al. 2008).

Inflammatory stresses often result in significant alterations in HSPCs function and output. Initially, it was believed that HSCs were incapable of detecting and responding directly to inflammatory signals (King and Goodell et al. 2011). Consequently, the changes in the function and distribution of the HSPCs population after infections have been interpreted as a response to replenish apoptotic cells rather than a direct response to the infection itself. Recent research has shown that HSCs can respond to bacterial and viral components via toll-like receptors (TLRs) and cytokine receptors (Baldridge, King, and Goodell et al. 2011; King and Goodell et al. 2011). Moreover, subsequent studies have confirmed that HSCs respond directly to the proinflammatory cytokines released under stress conditions rather than sensing a loss of progeny cells. In this regard, King and Goodell et al. (King and Goodell et al. 2011) classified four mechanisms by which infections can affect HSCs biology, the first two having direct effects on HSCs (direct infection or direct pathogen recognition) and the other two having indirect effects via proinflammatory cytokines or changes in the bone marrow microenvironment. (King and Goodell et al. 2011).

Inflammatory signals that arise in response to severe systemic infection or injury activate HSCs, initiating "emergency myelopoiesis." (Manz and Boettcher 2014) It is important to note that myeloid cells, such as macrophages and neutrophils, have a low proliferative capacity and must be replenished from HSPCs in the BM, unlike adaptive immune cells, such as T and B cells. Recent research has highlighted the critical role of proinflammatory cytokines in this complex and finely-tuned process of regulating myelopoiesis in the BM (Chiba et al. 2018). These cytokines elicit inflammatory signals

that lead to the differentiation of HSPCs and the initiation of signal transduction pathways. This ultimately results in various transcription factors that drive the

production of myeloid lineage-restricted hematopoietic progenitors, which replenish mature myeloid blood cells (Chiba et al. 2018). Although the effects of various proinflammatory cytokines on HSCs can vary significantly, there are still some conserved features (Caiado, Pietras, and Manz et al. 2021). Inflammation triggered by an infection often leads to a loss of function of the HSCs, resulting in decreased repopulation capacity and increased proliferation associated with myeloid lineage bias. This decline in function is often associated with chronic infection, suggesting that prolonged inflammation and demand may have cumulative effects on HSCs function (Caiado, Pietras, and Manz et al. 2021).

Proinflammatory cytokines can act directly on HSCs and indirectly by triggering secondary inflammatory signal production by BM niche cells such as mesenchymal stromal cells (MSCs), endothelial cells, and mature cells (Hurwitz, Jung, and Kurre et al. 2020). However, the mechanism by which HSCs sense proinflammatory cytokines is still under investigation. Proinflammatory cytokines such as Interferons (IFNs), Interleukin 1 (IL1), Tumor necrosis factor (TNF), and Interleukin 6 (IL6) play a role in regulating HSCs function (Pietras et al. 2017; Caiado, Pietras, and Manz et al. 2021). The question of how these proinflammatory signals affect HSCs biology under stress and homeostasis is a subject of an ongoing scientific investigation (Clapes, Lefkopoulos, and Trompouki et al. 2016; Caiado, Pietras, and Manz et al. 2021; Collins, Mitchell, and Passegué et al. 2021). The following sections will focus primarily on interferon alpha (IFNα) and its role in regulating HSCs activity and hematopoiesis. In a later section, I will also discuss the role of other cytokines, such as Interferon gamma (IFNγ), IL1, TNF, and IL6, in regulating HSCs activity and hematopoiesis.

1.2.1 Interferon-alpha mediated regulation of HSCs

1.2.1.1 Interferon Signaling

A decade ago, our group discovered that IFNs play an important role in the biology of HSCs (Essers et al. 2009) . IFNs, discovered in 1957, are a group of signaling proteins produced and released primarily by immune cells and other cell types after interaction with pathogens or cancer cells. They were originally named for their ability to "disrupt" viral infection of cells. They act as the first line of defense against viral infections and are an important component of innate immunity (Borden et al. 2007; Lee and Ashkar et al. 2018; Taylor et al. 2014) . In response to viral infection, infected cells produce

IFNs, which induce an antiviral state in infected and uninfected cells that blocks viral replication and the spread of infection. In addition to their role as antiviral cytokines, they also play a role in bacterial infections and in immune surveillance of malignant cells. It is now known that IFNs influence various cellular processes (Borden et al. 2007; Lee and Ashkar et al. 2018; Taylor et al. 2014) Endogenous IFNs production can also be triggered by sensing self-ligands (such as dsDNA and dsRNA) or TLR agonists. The cGAS/ STING (DNA) or RIG-I and MDA5 (RNA) pathways are intrinsically stimulated by these stimuli, leading to steady-state IFNs production during homeostasis (Liu, Sarhan, and Poltorak 2018). Although IFNs are expressed at low levels in the body under normal circumstances, their role in the immune response is dynamic and pathogen-specific, with members of the IFNs family induced to varying degrees depending on the stimulus. Following production and secretion by immune cells, IFNs modulate immune system activity by inducing the transcription of interferon signaling genes (ISGs) (Lee and Ashkar et al. 2018).

The three main types of IFNs are type I IFNs (IFNα and IFNβ), type II IFNs (IFNγ), and type III IFNs (IFN-like cytokines and IFNλ). Several criteria, including sequence identity, genetic loci, cell of origin, receptor distribution, and downstream responses, classify the IFN types (Borden et al. 2007; Lee and Ashkar et al. 2018; Taylor et al. 2014). Type I IFNs are the largest and best-characterized group, with IFNα and IFNβ being the best-defined. IFNα is predominantly produced by plasmacytoid dendritic cells (DCs), whereas most hematopoietic cell types produce IFNβ. Type I IFNs are produced during viral infection in response to pattern recognition receptor (PRR) stimulation and are important regulators of innate immunity. They restrict viral replication in infected cells and promote an antiviral state in bystander cells. In addition, type I IFNs promotes antigen presentation, natural killer (NK) cell function, and adaptive immune cell activation. Both IFNα and IFNβ bind to the IFNα receptor (IFNAR) which is associated with Janus-activated kinases (JAKs). Upon receptor activation, the JAKs are activated, leading to subsequent tyrosine phosphorylation and activation of signal transducer and activator transcription (STAT) proteins. The STATs then translocate to the nucleus and can dimerize with IFN-regulatory factor 9 (IRF9). The complex binds to IFN-stimulated

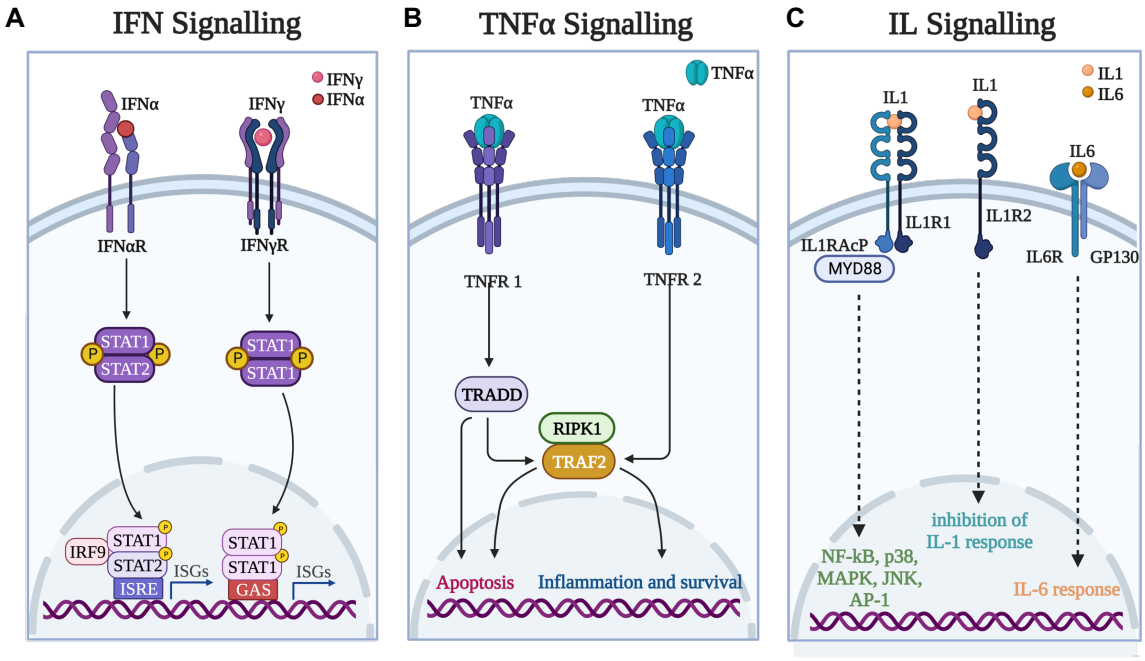

Figure 1.2 Overview of cytokine signaling pathways.

(A) When IFNα/β and IFNγ bind to their respective receptors, they activate separate intracellular signaling pathways, resulting in the transcription of interferon response genes (ISGs). The signal is transmitted through the phosphorylation of Signal Transducer and Activator of Transcription (STAT) proteins, which then move to the nucleus and bind to the transcription regulatory elements, namely IFN-stimulated response element (ISRE) and Gamma Interferon activation site (GAS). **(B)** TNFα signaling is mediated through TNFR1 and TNFR2 which activate two separate intracellular signaling pathways. Signaling by TNFR1 leads to activation of TNFR-associated death domain DD (TRADD) protein which then lead to activation of downstream kinases and eventually NF-κB activation which then mediate apoptotic activities. TNFR2 lacks an intracellular death domain and its engagement with TNF-α leads to MAPK and NF-κB activation to mediate angiogenic and proliferative effects. **(C)** The binding of IL1 to the IL1 receptor 1 (IL1R1) causes the binding of the IL1 receptor 1 accessory protein (IL-1RAcP) and the myeloid differentiation primary response 88 (MYD88) protein that activate intracellular pathways. When IL1 binds to the IL1 receptor 2 (IL1R2), the IL1 response is inhibited. Upon the binding of IL6 to the IL6 receptor (IL6R), the signal-transduction β-receptor subunit GP130 associates and transduces the signal into the cell. Created based on (Platanias 2005, Moelants, Mortier et al. 2013, Turner, Nedjai et al. 2014).Created with BioRender.com

response elements (ISREs) in DNA to initiate gene transcription of IFN-stimulated genes (ISGs), which then mediate the various biological responses of IFNs (Figure 1.2A) (Ivashkiv and Donlin et al. 2014; Platanias et al. 2005).

1.2.1.2 IFNα as therapeutics

IFNα was the first cytokine produced by the pharmaceutical industry and has been used to treat chronic myeloid leukemia, melanoma, and chronic Hepatitis B and C infections (Yang et al. 2012; Huang, Chintalacharuvu, and Morrison 2007); (Borden et al. 2007) In a therapeutic context, IFNα can promote cancer cell differentiation, inhibit proliferation and cell cycle progression, and induce apoptosis by activating IFNAR signaling (Figure 1.4) (Borden et al. 2007; Lee and Ashkar 2018; Taylor 2014). However, IFNα therapy is limited by its short half-life in the bloodstream, high myelotoxicity, and paradoxical immunosuppressive effects (Borden et al. 2007; Lee and Ashkar 2018; Taylor 2014). Despite these challenges, clinical trials using IFNα to treat viral and hematological disorders, such as HIV, thrombocytopenia, AML, and CML, are ongoing (www.clinicaltrials.gov). By repurposing these older therapeutic approaches, new methods for treating infections and malignancies can be developed without the need for novel drugs or in combination with newly invented immunotherapies. A thorough understanding of the impact of IFNs on the immune system and hematopoiesis could reveal significant opportunities for their use in immunology and oncology.

1.2.1.3 Role of IFNα on adult HSCs biology

Several recent studies have demonstrated the regulatory effect of IFNs on HSCs activity. Initially, it was observed that IFNs have anti-proliferative properties on hematopoietic progenitors in tissue culture systems, consistent with their role as antiviral agents (Paucker, Cantell, and Henle et al. 1962). These suppressive effects were mediated by the activation of protein kinase Cn (PKCn) and p38 mitogen-activated protein kinase (Verma et al. 2002; Redig et al. 2009). However, it was later discovered that treatment of mice with IFNα induces the proliferation of dormant HSCs (Essers et al. 2009). Furthermore, injecting mice with the immune-stimulant polyinosinic:polycytidylic acid (pIC), a synthetic double-stranded RNA that mimics viral infections, stimulated HSCs to exit G0 and enter the cell cycle in an IFNAR-dependent manner. The HSCs' response to IFNα was mediated by increased STAT1 and PKB/Akt phosphorylation and increased expression of Sca-1. In addition to stabilizing Myc, IFNα treatment has been associated with decreased expression of cyclin-dependent

kinase inhibitors and transcriptional programs that enforce quiescence, including FoxO3a, Notch, and TGFβ (Essers et al. 2009; Pietras et al. 2014). Intriguingly, HSCs that lacked IFN-α/β receptor, STAT1, or Sca-1 were rescued from IFNα treatment, suggesting that IFNAR, STAT1, and Sca-1 mediate the IFNα-induced proliferation of HSCs. While this data suggests a direct effect of IFNα on HSCs (Figure 1.3), an indirect effect has been proposed as HSCs lacking the IFN-α/β receptor still respond to IFNα treatment when present with wildtype (WT) HSCs during BM transplantation (Essers et al. 2009).

Since the effects of IFNα on HSCs *in vivo* are in contrast to the *in vitro* situation (Mirantes, Passegué, and Pietras et al. 2014; Pietras et al. 2014), this suggests a role for the BM niche environment in mediating the IFNα effect on HSCs *in vivo*. It is known that the cellular composition of the niche, which includes but is not limited to osteoblasts, endothelial cells, mesenchymal stromal cells (MSCs), and hematopoietic cells such as megakaryocytes and monocytes, play an important role in HSC maintenance and homeostasis (Ehninger and Trumpp 2011; Morrison and Spradling 2008). Our group has shown that BM endothelial cells are activated in response to acute IFNα exposure in vivo, which increases vascularity and vessel permeability (Prendergast et al. 2017; Negrotto et al. 2011). Interestingly, we were able to show that part of this activation is indirectly mediated via signaling from IFNα stimulated HSCs in the BM (Prendergast et al. 2017; Negrotto et al. 2011). Other studies have shown that IFNα plays a role in megakaryocyte distribution in the BM niches (Prendergast et al. 2017; Negrotto et al. 2011). This data provides evidence for crosstalk between HSCs and the BM niche cells under inflammatory stress conditions. The effects of IFNα signaling on HSCs responses can vary depending on the context and duration of exposure (Figure 1.3 & 1.4). While it can induce HSCs division in response to an infection or other assaults, prolonged exposure can result in HSCs exhaustion and loss of the stem cell pool. It has been shown that in contrast to acute IFNα stimulation, chronic IFNα treatment compromised HSCs repopulation capacity and led them back to quiescence, protecting them from IFNα induced apoptosis (Figure 1.3) (Pietras et al. 2014). The effects of short-term and long-term IFNα in various disease contexts differ significantly. During an acute viral infection, IFNα, along with TNFα and lymphotoxin (LT), can have a transient effect on hematopoiesis.

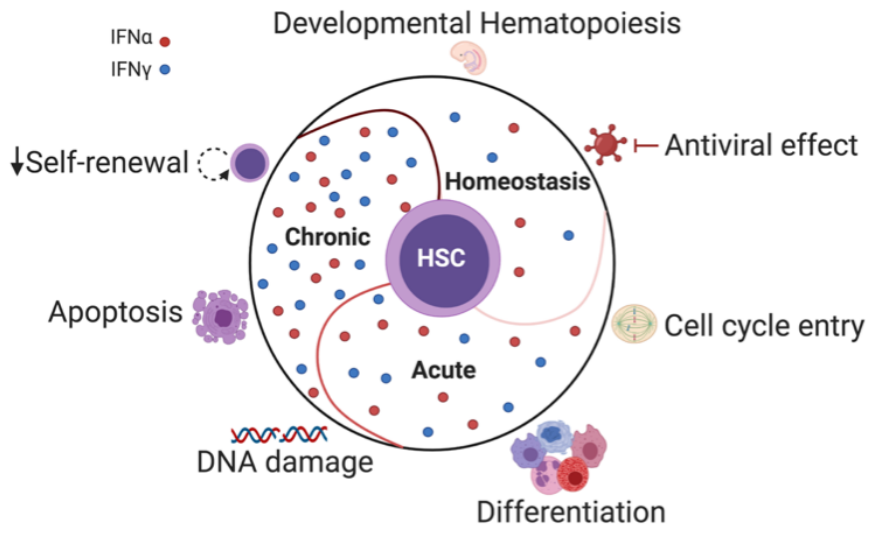

Figure 1.3 The multifaceted impact of IFNs on HSCs.

During homeostasis, basal IFNs signaling plays a role in regulating HSCs emergence during early development. In response to acute IFNs exposure, HSCs exit their quiescent state, start cycling and its differentiation is impacted. Chronic exposure to IFNs can lead to increased DNA damage, activation of apoptotic pathways. And compromised self-renewal and repopulation capacity. Thus, the role of IFNs on HSCs biology is complex and highly dependent on the stimulation conditions. Adapted from (Demerdash et al. 2021)

Nevertheless, acute viral infections also impair the reconstitution potential of HSCs even after the resolution of the infection, indicating the existence of lasting reprogramming effects following pathogen clearance (Hirche et al. 2017). Persistent IFNα signaling induced by non-acute murine cytomegalovirus (MCMV) infection leads to a prolonged inflammatory state in the BM, resulting in long-lasting impairment of HSC function (Figure 1.4). Moreover, studies have shown that IFNα-dependent BM aplasia occurs after LCMV infection (Binder et al. 1997). In support of these findings, studies by Michael Milsom's group have demonstrated that extensive treatment with IFNα can cause high levels of DNA damage in HSCs due to the increased proliferation of these typically quiescent cells (Binder et al. 1997; Walter et al. 2015). In a mouse model of Fanconi anemia, it was shown that prolonged exposure to IFNα led to severe aplastic anemia (SAA) by depleting the HSCs pool (Kaschutnig et al. 2015). More recently, a study by the same group observed a permanent reduction in functional HSCs, which did not recover even after one year following pIC treatment (Bogeska et al. 2022). HSCs from challenged mice displayed various characteristics of advanced

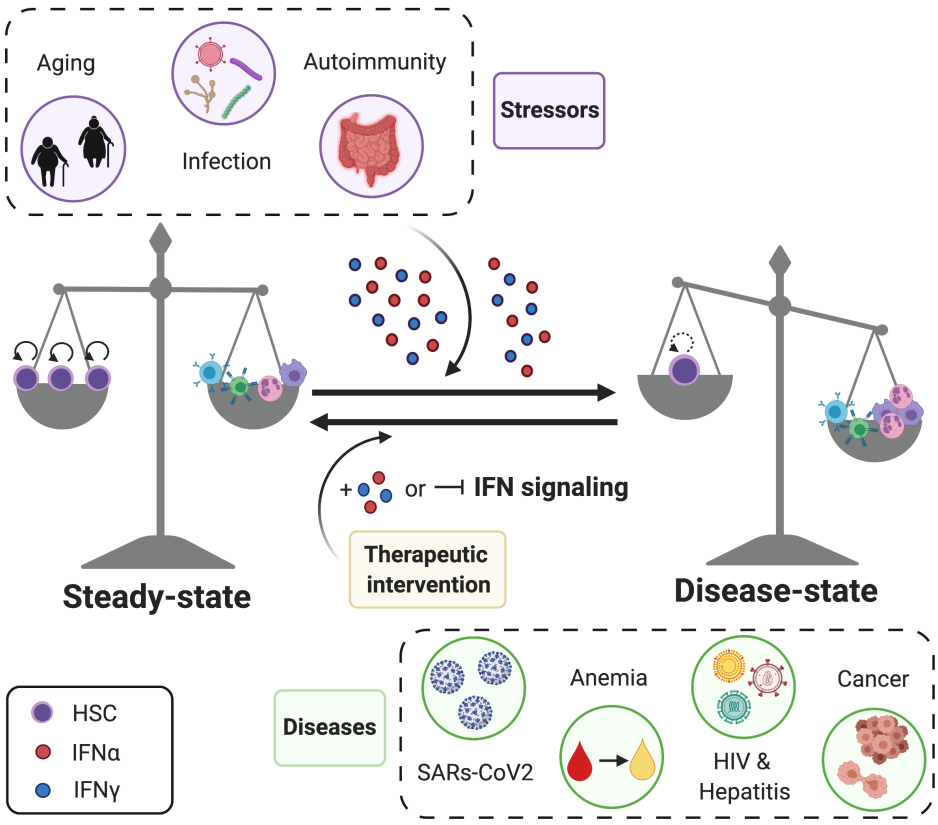

Figure 1.4 : The balance of IFNs signaling during homeostasis and disease.

HSCs are typically in a state of equilibrium, with self-renewal and differentiation into mature blood cells in balance. However, various internal and external stressors such as infection, aging, and autoimmunity can disrupt this homeostasis by increasing IFNα or IFNγ signaling. In the presence of excessive IFNs signaling, HSCs lose their ability to self-renew and instead differentiate. Treating patients with recombinant IFNs or inhibiting IFNs signaling pathways has been shown to be a successful approach to modulating IFNs signaling and managing these conditions. Adapted from (Demerdash et al. 2021)

aging at the cellular and molecular levels. Throughout the challenge and recovery periods, there was a lack of *in vivo* HSCs self-renewal divisions. The inhibition of HSCs by temporally distinct inflammatory events was cumulative and progressive (Bogeska et al. 2022). The differences in HSCs response to IFNα between sterile stimulus models that induce proliferation and viral infection models that lead to stem cell exhaustion suggest that the duration and source of IFNα may impact the balance of HSC self-renewal and homeostasis. In addition to their effects on HSCs cycling, IFNs have distinct effects on HSCs differentiation (Figure 1.3). Haas et al. have shown that IFNα rapidly activates a posttranscriptional megakaryopoiesis program in stem-like megakaryocyte-committed progenitor, which later leads to the efficient replenishment of platelets that are lost during inflammatory insults (Haas et al. 2015). Thus far, there

is no clear evidence that IFNα promotes HSCs myeloid differentiation. However, a recent study by Khan et al. investigated whether the virulent Mycobacterium tuberculosis (M.tb) strain, H37Rv, induces trained immunity and found results that diverged significantly from those observed with Bacille Calmette-Guérin (BCG) and M.tb infection (Khan et al. 2020; Cirovic et al. 2020). They found weakened host resistance against subsequent M.tb infections that lasted for at least a year (Khan et al. 2020). The weakened resistance was linked to Type I IFN signaling. While both M.tb and BCG expanded HSCs and MPPs, M.tb uniquely suppressed myelopoiesis, which caused a significant reduction in peripheral neutrophils and Ly6C^{hi} monocytes. Neutrophil deficiency was attributed to RIPK1-dependent necroptosis. Additionally, BM-derived macrophages from naïve mice administered HSCs from M.tb infected mice displayed reduced cell yield and were deficient in clearing M.tb *in vitro*. The critical role of type I IFN signaling was observed in *Ifnar1*$^{-/-}$ mice as it displayed better survival after M.tb infection than WT mice (Khan et al. 2020). These findings show that M.tb trains HSCs paradoxically to reduce the host's innate resistance (Khan et al. 2020).

1.2.1.4 Marker changes and implications for function under inflammatory stress

The responses of hematopoietic cells to IFNs may vary due to differences in the types of cells being studied. Phenotypic shifts have been one of the hallmarks following inflammatory stress, which complicates the molecular and functional identification of HSCs under non-homeostatic conditions (Demerdash et al. 2021; Ali and Park 2020). This is because Sca-1, a critical marker for identifying HSCs during steady-state hematopoiesis, is induced in response to inflammatory stimuli. IFN-induced signaling causes the stem cell marker Sca-1 to be highly upregulated on HSCs, as well as on CMPs and GMPs, which do not typically express Sca-1, leading to the shift of these cells into the LSK gate as demonstrated by in vitro clonogenic and differentiation assays (Kanayama et al. 2020). In addition, IFN treatment can also cause slight alterations in the expression of other stem cell markers, such as CD48 and CD150 (Demerdash et al. 2021). To improve the interpretation of results related to HSCs function, particularly when HSCs are exposed to inflammatory stressors, it is crucial to use stringent markers to exclude other cell types. However, one must be cautious in interpreting the data, and phenotypic studies should be complemented by functional

studies. Further research is needed to understand the complex relationship between inflammation and the adaptations in the HSPCs compartment.

1.2.2 The effects of proinflammatory cytokines on HSCs

1.2.2.1 Interferon gamma

IFNγ is the only member of the IFN type II family and mediates the host immune system and anti-tumor responses. IFNγ is secreted primarily by T cells and NK cells in response to Th1-inducing pathogens but can also be secreted by professional antigen-presenting cells (APCs), B cells, and NKT cells (Ivashkiv and Donlin et al. 2014; Platanias et al. 2005). The cellular source of IFNγ secretion corresponds with unique functions in response to pathogens. IFNγ can be stimulated by cytokines produced by APCs (e.g., IL12, IL15, and IL18), type I IFNs, and pathogen-associated molecular patterns (PAMPs). Negative regulators of IFNγ production include IL4, IL10, TNFα, and glucocorticoids. IFNγ binds to its receptor (IFNGR), which consists of both an alpha (IFNGR1) and beta (IFNGR2) chain. IFNGR1 can mediate biological responses to IFNγ alone, independent of the presence of IFNGR2. Intracellular signaling through IFNGR is mediated via STAT1 homodimers (Figure 1.2A). The signaling pathways used by IFNα and IFNγ overlap and act synergistically because IFNγ signaling can induce IFNα production (Ivashkiv and Donlin 2014; Platanias 2005).

Besides IFNα, IFNγ can directly enhance the proliferation of HSCs (Figure 1.3). This effect was demonstrated following infection of mice with the M.avium bacterium (Baldridge et al. 2010). It was shown that IFNγ is strongly upregulated during M.avium infection and that it is IFNγ but not IFNα that plays an essential role in the proliferative activation of HSCs in response to infection by M.avium (Baldridge et al. 2010), Confirming these findings, ablation of the p47 GTPase Irgm1 which is a negative regulator of IFNγ responses lead to hyper-proliferation and depletion of the stem cell compartment as indicated by the decrease in the HSC number in mice lacking Irgm1 (King et al. 2011). In the context of infection-related emergency myelopoiesis, IFNγ was identified as a potential mediator of stress-induced myeloid specification. Specifically, IFNγ can activate the transcription factors BATF2 and C/EBPb, inducing myeloid differentiation in myeloid-biased HSCs (Figure 1.3) (Matatall et al. 2014, 2016). Treatment with IFNγ also upregulates the monocyte promoting transcription

factor PU.1 while inhibiting STAT3 activation induced by the granulocyte colony-stimulating factor (G-CSF), which is necessary for emergency granulopoiesis (Matatall et al. 2014, 2016). In support of this, IFNγ-deficient mice infected with viruses that typically induce monopoiesis in WT mice displayed extreme granulocytosis and a strong increase in neutrophil development (de Bruin et al. 2012; H. Zhang et al. 2010). In contrast, there is no clear evidence that IFNα promotes HSC myeloid differentiation, and no parallel analysis was performed.

1.2.2.2 Tumor necrosis factor alpha

Tumor necrosis factor alpha (TNFα) is a proinflammatory cytokine implicated in a diverse range of inflammatory, infectious, and malignant conditions. It is produced by various cell types, with activated macrophages and T-lymphocytes being the most predominant (Bradley et al. 2008). TNFα signals through two specific cell surface receptors, tumor necrosis factor receptor 1 (TNFR1) and tumor necrosis factor receptor 2 (TNFR2), with TNFR1 being ubiquitously expressed and mainly implicated in pro-inflammatory and apoptotic pathways, while TNFR2 expression is restricted to hematopoietic and endothelial cells, and is involved in tissue repair, cellular proliferation, and angiogenesis (Bradley et al. 2008). Downstream signaling pathways following the activation of both TNFR1 and TNFR2 are summarized in Figure 1.2B.

The effect of TNFα on HSCs is a much-debated topic. TNFα has been extensively studied, but its effect on HSCs remains controversial. Early studies provided conflicting results. Some showed inhibition of HSC proliferation after TNFα stimulation (Broxmeyer et al. 1986), whereas others showed stimulation (Caux et al. 1990). Therefore, it is clear that the concentration and context in which TNFα is present may have a significant impact on HSCs. *In vitro* studies have shown that TNFα treatment inhibits the proliferation of mouse hematopoietic progenitor cells and their potential to form colonies (Bradley 2008; Y. Zhang et al. 1995). Similarly, treatment of human $CD34^{+}CD38^{-}$ cells with TNFα suppresses the ability of these cells to maintain multilineage hematopoiesis after transplantation (Dybedal et al. 2001). *In vivo* transplantation studies have shown that HSCs from TNF receptor knockout (KO) mice enhance long-term repopulating capability (Pronk et al. 2011). Conversely, when studies were conducted using older mice (>6 months), HSCs from TNF receptor KO mice had reduced repopulation activity compared to age-matched WT mice (Rebel et

al. 1999). Moreover, TNFα production by CD8+ cells has been shown to enhance the function of HSCs *in vitro*. Those cells demonstrated better engraftment upon transplantation (Rezzoug et al. 2008), while *in vivo* administration of TNFα resulted in suppression of cycling HSCs and decreased HSCs long-term repopulating capacity (Pronk et al. 2011). Exposure to lipopolysaccharide (LPS) induces the expression of TNFα, IL6, and the chemokine CCL2, which stimulates the proliferation and differentiation of HSCs (Chen et al. 2010). However, inhibition of these three proinflammatory cytokines induced by LPS exposure can rescue the functional effects of LPS on HSCs, suggesting that TNFα is a crucial mediator of LPS-induced activation of HSCs (Chen et al. 2010). These findings were further supported by a recent study by our group, which demonstrated that activation of HSCs in response to LPS *in vivo* requires the collective action of several cytokines, including IFNα, IFNγ, TNFα, IL1α, and IL1β (Demel et al. 2022).

Recent studies have shown that TNFα plays a role in emergency hematopoiesis and can instruct HSCs to adopt lineage-specific gene programs, suggesting that its effects on HSCs are complex (Bowers et al. 2018; Haas et al. 2015). Yamashita et al. highlight that TNFα has differential effects on HSCs and progenitor cells (Yamashita and Passegué et al. 2019). They found that TNFα promotes necroptotic cell death in myeloid progenitor cells while supporting HSCs survival and myeloid cell differentiation through activation of the NF-kB pathway. Activation of the NF-kB pathway also inhibits necroptosis, supports immunomodulatory functions, and promotes differentiation of myeloid cell differentiation in HSCs. Therefore, the cellular survival mechanisms stimulated by TNFα were thought to be unique to HSCs, suggesting that TNFα is a critical mediator of HSC regeneration and survival (Yamashita and Passegué et al. 2019).

1.2.2.3 Interleukin 1

The interleukin 1 family of cytokines plays a significant role in innate immune responses and inflammation, acting as critical signals to activate host defense and repair during infections. The family comprises 11 members, with IL1β and IL1α being the most well-known. Although they share only 24% of their amino acid sequence, IL1β and IL1α have largely identical biological functions (Dunn et al. 2001). However, they differ in several ways. IL1α is primarily membrane-bound, while IL1β is secreted and

circulates systemically. IL1β is produced by hematopoietic cells, whereas IL1α expression is more widespread, constitutively present in epithelial layers of the gastrointestinal tract, lung, liver, endothelial cells, and astrocytes (Garlanda, Dinarello, and Mantovani 2013). Both interleukins can signal independently through the same receptor complex, consisting of two types of receptors. Type I IL1 receptor (IL1R1) is ubiquitously expressed and requires the co-receptor IL1R Accessory Protein (IL1RAcP) for activation by IL1 family members. Type II IL1 receptor (IL1R2) lacks a signaling-competent cytosolic part and thus acts as a negative regulator of IL1 signaling (Figure 1.2C) (Weber, Wasiliew, and Kracht et al. 2010).

IL1 has been shown to regulate BM HSPCs as these cells express the cytokine and its receptor (IL1R1). One study demonstrated that HSCS and progenitors' proliferative responses were suppressed in IL1RI KO mice and that IL1 directly drives increased HSCS proliferation *in vitro* (Weber, Wasiliew, and Kracht et al. 2010; Ueda et al. et al. 2009). *In vitro* studies have revealed that IL1 can extend the survival of CFU-GM and BFU-E (Hangoc et al. 1989). This finding is further supported by *in vivo* experiments where the administration of an IL1 receptor antagonist resulted in a significant decrease in the number of femoral CFU-GM and BFU-E (Jovcic et al. 1996). These results suggest that the basal tone of IL1 signaling plays an essential role in constitutive hematopoiesis. A recent study showed that chronic exposure of HSCs to IL1 resulted in increased cycling and massive differentiation towards myeloid cells, driven through activation of a PU.1-dependent myeloid gene program. The effects of IL1 depend on the presence of the IL1 receptor, as IL1β fails to accelerate myeloid differentiation in $Il1r^{-/-}$ HSCs (Pietras et al. 2016).

1.2.2.4 Interleukin 6

Another interleukin that plays a role in hematopoiesis is interleukin 6 (IL6). The receptor for IL6 comprises the ligand-binding IL6-receptor α chain (IL6Rα) and the signal-transducing subunit β-receptor glycoprotein 130 (gp130), which are associated with Janus kinase (JAK) 1/2, tyrosine kinase 2, and STAT3. Unlike other cytokines, IL6 has the unique ability to signal not only through membrane-bound IL6Rα but also through sIL6Rα together with ubiquitously expressed gp130 (Figure 1.2C) (Scheller et al. 2011). The lack of the GP130 signal transducer was shown to cause fewer numbers of HSPCs and T cells (Yoshida et al. 1996).

IL6 is produced by T cells and macrophages in response to infection, trauma, burns, and other forms of tissue damage, which cause inflammation. As a result of its production, IL6 is responsible for inducing the synthesis of acute-phase proteins and promoting the production of neutrophils in the BM (Scheller et al. 2011; Schaper and Rose-John 2015). Interestingly, HSPCs produce more IL6 than conventional immune cells. They respond directly to bacterial components via the TLR/nuclear factor κB pathway and produce multiple cytokines, with IL6 being secreted the strongest (Zhao et al. 2014). The expression of IL6 by HSPCs has been shown to play a crucial role in the paracrine mediation of stress-induced myelopoiesis and HSPC proliferation. When IL6 was neutralized, the differentiation of LSK cells into myeloid lineages was significantly reduced, and the number of LSK cells was reduced as well, indicating that the cytokines secreted by LSK cells cause positive feedback to their proliferation and survival (Zhao et al. 2014). Furthermore, it was found that IFNγ-mediated myelopoiesis in HSPCs occurs indirectly through IL6 secreted by mesenchymal stromal cells (MSCs). The production of IL6 by BM MSCs leads to an increase in the number of early MPPs and committed myeloid precursors in the BM, facilitating the accumulation of myeloid cells in the periphery, resulting in the elimination of the infection (Schürch, Riether, and Ochsenbein et al. 2014). Additionally, recent studies have discovered that IL6 plays a crucial role in hematopoietic regeneration. One study showed that stress-induced IL6 drives lymphatic vessel expansion and bone lymphangiogenesis (Biswas et al. 2023).

1.3 The role of baseline proinflammatory signaling in HSC biology

Recent research has revealed that the proinflammatory cytokines regulating HSC stress responses also regulate the emergence of definitive HSCs during embryonic development (Espin-Palazon et al. 2018). They play a significant role in shaping the adult hematopoietic compartment not only during periods of pathogenic insults but also through tonic inflammatory signals originating from commensal microbiota (Collins, Mitchell, and Passegué et al. 2021). Recent discoveries have revealed the crucial role played by proinflammatory cytokines such as TNFα, IFNγ, and IL1β, as well as TLR4 signaling, in the fate determination of HSCs derived from the hemogenic endothelium (HE) (Espin-Palazon et al. 2018; Mancini, Bonnet, and Arrieta et al. 2022). The first evidence for the involvement of inflammatory signals in HSPCs specification came from discovering that TNFα signaling is necessary for endothelial cell development. It

was shown that activation of TNFR2 is required for the expression of jag1a, a Notch ligand essential for HSC specification, and that the resulting signaling to the Notch1a receptor on the adjacent HE helps to determine the fate of HSCs (Espín-Palazón et al. 2014). The study revealed that the proinflammatory transcription factor NF-kB is also active in nascent HSCs and essential for their specification. These results were consistent across zebrafish and mouse embryos. Inflammatory signaling pathways play a role in relaying the Notch-to-Runx1 signal, which is essential for specifying definitive HSPCs (Hadland et al. 2004; Bigas and Espinosa et al. 2012). Notch signaling results in Il6r up-regulation in zebrafish, rendering endothelial cells receptive to IL6 secreted by primitive neutrophils. IFN signaling has also been described to be involved in HSC emergence in mice (Sawamiphak, Kontarakis, and Stainier et al. 2014; Kim et al. 2016). Moreover, IL1β, together with the proinflammatory cytokines TNFα and IFNγ, have been identified as key determinants of HSC specification during embryonic development (Y. Li et al. 2014). It has been shown that at around E11, murine IL1 is highly expressed by HSCs and enhances HSC expansion (Orelio et al. 2008).

This discovery raises many questions in the field. One of the most important questions is whether basal activation of proinflammatory cytokine signaling is important for steady-state adult hematopoiesis. Although the role of IFNs in hematopoietic homeostasis has not been studied in detail, previous results show that HSCs from mice lacking IFNγ signaling have a lower proliferation rate and a better reconstitution capacity at steady state (Baldridge et al. 2010). Another study showed that mice lacking interferon regulatory factor 2 (Irf2) a negative regulator of Type I IFN signaling, had high numbers of proliferating HSCs (Sato et al. 2009). These findings implicate IFNs as regulators of HSCs under conditions of infectious stress and during homeostasis.

The understanding that proinflammatory signals play a crucial role in shaping the hematopoietic system has been slow to develop, likely because many adult KO mice lacking proinflammatory signals do not exhibit obvious hematological defects. This could be due to genetic compensation or redundancy between proinflammatory pathways. Supporting the idea of redundancy, simultaneous knockdown of both TNFα and IFNγ has led to a significant decrease in HSC numbers compared to single

knockdown (Y. Li et al. 2014). Previous studies by our group have shed light on existing crosstalk between the different proinflammatory cytokines. We have shown that the LPS-induced activation of HSCs is indirectly mediated through the production of proinflammatory cytokines by myeloid cells. These cytokines include IFNα, IFNγ, TNFα and IL1β. It was also shown that these cytokines lead to direct and indirect activation of HSCs (Demel et al. 2022) Moreover, we found that IL1β is highly induced upon TNFα treatment suggesting that IL1β is one of the factors leading to TNFα induced activation of HSCs (Unpublished data).

Treatment of any of these cytokines can likely activate HSCs indirectly by altering the niche environment, promoting the release of more proinflammatory cytokines, which then lead to the subsequent activation of HSCs (Zhao et al. 2014; Goedhart et al. 2018). The fact that a massive amount of cytokines are produced during an inflammatory reaction excludes the dependency of HSCs activation on only one proinflammatory cytokine. This data supports the hypothesis of the presence of crosstalk of proinflammatory cytokines on HSCs quiescence. Furthermore, since most of the proinflammatory cytokines are present in small concentrations under homeostatic conditions, we hypothesize that the combined proinflammatory cytokine signaling plays a role in regulating HSC biology at a steady state. A better understanding of the overlapping and unique features of the proinflammatory signaling mechanisms that regulate the functions of hematopoietic stem and progenitor cells throughout an individual's lifespan and state of health could lead to improved diagnostic and therapeutic strategies for hematopoietic disorders and malignancies.

2 Aims of the thesis

Our group has shown that treating mice with IFNα induces cell cycle entry of quiescent HSCs. However, the detailed mechanism of IFNα induced activation of HSCs remains unknown, and studies investigating the mechanisms controlling reversible cycle entry of quiescent HSCs are lacking. In addition, the heterogeneity of response between HSCs and downstream progenitors in the context of IFNα has not been investigated before.

Furthermore, induction of HSC's proliferation is a common response observed with many proinflammatory cytokines, which raises the question of whether there is a common stress mechanism activated in response to these different proinflammatory stimuli. Another interesting question is whether the same proinflammatory cytokines that activate HSCs in response to stress also play a role in regulating HSCs quiescence and activation under homeostasis.

This work aims to answer these open questions as follows:

2.1 Aim 1: Uncover the mechanisms and dynamics of the stress response of HSCs to IFNα

To understand the dynamics of the acute response of HSCs to IFNα treatment, I aimed to analyze the changes in gene expression in HSCs over time by performing bulk RNA sequencing at time points representing the three phases of HSCs response to acute IFNα treatment (sensing (3h), proliferation (24h), and recovery (72h)).

2.2 Aim 2: Understanding the heterogeneity of HSPCs response to IFNα

To investigate the kinetics of activation of the whole stem and progenitor cell compartment, I performed a single-cell RNA sequencing experiment under the same treatment conditions as the bulk sequencing of HSCs in aim1. With this experiment, I aimed to determine which cell populations respond and which do not and to define the major regulatory changes in the differentiation trajectory upon stress.

2.3 Aim 3: Dissect the interplay of proinflammatory cytokines in the acute response of HSCs to stress

To find out if there is a common mechanism that regulates the increase in HSCs proliferation after stress conditions. I performed a microarray on HSCs 3h after treating mice with various recombinant proinflammatory cytokines (IFNα, IFNγ, TNFα, IL1α, IL1β, IL6, LPS, and pIC). Using this approach, I aimed to determine whether converging gene expression programs are elicited and which key proinflammatory cytokines mediate HSCs activation.

2.4 Aim 4: Investigating the net impact of proinflammatory cytokine receptor signaling in hematopoiesis under homeostasis

Many single knockout (KO) mice in which a proinflammatory pathway is knocked out show little effect on basic blood homeostasis. Therefore, I hypothesized that because of the convergence of their intracellular signaling pathways, they have overlapping and redundant effects and therefore, most likely compensate for each other. Thus, I characterized the hematopoietic system in KO mice in which all five major proinflammatory cytokine receptors which are known to impact HSCs function under stress (*Ifnar*$^{-/-}$,*Ifngr*$^{-/-}$,*Tnfrsf1a*$^{-/-}$, *Tnfrsf1b*$^{-/-}$, and *Il1r*$^{-/-}$) were removed (5KO). Other precursor KO mouse lines were used as controls in our experiments.

3 Results

3.1 Uncover the mechanisms and dynamics of the stress response of HSCs to IFNα

3.1.1 Dynamic analysis of HSCs response to acute IFNα treatment

Our group has shown that treating mice with acute IFNα induces transient proliferation of HSCs (Essers et al. 2009). The response of quiescent HSCs to IFNα involves increased *STAT1*, PKB/Akt phosphorylation, and increased expression of *Sca-1* (Pietras et al. 2014; Essers et al. 2009). Nevertheless, the detailed mechanisms involved in stress-induced HSCs activation and the dynamics regulating the response and recovery of HSCs to acute IFNα remain poorly understood. To gain insights into the different phases of this stress response, I performed a dynamics analysis of the response of HSCs to acute IFNα treatment, which showed that the mRNA levels of interferon-stimulated genes (ISG) in HSCs (Lin^- $Sca\text{-}1^+$ $cKit^+$ $CD150^+$ $CD48^-$ $CD34^-$) were upregulated as early as 3 hours (3h) and returned to basal expression levels at 72 hours (72h) after IFNα treatment (Figure 3.1A), suggesting that HSCs shows first signs of sensing IFNα at 3h by increasing expression of ISGs. Moreover, the data confirmed that HSCs reached the maximal increase in proliferation at 24 hours (24h) and returned to quiescence at 72h, as measured by BrdU proliferation assay (Figure 3.1B). In addition, the mean cell number of HSCs calculated based on their abundance in the BM and the actual BM cellularity did not change significantly (Figure 3.1C). Using these analyses, I found that the three-time points (3h, 24h, and 72h) effectively elucidated the dynamics of the HSCs response to acute IFNα treatment: sensing (3h), proliferation response (24h), and recovery back to quiescence (72h).

3.1.2 Time-series global transcriptional profiling of HSCs response to IFNα treatment

To decipher the mechanisms regulating sensing, response, and recovery of HSCs to acute IFNα treatment, time-series bulk RNA sequencing was performed to identify the major changes in gene expression at each of the three-time points identified in section 3.1.1. Mice were treated with IFNα, and BM was isolated after 3h, 24h, and 72h. Three to four biological replicates were used per treatment time point, and I sorted between

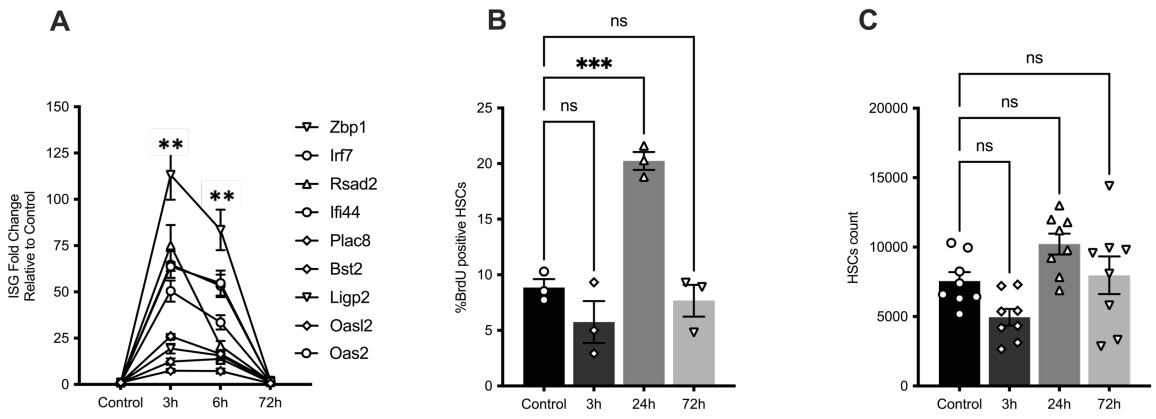

Figure 3.1: Dynamics analysis of HSCs response to acute IFNα treatment reveals distinct phases. Wild type (WT) mice were treated subcutaneous (s.c.) with either 100 µl PBS control or IFNα (50.000 international units (IU) per 20g mouse) and sacrificed after 3h, 6h, and 72h (for panel A) or after 3h, 24h, and 72h (for panels B and C). **(A)** Interferon response genes (ISGs) transcriptional levels were quantified using qPCR in HSCs (Lin^- $Sca\text{-}1^+$ $cKit^+$ $CD150^+$ $CD48^-$ $CD34^-$). 3 biological replicates were used in the analysis. **(B)** Cell proliferation in HSCs (Lin^- $Sca\text{-}1^+$ $cKit^+$ $CD150^+$ $CD48^-$ $CD34^-$) was measured using 14h BrdU (18 mg/kg) uptake. 3 biological replicates were used in the analysis. **(C)** The absolute numbers of indicated bone marrow (BM) HSCs were counted, with 8 biological replicates per group from two independent experiments. Statistical significance was evaluated using an ordinary one-way ANOVA with Holm-Šídák's multiple comparisons test. The data represent mean ± standard error of the mean (SEM) from at least two independent experiments. The significance level was set at ns; non-significant, **P≤ 0.01, ***P≤ 0.001.

3000-5000 HSCs (Lin^- $ckit^+$ $CD150^+$ $CD48^-$ $CD34^-$) from each biological replicate. I excluded Sca-1 from the gating strategy because it has been reported to be abnormally expressed in most HSPCs following inflammation, posing a major challenge in identifying HSCs under inflammatory conditions (Kanayama et al. 2020; Pietras et al. 2014). Total RNA was isolated, and samples were measured by the Genomics and Proteomics Core Facility of the German Cancer Research Center (DKFZ) in Heidelberg (Figure 3.2A). The facility prepared sequencing libraries and performed quality control and sequencing. Raw sequencing data in FASTQ format were aligned and quantified by the Omics IT and Data Management (ODCF) Core Facility. Subsequently, I performed the downstream analysis. I first wanted to generate a global overview of the gene expression time-course data and determine intra- and inter-group variability. Hierarchical clustering confirmed that all the samples at a given time point clustered together and were separated from each other (Figure 3.2B).

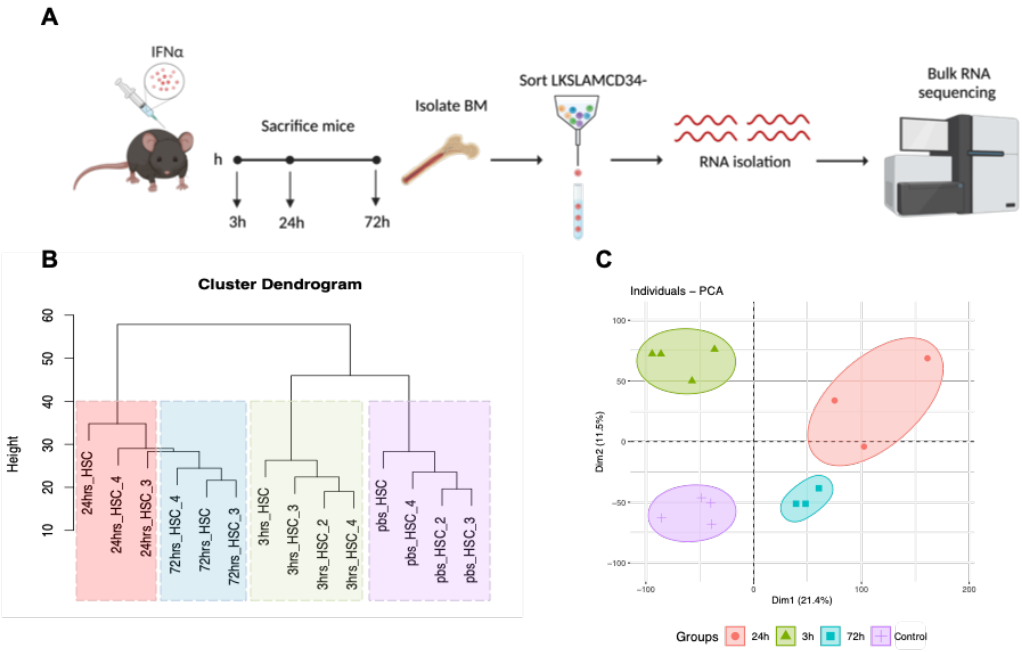

Figure 3.2: Time-series bulk RNA sequencing of HSCs following IFNα treatment.
(A) Scheme for Bulk RNA sequencing experimental procedure. Mice were treated with IFNα and sacrificed after 3h ,24h and 72h. 3-4 biological replicates were used per condition. Bones (tibia, femur and hips) were isolated, cleaned and then flushed. Cells were then stained with markers for HSCs (Lin^- $cKit^+$ $CD150^+$ $CD48^-$ $CD34^-$) then sorted. RNA was isolated from sorted cells; libraries were then prepared and sequenced. **(B)** Hierarchical clustering based on Euclidian distance was performed with the hclust function implemented in R. **(C)** Principal component analysis (PCA).

Moreover, principal component analysis (PCA) demonstrated robust grouping among biological replicates within each time point, and the sample groups spread among principal component (PC) 1, which accounted for 21.40% of the variance, and PC 2 which accounted for an additional 11.48% (Figure 3.2C). 3h separated on PC2, 24h separated based on a combination of PC2 and PC1 whereas 72h separated on PC1 (Figure 3.2C). The top 50 variable genes in the dataset were found to be ISGs and were highly increased in expression at the 3h time point, decreased again at 24h, and returned to baseline at 72h (Figure 3.3A). This suggests that the immediate response to IFNα occurs at an early stage and is driven mainly by ISGs. Next, I performed differential gene expression analysis. Because our dataset consisted of three treatment timepoints, I used the negative binomial distribution in DESeq2 (Love et al. 2014) and performed three pairwise comparisons with the PBS control samples.

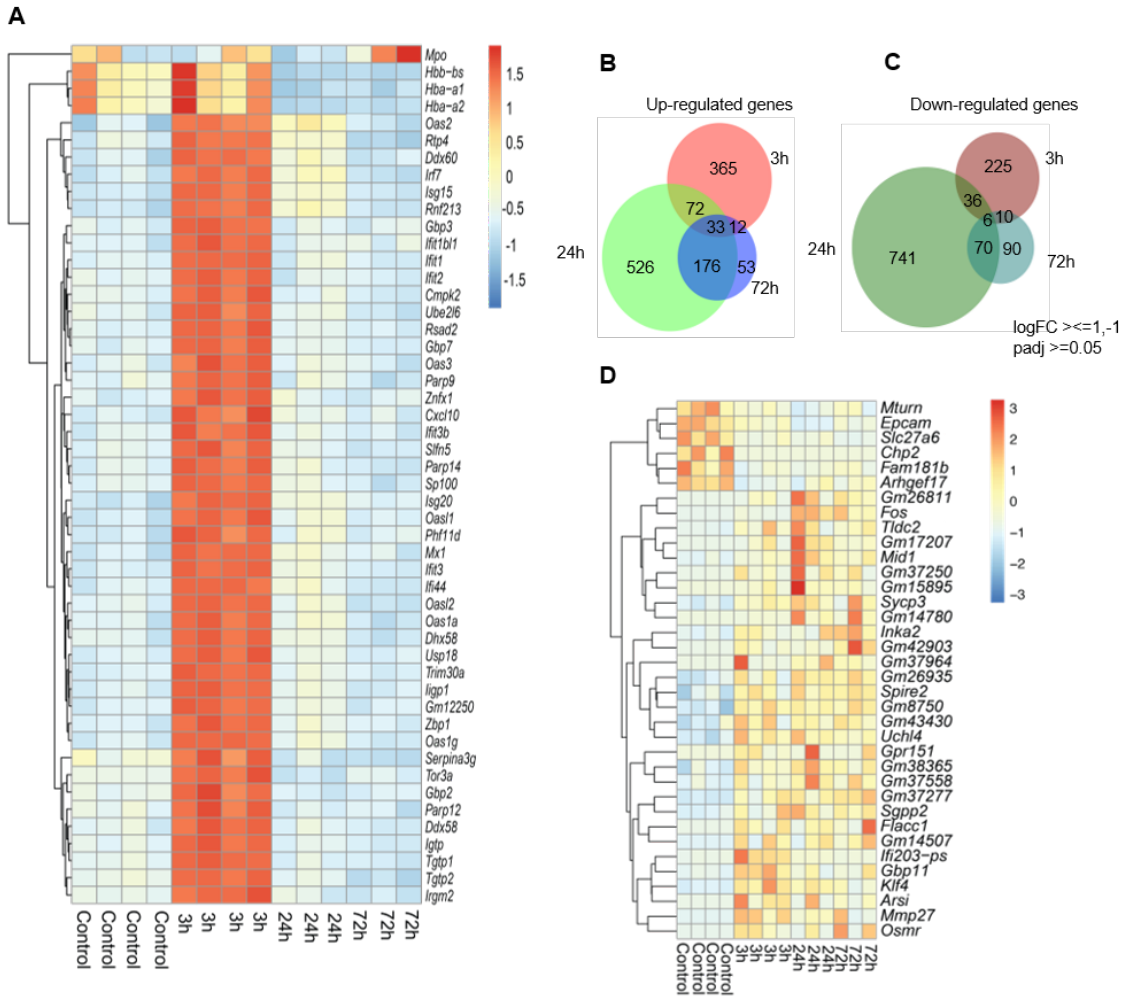

Figure 3.3: Time-dependent molecular signatures in HSCs following IFNα treatment.

(A) Heatmap showing the top 50 variable genes. Analysis was applied to read counts that were normalized with the variance stabilizing transformation (VST) implemented in the R package Deseq2. **(B-C)** Venn diagram illustrating the number of unique and shared differentially expressed genes (DEGs) for each comparison. Venn diagram showing the DEGs of upregulated **(B)** and downregulated genes **(C)** in HSCs at all three time points in comparison to the PBS control. Differential gene expression analysis was performed using DEseq2 package. **(D)** heatmap showing the common signature of upregulated and downregulated genes in HSCs at all time points.

I obtained 759, 1660, and 450 differentially expressed genes (padj ≤ 0.05, logFC ≥ 1, ≤-1) for the 3h, 24h, and 72h time points, respectively, compared to the PBS control samples (Figure 3.3B,C). I have noted a strong overlap in the global expression and the differentially expressed genes (DEGs) between the 24h and 72h timepoints compared to the 3h timepoint (Figure 3.3B,C).

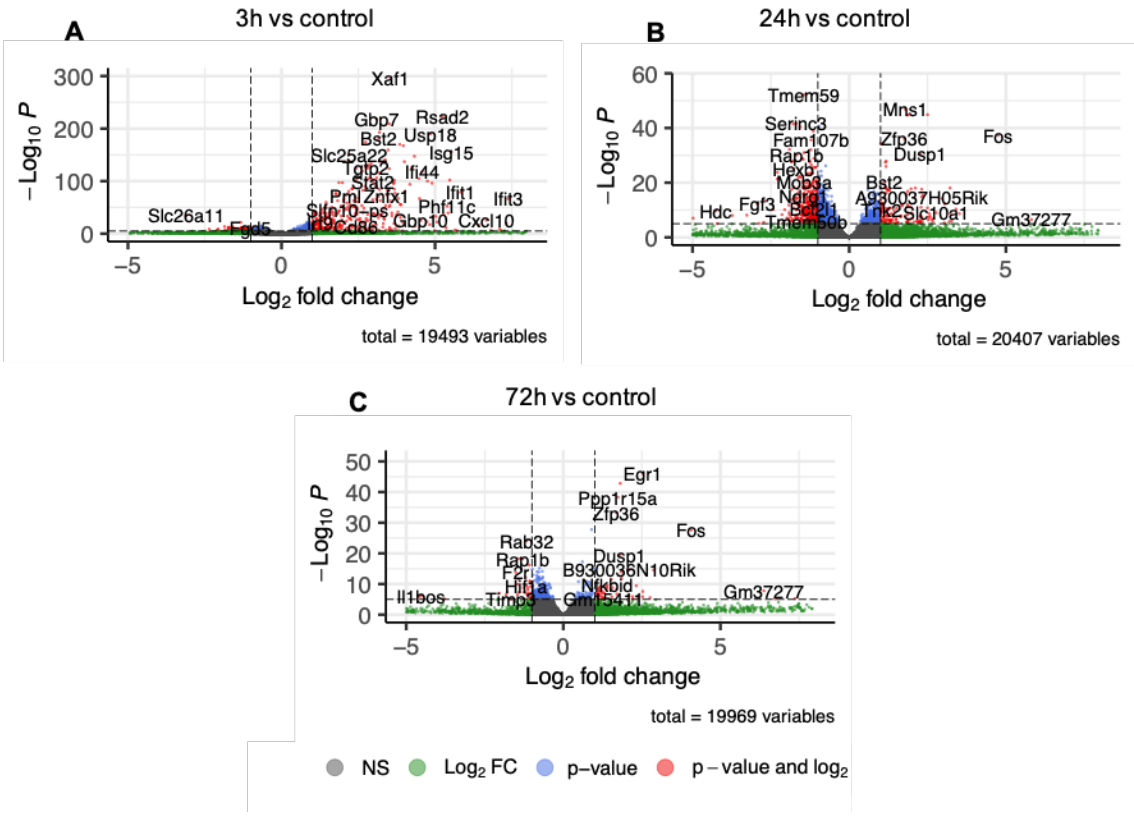

Figure 3.4: Differential gene expression analysis reveals unique molecular signatures in HSCs following IFNα treatment at various time points.

(A-C) Volcano plots showing differentially expressed genes (DEGs) in HSCs at 3h **(A)**, 24h **(B)**, 72h **(C)** compared to the PBS control samples.

Indeed, out of 274 upregulated and 159 downregulated DEGs at the 72h timepoint, 176 (64%) and 70 (44%) DEGs were also found to be significantly increased or decreased, respectively at the 24h timepoint (Figure 3.3B,C). Next, I looked for DEGs that were concurrently downregulated or upregulated at all three time points. Strikingly, I found a common signature of 33 upregulated and 6 downregulated genes (padj ≤ 0.05, logFC ≥ 1, ≤-1) (Figure 3.3D). The upregulated signature included genes reported to play a role in apoptosis (*Fos*), DNA repair (*Spire2*), self-renewal, lineage differentiation (*Klf4*), and extracellular matrix remodeling (*Mmp27*). The downregulated signature included genes involved in fatty acid metabolism (*Slc27a6*), cell adhesion (*Epcam*), and actin cytoskeleton organization (*Arhgef17*) (Figure 3.3D). Thus, the results of differential gene expression analysis showed a common signature of up and downregulated genes across all three treatment time points, indicating potential key IFNα factors. The top DEGs at the different time points are presented in the volcano plots (Figure 3.4A-C). This highlighted a large group of ISGs (*Usp18, Stat2, Ifit1,* and *Ifit3*) being expressed at 3h compared to the rest of the time points (Figure 3.4A).

Interestingly, I noted a marked reduction in the expression of genes that play a role in the early transcriptional priming of the myeloid lineage (*Hdc*) in the 24h dataset (Figure 3.4B). Remarkably, among the top-ranked downregulated genes in the 24h, I found *Serpine2*, which has been reported to play a role in protecting against death during stress, suggesting a mechanistic link for how IFNα can prime HSCs for apoptosis (Pietras et al. 2014) (Figure 3.4B). Genes known to regulate HSCs quiescence, such as *Egr1, Zfp36,* and *Fos*, were upregulated at 72h (Figure 3.4C), suggesting a genetic program to revert to quiescence at the acute-activation stage. In conclusion, differential expression analysis revealed unique molecular signatures for HSCs following IFNα treatment at various time points.

3.1.3 Transcriptional signatures of HSCs at different phases of acute response to IFNα treatment

To gain insights into the biological processes differentially represented at each time point, I performed gene set enrichment analysis (GSEA) on the entire set of significant DEGs (padj ≤ 0.05) from each of the three comparisons using the MsigDB database (Subramanian et al. 2005; Liberzon et al. 2011). This analysis identified 173, 254, and 104 positively enriched gene sets (false discovery rate [FDR]<0.05) for the 3h, 24h, and 72h time points, respectively, compared to the PBS control samples (Figure 3.5A). Moreover, I found 510 and 209 negatively enriched gene sets (FDR <0.05) at the 24h and 72h time points, respectively (Figure 3.5B). There were no pathways negatively enriched for the 3h dataset at FDR <0.05. The Venn diagram shows that more than 50% of the gene sets enriched in the 72h were also enriched in the 24h dataset (Figure 3.5A,B). The top gene sets enriched in the 3h analysis included the categories “Interferon alpha response” (NES= 2.84), “Response to virus” (NES= 2.84), “Lipid Oxidation" (NES= -1.81), and “Bile acid metabolic processes” (NES= -2.0) (Figure 3.5C). While, the top gene sets for the 24h analysis were including “Ribosome” (NES= 2.99), “Mitochondrial respiratory chain complex” (NES= 2.85), “Myeloid “Leukocyte mediated immunity” (NES= -2.11), and “phagocytosis” (NES= -2.18) (Figure 3.5D).

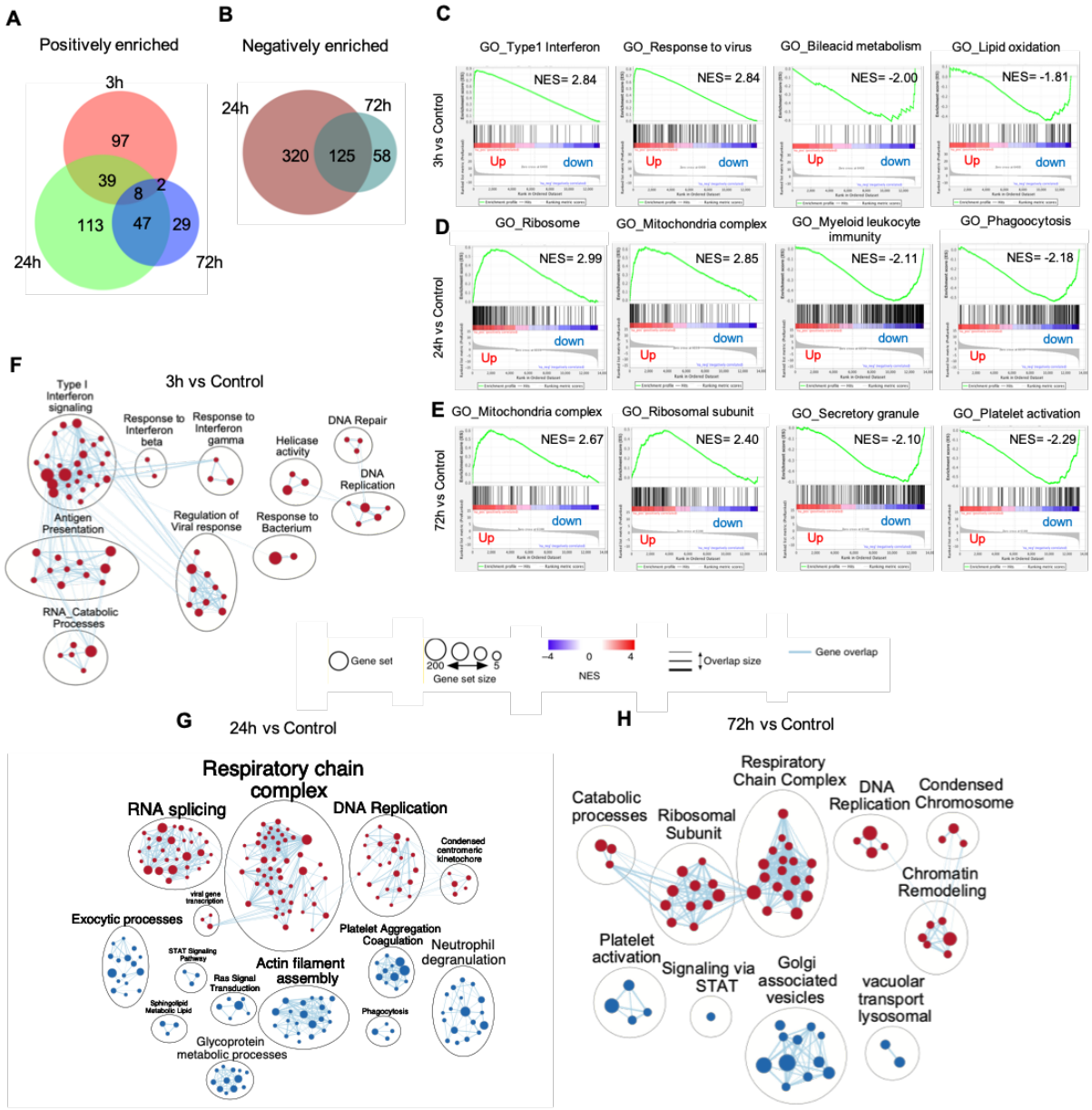

Figure 3.5: GSEA reveals time-dependent regulation of biological processes in HSCs after IFNα treatment.

(A-B) Venn diagram illustrating the number of unique and shared up **(A)** and downregulated **(B)** GO terms for each comparison (3h vs control, 24h vs control, and 72h vs control). **(C-E)** Enrichment plots for top four data sets enriched in GSEA 3h vs control analysis **(C)**, 24h vs control analysis **(D)** and in 72h vs control analysis **(E).** NES, normalized enrichment score. **(F-H)** Enrichment maps created and modified by cytoscape showing gene sets with FDR<=0.01 for 3h vs control analysis **(F)**, 24h vs control analysis **(G)** and in 72h vs control analysis **(H)**. Red and blue circles represent distinct pathways that are positively or negatively enriched respectively, in the treatment timepoint vs the control.

For the 72h analysis, the most enriched gene sets included “Mitochondrial Respiratory chain complex assembly” (NES= 2.67), “Ribosome” (NES= 2.40), “Secretory Granule membrane” (NES= -2.10), “Platelet Activation” (NES= -2.29) (Figure 3.5E). To obtain a better overview of all biological processes suggested to be differentially regulated at each time point, enrichment maps were created to organize the large number of gene sets obtained in a network. The enrichment maps showed the most significantly enriched gene ontology (GO) categories (FDR ≤ 0.01). This analysis revealed that processes associated with DNA metabolic processes, replication, and nuclear division, in addition to cell cycle and chromatin remodeling processes, were positively enriched at all three-time points (Figure 3.5F-H). Furthermore, the enrichment map showed that the 3h time point was further enriched in gene categories related to immune processes, such as defense response to viruses, regulation of innate immune responses, antigen presentation, processing, and interferon response processes (Figure 3.5F). Most of the processes enriched in the 24h and 72h datasets were related to energy metabolism, as I found an overrepresentation of processes related to the respiratory chain complex, including increased mitochondrial activity, oxidative phosphorylation, ATP metabolic processes, oxidoreductase activity, and ribosomal activity (Figure 3.5G,H), which is consistent with the aerobic metabolic program employed by cycling HSCs (Suda, Takubo, and Semenza 2011). It is interesting to note that HSCs remain metabolically active at 72h (Figure 3.5H), despite phenotypically returning to quiescence.

The categories negatively enriched in the 24h and 72h datasets related to the regulation of cytoskeleton organization, including actin filament assembly, exocytic processes, and Golgi-associated vesicles, specifically COPII-coated vesicle membranes, in addition to platelet aggregation processes (Figure 3.5G,H). The 24h dataset further included other metabolic categories that were negatively enriched, including glycoprotein metabolic, carbohydrate biosynthetic, and lipid metabolic processes. Interestingly, the 24h negatively enriched categories also included terms involving the categories of “Neutrophil Degranulation” (Figure 3.5G). Through this analysis, I identified the dynamics of biological categories activated and suppressed in HSCs after IFNα treatment. This may contribute to our understanding of the mechanisms underlying HSCs quiescence and activation.

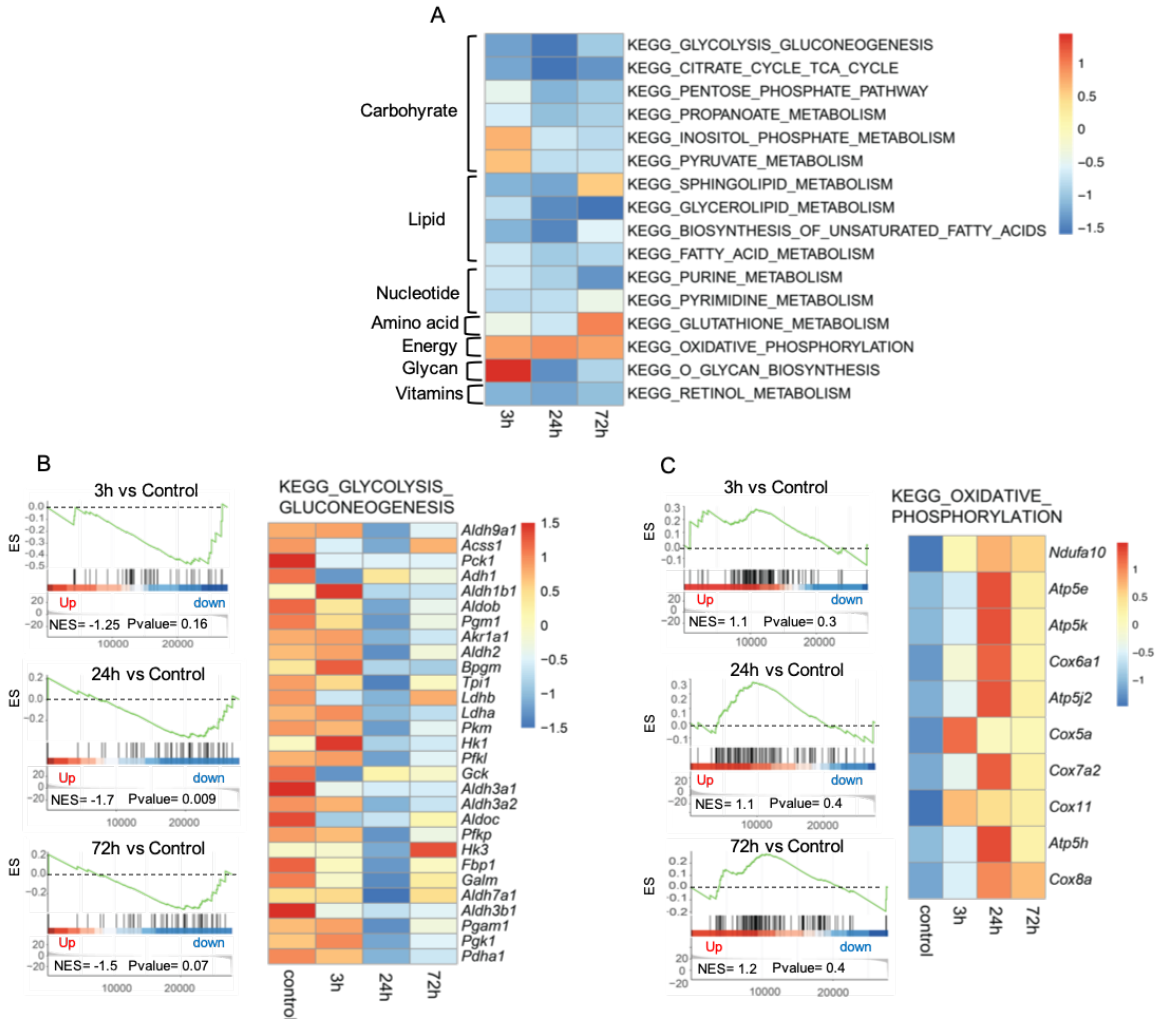

Figure 3.6: KEGG pathway GSEA analysis reveals changes in core metabolism in HSCs following IFNα treatment.

(A) The top enriched KEGG metabolic pathways. **(B-C)** GSEA plot and heatmap of genes enriched in KEGG Glyolysis_Gluconeogenesis **(B)** and in KEGG Oxidative Phosphoylation pathways **(C).** NES, normalized enrichment score.

3.1.4 Transcriptomic profiling of HSCs metabolism during the acute phases of IFNα treatment

The data shows that the exposure of HSCs to IFNα treatment predominantly activates the expression of genes related to metabolism (Figure 3.5G,H). Currently, the mechanisms by which HSCs metabolism is regulated in response to inflammatory challenges are not fully understood. Here, I used the transcriptomic data to interrogate the global metabolic changes in HSCs following IFNα treatment. By performing GSEA

using the Kyoto Encyclopedia of Genes and Genomes (KEGG) (M. Kanehisa and Goto 2000; Minoru Kanehisa et al. 2023) definition of metabolic pathways, I observed that the transition from quiescence to activation following IFNα treatment is accompanied by significant metabolic changes (Figure 3.6A). In line with the literature, the energy metabolism in HSCs is reprogrammed from anaerobic glycolysis to oxidative respiration (Suda, Takubo, and Semenza 2011). Within a 3h time frame, IFNα already induced metabolic changes, which facilitated a rapid shift within HSCs from glycolytic to OXPHOS, and this effect is sustained even at 72h post-injection when HSCs return to quiescence as indicated by a decrease in glycolytic genes including *Pdk2, Pkm* and *Ldha* (Figure 3.6B) and the concurrent upregulation of OXPHOS genes including *Atp5e, Cox5a,* and *Ndufa10* (Figure 3.6C). These results show that the transition from inactive to active HSPCs starts with an initial upregulation of glycolytic and a sustained upregulation of OXPHOS genes rather than a binary switch on/off pattern. In line with previous findings, retinoic acid metabolism is downregulated following IFNα (Cabezas-Wallscheid et al. 2017); however, here I show that this effect is still present even at 72h when the cells phenotypically are back to their quiescent state (Figure 3.6A). Both pyruvate and inositol phosphate carbohydrate metabolism pathways were upregulated shortly at 3h, and this effect was reversed at 24h (Figure 3.6A).

Notably, other carbohydrate metabolic pathways, including the pentose phosphate pathway (PPP) and citrate (TCA) cycle, were negatively enriched at 3h and stayed downregulated until 72h in comparison to PBS control samples (Figure 3.7A,B respectively). This contrasts with previous findings that have reported an increase in TCA and PPP in HSCs following inflammatory stress. While previous studies reported increased HSC purine metabolism in response to stress (Karigane et al. 2016), I found a sustained downregulation at all time points after IFNα treatment (Figure 3.7C). According to recent research by Mistry et al., the metabolism of HSCs shifts to fatty acid metabolism during lipopolysaccharide (LPS) triggered inflammation (Mistry et al. 2021). In contrast to this study, I found persistent downregulation of fatty acid metabolism throughout the treatment period (Figure 3.7D). In summary, HSCs showed a significant metabolic shift to OXPHOS that lasted up to 72h. In addition, HSCs showed an unprecedented decrease in TCA, PPP, fatty acid, and purine metabolism after IFNα treatment.

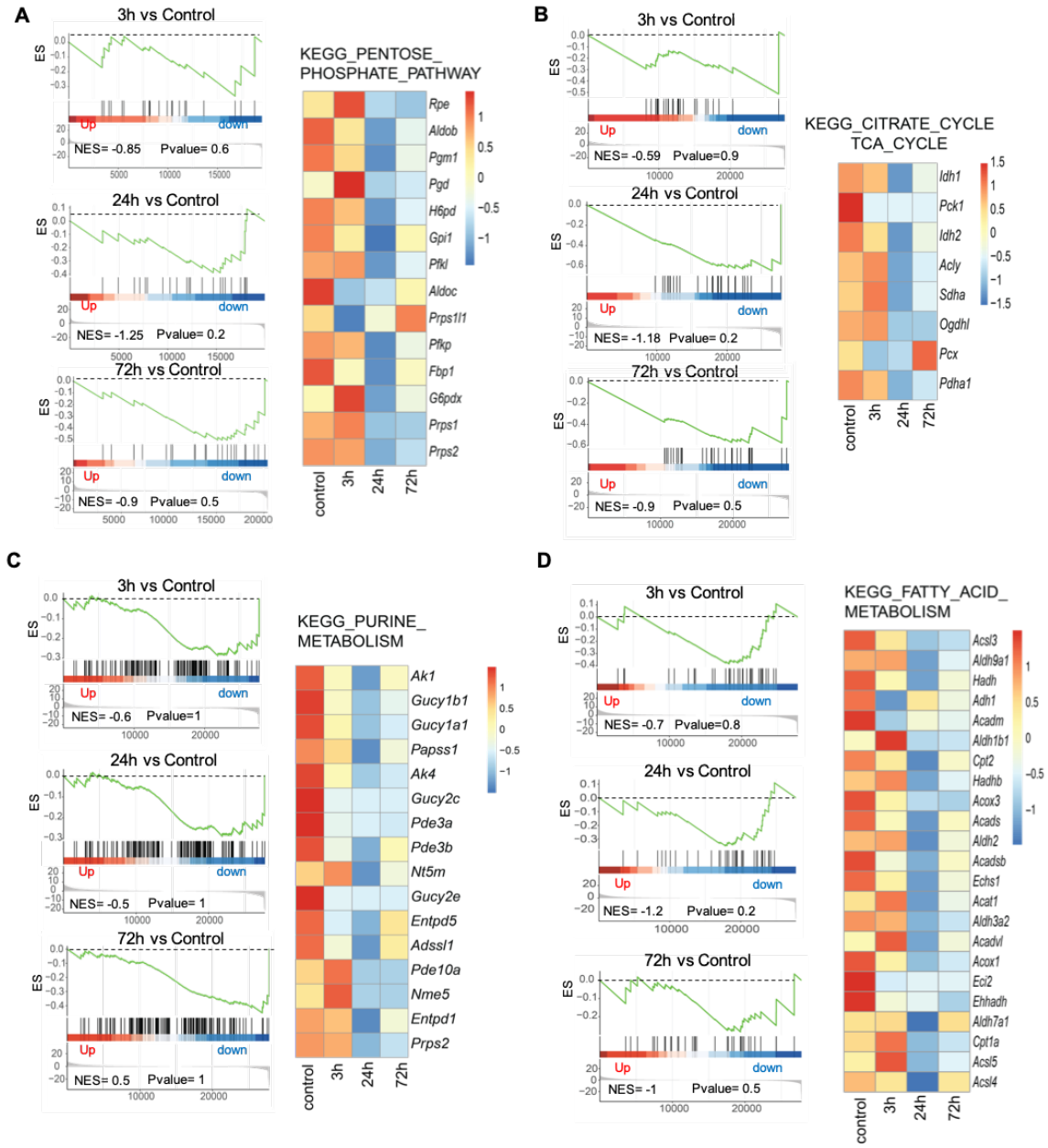

Figure 3.7: KEGG pathway reveals changes in core metabolism in HSCs following IFNα treatment.

(A-D) GSEA plot and heatmap of genes enriched in KEGG pentose phosphate pathway **(A)**, KEGG citrate cycle TCA cycle **(B)**, KEGG purine metabolism **(C),** and KEGG fatty acid metabolism **(D).** NES, normalized enrichment score.

3.1.5 HSCs are less myeloid primed following IFNα treatment

Metabolic cues play an important role in deciding the fate of HSCs (Morganti, Cabezas-Wallscheid, and Ito et al. 2022). Increased cellular metabolism during stress produces important metabolites used by HSCs as an energy source to promote differentiation

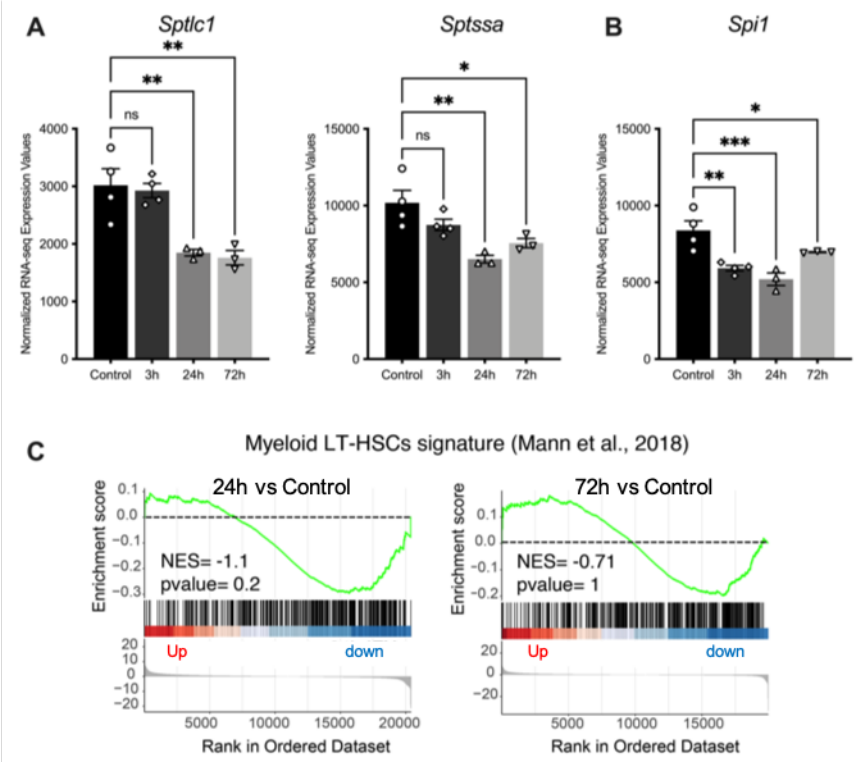

Figure 3.8: Impaired myeloid priming in HSCs following IFNα treatment.

(A-B) Bar plots showing DESeq2 normalized gene expression values for genes associated with lipid metabolism *Sptlc1* and *Sptssa* **(A)** and for the master myeloid transcription factor *Spi1* **(B)**. 3-4 biological replicates were used in the analysis. Statistical significance was determined by an ordinary one-way ANOVA using Holm-Šídák's multiple comparisons test. ns; non-significant, *P≤0.05, **P≤ 0.01, ***P≤ 0.001. Data represent mean ± standard error of the mean (SEM). **(C)** GSEA plots of Myeloid LT-HSC molecular signatures from *Mann et al.,* significantly enriched (pvalue <=1) over the 24h vs control (left) and 72h vs control (right). NES, normalized enrichment score.

and thus drive emergency hematopoiesis (Maryanovich and Ito et al. 2022). Therefore, the observed downregulation of TCA, PPP, fatty acid, and purine metabolism suggests that HSCs have a reduced differentiation capability following IFNα treatment. Accordingly, I found *Sptlc1* and *Sptssa* (Figure 3.8A,B) among the genes associated with deregulated fatty acid metabolism. Previous studies have shown that they play a central role in myelopoiesis (Parthibane et al. 2019). Interestingly, I found that the master regulator of myeloid differentiation *Spi1* was downregulated after 3h and was sustained up to 72h (Figure 3.8B). Next, I investigated whether myeloid priming was impaired in HSCs. The 24h gene expression signature showed significant downregulation of the previously reported myeloid-biased LT-HSC signature (Mann et al. 2018), and this effect persisted up to 72h (Figure 3.8C).

Taken together, the downregulation of myeloid priming of HSCs, along with the significant downregulation of leukocyte activation, phagocytosis, and neutrophil degranulation processes observed at 24h (Figure 3.5G), suggests that HSCs become less myeloid-biased following IFNα treatment.

3.2 Understanding the heterogeneity of hematopoietic stem and progenitor cells (HSPCs) response to IFNα

In the first part of my thesis, I focused on identifying the transcriptional changes of bulk HSCs after IFNα treatment. Building on these findings, the second part of my thesis aims to examine the heterogeneity of the response of HSCs and progenitor (HSPCs) cells to IFNα treatment, with the goal of gaining a more comprehensive understanding of the adaptations that occur throughout the compartment.

The results presented in this thesis section 3.2 are part of a manuscript currently under review for publication and is available online as a preprint at BioRxiv (Bouman, Demerdash et al. 2023) and some portions of the text, figures, and legends have been adapted from this co-authored manuscript. (see author contributions section 7 for more details)

3.2.1 Differential IFNα induced phenotypic alterations on the primitive LSKs and more committed LS-Ks

The molecular and cellular dynamics of HSPCs during inflammation remain poorly understood. To fill this gap and better understand the effects of IFNα-induced transient HSCs proliferation and correlate this effect with the response of downstream progenitor cells, I decided to examine the HSPCs dynamics in response to IFNα treatment, following the same time points I used to examine the response of bulk HSCs in the previous results section 3.1.2. I indeed observe that IFNα triggers a BM remodeling of HSPCs, as the FACs analysis data show potential alterations in population structure within the HSPCs (Figure 3.9A). However, one of the major limitations in studying the response of HSPCs to inflammatory stress is that the surface markers normally used to isolate these cells undergo massive changes upon inflammation. In accordance with previous results, I found similar dynamics in the expression of stem cell markers at the protein level as with the proliferation of HSCs (Figure 3.1B). This was most pronounced for Sca-1, which showed the greatest change at 24h (Figure 3.9B). The 3h time point showed no remarkable changes for the Sca-1 marker (Figure 3.9B), as reported by flow cytometry. Other stem cell markers such as cKit, CD150, and CD48 are not altered by the treatment (Figure 3.9C-E). Next, I analyzed changes in HSPCs abundance over time using common surface marker combinations (Table 7).

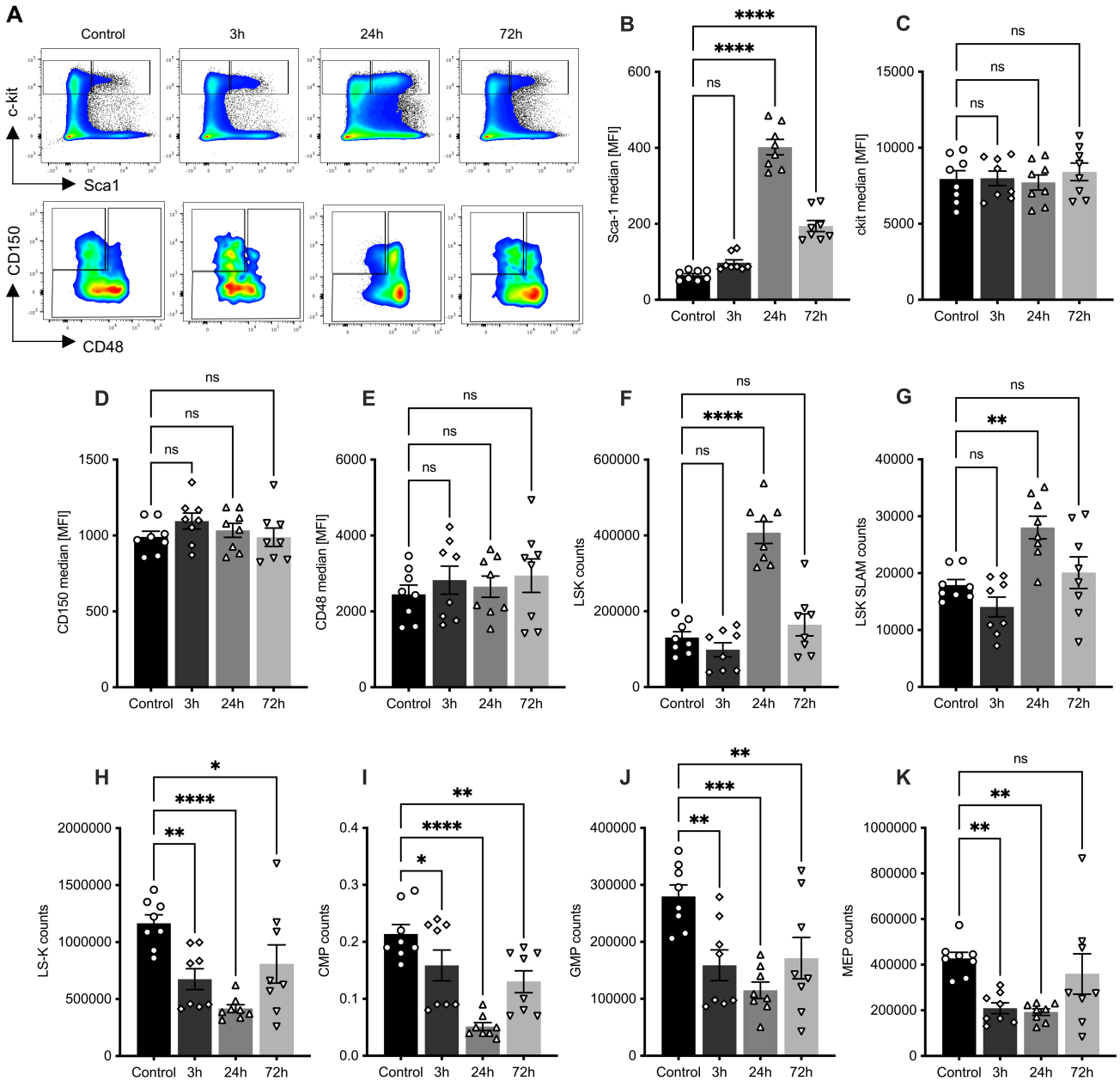

Figure 3.9: The primitive LSKs and more committed LS-Ks display differential phenotypic alterations upon IFNα treatment.

(A) Example of FACS plots of Lin$^-$ cKit$^+$ population of BM cells treated with PBS control or 3h, 24h and 72h with IFNα **(B-E)** Quantification of Sca-1 **(B)**, cKit **(C)**, CD150 **(D)**, CD48 **(E)** expression (calculated based on median fluorescence intensity) of HSCs (Lin$^-$ Sca-1$^+$ cKit$^+$ CD150$^+$ CD48$^-$ CD34$^-$). treated with control or 3h, 24h or 72h with IFNα. **(F-K)** Absolute numbers of the indicated BM populations. BM was isolated from tibia, femur and hips of the mice. Shown are LSK (Lin$^-$ Sca-1$^+$ cKit$^+$) **(F),** LSKSLAM (Lin$^-$ Sca-1$^+$ cKit$^+$ CD150$^+$ CD48$^-$) **(G),** LS-K (Lin$^-$ Sca-1$^-$ cKit$^+$) **(H),** CMP (Common Myeloid progenitors) **(I),** GMP (granulocytic monocytic progenitors) **(J),** MEP (Megakaryocytic erythroid progenitors) **(K).** 8 biological replicates per group from two independent experiments were used. Statistical significance in was determined by an ordinary one-way ANOVA using Holm-Šídák's multiple comparisons test. At least

2 independent experiments were performed; ns; non-significant, *P≤0.05, **P≤ 0.01, ***P≤ 0.001, ****P<0.0001. Data represent mean ± standard error of the mean (SEM).

The mean cell count for each of these populations was calculated based on their frequency in BM and the actual BM cell count at each time point. The results varied depending on the degree of stemness. In particular, the primitive cell populations, i.e., LSK (Lin^- $Sca\text{-}1^+$ $cKit^+$) and LSK SLAM (Lin^- $Sca\text{-}1^+$ $cKit^+$ $CD150^+$ $CD48^-$), increase significantly after 24h and return to homeostatic levels after 72h (Figure 3.9F,G). The opposite is true for the more committed LS-K (Lin^- $Sca\text{-}1^-$ $cKit^+$) progenitor cells and their associated subpopulations (CMP, GMP, and MEP). They show the greatest decrease in cell frequency after 24h (Figure 3.9H-K). Interestingly, the decrease was significant in the LS-K compartment much earlier than in the primitive cell populations starting at 3h (Figure 3.9H). At 72h, CMPs and GMPs still show a significant decrease compared to the PBS control level but a trend toward recovery (Figure 3.9I-J), whereas MEP numbers had already recovered at 72h (Figure 3.9K). Overall, our phenotypic analysis of HSPCs over time shows that IFNα-induced changes in Sca-1 marker expression follow similar dynamics to changes in the frequency of LSKs and proliferation of HSCs. It also shows that the effects of IFNα treatment on cell numbers are inversely correlated between LSKs and LS-Ks.

3.2.2 A longitudinal HSPCs single-cell dataset capturing inflammation dynamics

As a result of the massive changes in Sca-1 marker due to IFNα treatment, the molecular and functional analysis of HSCs and progenitors under stress is complicated (Ali and Park et al. 2020). Therefore, the effects observed in FACs-based analysis could be due to either actual changes in protein expression of cell markers in a given population or an actual increase or decrease in cell frequency, or even both. To circumvent this issue and study the inflammatory stress response cascade of the BM HSPCs populations in an unbiased manner, I performed a time course single-cell RNA sequencing experiment which is specifically designed to be unbiased and to overcome the limitations associated with conventional marker-based FACS. Accordingly, BM cells were collected from four different mice for each IFNα treatment timepoint (in addition to four control mice injected with PBS control). Using oligo-tagged antibodies,

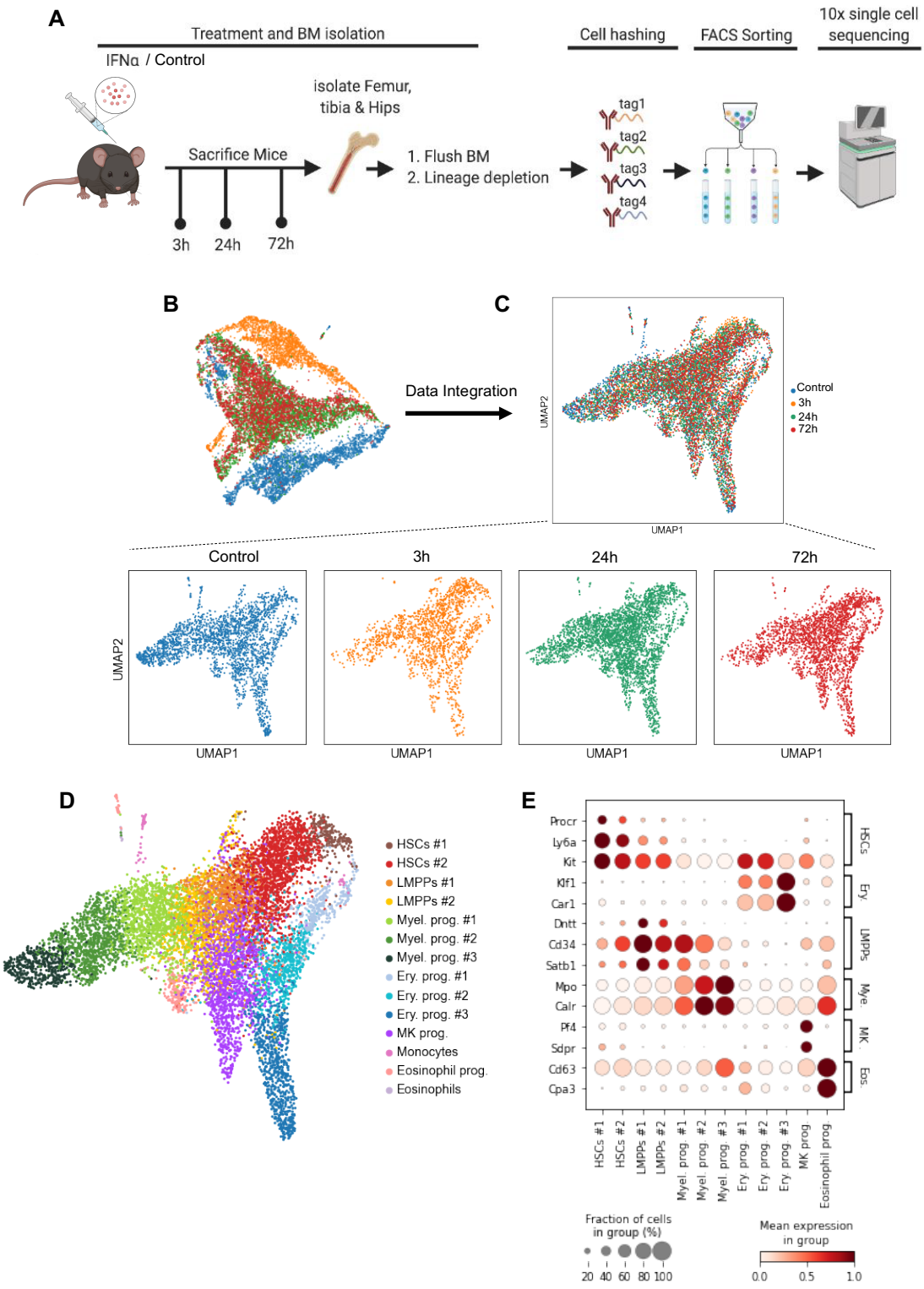

Figure 3.10: A single-cell time series RNAseq dataset to characterize the response of HSPCs to IFNα treatment.

(A) Scheme illustrating the experimental steps to acquire the single-cell time series RNA sequencing dataset. **(B-C)** UMAP plots of the 4 subsets before **(B)** and after integration **(C)** colored by subset. **(D)** Two-dimensional UMAP embedding of cells from all time points, colored for the different identified clusters as indicated in the legend. **(E)** Expression of marker genes in the different clusters in the control

dataset. Hematopoetic stem cells (HSCs); Erythroid (Ery.); LMPP (lymphoid primed multipotent progenitors); Myeloid (Mye.); Megakaryotic (MK.); Eosinophils (Eos.).

and so-called hashtags, I labeled the cells from each biological replicate and timepoint to address inter-animal heterogeneity of the inflammatory stress response. Following cell hashing, BM cells from mice of the same treatment were pooled together. BM cells were then sorted by using the broad lineage negative (Lin^-) and c-kit positive ($cKit^+$) (LK) gating strategy to capture a wide spectrum of the HSPCs transcriptional landscape independent of presumed changes in marker expression or cell frequencies. To guarantee sufficient numbers of HSCs for analysis, I additionally enriched the sorted populations with $LKSLAMCD34^-$ HSCs, since they are much less frequent than the other populations in the LK gate. The cells from all four experimental time points (control, 3h, 24h, and 72h) were sequenced simultaneously using the 10x Genomics platform (Figure 3.10A). For the data analysis, I collaborated with Brigitte Bouman from the division of computational methodologies and omic analytics in the Max-Delbrück-Centrum für Molekulare Medizin (MDC), Berlin. After filtering the datasets as described in the methods, the control, 3h, 24h, and 72h subsets contained 2472, 1661, 3462, and 2449 cells, respectively. Since we have single records with multiple conditions, we first executed each condition separately. By looking at the datasets before integration, we observe shifts in the perturbed system, with the 3h subset looking the most different (Figure 3.10B). In contrast, the 24h and 72h subsets look similar to each other (Figure 3.10B) in line with the bulk RNAseq analysis in results section 3.1.2 Next, we performed data integration to help us ensure that the same cell types cluster together and to identify if we have condition-specific clusters. The results show that no new cell states arise upon IFNα treatment as all cells of one subset align with the same cells of the other subsets (Figure 3.10C). Next, to determine the cell types present, we performed clustering analysis initially on the control subset, where we distinguished 14 clusters of cells. To get a more fine-grained understanding of the IFNα response, some cell types are subdivided into multiple clusters (e.g. HSCs #1 and #2) (Figure 3.10D). Cell clusters were annotated using known marker genes and by comparing our dataset to a previously published dataset (Nestorowa, Hamey, Sala, et al. 2016). HSCs are represented by genes such as *Procr (Epcr), Ly6a (Sca1),* and *kit* (Figure 3.10E). LMPPs share expression of *Procr (Epcr)* and *Ly6a (Sca1)* with HSCs but with lower

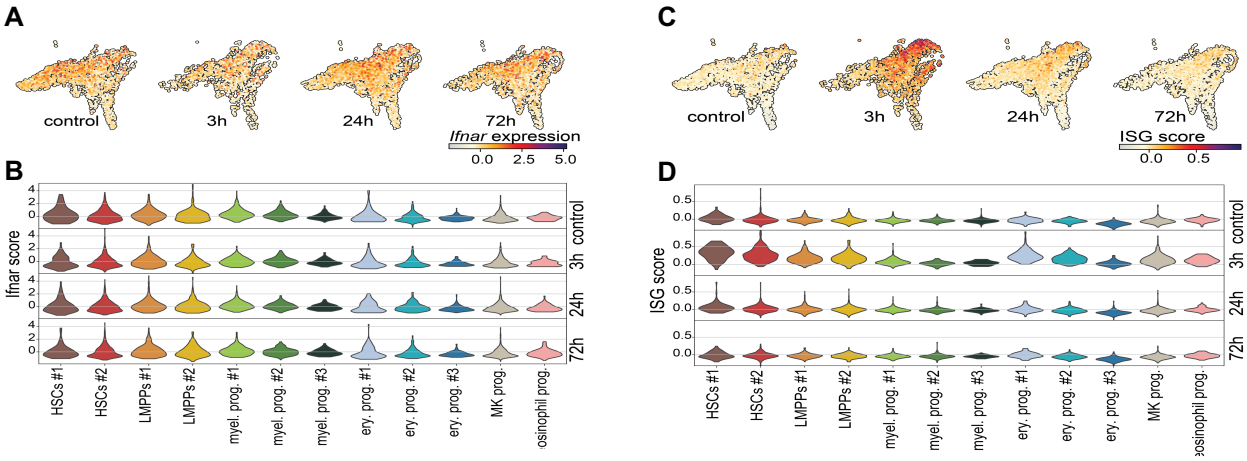

Figure 3.11: IFNα treatment induces heterogeneous ISG response in HSPCs.

(A-B) UMAP embedding **(A)**, and violin plot **(B)** of *Ifnar* expression in the four subsets (control, 3h, 24h, and 72h) **(C-D)** UMAP projection (**C**), and violin plot (**D**) of the ISG score in the different cell clusters in the four different time points. Figure is adapted from (Bouman, Demerdash et al. 2023).

expression and are differentiated by higher expression of *Cd34, Dntt,* and *Satb1*. Myeloid progenitors are characterized by the expression of genes such as *Mpo* and *Calr,* whereas erythroid progenitors were characterized by *Klf1* and *Car1* expression. Megakaryocytic progenitors were identified by having the highest expression of *Pf4* and *Sdpr*. Finally, Eosinophil progenitors were identified by the expression of *Cd63* and *Cpa3* (Figure 3.10E). The cell type labels in the control subset were transferred to the other three treatment time point subsets and marker gene expression confirmed the cell type labels in the response time points. The advantage of this approach is that it ensures that we can study the same cell type over time, as we avoid relabeling of the cells undergoing inflammation as separate populations. Hence, cell type identity is reliably retrieved, even though the conventional marker genes might be subject to changes, as is the case during inflammation.

Analysis of the hashtags confirms that the biological replicates in each timepoint had comparable abundances of each cell type label. To explore the effect of the IFNα treatment on a global scale, we checked the expression of the interferon α/β receptor (Figure 3.11A) to potentially highlight responsive single cell clusters. This result shows that all clusters express the receptor almost to the same extent and thus are able to directly respond to IFNα (Figure 3.11A,B). Next, we scored each cell for the expression of ISGs (Figure 3.11C). Similar to the bulk RNAseq analysis in results section 3.1.2 the

largest change in ISGs expression is seen in the 3h time point (Figure 3.11D). After 72h, the ISGs expression returned to the homeostatic state (Figure 3.11D). Interestingly, all clusters showed a change in ISGs expression at 3h, indicating that the whole HSPC compartment sensed an increase in IFNα. Despite this, the data indicate considerable heterogeneity in the ISGs response between the cell clusters, with HSCs showing the biggest change and more downstream progenitors displaying less change (Figure 3.11D).

3.2.3 Global and cell type-specific changes in gene expression define inflammation response

Next, we performed differential gene expression analysis to understand all genes that characterize the IFNα response comprehensively. DEGs were selected between the control subset and every treatment time point individually to get a set of response genes from any stage of the response. The sets of DEGs were independently found for each cell cluster in our dataset. The analysis identified a total of 2501 significant response genes. To investigate in which cluster(s) genes are changing the most, we scored the top 500 most significant response genes for the total expression change in each cluster. After calculating the total change for each cluster, the response genes were categorized into 14 different groups, using hierarchical clustering (Figure 3.12A). The different groups represent a wide variety of global (groups 1-5), and cluster-specific (groups 6-14) responding genes (Figure 3.12A). Response genes in groups 1-5 were universally altered, albeit not to the same extent, in all cell clusters. For example, response genes clustering in group 2 showed a global response, as the change score varied substantially upon IFNα treatment in all cell clusters (Figure 3.12A). Pathway enrichment analysis of the global inflammation signature from group 2 revealed an over-representation of terms associated with translation and ribosomal biogenesis (Figure 3.12B). The response genes in groups 1,3, and 4 also showed a global response response, but in that case was more specific to the progenitors as the stem cells were scored less for response genes in those groups (Figure 3.12A). Response genes from those groups were associated with metabolic processes involving oxidative phosphorylation, monosaccharide metabolic processes, and purine nucleoside biosynthetic processes (Figure 3.12C-E), consistent with the literature that HSPCs undergo massive changes in metabolism upon inflammatory stress (Karigane and Takubo et al. 2017).

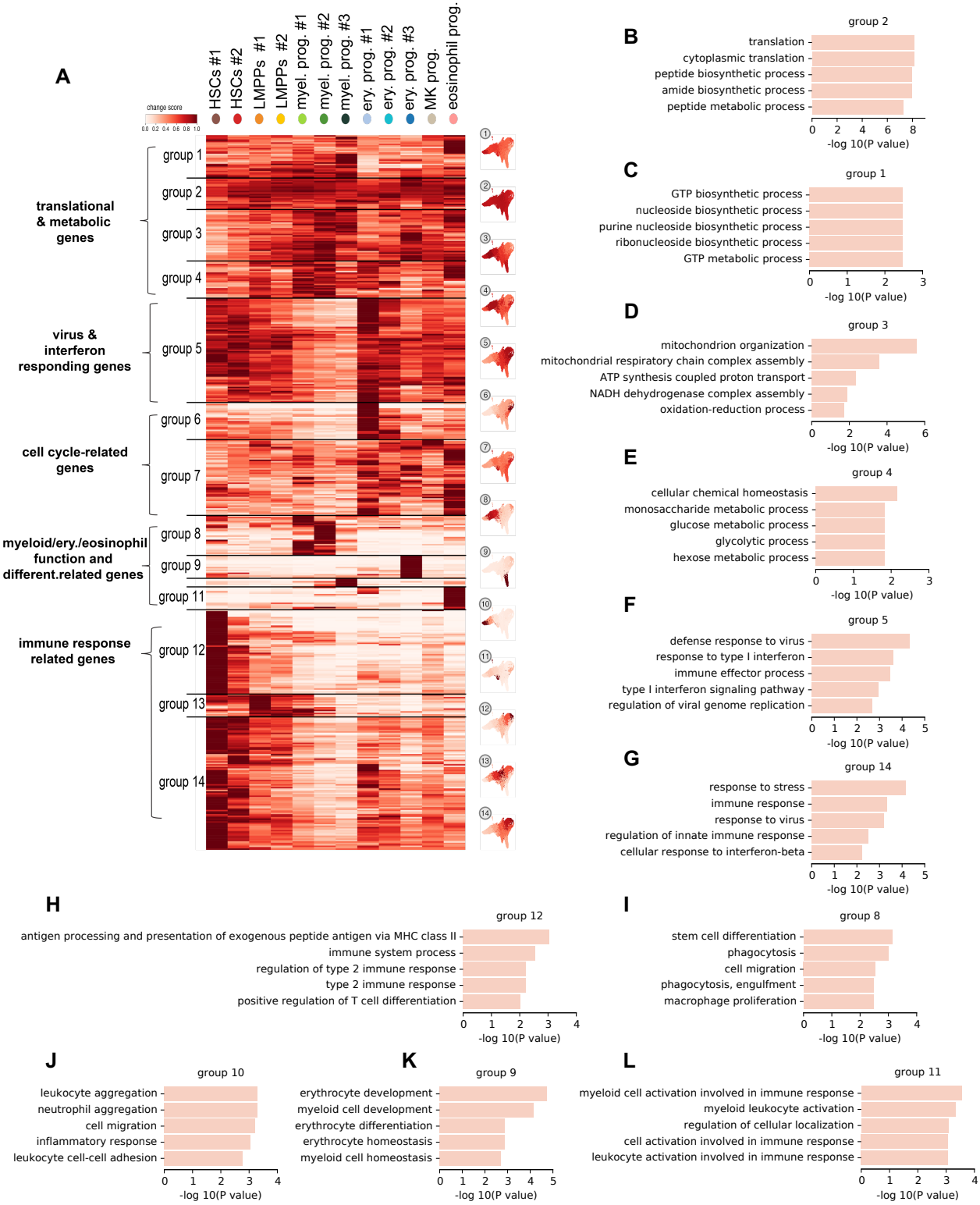

Figure 3.12 : Inter-cluster analysis of response genes shows both global and cluster-specific responding genes.

(A) Change score (see Methods) in each cluster for the top 500 response genes, grouped using hierarchical clustering. UMAPs on the right show the expression change for each cell cluster averaged over all response genes in the corresponding group. On the left are terms summarizing the functional

annotation of the response genes associated with the groups. **(B-L)** GO terms associated with group 2 (**B**), 1(**C**), 3(**D**),4(**E**), 5**(F)**, 14**(G)**, 12**(H)**,8**(I)**,10**(J)**,9**(K)**,11**(L)**. The length of each bar represents the statistical significance of each term. Figure is adapted from (Bouman, Demerdash et al. 2023).

DEGs belonging to group 5 showed a global response, but myeloid progenitors scored lower than the other progenitors in this group and HSCs scored highest (Figure 3.12A). Biological processes associated with immune response and response to type-I interferon were enriched in this group further supporting the ISGs expression data (Figure 3.12F), indicating that all cells sense the changes in IFNα levels. Interestingly, the expression changes in groups 12 and 14, which are enriched with HSCs, were also associated with immune response and response to type-I interferon (Figure 3.12G,H). However, these changes were distinct from those of the response genes in group 5. This indicates an HSC-specific immune response that differs from downstream progenitors. In addition, groups 12 and 14 included GO terms such as regulation of T cell activation and antigen processing and presentation (Figure 3.12G,H). These correspond to the recently identified role of HSCs as immunomodulators (Hernández-Malmierca et al. 2022), which further indicates that this response is specific to HSCs and not to progenitors. Therefore, our observations from the bulk HSCs data specifically in relation to antigen presentation and immune responses (Figure 3.5F) are HSC-specific and do not apply to progenitors.

Besides global and HSC-specific response genes related to immune response, change score analysis also identified groups of response genes enriched in committed progenitors and connected to progenitor-specific processes. For example, Change scores in groups 8 and 10 were largest for myeloid progenitors and connected with biological processes such as phagocytosis, myeloid leukocyte-mediated immunity, as well as stem cell differentiation, which are characteristic functions of this cell type (Figure 3.12I,J). Groups 9 and 11 showed erythroid and eosinophil progenitor-specific expression changes with an overrepresentation of processes related to erythrocyte differentiation terms and myeloid development (Figure 3.12K,L). Interestingly, HSCs had the highest score for the majority of the groups (Figure 3.12A) and showed a big change in the majority of response genes, confirming that HSCs are among the major responders in the HSPCs compartment. In summary, our analysis revealed both global and cell type-specific inflammatory signatures. We can conclude that although the

entire system responds to treatment, the identity of the response varies between cell groups, with HSCs exhibiting the greatest transcriptional changes.

3.2.4 Pseudotime analysis reveals a landscape of gene dynamics in HSPCs following IFNα treatment

In order to characterize the dynamics of gene expression during the IFNα response we wished to infer the trajectory of the response. However, current trajectory inference methods won't work because in our longitudinal dataset, both the response and recovery after a stimulus are covered. To perform such analysis our collaborators introduced a proximity-independent method to recover pseudotime. This novel approach transforms the discrete experimental time points into a continuous response pseudotime, which is optimally correlated with the actual time labels of the measurements. We then used this new response pseudotime approach to identify various temporal gene dynamics that follow IFNα treatment. Accordingly, we categorized the top 500 response genes into 16 patterns based on their expression dynamics in pseudotime, using hierarchical clustering (Figure 3.13A). Each pattern represents a group of genes with similar expression dynamics following IFNα injection. The patterns can be subdivided in upregulation (patterns 1-9 and 16) and downregulation (patterns 10-15). However, the patterns in both categories show a broad diversity in speed of response and recovery. The response genes in pattern 6 and 7 show a quick response and recovery, where the gene expression initially increases, but fully recovers to base-level expression within the response pseudotime margins (Figure 3.13A). These patterns represent a conventional response to IFNα, as can be seen by the number of ISGs that are assigned to this pattern (Figure 3.13B) and the GO analysis is enriched with processes related to response to virus, immune stimulus and regulation of type I interferon production (Figure 3.13B). Patterns 3 and 9 resemble patterns 6 and 7, however, the recovery to baseline is slower (Figure 3.13A). *Cox17, Pgk1, Ndufa1*, and *sec61g* are examples of genes in pattern 3 and GO analysis shows that this pattern is associated with metabolic processes, mainly carbohydrate biosynthetic processes (Figure 3.13C). Pattern 9 is enriched in genes such as *H2-T23, Gadd45g, Il18* and *Tap1* and the GO analysis shows enrichment of immune related processes such as T-cell differentiation involved in immune response (Figure 3.13D).

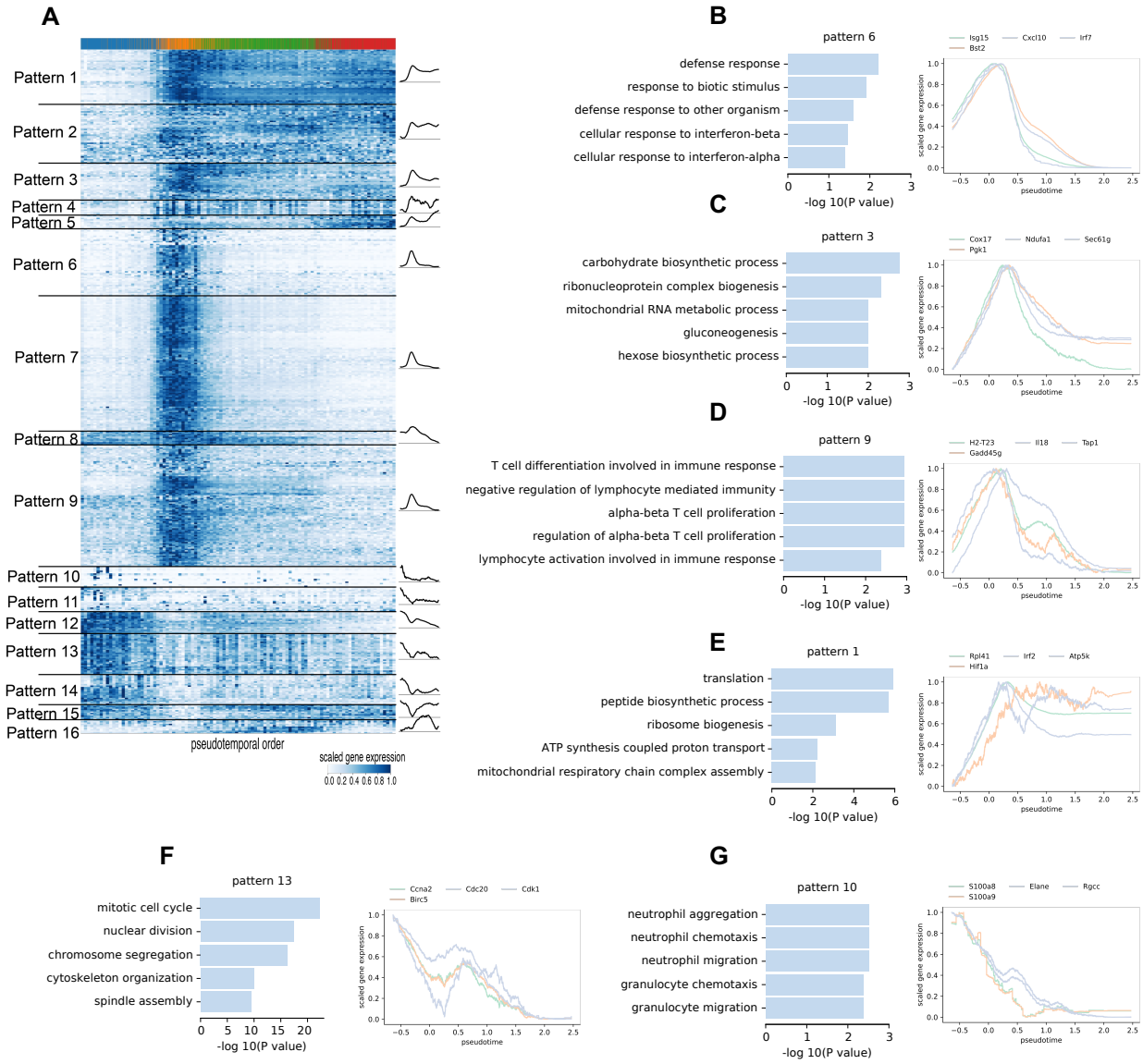

Figure 3.13: Response pseudotime reveals a landscape of gene dynamics in HSPCs following IFNα treatment.

(A) (smoothed) Expression of the top 500 response genes, with cells ordered by pseudotime and genes grouped by pattern using hierarchical clustering. A graphical representation of the mean pattern in each pattern group is shown on the right. (**B-G)** GO terms and example of gene expression in pseudotime associated with the indicated gene patterns 6(**B**), 3(**C**), 9(**D**), 1(**E**), 13**(F),** 10**(G).** The length of each bar represents the statistical significance of each term. Figure is adapted from (Bouman, Demerdash et al. 2023).

For other patterns such as pattern 16 their phase of upregulation takes longer (Figure 3.13A). Additionally, the heatmap showcases a variety of gene profiles with a sustained upregulation (pattern 1&2), which are associated with translation and other biosynthetic processes (Figure 3.13E). On the contrary we also identify genes that fail to recover to initial expression levels after downregulation (patterns 10-14). These patterns included genes linked to cell cycle such as *Ccne2, Cdc20,* and *Cdk1*, and other genes related to apoptosis such as *Birc5* (Figure 3.13F). Interestingly, the majority of these downregulated patterns included genes that were linked to myeloid cell activity such as *S100a8, S100a9, Rgcc* and *Elane* (Figure 3.13G). This would suggest that myeloid cell biology is impaired upon the IFNα treatment, an observation described for many other proinflammatory cytokines (Matatall et al. 2014; Pietras et al. 2016; Yamashita and Passegué 2019) but IFNα. Taken together, the IFNα responding genes show a variety of expression patterns, with different biological functions. Among the upregulated patterns are mainly those related to metabolic, translational, immune, and interferon processes. Conversely, downregulated patterns are related to myeloid function, cell cycle, and other processes that inhibit apoptosis.

3.2.5 Cluster-specific dynamics of response genes

Next, we wanted to understand the dynamic changes of the global and cluster-specific inflammation signature. Therefore, we combined the results on how response genes changed their expression (Figure 3.13A), whether these changes were global or cluster-specific (Figure 3.12A), as well as the biological functions these genes were linked to. Figure 3.14A shows response genes from the cell type specificity groups assigned to their pattern. Patterns 2 and 9, showing a fast increase combined with a slower (pattern 2) or fast (pattern 9) recovery, were the two most commonly found patterns among the groups, as 12 of the 14 groups had response genes associated with these patterns (Figure 3.14A). Genes from these patterns were mainly related to immune responses (Figure 3.13D), highlighting that the sensing and response to IFNα is fast and present in all groups and clusters. The majority of the global response genes from groups 1-4 are assigned to pattern 1, showing that the identified global biosynthetic activity (Figure 3.12B) enriched in ribosomal genes (e.g *Rpl35*, *Rps27*) is increased in HSPCs early in the treatment and remained active even in the recovering phase (Figure 3.14B).

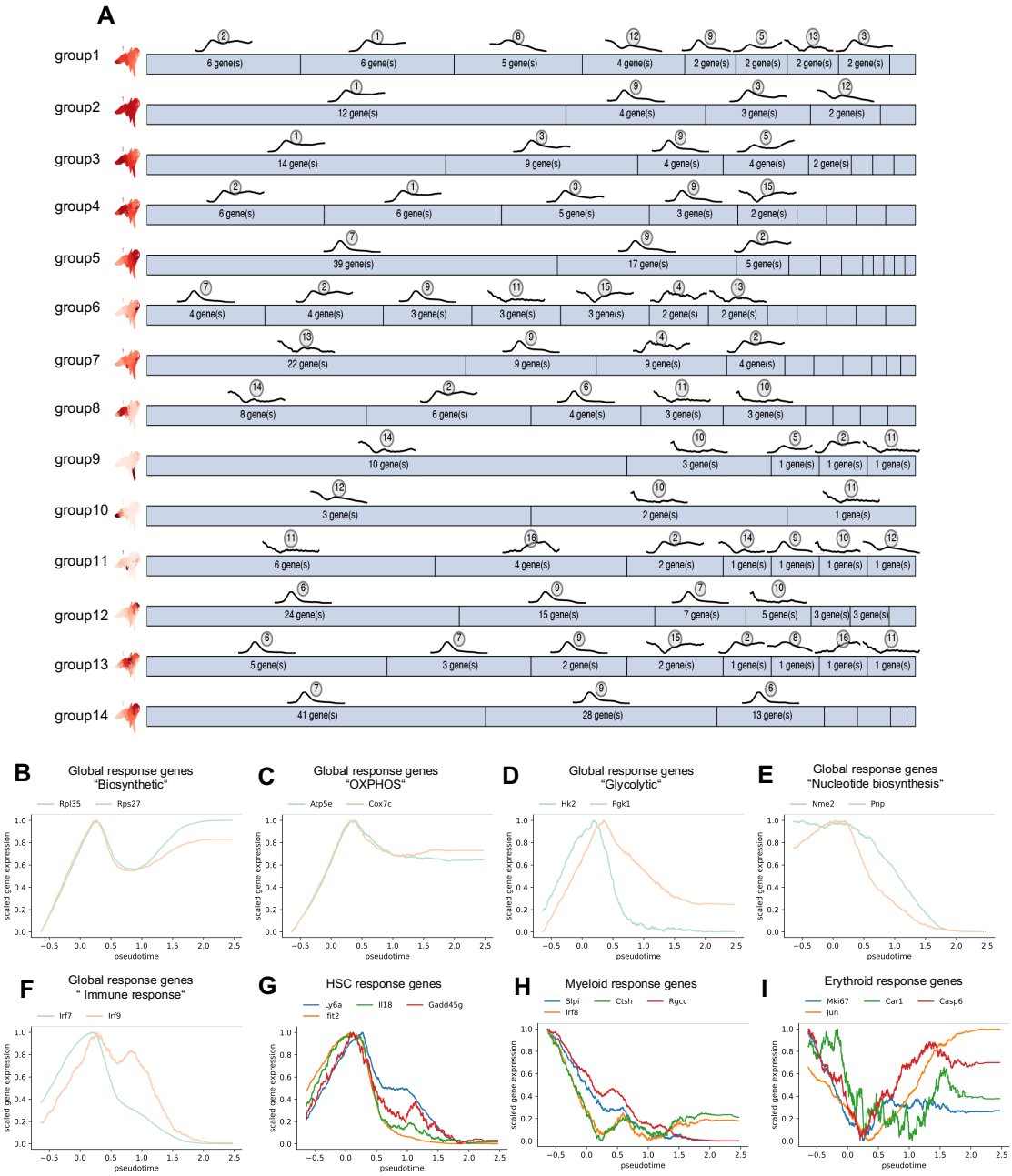

Figure 3.14: Dynamic Changes in Global and Cluster-Specific Inflammation Signatures in HSPCs Compartment.

(A) A breakdown of the response gene patterns in each change score group. Each bar represents the total amount of response genes within that pattern in the group and how abundant each pattern is within the total. **(B-F)** Examples of gene expression in pseudotime for translation (*Rpl35*, *Rps27*) (**B**), metabolism (*Atp5e*, *Cox7c*, *Hk2*, *Pgk1, Nme2, Pnp*) (**C-E**), and immune response (*Irf7*, *Irf9*) (**F**) specific genes **(G-I)** Pseudotemporal expression of HSC-specific genes (*Ifit2, Sca-1*) (**G**) and myeloid-specific genes (*Csf1r, Irf8*) (**H**) and erythroid specific genes (*Mki67, Car1, Casp6, Jun*) (**I**)**.** Figure is adapted from (Bouman, Demerdash et al. 2023).

Moreover, the metabolic signature observed for groups 1, 3, and 4 (Figure 3.12 C-E) is dynamically regulated. An increase in oxidative phosphorylation (OXPHOS) genes in HSPCs has been reported in inflammation (Suda, Takubo, and Semenza et al. 2011), which is also observed here, with a rapid (3h) and sustained increase in *Atp5e* and *Cox7c*, for example (Figure 3.14C). On the other hand, there is also a rapid response and recovery in glycolytic genes *Hk2* and *Pgk1* (Figure 3.14D). Overall, these data suggest that the transition from inactive to active HSPCs starts with an initial upregulation of glycolytic and a sustained upregulation of OXPHOS genes rather than a binary (on/off) switch between glycolysis and OXPHOS. Moreover, among the globally changing metabolic genes, we observe genes involved in nucleotide biosynthesis, e.g., *Pnp* and *Nme2*, following an initial upregulation followed by a sustained downregulation (Figure 3.14E).

In addition to the diversity of dynamics observed globally, there were also gene patterns enriched in specific clusters. For example, group 5 (global with the highest changes in HSCs) is mainly enriched with gene patterns that increase very early after treatment and also quickly return to homeostatic levels (such as *Irf7* and *Irf9*) (Figure 3.14F). Similar patterns are also found in HSC-specific groups 12 and 14 (for example *Ifit2*, *Sca-1, Il18*, *Gadd45g,* Figure 3.14G), showing that the HSC-specific response genes follow rapid interferon and immune response dynamics (patterns 6, 7, 9). Interestingly, the downregulated patterns [10-15] are mostly enriched with response genes from the myeloid (groups 8 and 10) and erythroid (groups 6 and 9) specific groups. Notably, myeloid-specific groups exhibited sustained downregulation (patterns 10,11,12 and 14) of response genes including *Slpi, Irf8, Ctsh,* and *Rgcc,* all associated with myeloid cell differentiation and functional programs (Figure 3.14H). Whereas, response genes associated with the erythroid progenitors have faster dynamics and recovery following pattern 15 and these include genes such as *Mki67, Casp6, Jun,* and *Car1* (Figure 3.14I). In conclusion, the behavior of cluster-specific signatures varies greatly. HSCs exhibit predominantly rapid upregulation dynamics, whereas downstream progenitors, especially those in the myeloid and erythroid lineages, mostly display downregulation of their response genes. The global signature, on the other hand, demonstrates sustained upregulation of biosynthetic activity and dynamic metabolic changes. These findings not only provide insight into gene dynamics during

inflammation induction in the HSPC compartment but also imply reduced myeloid differentiation in myeloid progenitor clusters.

3.2.6 Abundance analysis shows myeloid depletion and HSCs enrichment following IFNα treatment

Having understood the molecular properties of HSPC clusters after IFNα treatment, we next performed differential abundance analysis to investigate the possible effects of reduced transcriptional programs for myeloid differentiation and function on the size of the progenitor compartment. Thus far, it is not clear whether acute IFNα exposure affects the number/ abundance of HSPCs in the BM. In order to check this we used Milo package (Dann et al. 2022) which models cellular states as overlapping neighborhoods on a KNN graph rather than relying on clustering cells into discrete groups and thereby increasing the power and resolution of the differential abundance testing in a continuum system such as the hematopoietic system. At FDR 10%, we can observe multiple neighborhoods that are differentially abundant (Figure 3.15A). Each neighborhood was assigned to the cell type most commonly found within the neighborhood. The abundance of HSCs only slightly increased in HSCs #2 at 3h, but was back to normal at 72h (Figure 3.15B,C). Even though most progenitor-enriched clusters showed a reduction at 3h, the majority returned to normal by 24h or 72h (Figure 3.15B). Surprisingly, IFNα causes a strong reduction of the myeloid progenitors (Myel. prog. #3), which was not restored within 72h post-treatment (Figure 3.15 B,C). Thus, this unbiased (i.e., abundance analysis of cell types based on the expression of several genes rather than specific markers) single-cell investigation of the cell type frequency in the HSPC compartment showed that acute IFNα treatment resulted in a slight enrichment of HSCs at the early time point, but a sustained reduction in the most committed myeloid progenitors over the whole time course of the response (Figure 3.15B,C). This is consistent with our phenotypic analysis in section 3.2.1. However, this is in contrast to the widely held view that the decreased frequency of LS-K (consisting of myeloid, erythroid, and megakaryocytic progenitor cells) and the concomitant increase in LSKs (consisting of HSCs and LMPPs) after IFNα stimulation is mainly due to contaminated myeloid progenitor cells that have reacquired *Sca-1* expression (and would fall into the LSK gate) upon inflammation (Pietras et al. 2014; Kanayama et al. 2020).

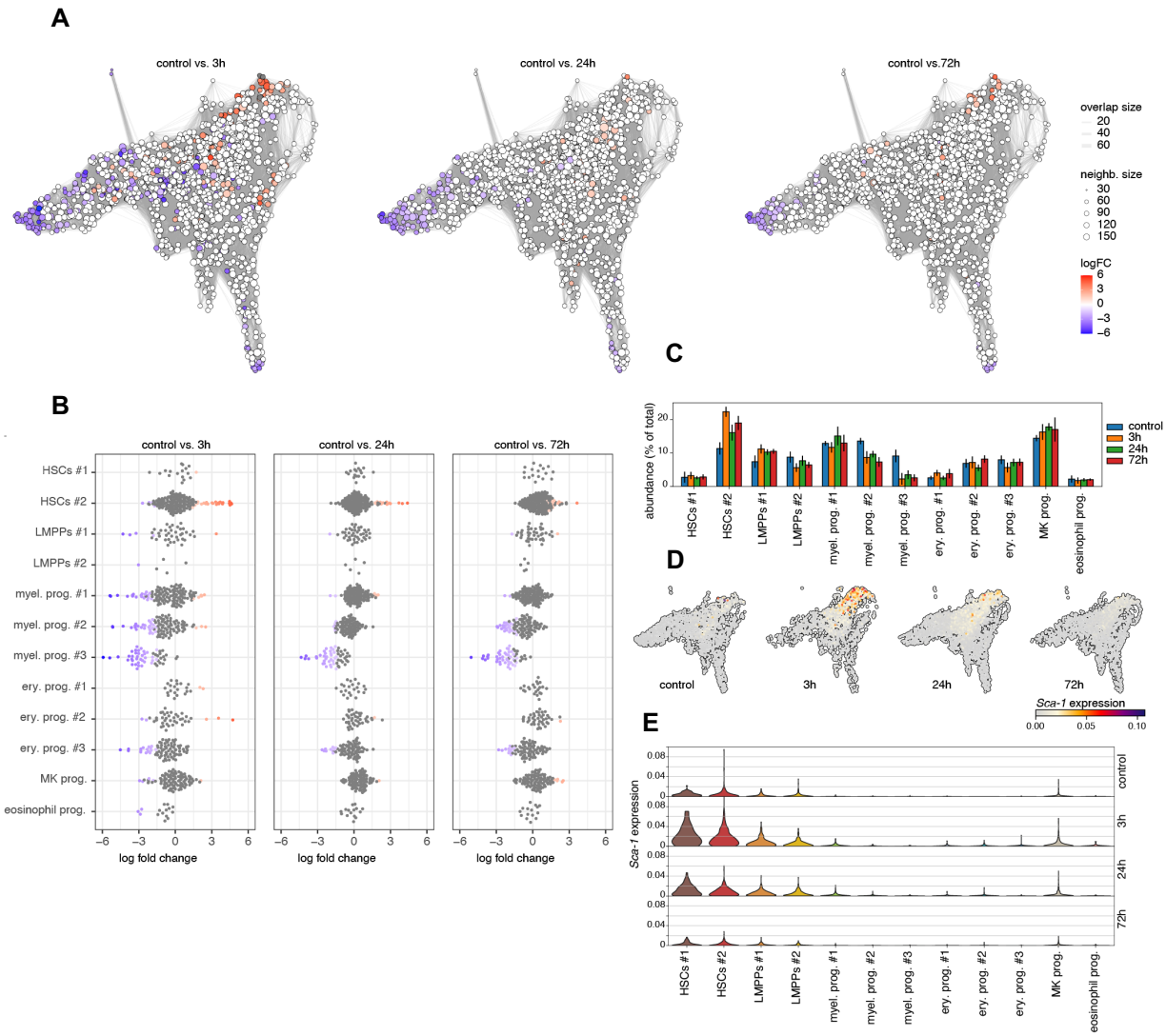

Figure 3.15: Abundance analysis reveals a sustained reduction in myeloid progenitors following IFNα treatment.

(A) Neighborhood graphs with the results from Milo differential abundance testing between the control dataset and post IFNα treatment subsets (3h, 24h, 72h). Nodes represent neighborhoods, coloured by their log fold change (red: more abundant, blue: less abundant, white: non-differentially abundant.) Graph edges represent the number of cells shared between two neighborhoods. **(B)** Beeswarm plot of the distribution of log fold changes in each cluster. Neighborhoods are assigned to clusters based on the most commonly found cluster label in the neighborhood. **(C),** Relative abundance of clusters in each time point. **(D-E)** UMAP embeddings **(D)** and violin plot **(E)** of *Sca-1* expression in the control, 3h, 24h, and 72h timepoints. Figure is adapted from (Bouman, Demerdash et al. 2023).

However, when analyzing *Sca-1* gene expression in our dataset, no change in *Sca-1* mRNA transcripts could be observed in myeloid progenitors (Figure 3.15D,E). In contrast, IFNα induced upregulation of *Sca-1* was solely observed in HSC and LMPP clusters, with the strongest increase in the HSCs (Figure 3.15D,E). Hence, this

unbiased investigation of the different clusters based solely on their gene expression identifies a true change in myeloid population size and not a shift in populations due to marker change.

3.2.7 Suppression of emergency myelopoiesis by IFNα treatment

Proinflammatory cytokine-triggered inflammatory signals tightly regulate myelopoiesis in the BM, but there is currently no clear evidence of IFNα's contribution to emergency myelopoiesis. As defined by Manz et al.,(Manz and Boettcher 2014) emergency myelopoiesis is a term that describes the activation of hematopoietic progenitors in the BM, resulting in their enhanced proliferation and differentiation and, thereby the increased de novo production of neutrophils in response to stress. Our findings reveal a decrease in myeloid progenitor abundance (Figure 3.15B,C) and a decrease in myeloid differentiation genes (Figure 3.14H) in these progenitors. To explore this further, I examined the expression patterns of *Cebpb*, *Spi1*, and *Stat3*, which are known to regulate emergency myelopoiesis. I identified *Cebpb* as one of the differentially expressed genes associated with pattern 8, showing an initial up-regulation followed by a sustained downregulation (Figure 3.16A). Notably, HSC, LMPPs, and Myeloid progenitors 1&2 showed an initial increase in *Cebpb* followed by downregulation (Figure 3.16E,F,H,I) whereas Myeloid progenitors 3 showed sustained downregulation (Figure 3.16G). *Stat3*, shows an initial decrease in expression that normalizes back to normal (Figure 3.16B), whereas, *Spi1* which is the main myeloid transcription factor, shows a sustained decrease in expression (Figure 3.16C). To test whether other members of the CCAAT-enhancer–binding protein (C/EBP) play a role in the IFNα response, I checked the expression of *Cebpa* and *Cebpe* which shows a sustained downregulation (Figure 3.16D). To assess the impact of these transcriptional changes on the mature myeloid compartment, I analyzed mature myeloid cells in the blood. The results indicate a continuous decrease in neutrophils over time (Figure 3.16J), in contrast to monocytes, whose numbers initially decreased and then normalized (Figure 3.16K). In conclusion, our findings suggest that IFNα treatment can suppress emergency myelopoiesis by downregulating critical transcription factors and myeloid differentiation genes, resulting in decreased myeloid progenitor abundance and impaired de novo production of neutrophils.

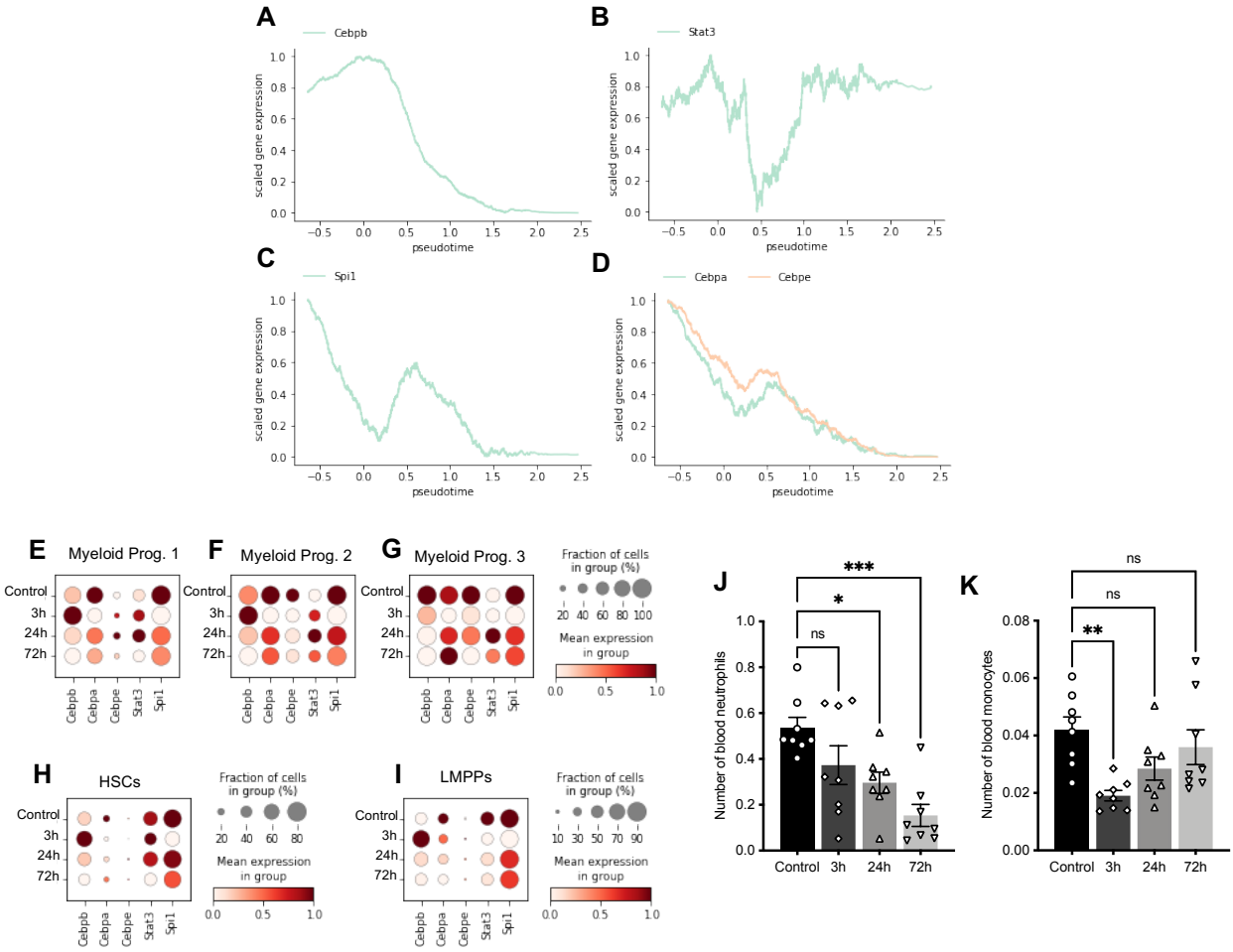

Figure 3.16: IFNα treatment suppresses emergency myelopoiesis.

(A-D) Gene expression in pseudotime for important players in emegancy myelopoesis, *Cebpb* **(A)**, *Stat3* **(B),** *Spi1* (**C**), *Cebpe*, and *Cebpa* **(D). (E-I)** Heatmap showing the expression of the same genes in myeloid progenitor #1 **(E)**, myeloid progenitor #2 **(F)**, myeloid progenitor #3 **(G)**, HSCs **(H)**, LMPPs **(I)** in the four experimental subsets. **(J-K)** Flow cytometric analysis of blood neutrophils ($B220^-$ $CD4^-$ $CD8^-$ $Ly6G^+$ $CD11b^+$) **(J)** and monocytes ($B220^-$ $CD4^-$ $CD8^-$ $Ly6G^-$ $CD11b^+$ $CD11c^-$ $F4/80^-$) **(K)** normalized to the whole blood leukocyte count as measured by hemavet at 3h, 24h, and 72h injection of IFNα or control (PBS) treatment in WT mice. n= 8 biological replicates. Statistical significance in **J,K** was determined by an ordinary one-way ANOVA using Holm-Šídák's multiple comparisons test and at least 2 independent experiments were performed; ns; non significant, *P≤0.05, **P≤ 0.01, ***P≤ 0.001,. Data represent mean ± standard error of the mean (SEM).

3.2.8 Mechanisms underlying the sustained depletion of myeloid progenitors following IFNα treatment

The reduction in the abundance of myeloid progenitor cells could be explained by reduced differentiation towards myeloid progenitor cells, loss of these cells by cell

death, or increased egress of these cells from the BM. However, myeloid progenitors were not observed in the blood following IFNα treatment (data not shown). Moreover, the number of myeloid progenitors in the spleen decreases at 24h, in line with the reduction in the BM (Figure 3.17A). This suggests that the reduced abundance of the myeloid progenitors in the BM is not due to increased egress into the blood or spleen but rather there is a total reduction of myeloid progenitors both in the BM and the periphery.

To investigate whether reduced levels of myeloid progenitors were the result of increased cell death we analyzed gene patterns of pro-survival genes (*Bcl2, Birc2*, and *Birc5*) and found an initial decrease in expression following IFNα treatment (Figure 3.17B). However, in *Bax*$^{-/-}$*Bak*$^{-/-}$ double-knockout mice, in which cells are unable to undergo apoptosis, a similar reduction of myeloid progenitors was observed as in WT mice (Figure 3.17C), indicating that apoptosis was not the reason for the reduction in myeloid progenitors. This experiment does not exclude the involvement of other forms of cell death, like necroptosis and pyroptosis. Although we do not see an increase in necroptosis genes in the myeloid progenitors (Figure 3.17D), the pyroptosis signature suggests an early increase of pyroptosis in response to the treatment (Figure 3.17D,E). To investigate whether insufficient production of new cells could explain the sustained depletion of myeloid progenitors we focused on genes involved in myeloid lineage priming. By calculating a gene score for known myeloid transcription factors that have been reported to impact both stem and progenitor cells. This analysis has revealed that myeloid priming is downregulated along the stem cell differentiation axis in HSCs (Figure 3.17F). Moreover, it was observed that the more differentiated LMPPs also exhibited downregulation of myeloid priming (Figure 3.17G). In addition, a reduction in cell cycle and purine nucleotide synthesis genes was observed in the myeloid progenitors (Figure 3.17H,I), suggesting that both myeloid differentiation in the HSCs and LMPPs and cell production in the myeloid progenitors are affected. Furthermore, the transcriptional signatures of neutrophils and monocytes were found to be downregulated in myeloid progenitors over the pseudotime axis (neutrophil: myel. prog. #1; monocyte: myel. prog. #3) (Figure 3.17J,K), suggesting reduced differentiation of myeloid progenitors into mature myeloid cells.

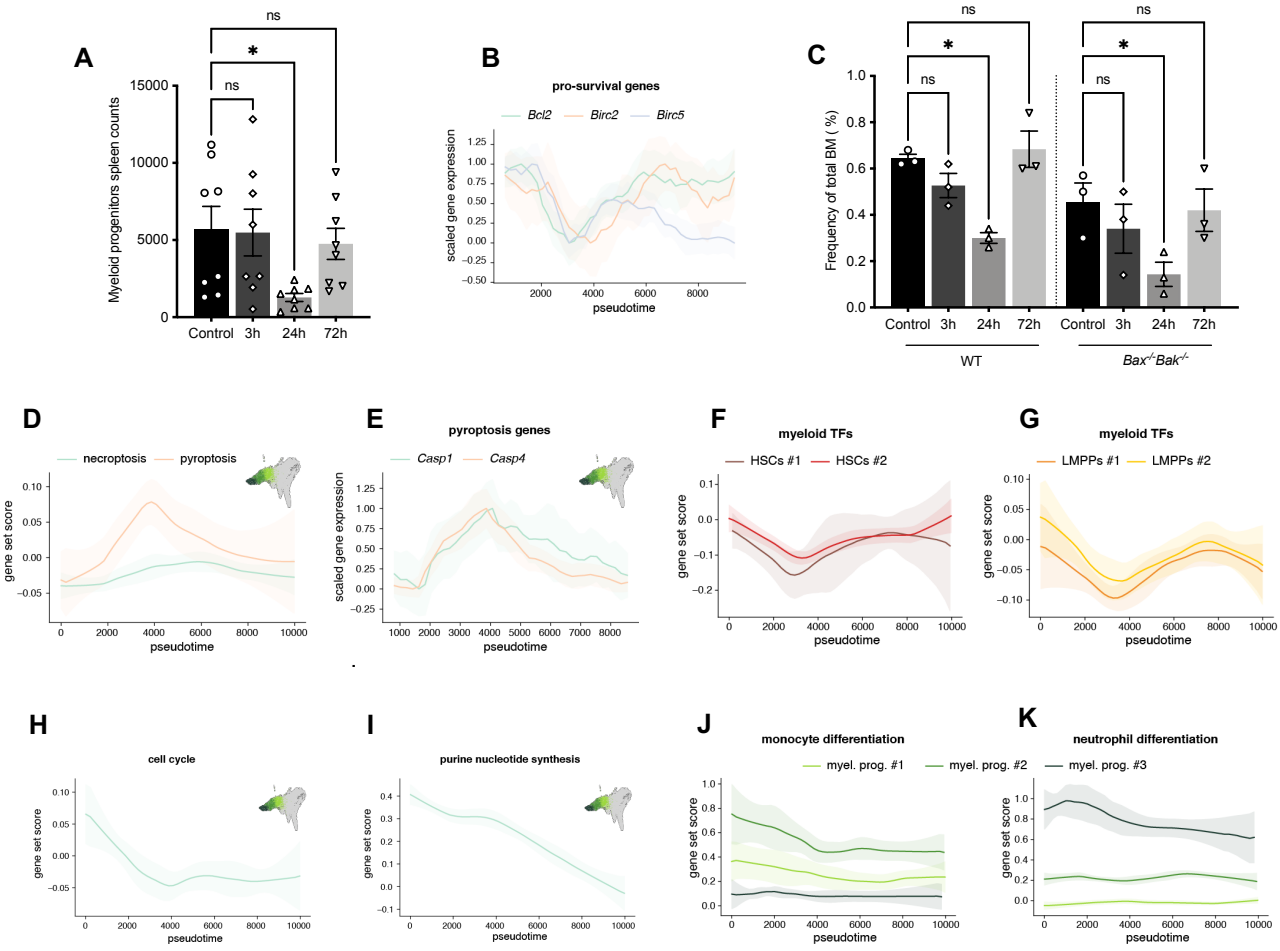

Figure 3.17: Reduced myeloid differentiation bias and increased cell death signature partially explain myeloid population's reduction upon IFNα treatment.

(A) Flow cytometric analysis of frequency of myeloid progenitors (Lin^- $Sca\text{-}1^-$ $cKit^+$ $CD34^+$ $CD16/32^+$) in WT mice at 3h, 24h and 72h following IFNα or control (PBS) treatment in spleen. n= 8 biological replicates. **(B)** Pseudotemporal expression of pro-survival genes (*Bcl2, Birc2, Birc5*). **(C)** Flow cytometric analysis of BM frequency of myeloid progenitors (Lin^- $Sca\text{-}1^-$ $cKit^+$ $CD34^+$ $CD16/32^+$) following IFNα treatment in WT and $Bax^{-/-}Bak^{-/-}$ double knockout mice at 3h, 24h, and 72h following IFNα or control (PBS) treatment. n= 3 biological replicates. **(D)** Score of necroptosis gene signature and pyroptosis gene signature in all myeloid progenitors plotted in pseudotime. **(E)** Pseudotemporal expression of two pyroptosis genes (*Casp1, Casp4*) in all myeloid progenitors **(F-G)** Score of (murine) myeloid transcription factors in HSCs **(F)**, and LMPPs **(G)** plotted in pseudotime. **(H-I)** Score of cell cycle **(H)** and purine nucleotide synthesis **(I)** genes in all three myeloid progenitor clusters plotted in pseudotime. **(J-K)** Score of monocyte **(J)** and neutrophil **(K)** differentiation genes in all three myeloid progenitor clusters plotted in pseudotime. Statistical significance for **A** and **C** was determined by an ordinary one-way ANOVA using Holm-Šídák's multiple comparisons test. At least 2 independent experiments were performed; ns; non significant *P≤0.05,. Data represent mean ± standard error of the mean (SEM). Figure is adapted from (Bouman, Demerdash et al. 2023).

This is consistent with the observed decrease in neutrophils in the blood (Figure 3.16J). Taken together, these *in vivo* cell analyses and gene expression data indicate reduced myeloid differentiation both at the stem cell level as well as in committed progenitors, combined with an increase in pyroptosis signature and a reduction in the cell production machinery. As a result, there are fewer myeloid progenitors in the BM and a lower level of mature myeloid cells in the blood.

3.3 Dissect the interplay of proinflammatory cytokines in the acute response of HSCs to stress

Type I interferons are not the only proinflammatory cytokines involved in the proliferative response of HSCs to inflammatory stress. HSCs have been shown to respond to bacterial and viral components via toll-like receptors (TLRs) and cytokine receptors (King and Goodell et al. 2011). In addition, studies show that HSCs are activated by other proinflammatory cytokines such as interleukin 6 (IL6) and tumor necrosis factor alpha (TNFα) and interleukin 1 (IL1) (Caiado, Pietras, and Manz et al. 2021). Thus, it appears that multiple pathways play an important role in activating HSCs triggered by inflammatory stress. Both direct and indirect mechanisms of HSCs activation have been proposed. Still, it remains unclear to what extent the various proinflammatory cytokines interact and overlap in their effects on HSCs quiescence.

3.3.1 Investigating the dynamics of HSCs responses to proinflammatory cytokines

Infections and general inflammatory settings produce not only one proinflammatory cytokine but rather a cascade of proinflammatory cytokines. The exit from the G0 phase and initiation of HSCs proliferation are common effects of different proinflammatory cytokines (Caiado, Pietras, and Manz et al. 2021). However, it is unknown whether these different agonists are equivalent in their mechanism of HSCs activation or in the response they provoke. Among the most commonly studied are IFNα, IFNγ, TNFα, and IL1β. In the previous section, I thoroughly investigated the molecular changes after IFNα treatment. In this section, I created comparative datasets to compare gene expression in HSCs treated with different proinflammatory cytokines. First, I analyzed the dynamics of HSCs responses to acute treatment with different proinflammatory cytokines to determine the timing of the initial signs of response in HSCs. To this end, I performed an acute time-course experiment to track phenotypic and cell cycle changes in HSCs after treatment with IFNγ, IL1α, IL1β, IL6, TNFα, LPS, and pIC at 3, 9, and 12h, which I compared to previously performed experiments of the HSCs response upon treatment with IFNα and pIC. The treatment of HSCs with pIC and LPS, which mimic viral and bacterial infection, was shown to cause the upregulation of the expression of different proinflammatory cytokines and was therefore, included in these experiments.

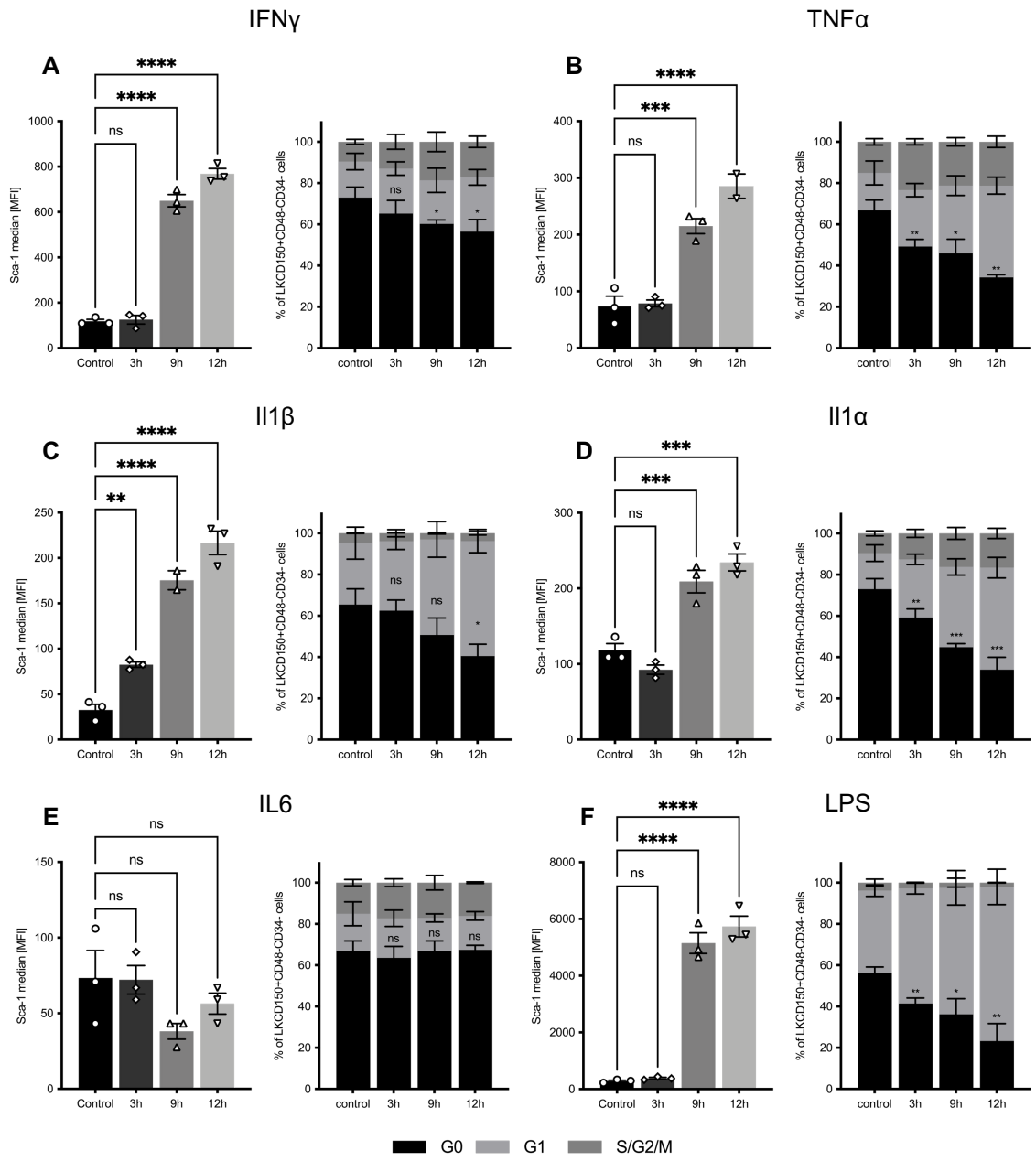

Figure 3.18: Response of HSCs to time course treatments with different proinflammatory cytokines.

(A-F) Cell cycle analysis of using Ki67 and Hoechst 33342 to detect HSCs (Lin^- $Sca1^+$ $cKit^+$ $CD150^+$ $CD48^-$ $CD34^-$) in G_0 ($Ki67^{neg}Hoechst^{low}$), G_1 ($Ki67^{High}Hoechst^{low}$) and SG_2M ($Ki67^{High}$ $Hoechst^{high}$) and quantification of cell cycle distribution and Sca-1 expression (calculated based on median fluorescence intensity) of HSCs treated with PBS control or 3h, 9h or 12h with IFNγ (**A),** TNFα (**B**)**,** IL1β (**C),** IL1α (**D**), IL6 (**E),** LPS **(F)**. Error bars indicate the standard error of the mean of HSCs in the G0 phase and expressing Sca-1 when compared to PBS controls. Statistical significance was determined by an ordinary one-way ANOVA using Holm-Šídák's multiple comparisons test. At least 2 independent experiments were performed; ns; non-significant, *P≤0.05, **p<0.01 ***P≤ 0.001, ****P<0.0001, Data represent mean ± standard error of the mean (SEM).

Mice were sacrificed at these time points, and the BM was isolated. The increases in Sca-1 expression and the distribution of HSCs in the different cell cycle stages by flow cytometry were analyzed to quantify HSCs response following proinflammatory cytokine treatment. For IFNγ treatment, the cells in the G0 phase decreased gradually with increasing treatment duration, although only significant at 9h of treatment. The Sca-1 upregulation showed a similar trend of increase (Figure 3.18A). In samples treated with TNFα (Figure 3.18B), the decrease in cells in the G0 phase was significant at all measured time points; However, Sca-1 expression was significantly upregulated only after 9h and 12h of treatment (Figure 3.18B). For IL1β treatment, the cells in the G0 phase decreased gradually with increasing treatment duration, although only significant at 12h of treatment (Figure 3.18C). In contrast, the constant upregulation of Sca-1 expression was already significant at 3h of treatment (Figure 3.18C). IL1α and LPS treatments showed a comparable decrease in cells in the G0 phase and an increase in Sca-1 expression following treatment with TNFα (Figure 3.18D,F respectively).

In contrast to the other samples, cells treated with IL6 did not exhibit the same pattern of cell cycle distribution and Sca-1 expression (Figure 3.18E). Compared with the PBS control sample, there was no significant difference in the number of cells in the G0 phase or Sca-1 expression at any of the tested treatment durations (Figure 3.18E). Despite being initially described as an IFN-stimulated gene, I was able to demonstrate that Sca-1 expression also increased when exposed to other cytokines, confirming previous work from our group (Demel et al. 2022). In summary, the results confirmed the inflammatory response of HSCs to various inflammatory cytokines, except for IL6, and that HSCs responded to cytokine treatments immediately after 3h; however, the responses were not significant for all cytokine treatments. These results fit to the observations I made in previous experiments with the treatment of HSCs for 3h with IFNα and pIC.

To analyze the HSCs response to proinflammatory cytokines using microarray analysis in the next section, I aimed to capture the time point when the inflammatory response first induces HSC proliferation, minimizing indirect effects. As multiple cells in the BM may respond to these cytokines, later time points could reflect a combination of direct

HSCs response and indirect signaling from other BM cells. Therefore, I chose to conduct the microarray analysis after a 3h treatment.

3.3.2 Investigating proinflammatory cytokines' early effects on HSC gene expression using microarray

To gain a deeper understanding of the molecular mechanisms underlying the phenotypic changes I observed in HSCs after acute treatment with proinflammatory cytokines, I treated WT mice with the various proinflammatory cytokines for 3h and collected RNA from HSCs (Lin^- $ckit^+$ $CD150^+$ $CD48^-$ $CD34^-$) for microarray analysis (Figure 3.19A). RNA samples were submitted to the genomics and proteomics core facility at the DKFZ, and global gene expression was measured using Affy Clariom S mouse chip. Differential gene expression of each treatment compared to the PBS controls was performed. To explain the relationships between the gene sets, an upset plot visualizing the number and overlap of DEGs ($p < 0.05$ and log FC <0.5, <-0.5) was created (Figure 3.19B-E). Among the gene sets, IL1β and IFNα showed the highest responses with 779 and 772 DEGs (Figure 3.19B), respectively. Similar numbers of DEGs were observed for the other treatments (288-211 DEGs), whereas IL6 exhibited the weakest response with 92 DEGs (Figure 3.19B). Together with the FACS analysis, these data indicated no strong response of the HSCs to the treatment with IL6. The numbers of unique genes identified for IL1β, IFNα, LPS, TNFα, IL1α, pIC, IFNγ, and IL6, were 477, 424, 97, 72, 64, 111, 82, and 53, respectively (Figure 3.19B). This shows that IFNα has the highest number of unique DEGs (62%) and IL1α has the lowest number of unique DEGs (28%); most of the DEGs for IL1α overlapped with other DEG responses, particularly IL1β (Figure 3.19B). By analyzing the set interactions, I found that with 66 genes (43 upregulated and 24 downregulated DEGs), the intersection between TNFα and IL1β cytokines had the largest overlap, followed by that between IFNα and IFNγ with 43 genes (39 upregulated and 6 downregulated DEGs) (Figure 3.19C,D, respectively). Some DEGs were unique to LPS (33%) and pIC (50%); however, many were shared with other cytokines (Figue 3.19B). In line with our recent study, I found a strong overlap in transcriptional responses between LPS and IFNα (Demel et al. 2022). In addition, I demonstrate that LPS shares transcriptional similarities with IL1α, IL1β, and TNFα (Figure 3.19B). Although pIC and IFNα treatments are often used redundantly in hematopoietic research (Essers et al. 2009)

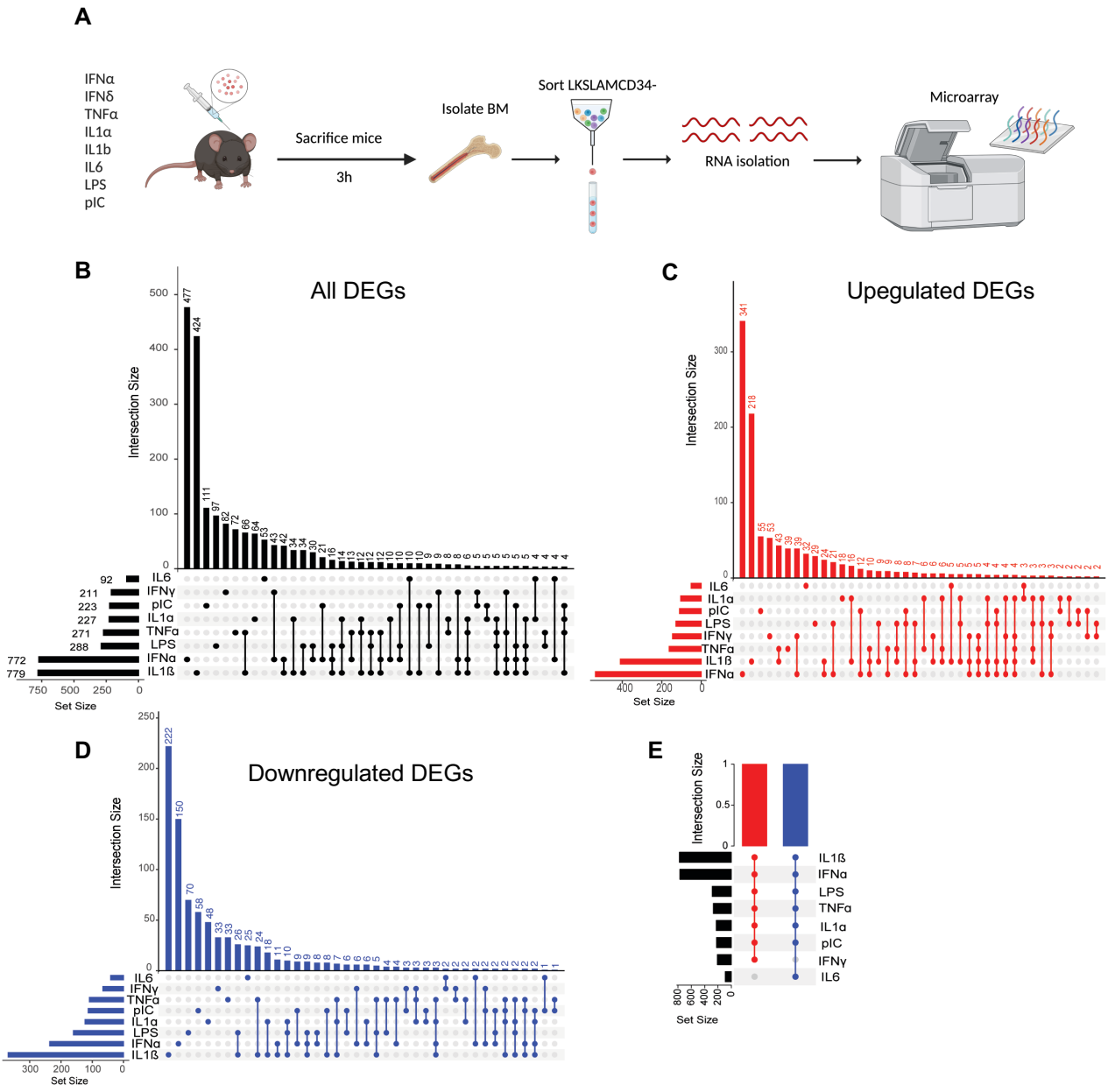

Figure 3.19: Microarray comparative analysis of HSC's response to various proinflammatory cytokines.

(A) Scheme for microarray experimental procedure. Mice were treated with the indicated proinflammatory cytokine and sacrificed after 3h. 3-4 biological replicates were used per condition. Bones (tibia, femur and hips) were isolated, cleaned and then crushed. Cells were then stained with markers for HSCs (Lin^- $cKit^+$ $CD150^+$ $CD48^-$ $CD34^-$) and sorted. RNA was isolated from sorted cells and libraries were prepared for microarray analysis. **(B-D)** UpSet plot showing relationships of all differentially expressed genes (DEGs) **(B)**, upregulated DEGs **(C)**, and downregulated DEGs **(D)** of the different proinflammatory cytokines datasets. **(E)** UpSet plot showing the intersection between at least seven of the datasets. Bars colored in black, red and blue show all, upregulated and downregulated DEGs respectively. The horizontal bars represent the datasets. The vertical bars represent the intersection of datasets. The length of the vertical bar indicates the number of items shared by the

datasets. The numbers above the vertical bars represent the size of the intersection. Dark circles in the matrix indicate sets that are part of the intersection.

only 10% (21 genes) of pIC DEGs were upregulated following IFNα treatment (Figure 3.19B), implying that HSCs respond differently to these treatments at the transcriptional level. Because many gene sets had an intersection of one gene, it was impossible to view all of them in a single plot. A plot showing the intersection between at least 7 datasets is presented in Figure 3.19E. I did not identify a common set among the 8 different cytokines. However, one gene (*serpina3g*) was upregulated, and one gene (*Tmem121*) was downregulated for seven different treatments (Figure 3.19E). *Serpina3g* was common between IL1β, IFNα, LPS, TNFα, IL1α, pIC, and IFNγ, and this gene plays a very important role in the T-Cell immunity (Ashton-Rickardt et al. 2012), going in line with the immunomodulatory function of HSCs. Whereas *Tmem121* gene had no role reported in hematopoesis. In summary the results showed unique and overlapping gene expression patterns among the different cytokines.

3.3.3 Analysis of gene ontology categories in proinflammatory cytokine treatments

Next, I investigated whether I could identify common processes after treatment with the different proinflammatory cytokines. Enriched gene ontology categories were analyzed separately for upregulated and downregulated genes (Figure 3.20). The top biological pathways for each cytokine are based on the significance of the enrichment pvalueCutoff = 0.5. Pathways pertaining to T-cell immune responses were significantly upregulated in all proinflammatory cytokine treatments (Figure 3.20A-G). In contrast, myeloid differentiation signaling pathways were significantly overrepresented only following TNFα, IL1β, IL1α, and IL6 treatments (Figure 3.20B-E, respectively). IFN signaling pathways were among the top biological processes for both LPS and pIC (Figure 3.20F,G, respectively). There was also a significant underrepresentation of metabolic processes. Similar to IFNα, lipid metabolic pathways were downregulated for TNFα, IL6, and pIC (Figure 3.20I,L,N, respectively). For both IL1β and LPS, the most significantly downregulated categories were those related to iron ion, sulfate, and glutathione metabolic processes (Figure 3.20J,M, respectively). Processes related to cell cycle and DNA replication were downregulated after treatment with IL1α and IL6 (Figure 3.20K,L, respectively).

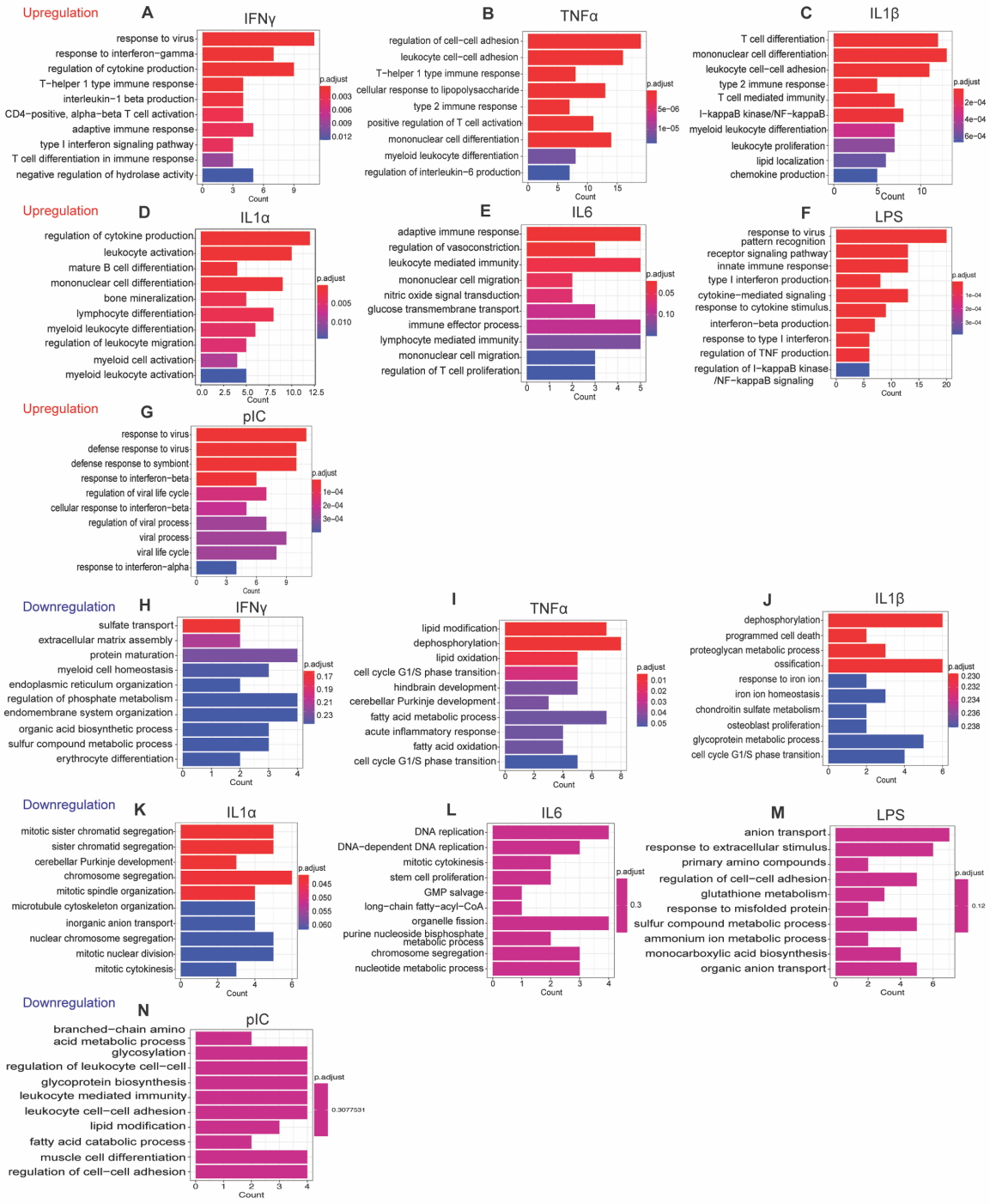

Figure 3.20: Enriched gene ontology (GO) categories following treatment with proinflammatory cytokines.

(A-G) Bar plots showing enriched GO terms of upregulated genes following treatment with IFNγ **(A),** TNFα (**B**), IL1β (**C),** IL1α (D), IL6 **(E),** LPS **(F)**, pIC **(G)**. **(H-N)** Bar plots showing enriched GO terms of downregulated genes following treatment with IFNγ **(H),** TNFα (**I**), IL1β (**J),** IL1α (**K**), IL6 (**L),** LPS **(M)**, pIC **(N)**. Number of genes is represented on the x-axis with adjusted significance ($P < 0.5$) indicated by order and colour trend.

Our results revealed significant alterations in multiple pathways associated with inflammation and cell cycle regulation. Despite similarities in the processes, it is noteworthy that distinct genes were up or downregulated for each cytokine, which is linked to the same biological processes, suggesting differences in the mechanism leading to the same biological outcome. These findings provide insight into the molecular mechanisms underlying the response of HSCs to proinflammatory cytokines.

3.3.4 Examination of the myeloid priming in HSCs following treatment with the different proinflammatory cytokines

Inflammatory signals triggered by proinflammatory cytokines during emergency myelopoiesis have been shown to tightly regulate myeloid cell production in the BM (Chiba et al. 2018). Thus, I investigated whether myeloid priming is affected in HSCs. Positive enrichment of HSCs with myeloid signature was observed following all proinflammatory cytokine treatments (Figure 3.21A-G). However, IFNγ and LPS had lower NES values than the other treatments (Figure 3.21A,F, respectively). IFNα, on the other hand, had the lowest NES value (Figure 3.21H). Compared with the bulk RNA sequencing data in section 3.1.5 which showed that HSCs, 24h after IFNα treatment exhibited a significant downregulation of myeloid gene expression signature, and this effect persisted up to 72h, suggesting that HSCs are less targeted to myeloid cells by IFNα treatment. Interestingly, the positive enrichment of the myeloid signature of HSCs was accompanied by downregulation of the lymphoid signature for all cytokine treatments except IFNγ, pIC, and IL6 (Figure 3.21I). In summary, these results provide new insights into the impact of proinflammatory cytokines on myelopoiesis in HSCs and highlight the complex regulation of this process.

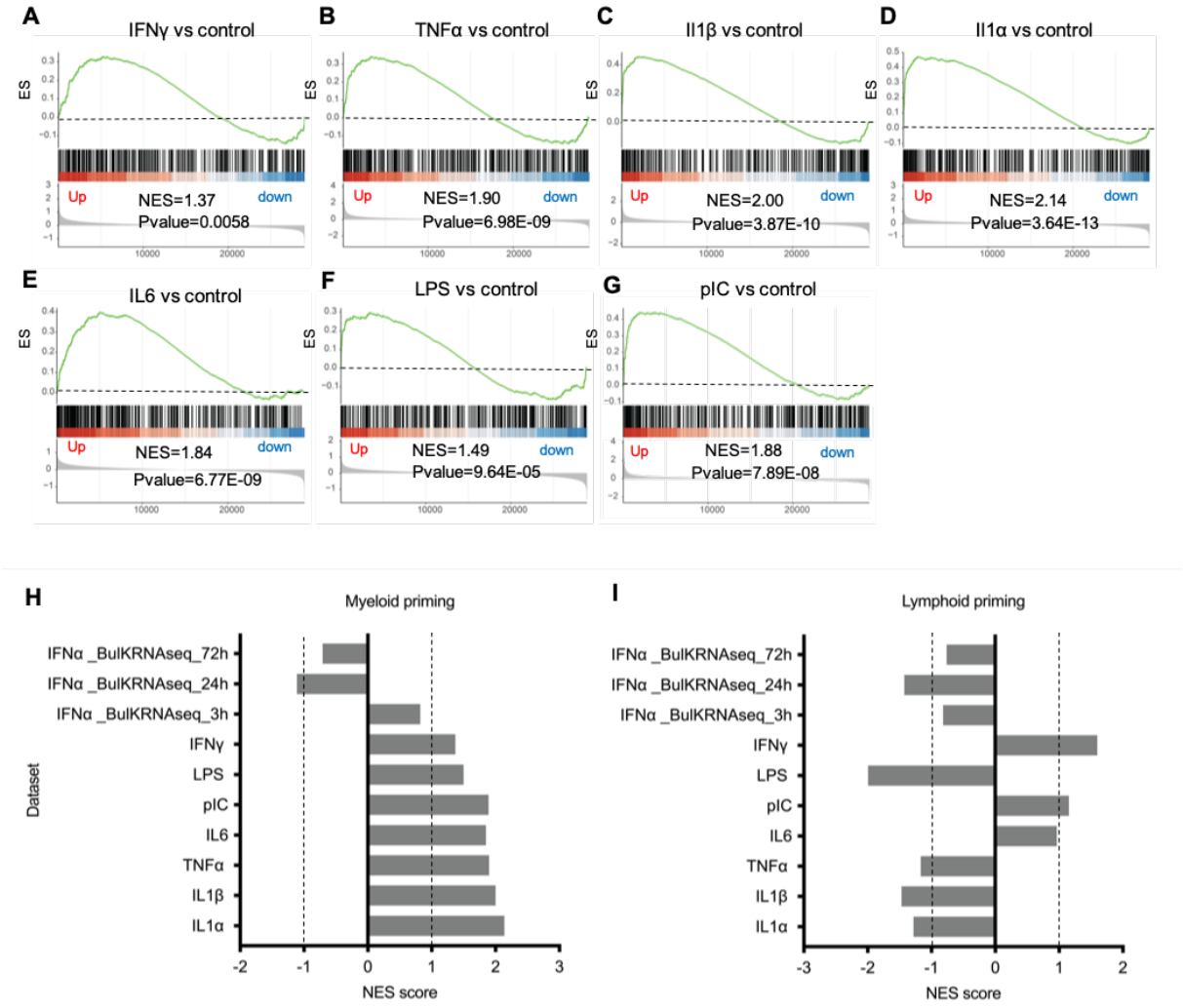

Figure 3.21: Proinflammatory cytokines regulate myeloid priming and lymphoid signatures in HSCs.

(A-G) GSEA plots of Myeloid LT-HSC molecular signatures from *Mann et al.,* significantly enriched (pvalue <=0.05) of HSCs following treatment with IFNγ, **(A),** TNFα, (**B**)**,** IL1β, (**C**)**,** IL1α (**D**), IL6, (**E**)**,** LPS **(F)**, pIC **(G)** vs PBS control treatment. Gene list ordered by log2 fold change. NES, normalized enrichment score. ES, Enrichment score. **(H-I)** GSEA of Myeloid molecular signatures from Mann et al. 2018 **(H)** and Lymphoid signatures from Izzo et al., 2020 **(I)** significantly enriched (pvalue <=0.05)

3.4 Investigating the net impact of proinflammatory cytokine receptor signaling in hematopoiesis under homeostasis

The role of proinflammatory cytokines in mediating hematopoiesis and HSCs quiescence under homeostatic conditions has yet to be fully elucidated. To better understand the function of these proinflammatory cytokines, in this section, I have investigated the effect of basal activation of proinflammatory cytokine signaling on steady-state adult hematopoiesis and HSCs quiescence.

3.4.1 Loss of Interferon receptor expression leads to reduced frequency of HSCs and LSKs

The role of basal IFNs in shaping the hematopoietic system develops relatively slowly, as individual knockout mice (KO) for the interferon-alpha receptor (*Ifnar*$^{-/-}$) or the interferon-gamma receptor (*Ifngr*$^{-/-}$) have no obvious hematologic defects (Essers et al. 2009; Matatall et al. 2014). I hypothesize here that because of the convergence of their intracellular signaling pathways, there is overlap and redundancy between their effects, and therefore, they most likely compensate for each other. Hence, I analyzed the hematopoietic system of mice lacking both Ifnar and Ifngr, hereafter referred to as *Ifnar*$^{-/-}$*Ifngr*$^{-/-}$ double KO (2KO). Similar to the single KO mice, there were no differences in the total number of BM cells in the 2KO mice compared with the WT mice (Figure 3.22A). Flow cytometric analysis of the mature lineage composition show that 2KO mice have mostly normal frequencies of differentiated cells with only slight increase in Gr1^{+}CD11b^{+} myeloid cells in the BM (Figure 3.22B). I did not detect any changes in the composition of the differentiated cells in the blood and spleen (data not shown). Moreover, frequencies of LS-Ks progenitors (Figure 3.22C) and its associated subpopulations (CMP, GMP, and MEP) (Figure 3.22D) did not change in the 2KO mice compared to WT controls. On the contrary, 2KO shows a profound decrease in the frequency of BM LSKs (Figure 3.22E). Subsequently, I analyzed the effect of IFNs signaling deletion on the multipotent progenitor (MPP) compartment. I observed a decrease in the frequency of MPP3 and MPP4, whereas MPP1 and MPP2 were not affected (Figure 3.22F). Interestingly, 2KO mice showed decreased HSCs frequency in the BM (Figure 3.22G). Although IFNs are strong inducers of HSCs cycling under stress conditions (Essers et al. 2009; Baldridge et al. 2010), steady-state cell cycle

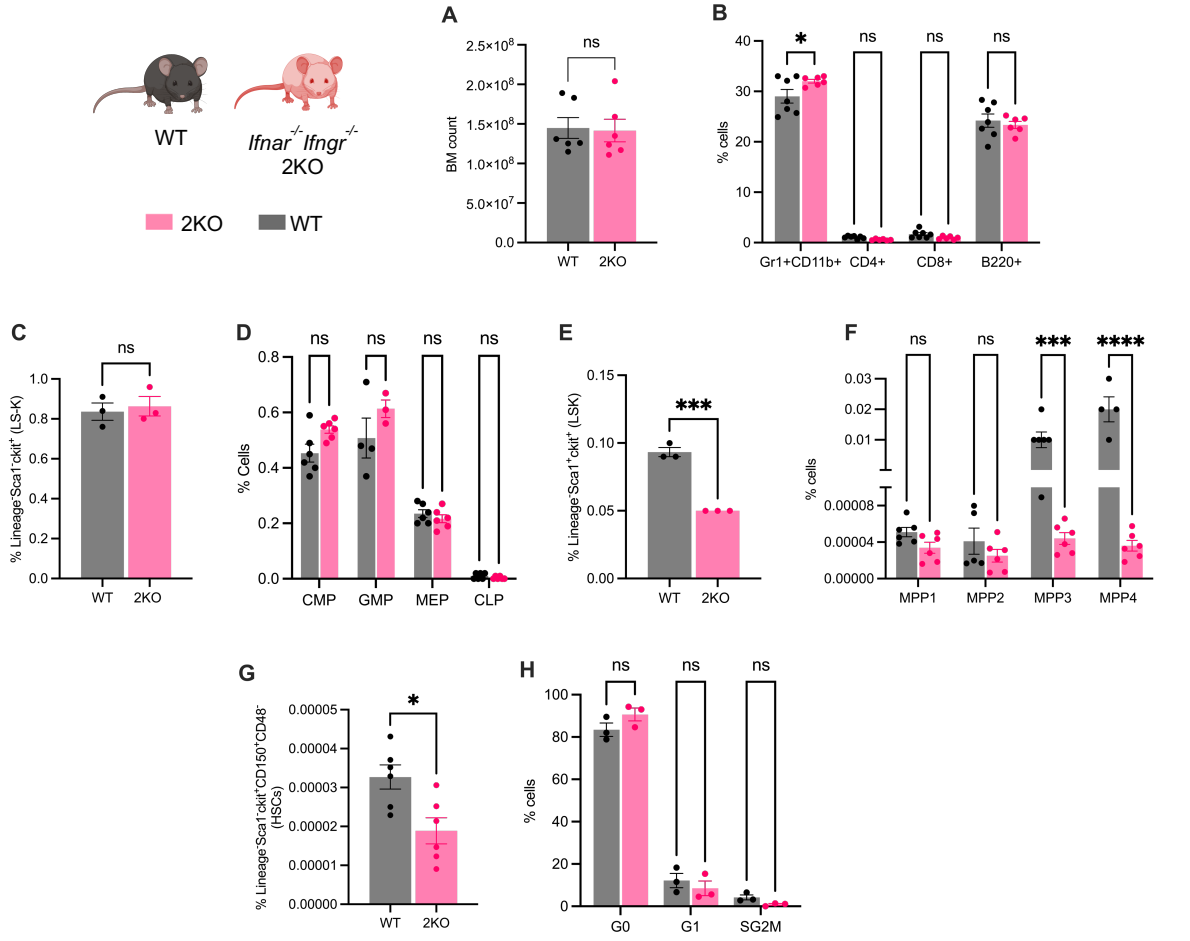

***F*igure 3.22: *Ifnar*$^{-/-}$*Ifngr*$^{-/-}$ (2KO) mice have decreased LSK and HSC numbers yet no change in cell cycle behavior and on differentiated cells.**

(A) BM cellularity determined by Vi-CELL counter. **(B-G)** Percentage (%) frequency of total BM of differentiated mature cells: B-cells (B220^{+}), T-cells (CD4^{+} and CD8^{+}), granulocytes (B220^{-} CD3^{-} CD11b^{+}Gr1^{+}) **(B),** LS-K (Lin^{-} Sca1^{-} cKit^{+}) **(C),** committed progenitor: CMP (Lin^{-} Sca1^{-} cKit^{+} CD16/CD32^{-} CD34^{+}); GMP (Lin^{-} Sca1^{-} cKit^{+} CD16/CD32^{+} CD34^{+}); MEP (Lin^{-} Sca1^{-} cKit^{+} CD16/CD32^{-} CD34^{-}), CLP (Lin^{Low} cKit^{low} CD127^{+} CD125^{+}) **(D),** LSK **(**Lin^{-} Sca1^{+} cKit^{+}) **(E),** multipotent progenitors (MPPs): MPP1 (Lin^{-} Sca1^{+} cKit^{+} CD135^{-} CD34^{-} CD150^{+} CD48^{-}); MPP2 (Lin^{-} Sca1^{+} cKit^{+} CD135^{-} CD34^{+} CD150^{+} CD48^{+}); MPP3 (Lin^{-} Sca1^{+} cKit^{+} CD135^{-} CD34^{+} CD150^{-} CD48^{+})**(F),** HSCs (Lin^{-} Sca1^{+} cKit^{+} CD150^{+} CD48^{-} CD34^{-}) **(G). (H)** Cell cycle analysis using Ki67 and Hoechst 33342 to detect HSCs in G_0 (Ki67^{neg}Hoechst^{low}), G_1 (Ki67^{High}Hoechst^{low}) and SG_2M (Ki67^{High} Hoechst^{high})**.** 3-6 biological replicates per group from two independent experiments. Statistical significance for **B, D, F** and **H** was determined by an ordinary one-way ANOVA using Holm-Šídák's multiple comparisons test. Statistical significance for **A, C, E,** and **G** was determined by unpaired t-test analysis. At least 2 independent experiments were performed;

*P≤0.05, ***P≤ 0.001, ****P<0.0001, ns; non-significant. Data represent mean ± standard error of the mean (SEM).

analysis of 2KO HSCs revealed no changes in the percentage of quiescent cells compared to WT HSCs (Figure 3.22H). This data suggests that maintaining differentiated cells in the BM, blood, and spleen is dispensable of interferon signaling. Whereas the significant decrease in HSCs and LSKs frequencies in 2KO mice suggest a role for interferon signaling in the maintenance of HSCs and early progenitors.

3.4.2 IFNs deficient progenitors show decreased colony formation in secondary CFU and early competitive advantage than WT cells *in vivo*

To functionally assess the effects of reduced frequencies of HSCs and LSKs, I performed an *in vitro* colony formation assay to determine whether the expansion and progenitor differentiation abilities of BM cells are impaired in the absence of interferon signaling. For this assay, I isolated BM cells from 2KO and WT mice and cultured them in a methylcellulose-based medium (Figure 3.23A). During primary colony formation, I did not detect changes in the colony forming unit (CFU) (Figure 3.23B). However, after the secondary plating of the primary colonies, the total number of colonies was reduced in the 2KO cells compared to the WT cells (Figure 3.23B). To further investigate the self-renewal potential and lineage contribution of 2KO stem cells *in vivo*, I performed a competitive transplantation assay. I isolated BM cells from 2KO and WT mice and then sorted for LSKs from each strain. Next, I mixed LSKs from CD45.2 mice of the KO strain or control WT mice with CD45.1/2 LSKs of WT strain in a 1:1 ratio. This mixture was transplanted intravenously into lethally irradiated CD45.1 WT recipient mice, along with cKit-depleted WT cells as supportive BM. Chimerism of KO and WT in the blood of recipients was determined every 4 weeks for a period of 18 weeks (Figure 3.23C). At 18 weeks after transplantation, BM cells from primary graft recipient mice were transplanted into lethally irradiated recipients to assess long-term engraftment (Figure 3.23C). In this competitive setting, hematopoietic reconstitution from 2KO donor LSK cells showed a competitive advantage in the primary transplants up to 16 weeks (Figure 3.23D).

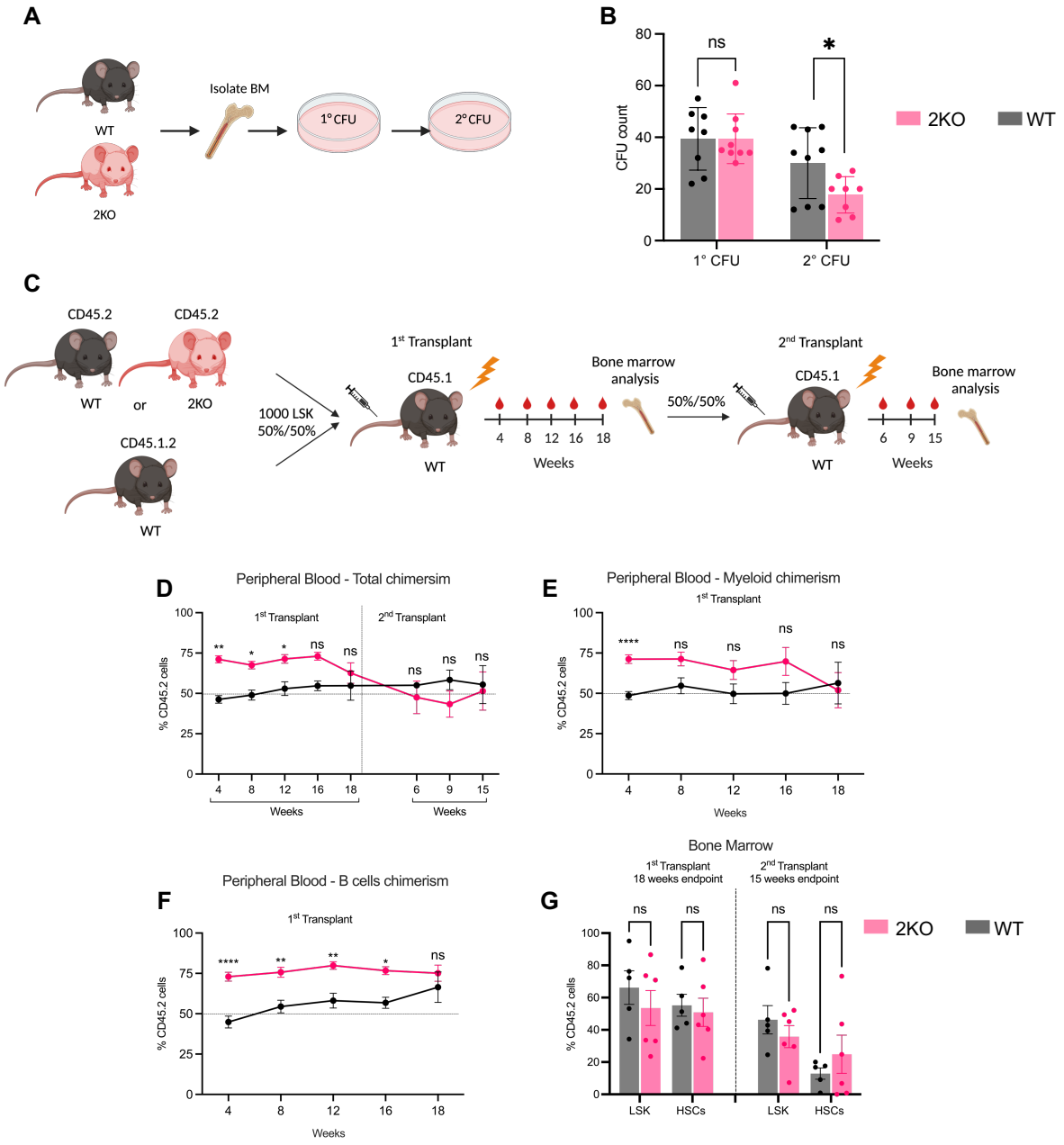

Figure 3.23: 2KO LSKs have early competitive repopulation advantage over WT LSKs.

(A) Schematic overview of colony forming unit (CFU) assay: WT and 2KO mice were sacrificed, BM was isolated and 20,000 cells from each genotype were cultured in methylcellulose medium for 7 days. Colonies were then counted. **(B)** Number of colonies from serial CFU assay. 4 biological replicates from two independent experiments were performed. **(C)** Schematic overview of competitive transplantation assay. LSKs from 2KO and WT mice (CD45.2) were sorted and mixed with LSKs from CD45.1/2 WT mice (1:1 ratio). This mixture was transplanted into lethally irradiated CD45.1 WT recipient mice. Peripheral blood chimerism was analyzed every 4 weeks up to 18 weeks. BM cells from primary recipients were transplanted into secondary recipients and peripheral blood chimerism was analyzed over time. **(D-F)** Flow cytometry-based analysis of serial competitive transplantation experiments. CD45.2% outcome is shown for peripheral blood chimerism **(D),** myeloid cells **(E),** and B cells **(F). (G)**

Flow cytometry-based analysis of endpoint of competitive transplantation experiment. CD45.2% outcome is shown for BM HSCs and LSK. 4-6 biological replicates were used. Statistical significance for **(B)** and **(G)** was determined by two-way ANOVA using Holm-Šídák's multiple comparisons test. Statistical significance for **(D-F)** was by unpaired t-test. One independant experiment was perfomed. *P≤0.05, **p<0.01 ns; non-significant. Data represent mean ± standard error of the mean (SEM).

Although engraftment of $Gr1^+CD11b^+$ was not significant (Figure 3.23E), the proportion of $B220^+$ chimerism from 2KO donor was substantial up to 16 weeks (Figure 3.23F). Moreover, the BM donor-derived chimerism and frequency of LSKs, HSCs, and mature cells were similar for 2KO and controls at the 18 weeks endpoint analysis (Figure 3.23G). I did not observe any change in peripheral blood contribution over time in the secondary transplants between the KO and WT (Figure 3.23D). In addition, no differences in BM contribution and generation of differentiated cells as well as for HSCs and LSKs were detected between KO and WT in the secondary recipients (Figure 3.23G). Overall, these results suggest that the absence of interferon signaling does not significantly impair the expansion or differentiation capabilities of progenitors. However, the reduced frequency of stem and progenitor cells in 2KO mice does lead to a temporary competitive advantage for 2KO LSKs in the early stages of hematopoietic reconstitution in a competitive transplantation assay.

3.4.3 5KO mice have decreased LSKs and HSCs numbers and increased myeloid committed progenitors

As the numbers of LSKs and HSCs were reduced in 2KO mice (Figure 3.22E,G), I wanted to determine whether additional proinflammatory cytokines contribute in combination with IFNs to the maintenance of the stem cell compartment under homeostasis. Since little research has been done on the simultaneous switching off of receptors of several proinflammatory cytokines, we generated homozygous KO mice that lack both receptors for TNFα and receptors for both IFNα and IFNγ, in addition to IL1 receptors. These ‘genotype’ mice are hereby called 5KO. These mice had a shorter lifespan compared to normal WT mice. They die at a younger age of approximately 50 weeks without signs (Figure 3.24A), unlike WT mice which can survive up to 150 weeks (Flurkey, Mcurrer, and Harrison et al. 2007). In addition, the breeding performance of

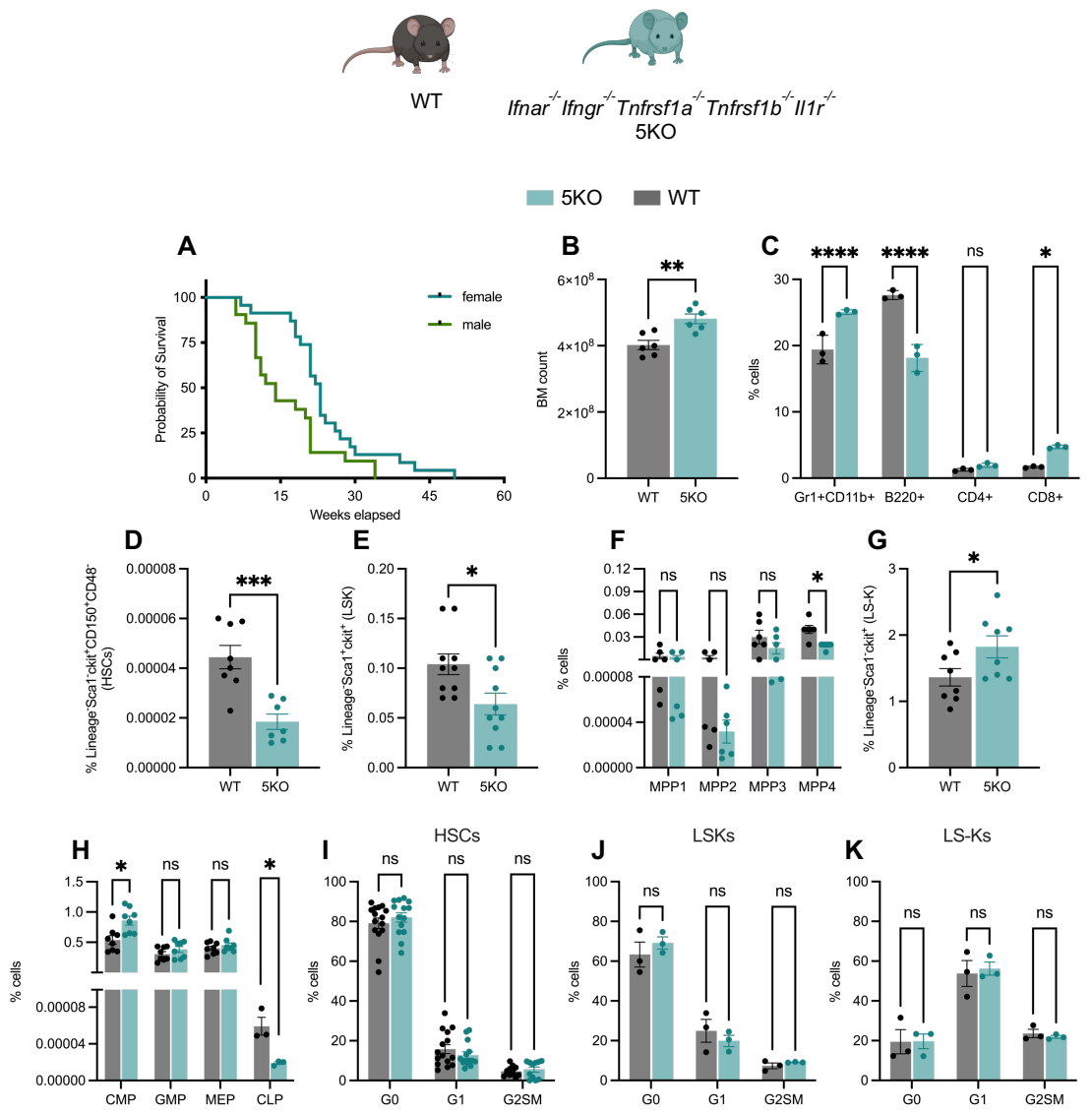

Figure 3.24*: Ifnar$^{-/-}$Ifngr$^{-/-}$Tnfrsf1a$^{-/-}$Tnfrsf1b$^{-/-}$Il1r$^{-/-}$ (5KO)* mice have decreased LSKs and HSCs numbers and increased myeloid committed progenitors.

(A) Kaplan-Meier survival curve of 5KO mice. **(B)** BM cellularity determined by Vi-CELL counter. **(C-G)** Percentage (%) frequency of total BM of differentiated mature cells: B-cells (B220$^+$), T-cells (CD4$^+$ and CD8$^+$), granulocytes (B220$^-$ CD3$^-$ CD11b$^+$ Gr1$^+$) **(C),** HSCs (Lin$^-$ Sca1$^+$ Ckit$^+$ CD150$^+$ CD48$^-$ CD34$^-$) **(D),** Lin$^-$ Sca1$^+$ cKit$^+$ (LSK) **(E),** multipotent progenitors (MPPs): MPP1 (Lin$^-$ Sca1$^+$ cKit$^+$ CD135$^-$CD34$^+$ CD150$^+$ CD48$^-$); MPP2 (Lin$^-$ Sca1$^+$ cKit$^+$ CD135$^-$ CD34$^+$ CD150$^+$ CD48$^+$); MPP3 (Lin$^-$ Sca1$^+$ cKit$^+$ CD135$^-$CD34$^+$ CD150$^-$ CD48$^+$) **(F)** Lin$^-$ Sca1$^-$ cKit$^+$ (LS$^-$K) **(G),** committed progenitor: CMP (Lin$^-$ Sca1$^-$ cKit$^+$ CD16/CD32$^-$ CD34$^+$); GMP (Lin$^-$ Sca1$^-$ cKit$^+$ CD16/CD32$^+$ CD34$^+$); MEP (Lin$^-$ Sca1$^-$ cKit$^+$ CD16/CD32$^-$ CD34$^-$); CLP (Lin^{Low} cKit^{low} CD127$^+$ CD125$^+$) **(H). (I-K)** Cell cycle analysis using Ki67 and Hoechst 33342 to detect HSCs **(I),** LSKs **(J),** LS$^-$K **(K)** in G_0 (Ki67^{neg}Hoechst^{low}), G_1 (Ki67^{High}Hoechst^{low}) and SG_2M (Ki67^{High} Hoechst^{high}) **(I).** 3-6 biological replicates per group from two independent experiments. Statistical significance for **C, F, H, I, J,** and **K** was determined by an ordinary one-way ANOVA using Holm-Šídák's

multiple comparisons test. Statistical significance for **B, D, E,** and **G** was determined by unpaired t-test analysis. At least 2 independent experiments were performed; *P≤0.05, ***P≤ 0.001, ****P<0.0001, ns; non-significant. Data represent mean ± standard error of the mean (SEM).

those mice is limited. This phenotype was not present in mice only lacking one or up to 4 cytokine receptors (Data not shown). Analyzing the BM composition of 5KO mice revealed an increase in total BM cells (Figure 3.24B), a decrease in $B220^+$ frequencies, and an increase in $Gr1^+CD11b^+$ myeloid cells (Figure 3.24C). I found no changes in the composition of mature cells in the peripheral blood and spleen of the 5KO mice compared with the WT mice (data not shown). Interestingly, there was a decrease in the number of LSKs and HSCs (Figure 3.24D,E), similar to the 2KO mice, and a decrease in the frequency of MPP4 (Figure 3.24F). However, there was an increase in LS-K frequency (Figure 3.24G) associated with a significant increase in CMPs and a significant decrease in CLP frequency (Figure 3.24H). Cell cycle analysis using Ki67/Hoechst 33342 staining shows that the receptor signaling did not affect the cycling of HSCs, LSKs, and LS-Ks under homeostasis (Figure 3.24 I-K, respectively). These results suggest that IFNs and other proinflammatory cytokines play a role in regulating stem cell numbers but not their cycling under homeostasis.

3.4.4 5KO deficient progenitors show increased colony formation in secondary CFUs

To assess the function of the altered stem and progenitor cell composition in the BM of 5KO mice, I performed an *in vitro* colony formation assay by culturing total BM cells in a 1:1 ratio of WT and 5KO in methylcellulose-based medium (Figure 3.25A). The results showed that 5KO exhibited an increase in CFU only when serially plated out into a secondary CFU (Figure 3.25B). Additionally, an increase in LS-Ks and myeloid progenitor cells in 5KO compared to WT was observed as early as 7 days after primary CFU culture (Figure 3.25C). To exclude the possibility that the results of BM CFU were affected by the reduction of LSKs or the propagation of LS-Ks in the 5KO mice and to confirm these results, the assay was repeated by sorting an equal number of LSKs from each genotype. The increase in colony-forming potential in the secondary CFUs of the 5KO mice compared to the WT controls was confirmed (Figure 3.25D). Furthermore, a competitive re-population transplantation assay was performed to determine whether the self-renewal potential and lineage contribution of the 5KO stem

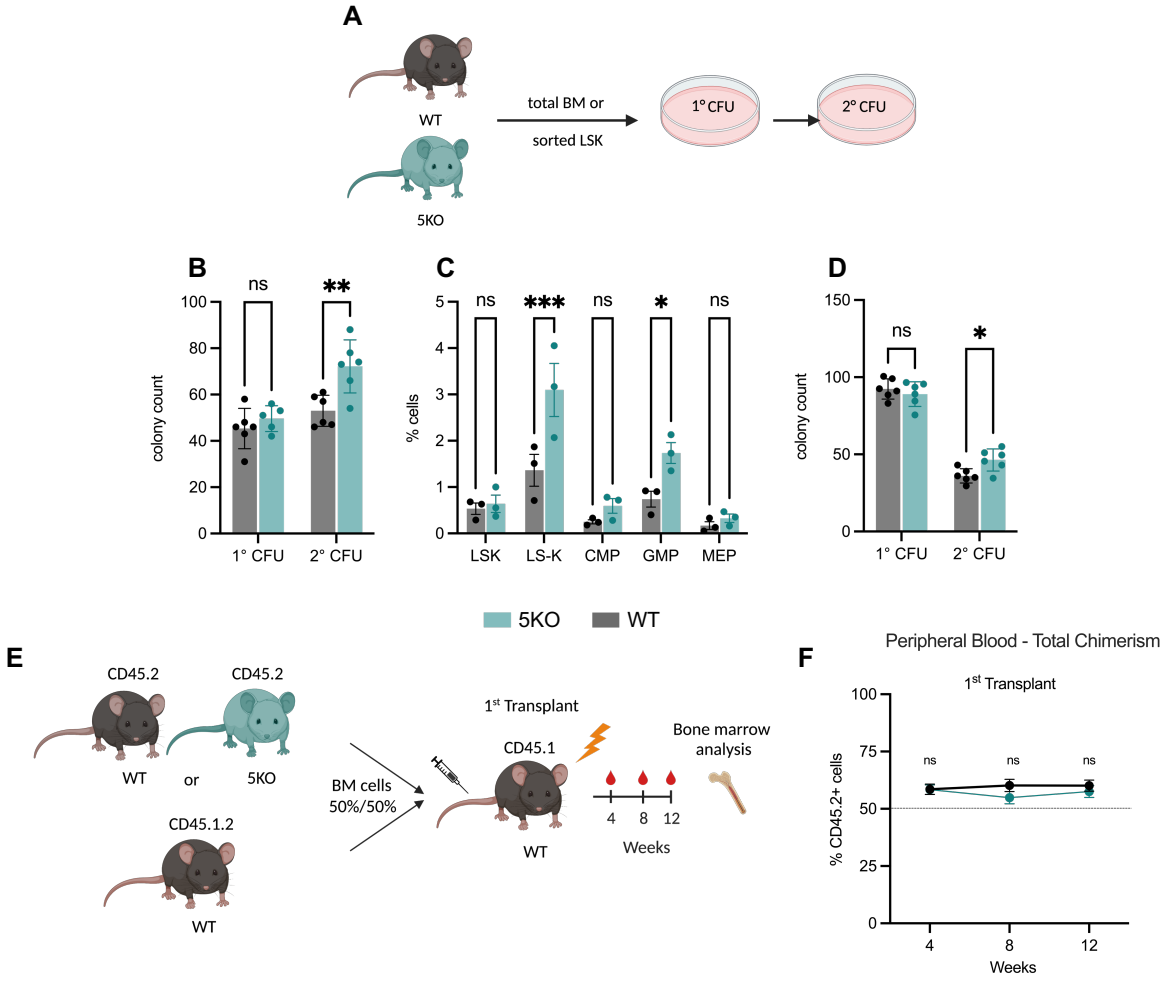

Figure 3.25*:* 5KO progenitors exhibit an increase in colony formation in secondary colony-forming units (CFUs).

(A) Schematic overview of colony forming unit (CFU) assay: WT and 5KO mice were sacrificed, BM was isolated and 20,000 cells from each genotype or sorted for LSKs and were cultured in methylcellulose medium for 7 days. Colonies were then counted. **(B)** Number of colonies from serial CFU assay of cultured BM cells. **(C)** Percentage (%) frequency of progenitors after 7 days in culture as quantified by FACs analysis. **(D)** Number of colonies from serial CFU assay of cultured LSKs cells. 4 biological replicates from two independent experiments were performed. **(E)** Schematic overview of competitive transplantation assay. BM cells from 5KO and WT mice (CD45.2) were mixed with BM from CD45.1/2 WT mice (1:1 ratio). This mixture was transplanted into lethally irradiated CD45.1 WT recipient mice. Peripheral blood chimerism was analyzed every 4 weeks up to 12 weeks. **(F)** Flow cytometry-based analysis of serial competitive transplantation experiments. CD45.2% outcome is shown for peripheral blood chimerism. 6 biological replicates were used. Statistical significance for **(B-D)** was determined by two-way ANOVA using Holm-Šídák's multiple comparisons test. Statistical significance for **(F)** was by unpaired t-test. One independant experiment was perfomed. *P≤0.05, **p<0.01 ns; non-significant. Data represent mean ± standard error of the mean (SEM).

cells were impaired. Accordingly, BM cells were isolated from CD45.2 mice of the 5KO strain or from control mice WT and mixed with BM from CD45.1/2 WT strain in a 1:1 ratio. This mixture was transplanted intravenously into lethally irradiated CD45.1 WT recipient mice, along with cKit-depleted WT cells as supporting BM cells (Figure 3.25E). The results showed no functional defect, as chimerism in blood remained at ~50% up to 12 weeks after transplantation (Figure 3.25F). These experiments are currently ongoing, and the endpoint will be in April 2023. In summary, these experiments suggest that the altered stem and progenitor cell composition in the BM of 5KO mice may play a significant role in the observed increase in secondary CFU.

3.4.5 5KO mice show delayed recovery following chemotherapeutic 5-FU treatment

As IFNs, TNF, and IL1 are known to play a role in cell cycle control under stress conditions, I investigated whether deleting the cytokine receptors could affect HSC activation or their return to quiescence in response to treatment with 5-fluorouracil (5-FU). 5-FU is a cytotoxic drug that decimates the differentiated blood cells and activates dormant HSCs to divide (Randall and Weissman et al. 1997). Following 5-FU treatment, I monitored the rate at which HSCs could renew the blood cell pool and whether this rate differed between 5KO and WT mice due to the lack of cytokine signaling pathways. Although there was no difference in the survival of WT and 5KO mice 10 days after a single 5-FU treatment, a greater percentage decrease of 22.6% in BM cellularity was observed in the 5KO mice compared to the WT mice (Figure 3.26A). The treatment increased the LSKs counts in the BM. Even though the 5KO had a 2-fold decrease in their LSKs counts compared to WT at homeostasis (Figure 3.24E), I observe a 16.8-fold increase in the LSKs frequency of the 5KO compared with only a 6.8-fold increase in WT LSKs frequency following 5-FU treatment relative to PBS controls (Figure 3.26B). Likewise, 5KO HSCs had an 18.4-fold increase in frequency compared to 14.7 fold increase in the WT HSCs following the treatment (Figure 3.26C). Interestingly, I observed significant differences in the HSCs and LSKs' return to a quiescent state between the 5KO and WT mice. WT HSCs returned to quiescence 10 days following treatment, whereas the 5KO HSCs and LSKs were still cycling (Figure 3.26D,E). This is consistent with the increased sensitivity of 5KO stem cells to 5-FU.

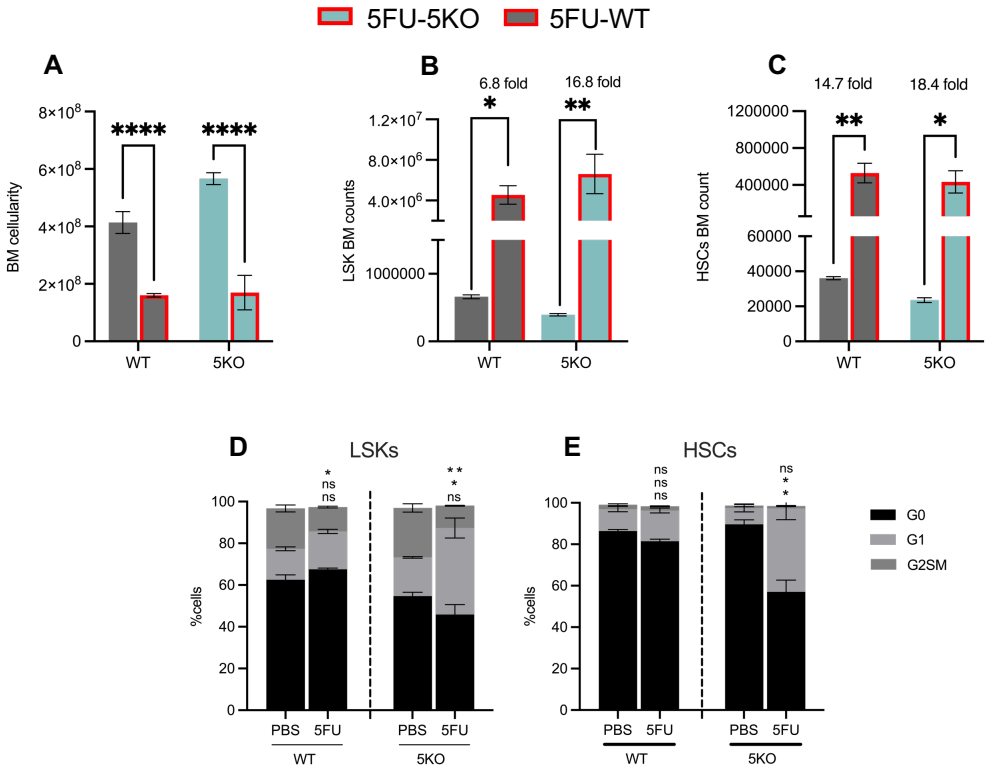

Figure 3.26: 5KO stem and progenitor cells have delayed recovery after 5-FU treatment.

(A) BM cellularity determined by Vi-CELL counter in WT and 5KO mice after 10 days of *in vivo* PBS or 5-FU (150 mg/kg) treatment. **(B-C)** Flow cytometric analysis of BM LSK ($Lin^-Sca1^+cKit^+$) **(B)** and HSCs ($Lin^-Sca1^+cKit^+CD150^+CD48^-CD34^-$) **(C)** in WT and 5KO mice after 10 days of in vivo PBS or 5-FU treatment. **(D-E)** Cell cycle analysis using Ki67 and Hoechst 33342 to detect LSKs **(D)** and HSCs **(E)** in G_0 ($Ki67^{neg}Hoechst^{low}$), G_1 ($Ki67^{High}Hoechst^{low}$) and SG_2M ($Ki67^{High}$ $Hoechst^{high}$). 2-3 biological replicates were used. One experiment was performed. Statistical significance for **(A-D)** was determined by two-way ANOVA using Holm-Šídák's multiple comparisons test. Statistical significance for **(D-E)** was by unpaired t-test. *P≤0.05, **p<0.01, ****P<0.0001, ns; non-significant. Data represent mean ± standard error of the mean (SEM).

These results suggest that the absence of proinflammatory cytokine receptors in 5KO mice affects HSC activation and response to stress, making them more sensitive to the effects of 5 FU.

3.4.6 Bulk transcriptional profiling reveals altered metabolic and cell cycle pathways in HSCs of 5KO mice

To characterize the transcriptional profile of HSCs in the 5KO mice, I performed bulk RNA sequencing. I sorted HSCs from 5KO and WT mice into lysis buffer to isolate RNA, which was then submitted to the Genomics and Proteomics Core Facility at the DKFZ, Heidelberg. The Facility prepared the sequencing libraries and performed the quality control and sequencing. The raw sequence data in FASTQ format was aligned and quantified by the Omics IT and Data Management Core Facility. Afterward, I performed the downstream analysis. Hierarchical clustering confirmed that all samples of a given genotype cluster together and separate (Figure 3.27A). Moreover, PCA shows robust segregation of 5KO HSCs from WT control HSCs (Figure 3.27B). I next performed differential gene expression analysis using DESeq2 and identified 1139 DEGs (padj <=0.05) with 561 genes being upregulated and 578 genes being downregulated between the 5KO and WT HSCs. I then performed GSEA, using the Molecular Signatures Database (MSigDB) Hallmark gene set, which showed that genes upregulated in the 5KO HSCs were significantly enriched in pathways related to the glycolysis metabolic processes (Figure 3.27C). In contrast, the downregulated genes were enriched in processes related to the inflammation system (Figure 3.27D) and cell cycle (Figure 3.27E). Furthermore, analysis using the REACTOME database shows that the down-regulation of cell cycle processes dominates the variability between the 5KO and WT HSCs (Figure 3.27F). Of note, processes related to extracellular matrix organization were upregulated in the 5KO HSCs (Figure 3.27F). Thus transcriptional profiling showed that 5KO HSCs have a distinct transcriptional profile characterized by upregulation of metabolic and signaling pathways and downregulation of cell cycle and inflammatory processes.

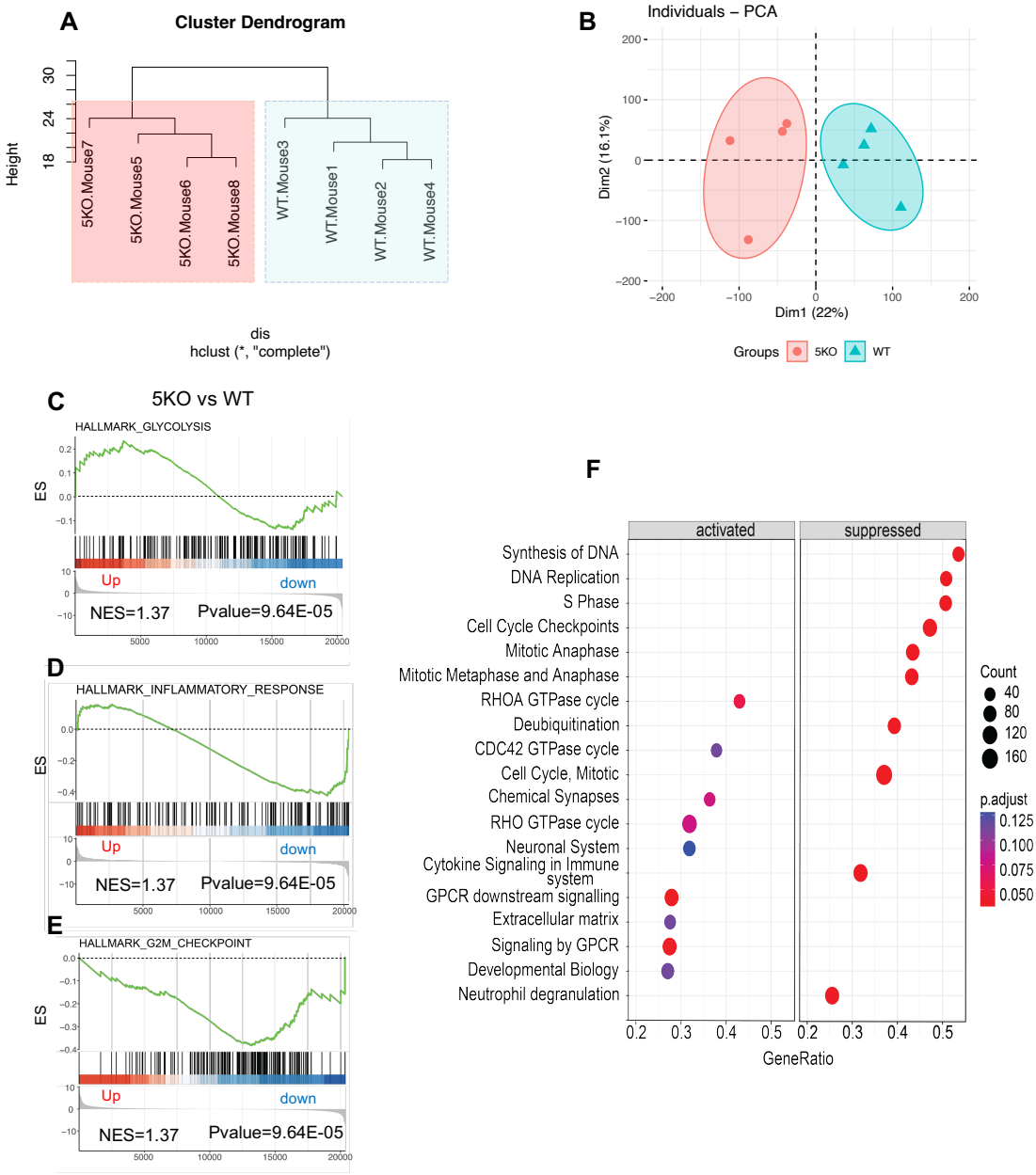

Figure 3.27: Bulk transcriptional profiling of HSCs from 5KO mice indicates changes in metabolic and cell cycle pathways.

(A) Hierarchical clustering based on Euclidian distance was performed with the hclust function implemented in R. **(B)** Principal component analysis (PCA). **(C-E)** GSEA plots of 5KO vs. WT HSCs (Lin^- $Sca1^+$ $cKit^+$ $CD150^+$ $CD48^-$ $CD34^-$) analysis. **(F)** Dot plots showing activated and suppressed GO terms in 5KO vs. WT HSCs using REACTOME database.

4 Discussion

4.1 Longitudinal analysis of hematopoietic stem and progenitor cell responses to IFNα treatment

Biological responses, such as acute inflammation, are dynamic processes in which cells, tissues, and organisms undergo different phases of sensing differences, responding to changes, and recovering after a successful response. To understand biological systems, it is critical to recognize their dynamic nature (Bar-Joseph, Gitter, and Simon et al. 2012). In the context of hematopoiesis, the role of inflammation in HSCs function has been widely studied (Caiado, Pietras, and Manz et al. 2021). However, most studies have concentrated on single time points, and there is limited knowledge of the molecular alterations that occur across the HSPCs compartment over time. While bulk and single-cell RNAseq can provide static snapshots of cellular state at the time of measurement, longitudinal data can offer valuable insights into how biological systems transform over time (Saelens et al. 2019; Treutlein et al. 2016; Petropoulos et al. 2016). Despite the challenges that come with analyzing longitudinal data sets (Saelens et al. 2019), this is a critical area of research because of the potential for gaining a deeper understanding of the dynamics of biological systems. Currently, few computational methods exist to infer time series specific changes in the transcriptome (Shao et al. 2021; Tran and Bader et al. 2020). Unsupervised pseudotime methods are often used, but they are not suitable for identifying genes that exhibit coherent variation across time series. Moreover, the orders these methods estimate may not correspond to the processes associated with the real-time. In this work, I used comprehensive bioinformatics analysis to identify qualitative changes in cellular abundance and the specific molecular changes likely responsible for these changes. I presented a longitudinal analysis of transcriptional changes of bulk HSCs and the whole HSPCs on the single cell level across the three phases (sensing, response, and recovery) of the acute inflammatory response to IFNα treatment. The datasets generated are a powerful resource for studying the heterogeneity and dynamics of the inflammatory response of HSPCs. The results show diversity in the response of HSPCs to IFNα; I highlighted different expression patterns that define early and late transcriptional responses, as well as global and cell type-specific signatures.

The study also revealed that HSPCs respond differently to treatment and exhibit different biological responses depending on the cell type.

4.1.1 IFNα-Induced Inflammation Primes Hematopoietic Stem Cells for Ongoing Molecular Changes

The discovery that IFNα affects HSCs function has opened an area of research that has produced conflicting data on HSCs development and maintenance (Demerdash et al. 2021). Short-term exposure to IFNα has been found to stimulate HSCs proliferation, while long-term exposure has been associated with stem cell depletion and exhaustion (Essers et al. 2009; Pietras et al. 2014). Chronic and acute viral infections have also been linked to HSCs impairment through continuous IFNα signaling (Hirche et al. 2017; Binder et al. 1997). However, thus far, it is unclear whether IFNα preprograms the transcriptional machinery in HSCs for functional impairment. Previous work suggests that the regenerative capacity of HSCs decreases with each cell division (Qiu et al. 2014), raising intriguing questions about the potential existence of cellular memory of division and the responsible factors for this memory. To gain insight into this process, RNA sequencing was performed on HSC populations at different stages, including 3h, 24h, and 72h. My results challenge conventional wisdom by showing that transcriptional activity in HSCs persists until 72h, in contrast to phenotypic FACs analysis. My data indicates that certain genes in HSCs are still undergoing changes at this time point, suggesting an ongoing cascade of molecular changes or even irreversible changes that have a lasting impact on activated cells. These results support the theory that deterioration of HSCs function begins immediately after initial cell division and worsens over time. This is consistent with recent work showing that discrete inflammatory events can irreversibly attenuate HSC function, underscoring the cumulative inhibitory effect of such events (Bogeska et al. 2022). However, the precise molecular mechanisms underlying this loss of function were previously unknown. My study suggests that a single dose of IFNα may prime HSCs for irreversible loss of function. This hypothesis is supported by the concept of cellular memory (Saeed et al. 2014; Netea et al. 2016); Bernitz et al. 2016), which allows cells to alter their response to secondary stimuli. The ability of HSCs to modulate their response may be compromised after exposure to IFNα, potentially leading to a functional decline from which they cannot recover.

4.1.2 Metabolic Insights from transcriptomics into HSC proliferation and activation under IFNα-Induced Stress

My findings revealed that during HSCs proliferation, there are significant transcriptional, mitochondrial, and metabolic changes that last up to 72h. These findings have implications for understanding the underlying mechanisms behind HSCs attrition and the loss of regenerative potential that occurs when dysfunctional mitochondria accumulate after cell division (Chan et al. 2012). My work also sheds light on the concept of HSCs divisional memory, which is thought to be driven by long-lasting epigenetic modifications that enable rapid re-expression of genes upon secondary challenge (Saeed et al. 2014; de Laval et al. 2020). Interestingly, the data suggest that abnormal mitochondria acquired during initial division may play a role in holding this memory, including in cases of IFNα-induced activation (Filippi et al. 2021). While the concept of HSCs divisional memory is still being investigated, these findings have the potential to open up new avenues for research on the fundamental mechanisms governing HSCs function and their responses to external stressors.

My investigation into the activation of HSCs has revealed a temporal relationship between mitochondrial activation and the initiation of the cell cycle. Furthermore, I observed sustained mitochondrial activity even after HSCs returned to a quiescent state, suggesting a crucial role for these organelles in HSCs regulation. This coincides with increased chromatin remodeling processes, potentially enabling HSCs to retain a memory of previous cell division and programming for extinction. Recent work has emphasized the interplay between mitochondrial function, metabolism, and epigenetic changes in HSCs, highlighting the need for a deeper understanding of these factors in HSC biology (Filippi et al. 2021; Morganti, Cabezas-Wallscheid, and Ito et al. 2022).
Mitochondria plays a pivotal role in regulating HSCs function by facilitating energy production, fatty acid metabolism, nucleotide synthesis, and amino acid production (Papa, Djedaini, and Hoffman et al. 2019). The exact mechanisms by which mitochondria regulate HSCs activity are not yet clear, but their crucial role in maintaining cellular homeostasis underscores their importance (Chan et al. 2012). Further exploration of HSCs metabolic plasticity in various states, including during activation and under regenerative stress, is essential to uncovering the intricate relationships between mitochondrial function and HSCs regulation.

Stress-induced increases in cellular metabolism produce important metabolites that HSCs use as an energy source to promote differentiation and drive emergency hematopoiesis under stress conditions, as shown by previous studies (Maryanovich and Ito et al. 2022; Mistry et al. 2020). The field of HSCs biology is interested in understanding how HSCs metabolic activities are fueled during specific conditions that require HSCs activation. Initial analyses of our HSC bulk RNAseq dataset have shown that metabolic pathways are enriched at different stages of the response. It is noteworthy that instead of the classic metabolic features typically associated with the activation of HSCs (Morganti, Cabezas-Wallscheid, and Ito et al. 2022), I observed the exact opposite. Analysis of metabolic properties at the transcriptional level revealed sustained downregulation in anabolic processes after IFNα treatment, suggesting that the functional and differentiation capacities of HSCs were diminished. These results suggest a unique IFNα response to cellular activation of HSCs compared with other inflammatory stimuli. While bulk sequencing of HSCs has provided a great tool to understand better the molecular basis of IFNα-induced proliferation with considerable depth. To comprehensively investigate the metabolic landscape of HSCs under IFNα-induced stress and to better understand the functional consequences of changes in these metabolic states. It would be necessary to integrate our transcriptomics data with proteomics and metabolomics data to correlate the mRNA and protein levels. This will allow us to perform a more comprehensive analysis of the metabolic profile in HSCs under IFNα-induced stress. It is tempting to postulate if the downregulation of fatty acid oxidation is associated with the absence of the regular emergency myelopoiesis phenotype upon IFNα treatment.

Despite significant progress in recent years, our understanding of the metabolic requirements of HSCs is limited because it is difficult to profile the metabolism of these rare cells using conventional mass spectrometry techniques. New techniques in metabolomics will improve our understanding of metabolic changes in HSCs. We can now get metabolic information from 10,000 cells (DeVilbiss et al. 2021), but more detailed analysis is needed to determine how metabolites are used and their role in epigenetic modifications. Much is still to be discovered about how HSCs metabolism is driven and the specificity of metabolite utilization in different contexts. Such knowledge could provide valuable insights into not only the stress response upon viral

infections but also the consequences of IFNα administration in treating hematological malignancies, such as myeloproliferative neoplasms (MPNs).

4.1.3 Differential IFNα induced stress responses in hematopoietic stem and progenitor cells

Although many studies have investigated the role of inflammation on HSCs function, changes in marker expression on these cells have made it challenging to examine the impact of inflammation on the heterogeneity and molecular changes over time in the HSPC compartment (Ali and Park et al. 2020). Single-cell profiling has improved our understanding of HSPCs heterogeneity, allowing for marker-independent analysis of their response to inflammation (Watcham, Kucinski, and Gottgens et al. 2019). Previous studies only captured a snapshot (Giladi et al. 2018), but our study investigates the progression of IFNα-induced processes over time, providing insight into the dynamics of the HSPCs response.

Analysis of single-cell RNA-seq time series is nontrivial because of its high complexity, regarding the inclusion of multiple cell types, the high number of genes, and the extra dimension of time. To overcome the challenges of analyzing such longitudinal datasets, together with our collaborators, we designed a computational pipeline for processing and analyzing single-cell RNA-seq time series, in which clusters were labeled based on the expression of multiple genes after correcting for treatment effects, thus avoiding relabeling of the cells undergoing inflammation as separate populations. This will ensure the study of the same cell type over time. Hence, cell type identity is reliably retrieved, even though the conventional marker genes might be subject to changes, as is the case during inflammation. Furthermore, we designed measures that make the temporal dynamics more comprehensible and provide a (visual) entry point into all the information in the data. Unsupervised methods based on cell-to-cell proximities cannot capture the pseudotemporal order of the cells in our data, where the cell states after relaxation become more similar to those before treatment. Therefore, our collaborators implemented a semi-supervised, i.e., using the experimental time labels information, method for inference of response pseudotime. Using a minimal linear regression model, our response pseudotime reconstruction enabled capturing the fine-grained expression changes and dynamical patterns

beyond the four discrete experimental time points. Recently, alternative semi-supervised methods such as psupertime (Macnair, Gupta, and Claassen 2022), or methods suitable for other temporal patterns (e.g., periodic dynamics) that linear matrix transformations may not capture are also being investigated. By utilizing our approach, we showed that the HSPCs response to IFNα has distinct molecular patterns of gene expression and biological processes depending on the cell type, highlighting the dynamic nature of HSPC's response to IFNα. Our single-cell data demonstrate while the whole stem and progenitor compartment do sense the treatment, there is a heterogeneous response of HSPCs to IFNα, with HSCs displaying the greatest response compared to other progenitors. Strengthening the idea that HSCs are a key determinant of the host response and a major player in inflammation (Pietras et al. 2017). For the first time, our data enabled a direct, systematic comparison of IFNα response among different HSPCs at the molecular level. Notably, the global HSPCs response shows a sustained increase in gene expression of metabolic and translational genes. In contrast, HSC-specific gene groups and patterns followed a rapid response and recovery. They were enriched in various inflammation-related genes, suggesting marked differences in how related cell types respond to the same inflammatory stimulus.

4.1.4 Emergent effects of IFNα treatment on myelopoiesis: An unanticipated role for IFNα on myeloid progenitor development

Our analyses not only provide insights into the dynamics of genes in the HSPCs compartment but also reveal previously unknown information about the effects of IFNα on myeloid progenitor cells, which has been controversial. Unexpectedly, I observed a persistent attenuation of myeloid differentiation genes in myeloid progenitor cells. Interestingly, I found that the persistent downregulation of myeloid differentiation genes was synchronized with the depletion of those cells from the BM. Several myeloid genes that did not reach convergence of their induced decreased expression along the response pseudotime of 72h post-treatment support a division memory of HSCs after IFNα treatment. Cellular memory is a process that allows cells to alter their response to secondary stimuli by enhancing or suppressing subsequent responses, depending on the type of stimulus received (Netea et al. 2016); (Saeed et al. 2014; Netea et al. 2016). In innate immune cells, this can lead to an intensified inflammatory response to

secondary pathogen infections, known as trained immunity. Conversely, cellular memory can also result in dampening subsequent responses, which is called immune tolerance (Burrill and Silver 2010; Bernitz et al. 2016; Netea et al. 2016). For example, b-Glucan, Bacille Calmette-Guerin (BCG), and Candida albicans induce trained immunity via a type II interferon (Kaufmann et al. 2018) and IL1 (Moorlag et al. 2020) response, while recently it was shown that Mycobacterium tuberculosis (Mtb) reprograms HSCs and limits myelopoiesis via a type I IFN/iron signaling axis, impairing trained immunity responses (Khan et al. 2020). Trained immunity is a non-specific response of the innate immune system that functions independently of the acquired/adaptive immune system and provides an enhanced immune response upon reinfection with invading agents (Moorlag et al. 2020; Netea et al. 2020). It was shown that BCG and Mtb uniquely reprogram HSCs for at least 1 year. It is yet to be established whether a single administration of IFNα is adequate to induce the myeloid signature I observed. Additional research is necessary to comprehend the duration and specificity of the cellular memory response elicited by IFNα treatment.

Emergency myelopoiesis, i.e., increased production of myeloid cells, has been described in response to many pro-inflammatory cytokines and infections (Manz and Boettcher et al. 2014). However, thus far, we have not identified any impact on myeloid production or differentiation upon IFNα treatment, due to extensive changes in stem cell-specific marker expression upon inflammation (Demerdash et al. 2021). Others claimed that decreased frequency of myeloid progenitors and the simultaneous increase in LSKs upon *in vitro* treatment of HSPCs with IFNα was mainly the result of myeloid progenitors reacquiring *Sca-1* expression (Pietras et al. 2014; Kanayama et al. 2020). This conclusion was made based on *in vitro* studies, which show that myeloid progenitors re-acquire *Sca-1* following IFNα treatment. However, the results of *in vitro* studies can be highly misleading, as when cells are removed from their niche, they are stressed and respond differently to the treatment. With our unbiased investigation of the different clusters, defined solely by their gene expression, I could now show that IFNα induced *Sca-1* gene expression only occurred in immature HSCs and LMPPs. Even though CITEseq analysis of HSPCs should be performed to confirm these results at the Sca-1 protein level, our data indicate that the LSK expansion observed in flow cytometry is mainly due to the enrichment of the HSCs and multipotent progenitors and not myeloid progenitor populations shifting into the LSK gate.

Unlike other proinflammatory cytokines such as TNFα (Yamashita and Passegué 2019) and IL1β (Pietras et al. 2016), I did not find characteristics typical of emergency myelopoiesis. Instead, abundance analysis showed a decrease in myeloid progenitor numbers; gene expression related to myeloid priming was downregulated in all cell clusters from immature HSCs to committed myeloid progenitors; and myeloid-derived mature neutrophils were continuously reduced in the blood. In addition, response pseudotime analysis revealed changes in expression of genes related to pyroptosis, suggesting that reduced levels of myeloid progenitors might result from a combination of impaired myeloid differentiation with increased cell death via pyroptosis. Interestingly, upon infection with Mtb, HSCs are reprogrammed to limit their commitment towards myelopoiesis via a type I IFN signaling axis (Khan et al. 2020). In this same study, they showed that IFNα induces RIPK3-mediated necroptosis in myeloid progenitors. However, RIPK3 is a component of both pyroptosis and necroptosis depending on other proteins participating in these pathways (Shlomovitz, Zargrian, and Gerlic et al. 2017). Differentiation and cell death pathways are not only regulated at the transcriptional level. Thus post-translational analysis and additional functional approaches need to be performed to unravel further the programs controlling the IFNα-induced reduction in the myeloid progenitors in the BM.

Thus, our time course data suggest an unanticipated impact of IFNα on the differentiation and production of myeloid cells, possibly indicating that while it was previously believed that the proliferative response of HSCs protects the system, IFNα appears to have a harmful effect on more downstream progenitors, highlighting the diverse impact of the same proinflammatory agonist on related but distinct cell types at different timepoints in the response. This link between IFNα and reduced production and levels of myeloid cells such as neutrophils not only helps us to understand better the impact of inflammation on the whole hematopoietic compartment. It will also help to understand better the role of IFNα in disease settings such as the autoimmune disease systemic lupus erythematosus (SLE) in which neutrophil dysfunction plays an integral role in disease pathogenesis (Kaplan et al. 2011), and IFNα is associated with adverse outcomes (Rönnblom and Leonard et al. 2019). Although our study provides intriguing observations regarding myeloid cell development, I didn't capture lymphoid progenitors with our single-cell experiment. Therefore, the impact of IFNα on

lymphopoiesis remains unknown, and experiments investigating this are required to address this important question.

While scRNA-Seq provides greater resolution than immunophenotyping, it does not fully capture the state of cells. A number of additional factors affect cell behavior, such as protein levels and chromatin state, which may manifest as unappreciated heterogeneity and dynamic properties. Nevertheless, the dataset that I provide is a very powerful resource that can be utilized to identify new FACs markers that remain unchanged with the treatment. This is because the dataset covers the full phase of acute inflammation, which provides almost a complete picture of the changes occurring in the cells during this period. By finding markers not affected by the treatment, we can have a better gating strategy for HSPCs, which will help us better study processes that occur during inflammation.

4.2 Early transcriptional responses of HSCs to multiple proinflammatory cytokines

The activation of HSCs triggered by inflammatory stress is not limited to IFNα as it is a general response of HSCs to a broad spectrum of proinflammatory agonists. During infections or general inflammation, a whole storm of cytokines is produced, including other proinflammatory cytokines such as IFNγ, TNFα, IL1, and IL6, which are also capable of inducing HSCs proliferation *in vivo* (Caiado, Pietras, and Manz et al. 2021). Whether there is crosstalk between the different proinflammatory cytokines on their effect on HSCs quiescence remains unclear. In this part of my thesis, I aimed to uncover the early transcriptional responses of HSCs to various proinflammatory cytokines. To increase the likelihood of studying the direct downstream effects of stimulants on HSCs, I selected a short treatment window of 3h. The analysis involved examining the transcriptional responses of HSCs to six different proinflammatory cytokines: IFNα, IFNγ, TNFα, IL1β, IL1α, and IL6, along with LPS and pIC. Through this analysis, I found that nearly all proinflammatory cytokines tested initially elicited a response at the 3h timepoint. I demonstrated that the eight distinct proinflammatory cytokines elicited unique gene alterations in HSCs, indicating a diverse range of proinflammatory cytokine responses in the HSCs. Consistent with our recent work showing that a complex network of proinflammatory cytokines mediates the proliferative response of HSC to LPS (Demel et al. 2022), I uncover here the strong overlap of the transcriptional responses of LPS with IL1β, IFNα, IL1α, and TNFα. Exploring the interplay and interdependence of proinflammatory cytokines is an interesting approach. To explore this further, we need to use different mouse models that lack specific cytokine receptors. This will allow us to analyze whether the response to cytokines is different in KO mice compared to WT mice.

Because many proinflammatory cytokines can induce the production of each other further experiments are needed. For this purpose, a cytokine array could be performed after a single proinflammatory cytokine treatment. Thus, we can investigate which proinflammatory cytokines are induced by the different treatments. In addition, mixed BM chimeras that include BM from WT and different receptor KO mice may be useful to reveal the interactions between the different proinflammatory cytokines. This may help to understand their effects on HSCs quiescence and the role that BM niche cells

play in mediating the indirect effects. Understanding the interactions between proinflammatory cytokines and their effects on HSCs behavior is critical to gain further insight into HSCs function and maintaining a functional hematopoietic system upon inflammation.

The findings demonstrate that proinflammatory cytokines can induce distinctive alterations in the genes of HSCs. Nevertheless, I also discovered that some of these proinflammatory cytokines activate similar processes in the HSCs, highlighting the intricacy of proinflammatory cytokine signaling in regulating both the function and fate of HSCs. Interestingly, one common characteristic of all the treatments was the upregulation of adaptive immune responses. This finding suggests that immunomodulatory processes are initiated soon after exposure to the stressors, with a mere 3h interval between stimulus and response. Furthermore, all treatments except IFNα and pIC enhanced myeloid priming in HSCs, consistent with prior research. Further studies are needed to gain a deeper understanding of how proinflammatory cytokines regulate myeloid priming in HSCs. Furthermore, to fully elucidate the common and unique responses to the treatments, it is necessary to analyze and identify specific signaling pathways or processes later in the response. To complement this, we need to understand further if all the HSCs pool responds to inflammation or there is only a specific subset that responds. And is there a common stress mechanism activated by those cytokines to mediate their effect on HSCs? Recent unpublished data by our group have shown that HSCs display increased IFN-stimulated gene (ISG) expression under homeostasis. Would this interferon priming within the HSCs pool poise the cells to respond differently to cytokine treatment? Gene expression profiling on the single cell level through RNA-sequencing analysis could help answer this question. With such experiments, we can identify the molecular determinants of proinflammatory cytokine responsiveness within the HSCs compartment and thereby have complete understanding of the effects induced by the single treatments. Through comparison of single cell RNA sequencing of the single proinflammatory cytokine treatments we could potentially identify a common mechanism that is regulating the increase in HSCs proliferation after the different proinflammatory cytokine treatments. In the future, this could be further expanded, and investigation of the effect of those proinflammatory cytokines on the different lineage-biased HSCs subtypes would be intriguing.

Although these proinflammatory cytokines use different genes to regulate similar processes, they share some commonly regulated genes. Interestingly, the *Serpina3g* gene has been found to be upregulated in response to all treatments except IL6. This gene is known to be involved in response to bacteria, cytokines, and adaptive immune responses. In addition, *Serpina3g* has been shown to act as a cytoprotectant against oxidative stress, protecting HSCs during inflammatory events and thereby possibly preventing cell death (L. Li et al. 2014). Moreover, this gene has been shown to play a role in regulating BM microenvironment and affecting the migratory behavior of HSCs. It was shown to be downregulated in mobilized progenitor cells (Winkler et al. 2005). Therefore, it might be interesting to compare its expression in mobilized progenitor cells and HSCs. The upregulation in HSCs might indicate a mechanism that prevents the mobilization of HSCs during the acute stress response. To better understand the mechanistic relationship between the activation of HSCs and different stimuli, future experiments should be conducted. Specifically, it is necessary to analyze whether *Serpina3g* activation within HSCs is essential for their activation by different stimuli. To answer this question, using different mouse models and KO of *Serpina3g in vivo* may prove helpful.

4.2.1 Cautionary remarks on the redundant use of pIC and IFNα treatments on HSCs

In hematopoietic research, the use of pIC and IFNα treatments are widespread; however, my findings suggest that these treatments may not be as redundant as previously believed. Specifically, I demonstrate that only a fraction of pIC DEGs are upregulated following IFNα treatment, indicating possible differences in the underlying molecular mechanisms and pathways involved. These results shed new light on the intricate interplay between these treatments and their impact on hematopoietic processes. Therefore, it is important to consider the differential effects of these treatments when designing hematopoiesis studies. For example, if investigating early responses to IFNα, caution should be taken when using pIC to infer transcriptional responses at the 3h timepoint, as our analysis revealed significant dissimilarities between these two treatments. This novel insight may lead to a more sophisticated approach to the use of these treatments in hematopoietic research, with the potential to develop more targeted and effective therapeutic interventions. However, despite this disparity, the processes mediated by the DEGs for both treatments appear to be

functionally related, with some ISGs being induced. As an interferon inducer, pIC has been demonstrated to increase IFNα protein levels in the serum as early as 2h post in vivo injection (Linehan et al. 2018). Additionally, studies in KO mice suggest that pIC-induced proliferation of HSCs relies on IFNα receptor signaling, warranting further exploration. For instance, the knockdown of cell cycle-related genes upregulated after IFNα treatment could determine whether the response of HSCs to inflammatory signals is modulated by the cell cycle. Alternatively, measuring the response of HSCs to pIC treatment after the KO of IFNα-specific genes (and vice versa) could determine whether these genes are specific to the treatment that upregulated them. Subsequent experiments should also validate the expression of differentially upregulated and downregulated genes after pIC and IFNα treatment by qPCR and determine their essential role in eliciting responses. These insights offer exciting avenues for future research in unraveling the complex mechanisms underlying the interplay between these treatments and their impact on hematopoietic processes.

4.2.2 The Impact of IL6 on Gene Expression and Hematopoiesis

In the context of hematopoesis, IL6 has been extensively studied due to its crucial role in the development of hematopoietic lineages in response to inflammatory stimuli. However, compared to other proinflammatory cytokines, my analysis revealed a weaker magnitude of gene expression changes induced by IL6 treatment. The production of IL6 is usually triggered by infection or the injection of other cytokines, resulting in massive IL6 production (Zhao and Baltimore 2015). The weak response of differentially expressed genes after IL6 treatment may be attributed to the low dose of injected IL6, which was lower than what animals typically encounter during actual injury or infection. Alternatively, IL6 may exert effects that have not been investigated, such as promoting lymphoangiogenesis in bone lymphatic vessels, as demonstrated in a recent study (Biswas et al. 2023). Although our findings do not rule out the possibility of IL6 playing a role in the activation of HSCs, administering a higher dose of IL6 may lead to a more pronounced activation of HSCs. Further experiments are required to investigate whether the dose or duration of IL6 treatment was incorrectly chosen or if IL6 does not promote HSCs proliferation. The microarray data, in conjunction with FACS analysis, suggest that IL6 treatment did not strongly activate HSCs, indicating a need for additional investigations into the role of IL6 in hematopoiesis.

4.3 The Complex Interplay of Proinflammatory Cytokines and Hematopoietic Stem cells under homeostasis

Extensive work has been conducted on the role of proinflammatory cytokines in regulating HSCs and hematopoiesis under stress conditions. However, their role in regulating HSC development during embryogenesis, even without infection, has recently been investigated, revealing the importance of tonic inflammatory signals in maintaining HSC pool homeostasis (Collins, Mitchell, and Passegué et al. 2021). Despite this, the basal activation of proinflammatory cytokines in homeostasis has been less studied.

Single-gene KO studies often face a challenge called genetic compensation or transcriptional adaptation. This occurs when the loss of one gene is compensated for by another gene with similar functions and expression patterns. Such compensation has been observed in multiple mutants of various model organisms (El-Brolosy and Stainier 2017). For instance, KO mice in which specific proinflammatory cytokine signals are turned off, like *Tnfrsf1dko*, *Il1r1*$^{-/-}$, *Ifngr*$^{-/-}$, and *Ifnar*$^{-/-}$ KO mice, show no significant hematologic defects (Pronk et al. 2011; Pietras et al. 2016; Matatall et al. 2014; Essers et al. 2009). Although they show minor changes in HSC pool size or lineage priming, their viability is unaffected. Conversely, animals lacking NF-kB subunits, a common downstream target of inflammatory cytokine signaling, display substantial impairments in hematopoiesis (Espín-Palazón and Traver et al. 2016). This suggests that individual cytokines, rather than inflammatory signals, are dispensable for hematopoietic development. In this work, investigating the hematopoietic system of *Ifnar*$^{-/-}$*Ifngr*$^{-/-}$ KO adult mice revealed a phenotypic change in the stem cell compartment as elucidated by a significant decrease in HSCs and LSKs. This is in contrast to previous results showing that single *Ifnar*$^{-/-}$ KO and *Ifngr*$^{-/-}$ KO adult mice have normal HSCs numbers (Matatall et al. 2014; Essers et al. 2009); this is likely due to redundancy in and cooperativity between both classes of IFNs (Platanias et al. 2005), which may explain why the removal of only one signaling pathway did not affect the stem cell number in adult mice.

IFN signaling has been shown to regulate embryonic HSC production; the authors showed that *Ifngr*$^{-/-}$ embryos exhibit a four-fold decrease in HSC numbers (Y. Li et al. 2014). Therefore, my results lead to the important hypothesis that the decrease in HSCs numbers in *Ifnar*$^{-/-}$*Ifngr*$^{-/-}$ KO adult mice may have originated during embryonic development and is not compensated by other proinflammatory cytokines in adulthood. It would be important to examine the number of HSCs in the double and single IFNs KO embryos in mating experiments to determine whether this decrease in the stem cell compartment arose during embryonic development or adulthood. The reduction in the number of HSCs in *Ifnar*$^{-/-}$*Ifngr*$^{-/-}$ KO adult mice was further highlighted by the reduction in differentiation potential observed in *in vitro* colony formation assays compared with WT mice. These findings are consistent with a study showing a similar phenotype in JAK1 KO mice, which have defects in type 1 and type 2 IFN signaling pathways, among others. In addition, JAK1-deleted stem cells exhibited downregulation of several members of the interferon-regulating transcription factor family (Kleppe et al. 2018). These findings underscore the critical role of IFN signaling in maintaining the HSCs compartment.

Although the deficiency in CFU differentiation may be attributed to a decline in proliferative capacity, I did not detect any alteration in the cycling pattern of the *Ifnar*$^{-/-}$ *Ifngr*$^{-/-}$ HSCs. Alternatively, it could be due to the limited number of functional HSCs in the 2KO mice. Despite this, the competitive repopulation assay indicated that 2KO LSKs had a transient competitive advantage in the early stages of hematopoietic regeneration, which emphasizes the crucial role of the BM microenvironment in stress-induced activation of HSCs. Notably, altered homing of LSK as a consequence of IFN receptor deficiency could likely explain the competitive advantage of the 2KO cells in the primary transplants, as only short-term reconstitution levels were affected. Therefore, it is imperative to generate reverse chimeras within a 2KO stromal microenvironment to determine whether the observed defect in the 2KO mice is due to the microenvironment or an inherent attribute of the 2KO cells. In addition, to distinguish between genes and functions that are important for all cells and those with specific functions for HSCs, it is important to perform studies with HSC-specific Cre recombinase (HSC-SCL-Cre-ERT transgenic mice) (Göthert et al. 2005) in combination with floxed IFN signaling genes. This allows direct investigation of the

effects of IFN in adult hematopoiesis, excluding potential developmental and microenvironmental impairments that may ultimately affect HSCs.

4.3.1 Insights from knockout mouse models and implications for understanding HSCs function in physiological environments

Lacking one or two proinflammatory cytokine receptors doesn't fully explain the complex interactions between HSCs and their microenvironment. Because many factors are involved in cytokine receptor signaling, compensatory mechanisms can occur when a single component is absent (El-Brolosy and Stainier et al. 2017). Therefore, it's crucial to understand the combined role of proinflammatory cytokines in a dynamic physiological environment rather than analyzing each proinflammatory cytokine separately. Our findings that 2KO mice had reduced function and number of HSCs prompted us to investigate whether the loss of other proinflammatory signaling pathways (TNFα and IL1) combined with IFNs could lead to more severe defects in the HSCs compartment. Remarkably, these mice exhibited a reduced lifespan of approximately 50 weeks, a phenotype absent in the precursor mice. However, it is currently unclear whether the cause of mortality originates during fetal development or manifests as an adult phenotype. To resolve this, conducting timed mating experiments is crucial to determine whether mortality occurs during embryonic development or adulthood.

The complex influence of proinflammatory cytokines on HSC function is highlighted by the finding that 5KO mice have an increased colony forming capacity which is in contrast to the results obtained with 2KO. Although I found no differences in competitive transplantation between 5KO mice, I used whole BM and did not perform HSCs equivalence. The results show that the transplanted cells were still evenly distributed, indicating an efficient repopulation. To gain a more comprehensive understanding of the functional differences in HSCs numbers among the 5KO mice and compare them to WT mice, future experiments should employ single-cell transplantation assays and limiting dilution assays.

Upon further analysis of mice post-chemotherapy, it was observed that stem and progenitor cells of 5KO mice exhibit increased proliferation and expansion in response to stress, leading to delayed recovery of their cell cycle. Even though no differences in cell cycle behavior were observed between wild-type and 5KO mice at baseline, given that proinflammatory cytokines can induce HSC activation and cycling following stress stimuli, I expected that baseline signaling of these cytokines would contribute to the homeostatic activation of HSCs. However, using Ki67/Hoechst staining to examine the cell cycle status of these 5KO mice did not reveal a role for proinflammatory cytokines in maintaining HSC quiescence under homeostasis. Nonetheless, I cannot exclude the possibility that proinflammatory cytokines play a role in regulating HSCs quiescence under homeostatic conditions. This is because using Ki-67/Hoechst 33342 staining provides only a snapshot of the cell cycle at a one-time point, and 70-80% of HSCs are already at G0. This method is not sensitive enough to detect small numbers of actively cycling cells. Therefore, label-retaining assays and methods that measure division kinetics in vivo (van der Wath et al. 2009) could help address this question. The gene expression data reinforces that proinflammatory cytokine receptor loss leads to changes in the cell cycle. Further studies are needed to functionally dissect the downstream targets of the proinflammatory cytokine receptors that confer the enhanced proliferation ability for stem/progenitor cells upon stress.

In aging, myelopoiesis becomes dominant over lymphopoiesis, and it is suggested that increased basal levels of proinflammatory cytokines observed during aging might be responsible for this effect (Geiger, de Haan, and Florian et al. 2013) Further experiments are required to determine how the different cell fates of HSCs are regulated by proinflammatory cytokines to help gain insights into the molecular mechanisms by which extrinsic factors control the fates of HSCs. Moreover, post-transcriptional regulatory mechanisms specific to HSCs, such as microRNA regulation, protein modifications, or substrate availability, may exist but are not readily obvious.

Currently, there is no literature showing the effect of multiple receptor KO on hematopoiesis. In summary, using our novel multiple receptor knockout mice, I reveal the complexity of proinflammatory cytokines in regulating the quiescence and differentiation of HSCs. These findings are critical to advance our knowledge of the relationship between inflammation and hematopoiesis. By exploring how inflammatory

signaling regulates hematopoiesis function and shapes the blood system, we can gain valuable insights into the changes that occur during aging and the development of various hematologic malignancies. Ultimately, these insights could lead to new therapies that target inflammatory pathways to improve outcomes in patients with hematologic diseases.

4.4 Concluding remarks and future perspective

The current state of research in stress hematopoiesis fails to recognize the significance of studying the temporal dynamics of these biological processes. Since all biological phenomena inherently involve changes over time, incorporating the temporal aspect into investigations is crucial to gain a comprehensive understanding of the underlying mechanisms. This study presents a novel approach to analyzing the molecular response of bulk HSCs to IFNα treatment throughout the three phases of acute inflammation: sensing, response, and recovery. The longitudinal transcriptional analysis of HSCs is the first of its kind and provides insights into the sequence of biological events that occur in HSCs during IFNα treatment. These findings were previously underrepresented in single end-point analyses. An exciting prospect for this study is the further investigation of the analysis at later time points. Understanding whether the system recovers and whether cellular memory has developed as a result of treatment. By focusing on the temporal dynamics of biological processes, this research can provide a more comprehensive understanding of stress hematopoiesis.
In addition to the longitudinal transcriptional analysis of HSCs during IFNα treatment, I have compiled a comprehensive resource of transcriptional features specific to HSCs and progenitor cells at the single-cell level. These features are crucial for responding to IFNα treatment during different stages of acute inflammation in stress hematopoiesis. By creating this resource, I have established a foundation for exploring the functional properties of the molecular signatures of HSPCs under inflammatory stress. Manipulating hematopoiesis requires an understanding of the underlying molecular mechanisms. While correlations inferred from expression data offer hypotheses for regulatory mechanisms, experimental testing is crucial for confirming these hypotheses. Furthermore, to comprehensively model regulatory and signaling networks that lead to changes in gene expression, we must integrate different types of biological data. Combining our time-series data with protein levels and chromatin features is essential for this comprehensive modeling. Techniques, such as CITE-Seq (Stoeckius et al. 2017) or REAP-Seq (Peterson et al. 2017), will enable the simultaneous detection of proteins or chromatin status. Additionally, imaging-based transcriptomics (Petukhov et al. 2022); (Haase et al. 2022) is being developed to provide spatial information that complements the data. Collectively, these advancements will provide near-complete information, including precise cell locations

in a multidimensional feature space, tying together information at molecular, cellular, and tissue levels. These efforts can uncover new insights into the complex regulatory networks that govern stress hematopoiesis and have significant implications for the development of novel therapeutic interventions.

My work delves into the previously unexplored area of how IFNα contributes to emergency myelopoiesis. The findings have revealed novel insights into the mechanisms governing this critical biological process and suggest that IFNα treatment may hold clinical promise for addressing diseases associated with emergency myelopoiesis. Looking ahead, I plan to investigate the mechanisms underlying the loss of myeloid progenitor cells, which I have observed to have strong death-signaling properties. Notably, the findings indicate an increased score for the pyroptosis gene signature, which highlights the significance of this pathway in regulating myelopoiesis. Newly developed single-cell lineage tracing strategies (Rodriguez-Fraticelli et al. 2020) will facilitate the assessment of treatment-induced transcriptional changes and the functional capacity of individual cells in a single experiment. By targeting multiple genes and observing the effects globally, we can understand how RNA, proteins, epigenetics, and extrinsic signals shape the differentiation landscape and drive cellular fluxes. For finer time scales and insight into cell cycle–related effects, pulse-chase experiments may become important. By elucidating the molecular mechanisms driving these processes, we can gain a more comprehensive understanding of the complex regulatory networks involved in myelopoiesis and potentially uncover new therapeutic targets for these debilitating diseases. The IFNα's impact on the myeloid differentiation pathway raises intriguing questions about its effects on other cellular differentiation lineages, especially the lymphoid arm. No conclusive evidence has been found to suggest an increase in lymphoid priming. However, the upregulation of GO terms related to antigen presentation and T-cell differentiation in HSCs suggests a potential impact on lymphoid differentiation. Further investigation is needed to determine whether this effect leads to increased lymphoid priming in HSCs. In addition, leveraging this dataset to identify markers that remain consistent throughout treatment for each cluster can aid in devising a more effective gating strategy for progenitors.

The current state of research in this field lacks the ability to compare proinflammatory cytokine responses due to the usage of varied techniques and gating strategies. To

address this issue, I started to perform a systematic analysis that will enable us to compare proinflammatory cytokine responses, determine the level of overlap and crosstalk, and facilitate our understanding of disease models. The transcriptional changes observed suggest both common and specific responses to various proinflammatory cytokines, warranting further validation. Numerous studies have linked inherited and acquired BM failure syndromes to increased inflammation during chronic infection, with inflammation increasing the risk of developing hematologic malignancies. By targeting specific cytokines, patients may receive more effective treatment. Our findings could enhance our comprehension of the hematopoietic system during inflammatory responses and its involvement in severe hematological disorders that demonstrate impaired HSCs function, such as leukemia and BM failure. Future work using genetic models is needed to dissect further indirect vs. direct effects of external stimulants on HSCs.

The present investigation of hematopoiesis and proinflammatory cytokines fails to account for the interconnections and overlaps among these cytokines and often studies them in isolation. However, in the actual setting of infection, it is rare for a single cytokine to function in isolation. Consequently, concluding the existing literature is difficult since different techniques are used, and it does not accurately reflect the actual situation. Thus, we aimed to address this issue by developing a mouse model with multiple proinflammatory cytokine signaling Knockedout to investigate their overall impact. However, further analysis and comparison with all progenitor knockouts are needed to gain a more comprehensive understanding of the signaling pathways involved in proinflammatory cytokines and their regulation of hematopoiesis. This research may also shed light on how human HSCs behave since humans are constantly exposed to various pathogens, unlike mice, which are maintained in a pathogen-free environment. This constant exposure to pathogens may contribute to the HSC defects that occur with aging. Blocking cytokines that trigger HSCs activation may be a potential treatment option for patients with immune deficiencies or age-related BM failure. Understanding the effects of individual proinflammatory cytokines and combinations of them may improve the treatment of patients suffering from BM failure due to chronic infections or defective DNA repair mechanisms.

5 Materials and Methods

5.1 Materials

Materials not listed in the 'Materials' section will be mentioned in the 'Methods' sections.

5.1.1 Antibodies

Table 1: List of antibodies for flow cytometry

Antigen	Label	Clone	Company
B220	PE-CY7	RA3-6B2	eBiosciences
B220	APC-Cy7	RA3-6B2	eBiosciences
B220	AF700	RA3-6B2	eBiosciences
B220	BUV661	RA3-6B2	BD Biosciences
BrdU	APC	RB6-8C5	eBiosciences
CD45.2	104	Pacific Blue	BioLegend
CD45.1	A20.1	FITC	eBioscience
CD105	Pacific Blue	MU7/18	eBiosciences
CD117	APC-Cy7	2B8	eBiosciences
CD117	PE	2B8	eBiosciences
CD117	BV711	2BB	Biolegend
CD117	APC	2B8	eBiosciences
CD11b	PE-CY7	M1170	eBiosciences
CD11b	AF700	M1/70	eBiosciences
CD11b	PE-CY5	M1/70	eBiosciences
CD11b	BUV805	M1/70	BD Biosciences

CD11c	PE-cy7	HL3	BD Pharmingen™
CD135	PE	A2F10	eBiosciences
CD150	PE-CY5	TC15-12F12.2	Biolegend
CD16/CD32	APC	93	eBiosciences
CD34	AF700	RAM34	eBiosciences
CD34	FITC	RAM34	eBiosciences
CD4	PE-CY7	GK1.5	eBiosciences
CD4	FITC	GK1.5	eBiosciences
CD41	FITC	eBioMWReg30	eBiosciences
CD41	PE	eBioMWReg30	eBiosciences
CD45.1	PE-CY5	A20	eBiosciences
CD45.2	PE-CY7	104	Biolegend
CD48	PE	HM48-1	eBiosciences
CD48	Pacific Blue	HM48-1	Biolegend
CD8a	PE-CY7	53-6.7	eBiosciences
CD8a	AF700	53-6.7	eBiosciences
F4/80	Pacific Blue	-	Bio-Rad
Gr.1	AF700	RB6-8C5	eBiosciences
Gr1	PE-CY7	RB6-8C5	eBiosciences
Gr1	APC	RB6-8C5	eBiosciences

Ki67	FITC	51-36524X	BD Pharmingen™
Ly6G	BUV395	1A8	BD Biosciences
Sca-1	APC	D7	eBiosciences
Sca-1	APC-Cy7	D7	BD Pharmingen™
Ter119	AF700	-	Biolegend
Ter119	PE-CY7	TER-119	eBiosciences
TotalSeq™ anti-mouse Antibody	A0301	Hashtag	BioLegend
TotalSeq™ anti-mouse Antibody	A0302	Hashtag	BioLegend
TotalSeq™ anti-mouse Antibody	A0303	Hashtag	BioLegend
TotalSeq™ anti-mouse Antibody	A0304	Hashtag	BioLegend

5.1.2 qRT-PCR primers

Table 2: List of qRT-PCR pimers and sequences

Gene	Primer	Sequence
Zbp1	fwd	CAGGAAGGCCAAGACATAGC
Zbp1	rev	GACAAATAATCGCAGGGGACT
Irf7	fwd	CTTCAGCACTTTCTTCCGAGA
Irf7	rev	TGTAGTGTGGTGACCCTTGC
Rsad2	fwd	GTGGACGAAGACATGAATGAAC

Rsad2	rev	TCAATTAGGAGGCACTGGAAA
Ifi44	fwd	CTGATTACAAAAGAAGACATGACAGAC
Ifi44	rev	AGGCAAAACCAAAGACTCCA
Plac8	fwd	CAGACCAGCCTGTGTGATTG
Plac8	rev	TCCAAGACAAGTGAAACAAAAGG
Bst2	fwd	GAAGTCACGAAGCTGAACCA
Bst2	rev	CCTGCACTGTGCTAGAAGTCTC
Ligp2	fwd	GCCTGGATTGCAGTTTTGTAA
Ligp2	rev	TCAAATTCTTTAACCTCAGGTGACT
Oasl2	fwd	AGGTGGCTGCAGAAGCTG
Oasl2	rev	TGTTTCACTCTCACCTGAACATC
Oas2	fwd	TAGACCAGGCCGTGGATG
Oas2	rev	GTTTCCCGGCCATAGGAG

5.1.3 Kits

Table 3: List of used kits

Kit	Source	Identifier
APC BrdU Flow Kit	BD Pharmigen	552598
Arcturus® PicoPure® RNA Isolation Kit	Life Technologies	KIT0204
Agilent RNA 6000 Pico Kit	Agilent RNA 6000 Pico Kit	5067-1513
Chromium Next GEM Single Cell 3' GEM, Library & Gel Bead Kit v3.	10x Genomics	1000121

Chromium Next GEM Chip G Single Cell Kit	10x Genomics	1000120
Dynabeads® Untouched™ Mouse Kit	ThermoFischer Scientific	11415D
SuperScript® VILOTM cDNA Synthesis Kit	Life Technologies	11754250

5.1.4 Reagents and cell culture medium

Table 4: Reagents and cell culture medium

Reagent	Source	Identifier
MethoCultTM GF M3434	StemCellTM Technologies	03434
RPMI-1640 Medium	Sigma-Aldrich	R8758
UltraPureTM Distilled Water DNase/RNase Free	ThermoFisher Scientific	10977-035

5.1.5 Equipment

Table 5: List of equipment

Instrument/Material	Source	Identifier
10X Chromium Controller	10x Genomics	1000202
BD LSRFortessa™ Flow Cytometer	BD	BD Fortessa
BD™ LSR II	BD	BD LSR

FACSAria™ Fusion Cell Sorter	BD	BD FACSAria
FACSAria™ I Cell Sorter	BD	BD FACSAria
FACSAria™ II Cell Sorter	BD	BD FACSAria
NovaSeq Sequencing System	Illumina	NovaSeq
Hiseq sequening system	Illumina	

5.1.6 Programs and software

Table 6: List of programs and softwares

Tool	From
FACSDIVA v8.0	BD Biosciences
Flowjo v10	TreeStar
DESeq2	Love, Huber and Anders, 2014
ClusterProfiler	Yu et al., 2012
Pheatmap v1.9.12	N/A
GraphPad Prism v8	GraphPad Software
Adobe illustrator CS6	Adobe systems
Rstudio	RStudio, Inc.

5.2 Methods

5.2.1 Animals

All animal experiments were approved by the local Animal Care and Use Committees of the German Regierungspräsidium Karlsruhe für Tierschutz und Arzneimittelüberwachung (Karlsruhe, Germany). Mice were kept under specific pathogen-free conditions (SPF) in ventilated cages (ICV) in the animal facility of the German Cancer Research Center (DKFZ). Mice used for experiments were 10-20 weeks old at the beginning of the respective experiments. All mice were on a C57Bl/6 background. Wild-type (WT) mice were bred at the DKFZ animal facility under pathogen-free conditions and in line with all standards of animal care or bought from the JANIVER lab. *Ifnar*$^{-/-}$*Ifngr*$^{-/-}$ knockout (KO) mice lack the receptors for both IFNα and IFNγ, leading to a defect in response to these cytokines. *Ifnar*$^{-/-}$*Ifngr*$^{-/-}$*Ilr*$^{-/-}$ *Tnfrsf1dKO* mice lack receptors for TNFα, IL1, IFNγ, and IFNα. Multiple receptor KO mice were generated at the DKFZ animal facility by mating single KO mice to produce homozygous multiple knockout mice finally. *SclCreERT bax*$^{fl-/fl-}$*bak*$^{-/-}$ mice were on a C57Bl/6 background (Takeuchi et al. 2005), and treated for 5 days with 2mg/day tamoxifen to delete bax. To determine the genotype of mice, DNA was extracted from tail biopsies, and genotyping PCR was performed. Mice were sacrificed by cervical dislocation according to German guidelines.

5.2.2 In vivo treatments

To treat the mice with the different pro-inflammatory cytokines and other reagents, the mice were weighed and injected with 200 µl 0,5 mg/kg IFNγ (eBiosciences), 0,25 mg/kg IL1α (Peprotech), 0,25 mg/kg IL1β (Peprotech), 0,05 mg/kg IL6 (R&D Systems), 0,25 mg/kg LPS (Sigma Aldrich), 5 mg/kg pIC (InvivoGen) and 0,75 mg/kg TNFα (Peprotech) intraperitoneally (i.p.), with 100 µl of 50.000 international units (IU) per 20g mouse IFNα (Miltenyi Biotec) subcutaneous (s.c.), and 150 mg/kg 5-FU (InvivoGen).
The reagents were diluted in phosphate-buffered saline (PBS), control mice were injected with 200 µl of PBS i.p., and IFNα control mice were injected with 100 µl PBS s.c. For the *bax*$^{-/-}$*bak*$^{-/-}$ mice, IFNα treatment was started 4 weeks post tamoxifen treatment. For the BrdU incorporation assay, BrdU (18mg/kg, Sigma-Aldrich) was administered i.p. for 14 hours prior to sacrifice.

5.2.3 Organ dissection and preparation of cell suspensions

5.2.3.1 Blood

Blood was collected from the vena facialis by sub-mandibular bleeding into EDTA-coated collection tubes. Blood was analyzed automatically with a Hemavet cell counter (Drew Scientific) or stained for flow cytometry after initial RBC lysis by incubation with ACK lysis buffer (LONZA) for 20 mins.

5.2.3.2 Spleen

The spleen is excised and kept in an RPMI medium. Splenocytes single cell suspension was then obtained by mashing the spleen through 40 µm EASYstrainerTM (Greiner bio-one) and washing with RPMI-1640 medium (Sigma-Aldrich) supplemented with 2% fetal bovine serum (FBS) for 5 min at 1600 rpm, 4°C. RBC lysis was performed by incubation with ACK lysis buffer (LONZA) for 5 mins at room temperature. The lysis reaction was stopped by adding PBS, and cells were washed as before. Cells were then stained for flow cytometry.

5.2.3.3 Bone Marrow

For flow cytometry analysis, BM was isolated from the tibia, femur, hips, and (if required) spine by crushing using mortar and pestle in 2x 5 ml cold RPMI-1640 medium (Sigma-Aldrich) supplemented with 2% fetal bovine serum (FBS). Cell suspensions were filtered through a 40 µm EASYstrainer^{TM} (Greiner bio-one), then counted, and the appropriate cell number was transferred, washed for 5 min at 1600 rpm, 4°C, and used for FACS staining. For cell sorting, an extra step of lineage depletion was performed. This was done by incubating the BM cells with a lineage antibody cocktail against CD4, CD8, CD11b, B220, Gr-1, and Ter119 in RMPI+2%FCS for 45 mins on ice. Afterward, cells were washed for 5 min at 1600 rpm, 4°C, and incubated with Dynabeads® Magnetic Beads (1 per mouse) (Invitrogen) on a wheel for 30 mins at 4°C. Cells were then exposed to a magnet to remove lineage marker-expressing cells. Cells were washed for 5 min at 1600 rpm, 4°C, and suspended in FACS staining buffer.

5.2.4 Cell counting

Cells were diluted with phosphate-buffered saline (PBS) in a ratio of 1:50 to a final volume of 600 µl, and cell numbers were then determined with a Vi-cell automated cell counter (Beckman Coulter).

5.2.5 Flow cytometry and cell sorting

Flow cytometric analyses were performed using fluorochrome-labeled monoclonal antibodies listed in table 1 Antibodies were titrated with the whole BM prior to use and used in concentration according to this titration. All cell suspensions were filtered through a nylon mesh filter (70 µm) prior to FACS analysis, and data were then acquired on the BD LSR Fortessa or LSRII (BD Biosciences). Cell suspension staining was performed in RPMI medium supplemented with 2% FCS. To achieve this, cells were incubated with specific antibodies for 30-60 minutes on ice in the dark. Subsequently, the cells were washed with PBS+2% FBS for 5 mins at 4°C. To identify HSC and progenitor subsets, the cell suspensions were stained with a combination of antibodies, including CD117, Sca-1, CD150, CD48, CD34, CD105, CD16/32, CD135, and lineage antibodies (CD4, CD8, CD11b, Gr-1, B220, and Ter119). In addition, we stained for differentiated cells using B220, CD4, CD8, Ter119, Ly6G, CD11b, CD11c, and F4/80 antibodies. Table 7 displays the surface marker combinations for the cell types investigated in this thesis. For cell sorting, lineage depletion was performed after BM was isolated. Cells were then stained, as mentioned above. Cell sorting was performed on a FACS-sorting Aria I/II or Fusion flow cytometers (BD Bioscience) at the DKFZ flow cytometry service unit.

Table 7: Combination of surface markers for cells studied in this thesis

Cell population	Surface markers
HSCs	$Lin^-Sca1^+cKit^+CD150^+CD48^-CD34^-$
LSK	$Lin^-Sca1^+cKit^+$
MPP1	$Lin^-Sca1^+cKit^+$CD34+CD135-$CD150^+CD48^-$
MPP2	Lin-Sca1+cKit+CD34+CD135-CD150+CD48+
MPP3	$Lin^-Sca1^+cKit^+CD34^+CD135^-CD150^-CD48^+$

MPP4	$Lin^-Sca1^+cKit^+CD34^+CD135^+CD150^-CD48^+$
LS$^-$K	$Lin^-Sca1^-cKit^+$
CMP	$Lin^-Sca1^-cKit^+CD34^+CD16/32^-$
GMP	$Lin^-Sca1^-cKit^+CD34^+CD16/32^+$
MEP	$Lin^-Sca1^-cKit^+CD34^-CD16/32^-$
CLP	$Lin^{Low}cKit^{low}$ $CD127^+CD125^+$
Monocytes	$B220^-$ $CD4^-$ $CD8^-$ $Ly6G^-$ $CD11b^+$ $CD11c^-$ $F4/80^-$
Neutrophils	$B220^-$ $CD4^-$ $CD8^-$ $Ly6G^+$ $CD11b^+$

5.2.6 Ki67 cell cycle analysis

For cell cycle analysis, Ki67-Hoechst staining is used. First surface stained BM cells were fixed with BDCytofix/Cytoperm™ Buffer for 15 mins at 4°C. Cells were then washed with 1x permeabilization buffer and stained with anti-Ki67 antibody overnight at 4°C. Cells were then co-stained with Hoechst 33342 (Molecular Probes) at a dilution of 1:400 for the final 10 min. Cells were washed and resuspended in 1x permeabilization buffer until the acquisition was made.

5.2.7 BrdU proliferation assay

For the BrdU incorporation assay, mice were injected i.p with 200 µL BrdU (18mg/kg, Sigma-Aldrich) for 14 hours prior to sacrifice. BM was isolated as described and stained for surface markers. Subsequently, cells were fixed, and BrdU staining was performed according to the instructions of the BrdU Flow Kit protocol (BD Pharmingen™).

5.2.8 RNA isolation, reverse transcription & quantitative real-time PCR

For all samples for qRT-PCR analysis, cells were sorted directly into 50 µl extraction buffer (Arcturus PicoPure Kit), then spun and frozen. RNA isolation was performed using the PicoPure RNA isolation kit (Arcturus Therapeutics) according to the manufacturer's instructions. Briefly, the isolated RNA samples were treated with 5 µl

DNase and 35 µl RDD buffer per sample with DNase and then incubated for 15 minutes at room temperature. Then, 40 µl wash buffer 1 was added and the samples were centrifuged at 8000 g for 1 minute. The elution step was performed with 16 µl H2O, and the resulting samples were stored at -80°C or used immediately for downstream experiments. To determine the quality and concentration of the isolated RNA, an RNA Pico Chip (Agilent Technologies) was used in the Agilent 2100 Bioanalyzer System (Agilent Technologies), following the instructions in the Agilent RNA 6000 Pico Kit manual (Agilent Technologies). Isolated RNA was reverse transcribed into cDNA using the SuperScript VILO cDNA Synthesis Kit (Invitrogen, ref. 11754-250) according to the manufacturer's protocol. The cDNA was diluted with H2O to the minimum required volume, and 6 µl of the cDNA samples were pipetted into a well of the 384-well plate. Technical triplicates were prepared for each sample. The primer mix contained 0.1 µl forward primer, 0.1 µl reverse primer, 0.8 µl RNase-free water, and 7 µl Power SYBR Green PCR Master Mix (Thermo Fisher Scientific) per sample. 8 µl of the primer mix was added to the cDNA in the 384-well plate, which was then sealed and centrifuged at 1200 rpm for several seconds. The Viia 7 Real-Time PCR System (Thermo Fisher Scientific) was set up according to the recommendations in the Power SYBR Green PCR Master Mix manual. The results were exported, and the fold change of each gene was calculated by normalizing to the housekeeper genes (GAPDH and β-actin) and the PBS control samples and using the ΔΔCT values and analyzed using GraphPad Prism analysis software (GraphPad Software).

5.2.9 Colony-forming assay

BM cells were prepared and stained as described above. 500 primary sorted LSK cells or 20,000 BM cells were plated in 1 ml Methocult 3434® (Stem Cell Technologies). Samples were plated in duplicates in 35 mm2 tissue culture dishes and incubated in a humidified atmosphere at 37°C and 5% CO2. Colonies were counted after 7 days using an inverted microscope. The total number of cells per well was also recorded using the Vi-cell automated cell counter to determine the number of cells/colony. For replating, cells were harvested by washing the culture plates with PBS. Cells were counted using a hemocytometer, and 20,000 cells of each technical replicate were mixed with 1 ml of MethoCult M3434 semisolid medium and applied to a 35-mm culture plate (1 ml/replicate). Colony counts were determined after 5-7 days.

5.2.10 Competitive transplantation assay

For 2KO competitive transplants, 1000 LSKs of CD45.2 experimental mice were mixed with equal numbers of CD45.1.2 WT competitor cells and 100,000 c-kit depleted bone marrow cells. This cell mixture was transplanted via tail vein injection into lethally irradiated (2x5 Rad) CD45.1 congenic WT recipients within 24h after irradiation. All mice were kept on an antibiotic (Cotrim) containing water for 3 weeks post-transplantation. Chimerism and lineage composition was measured by FACS in peripheral blood (PB) at weeks 4, 8, 12, 16, and 18 weeks after transplant. Total PB and chimerisms in the stem/progenitor compartment in BM were evaluated at 18 weeks via animal sacrifice and FACS analysis. At the 18 weeks endpoint, BM was isolated from the primary recipients, and $3x10^6$ cells were diluted in 200 µl PBS and i.v injected into lethally irradiated secondary recipients. The blood chimerism was again measured by FACS in peripheral blood (PB) at weeks 6, 9, and 15 weeks after the transplantation.

For the 5KO competitive transplants, $1.5x10^6$ BM cells of CD45.2 experimental mice were mixed with equal numbers of CD45.1.2 WT competitor cells. This cell mixture was transplanted via tail vein injection into lethally irradiated (2x5 Rad) CD45.1 congenic WT recipients within 24h after irradiation. All mice were kept on an antibiotic (Cotrim) containing water for 3 weeks post-transplantation. Chimerism and lineage composition was measured by FACS in peripheral blood (PB) at weeks 4, 8, and 12 weeks after transplant. This experiment is still ongoing.

5.2.11 Statistical analysis

Flow cytometry data were analyzed using FlowJo software. All graphs and statistical analyses were performed using GraphPad Prism. An unpaired T-test or two- or one-way ANOVA was used to analyze the differences between groups. Statistical significance is indicated by *P ≤ 0.05, ** P ≤ 0.01, ***P ≤ 0.001, **** P ≤ 0.000 Experiments were conducted with three- nine mice per condition, and the results were expressed as mean ± standard error of the mean (SEM). Error bars indicate SEM. For detailed information, please check the figure legends.

5.2.12 Microarray

5.2.12.1 Sample preparation

Total RNA isolation was performed using the PicoPure RNA isolation kit (Arcturus Therapeutics) according to the manufacturer's instructions. To determine the quality and concentration of the isolated RNA, an RNA Pico Chip (Agilent Technologies) was used in the Agilent 2100 Bioanalyzer System (Agilent Technologies), following the instructions of the Agilent RNA 6000 Pico Kit (Agilent Technologies) manual. RNA samples with an RNA integrity (RIN) higher than 7 were submitted to the genomics and proteomics core facility at the DKFZ. Global gene expression was measured using an Affy Clariom S mouse chip. An initial analysis of the results was performed by the core facility.

5.2.12.2 Scanning and preprocessing

The following steps were performed by the microarray unit of the genomics and proteomics core facility at the DKFZ.

Microarray scanning was done using an iScan array scanner. Data extraction was done for all beads individually, and outliers were removed when the absolute difference to the median was greater than 2.5 times MAD (2.5 Hampelís method). All remaining bead-level data points were then quantile normalized. As a test for significance, the studentís t-test was used on the bead expression values of the two groups of interest. In the case of the significance of expression against the background, we tested for greater than all negative beads for this sample. In the case of comparing separate groups, we tested for inequality of the means of the groups. In both cases, Benjamini-Hochberg correction was applied to the complete set of p-values of all ProbeIDs on the chip. The average expression value was calculated as the mean of the measured expressions of beads together with the standard deviation of the beads. The analysis was done with R on the bead-level data, which you can find in the raw data produced by the scanner (e.g. in 5282035051.7z the file 5282035051_A.txt, which holds bead-level data for all probeIDs of sample A). All analyses were done using the following mechanisms: outlier removal, average values over beads are means (not median), and statistical tests are t-tests over all beads (e.g for one probeID over all beads of all samples of a group) in original scale (not log2 scale). Benjamini-Hochberg correction was applied over all p-values of the differential expression analysis. Outliers were

removed by taking only beads with an expression value > 20 before using the 2.5 MADs rule. The ProbeIDs expression value was the mean of the remaining beads. The remaining bead level lists of different lengths for each sample were randomly filled with NAs (NA=not available) and built the bead level matrix on which quantile normalization was performed. Used R and Bioconductor packages: multicore, preprocessCore, affy, oligo, pd.hugene.2.0.st, pd.ragene.2.0.st, pd.mogene.1.0.st.v1

5.2.12.3 Downstream analysis

The provided data from the core facility was analyzed using BioVenn(Hulsen, de Vlieg, and Alkema 2008) web tool (https://www.biovenn.nl/) and R programming language, where the Clusterprofiler package(Yu et al. 2012) was used for Gene ontology analysis and UpSetR(Conway, Lex, and Gehlenborg 2017) was used for intersection analysis between the datasets.

5.2.13 Bulk RNA sequencing

5.2.13.1 Sample preparation and library generation

BM was isolated from 4 WT mice and surface stained as described above but with an additional step in which a live/dead marker was added. Cells were incubated for 15 minutes at room temperature with Zombie Yellow (BioLegend) (as described in the manufacturer's protocol), followed by 30 minutes at 4°C with the appropriate preconjugated surface antibodies (as described above). Cells were then washed twice in PBS. HSC populations from the 4 independent biological replicates were then sorted by FACS directly into RNase-free microfuge tubes (ThermoFisher) containing RNA extraction buffer (Arcturus Therapeutics) until 3000-5000 cells were collected. RNA isolation was performed using the PicoPure RNA isolation kit (Arcturus Therapeutics) according to the manufacturer's protocol (as described above). The quality of the isolated RNA was measured using a Bioanalyzer 2100 (Agilent, Waldbronn, Germany).

Library preparation and sequencing were performed at the Genomics and Proteomics Core Facility at DKFZ. Libraries were prepared using SmarTer Ultra Low Input RNA v4 and NEBNext ChIP-Seq (Takara Bio, USA) according to the manufacturer's instructions. For bulk RNA sequencing in the results section 3.1.2, sequencing was performed with Illumina HiSeq 2000 V4, paired-end 125bp, using the HiSeq Flow Cell v4 sequencing kit. For bulk RNA sequencing in the results section 3.4.6, sequencing

was performed with the Illumina HiSeq 4000, paired-end 100bp, using the HiSeq 3000/4000 sequencing kit PE.

5.2.13.2 Preprocessing and downstream analysis

Paired-end libraries were mapped against the mm10 reference genome with the STAR package version 2.5.3.a to generate the BAM files. Reads were annotated and counted against the GRCm38mm10_PhiX reference genome (Ensembl) using the htseq-count package.Downstream analysis was performed using R (v 4.1. 0). Differentially expressed genes were identified with the DESeq2 package(Love, Huber, and Anders 2014). Gene set enrichment analyses (GSEA) were performed and visualized using broad GSEA software. To visualize and summarize GO terms, enrichment maps(Merico et al. 2010) were made using the enrichment map Cytoscape plugin from the Cytoscape network visualization and analysis software(Cline et al. 2007). KEGG pathway enrichment analysis using the Kyoto Encyclopedia of Genes and Genomes (KEGG) database (http://www.genome.jp/kegg) and GO analysis were performed using the Clusterprofiler R package(Yu et al. 2012). Hierarchical Clustering was created using hclust function in R. Heatmaps were created using the pheatmap R package (https://CRAN.R-project.org/package=pheatmap). Volcano and PCA plots were created using the EnhancedVolcano, and FactoMineR(Lê, Josse, and Husson 2008) R packages, respectively.

5.2.14 Single-cell RNA sequencing

The content presented in this section on methods is sourced from my co-author manuscript which is currently under review for publication and, It is accessible online as a preprint (Bouman*, Demerdash* et al. 2023).

5.2.14.1 FACS sorting

For FACS sorting of single cells, BM cells were isolated, and RBC lysed as described above. This was followed by lineage depletion using a lineage antibody cocktail against CD4, CD8, CD11b, B220, Gr-1, and Ter119 and incubation with Dynabeads® Magnetic Beads (Invitrogen). Lineage-depleted BM cells were stained with Zombie Yellow viability dye (BioLegend) followed by incubation with the following antibodies: CD117, Sca1, CD150, CD48, CD34, and lineage antibodies (B220, CD4, CD8, Ter119, Ly6G, CD11b, CD11c, and F4/80) together with one of the hash antibodies (TotalSeq™-A0301 anti-mouse Hashtag 1 Antibody, TotalSeq™-A0302 anti-mouse Hashtag 2

Antibody, TotalSeq™-A0303 anti-mouse Hashtag 3 Antibody, TotalSeq™-A0304 anti-mouse Hashtag 4 Antibody) (BioLegend, TotalseqA antibodies). The 4 biological replicates of each time point were stained with one of the 4 unique hash antibodies. Cells were sorted using a FACSAria Fusion or FACSAria II equipped with a 100 µm nozzle (BD Biosciences).

5.2.14.2 Single-cell RNA library preparation and Sequencing

HSPC single-cell RNA-seq was performed using the 10X Genomics platform. The Chromium Next GEM single cell 3‘ reagent kits v3.1 were implemented to prepare the libraries, following the official instruction manual (https://www.10xgenomics.com/support/single-cell-gene expression/documentation/steps/library-prep/chromium-single-cell-3-reagent-kits-user-guide-v-3-1-chemistry). Briefly, 10,000 Lin^- $cKit^+$ cells were sorted and enriched for HSCs by sorting additional 3000-4000 Lin^- $cKit^+$ $CD150^+$ $CD48^-$ $CD34^-$ cells. Cells were super-loaded according to the manufacturer’s instructions until the cDNA amplification step. 1 ul/sample of HTO primers was spiked into the cDNA amplification PCR, and cDNA was amplified according to the 10x Single Cell 3′ v3.1 protocol aiming for a targeted cell recovery of 500-6000 cells. Following PCR, cDNA cleanup was performed using SPRI to separate the HTO-derived cDNAs (in the supernatant) from the mRNA-derived cDNAs (retained on beads). The cDNA fraction was processed according to the manufacturer's protocol to generate the transcriptome library. The quality of the obtained cDNA library upon adapter ligation and sample index PCR was assessed on an Agilent Bioanalyzer High sensitivity chip. Library sequencing was performed on the Novaseq 6000 Illumina sequencing platform.

5.2.14.3 Filtering longitudinal single-cell RNAseq dataset

All reads were aligned to the mm10 genome and the coverage of each gene in each cell was counted using version 3.1.0 of the cellranger pipeline. Cells were assigned to their corresponding time point (control, 3h, 24h, or 72h) and batch (four batches per time point) based on hashtag barcodes. Cells with multiple barcodes (multiplets) or missing barcodes (negatives) were excluded from the dataset. The resulting count matrix (cells x genes) had cells with a high percentage of mitochondrial genes (>5%) or a low number of unique genes (<700) removed. Following the filtering steps, the

respective number of cells present in each time point was as follows: control - 2474, 3h - 1661, 24h - 3462, and 72h - 2449

5.2.14.4 Clustering and cell type annotation

The 500 most highly variable genes (HVGs) were identified in the control subset using analytic Pearson residuals (Lause, Berens, and Kobak 2021). The control subset was subsetted for the 500 HVGs, and the counts were L2 normalized. Next, a neighborhood graph was computed using 10 out of 50 principal components and the 15 nearest neighbors. The Leiden algorithm (resolution = 0.8) identified 14 distinct clusters in the control subset (Traag, Waltman, and van Eck 2019). Each cluster was appointed to a cell type based on 1) differentially expressed genes (DEGs) between the cluster of interest and all other clusters, 2) the expression profiles of the HVGs, 3) known marker genes and 4) correlation with cell types in a previously published dataset of the HSPCs (Nestorowa, Hamey, Pijuan Sala, et al. 2016).

5.2.14.5 Label transfer and UMAP representation

In each subset, we identified the top 2000 highly variable genes (HVGs) and used the combined list to subset the complete dataset. The dataset was then L2 normalized, and the different subsets were integrated using Scanorama (Hie, Bryson, and Berger et al. 2019). We used all 100 Scanorama-reduced dimensions to calculate a neighborhood graph with nearest neighbors set to 15, and a two-dimensional UMAP representation was computed using the neighborhood graph. To transfer cell type labels from the control subset to the response subsets (3h, 24h, and 72h), cells in the response subsets were assigned the cell type label that was most common among their 15 nearest neighbors (Euclidean distance) in the control subset. The integrated data was only used for label transfer and visualization purposes. For other downstream analyses, we used the filtered-only dataset and removed eosinophils and monocytes due to the small number of cells assigned to those cell types (10 and 52, respectively)

5.2.14.6 Calculating gene set scores

The filtered dataset was L2 normalized and scaled to unit variance, and zero mean. The ISG score was calculated by subtracting the average expression of a random set of reference genes from the average expression of about 400 known ISGs (Scanpy

function score_genes). Similarly, the stemness (Giladi et al. 2018), necroptosis (GO:0070266), pyroptosis (GO:0070269), myeloid TF (Kwok et al. 2020), monocyte and neutrophil differentiation, cell cycle (Giladi et al. 2018) and purine nucleotide synthesis (Vogel et al. 2019) score were calculated. Genes for each signature are shown in Supplementary table 1. Necroptosis and pyroptosis gene sets were retrieved from the Mouse Genome Database (MGD), Mouse Genome Informatics, The Jackson Laboratory, Bar Harbor, Maine. World Wide Web (URL: http://www.informatics.jax.org). (The data was retrieved in the year 2022)

5.2.14.7 Differential abundance analysis

We used the R package Milo to perform an abundance analysis on the L2 normalized, filtered dataset (Dann et al. 2022b). A neighborhood graph was built using 30 out of 100 of the Scanorama-reduced dimensions (see *Label transfer and UMAP representation*) and 30 nearest neighbors. Afterward, we followed the steps described in the accompanying tutorial (*Milo example on mouse gastrulation dataset*) for each response subset (3h, 24h, and 72h). In each analysis, the control subset served as the reference, to which the response subset would be compared.

5.2.14.8 Identifying response genes

We used the edgeR-LRT method in the Libra R package to find the differentially expressed genes (DEGs) between the control and any of the response subsets, in each cluster (Robinson et al., 2010; Squair et al., 2021). We considered only DEGs with an adjusted p-value higher than 0.05 and a log-fold change higher than 1 in at least one cluster. For the downstream analyses of the response genes, we consider only the 500 DEGs with the highest p-values. In case a DEG is found in more than one cluster and/or time point, we take only the highest p-value into consideration.

5.2.14.9 Change score

We L2 normalized the filtered dataset per cell. For each response gene we took the mean expression in each cluster per time point. The expression change was calculated as the absolutes sum of the derivative of the mean expression across all time points. The result is a matrix with change scores per cluster for each of the response genes.

We applied hierarchical clustering and grouped the response genes into 14 groups by setting a threshold at the cophenetic distance of 3 (Scipy function cluster.hierarchy.linkage and cluster.hierarchy.fcluster).

5.2.14.10 Pseudotemporal ordering of cells during response

We opt to find a pseudotime axis that correlates with the actual arrow of time. Thus, we look for a transformation (W of size G,1) of the expression data from all time points that reconstructs the experimental time point of each cell with minimal error (ε):

$$X*W = T + \varepsilon$$

Here, X (of size N,G) is the filtered count matrix after L2 normalization, scaling and subsetting for all response genes. T is a vector (of size [G,1]) with an (experimental) time assignment for each cell, created by taking the experimental time points (control, 3h, 24h, and 72h) and converting those to 0, 1, 2, and 3 respectively (alternatively one could consider using the actual time values on a log-scale). The least squares solution for W (which minimizes $\varepsilon^T * \varepsilon$) is given by:

$$W = (X^T X)^{-1} * X^T * T$$

We used the expression matrix X with the size of 9983 cells and 2501 genes and the cells' corresponding time labels to solve the above linear regression problem. We note that in order to avoid over-parametrization and to ensure the identifiability of the solution, the number of cells has to be larger than the number of genes. After W has been retrieved, a pseudotime coordinate can be calculated for each cell by:

$$PT = X * W$$

5.2.14.11 Gene expression in pseudotime

Expression profiles of individual genes in response pseudotime were derived using a combination of bin smoothing and bootstrapping. To find the expression profile in the complete dataset, bin smoothing with a 600-cell window size was performed on a sample of 50% of the cells in the dataset. This was repeated 20 times to find the mean expression, which defines the expression profile. The 95% confidence intervals were calculated by multiplying the standard error with 1.96 and subtracting or adding to the mean. For the cluster-specific expression profiles of individual genes a 50-cell window size was chosen instead, because of the smaller number of cells in each cluster.

5.2.14.12 Gene score in pseudotime

The gene set score profile in response pseudotime was calculated using a combination of locally weighted least squares regression (LOESS) smoothing and bootstrapping. For each cluster LOESS smoothing with a first order regression model was applied to 50% of the cells. This was repeated 30 times. The score profile was derived by taking the mean and 1.96 times the standard error for the 95% confidence intervals.

5.2.14.13 Code availability

All scripts used in this study are available on Github: https://github.com/bjbouman/prj_HSPC.

5.2.14.14 Data availability

The single-cell RNA-seq data were deposited in the Gene Expression Omnibus (GEO) under accession code GSE226824.

6 Appendix

Supplementary table 1

Gene	Description
Abca9	Interferon stimulated gene (ISG)
Abce1	Interferon stimulated gene (ISG)
Ablim3	Interferon stimulated gene (ISG)
Abtb2	Interferon stimulated gene (ISG)
Acsl1	Interferon stimulated gene (ISG)
Adamdec1	Interferon stimulated gene (ISG)
Adar	Interferon stimulated gene (ISG)
Adm	Interferon stimulated gene (ISG)
Agpat9	Interferon stimulated gene (ISG)
Aim2	Interferon stimulated gene (ISG)
Akt3	Interferon stimulated gene (ISG)
Aldh1a1	Interferon stimulated gene (ISG)
Alyref	Interferon stimulated gene (ISG)
Amph	Interferon stimulated gene (ISG)
Angptl1	Interferon stimulated gene (ISG)
Ankrd22	Interferon stimulated gene (ISG)
Apol2	Interferon stimulated gene (ISG)
Apol6	Interferon stimulated gene (ISG)
Aqp9	Interferon stimulated gene (ISG)
Arg2	Interferon stimulated gene (ISG)
Arhgef3	Interferon stimulated gene (ISG)
Arntl	Interferon stimulated gene (ISG)
Atf2	Interferon stimulated gene (ISG)
Atf3	Interferon stimulated gene (ISG)
B2m	Interferon stimulated gene (ISG)
Bag1	Interferon stimulated gene (ISG)
Bak1	Interferon stimulated gene (ISG)
Banf1	Interferon stimulated gene (ISG)
Batf2	Interferon stimulated gene (ISG)
Bax	Interferon stimulated gene (ISG)
Bcl2	Interferon stimulated gene (ISG)
Bcl2l1	Interferon stimulated gene (ISG)
Bcl3	Interferon stimulated gene (ISG)
Birc2	Interferon stimulated gene (ISG)
Birc3	Interferon stimulated gene (ISG)
Blvra	Interferon stimulated gene (ISG)
Blzf1	Interferon stimulated gene (ISG)
Bst2	Interferon stimulated gene (ISG)

Bub1	Interferon stimulated gene (ISG)
C10orf10	Interferon stimulated gene (ISG)
C15orf48	Interferon stimulated gene (ISG)
C1S	Interferon stimulated gene (ISG)
C22orf28	Interferon stimulated gene (ISG)
C4orf32	Interferon stimulated gene (ISG)
C4orf33	Interferon stimulated gene (ISG)
C9orf91	Interferon stimulated gene (ISG)
Calr	Interferon stimulated gene (ISG)
Canx	Interferon stimulated gene (ISG)
Casp1	Interferon stimulated gene (ISG)
Casp7	Interferon stimulated gene (ISG)
Ccdc75	Interferon stimulated gene (ISG)
Ccl11	Interferon stimulated gene (ISG)
Ccl2	Interferon stimulated gene (ISG)
Ccl22	Interferon stimulated gene (ISG)
Ccl4	Interferon stimulated gene (ISG)
Ccl5	Interferon stimulated gene (ISG)
Ccna1	Interferon stimulated gene (ISG)
Ccr1	Interferon stimulated gene (ISG)
Ccr7	Interferon stimulated gene (ISG)
Cd163	Interferon stimulated gene (ISG)
Cd274	Interferon stimulated gene (ISG)
Cd38	Interferon stimulated gene (ISG)
Cd40	Interferon stimulated gene (ISG)
Cd69	Interferon stimulated gene (ISG)
Cd74	Interferon stimulated gene (ISG)
Cd9	Interferon stimulated gene (ISG)
Cdk17	Interferon stimulated gene (ISG)
Cdk18	Interferon stimulated gene (ISG)
Cdkn1a	Interferon stimulated gene (ISG)
Ces1	Interferon stimulated gene (ISG)
Cfb	Interferon stimulated gene (ISG)
Chmp5	Interferon stimulated gene (ISG)
Chuk	Interferon stimulated gene (ISG)
Ciita	Interferon stimulated gene (ISG)
Clec4d	Interferon stimulated gene (ISG)
Clec4e	Interferon stimulated gene (ISG)
Clec5a	Interferon stimulated gene (ISG)
Cnp	Interferon stimulated gene (ISG)
Commd3	Interferon stimulated gene (ISG)
Cpt1a	Interferon stimulated gene (ISG)

Creb3l3	Interferon stimulated gene (ISG)
Crebbp	Interferon stimulated gene (ISG)
Crebzf	Interferon stimulated gene (ISG)
Crp	Interferon stimulated gene (ISG)
Cry1	Interferon stimulated gene (ISG)
Csrnp1	Interferon stimulated gene (ISG)
Cx3cl1	Interferon stimulated gene (ISG)
Cxcl10	Interferon stimulated gene (ISG)
Cxcl9	Interferon stimulated gene (ISG)
Cxcr4	Interferon stimulated gene (ISG)
Cyp1b1	Interferon stimulated gene (ISG)
Cyth1	Interferon stimulated gene (ISG)
Dcp1a	Interferon stimulated gene (ISG)
Ddit4	Interferon stimulated gene (ISG)
Ddx58	Interferon stimulated gene (ISG)
Ddx60	Interferon stimulated gene (ISG)
Dhx58	Interferon stimulated gene (ISG)
Dtx3l	Interferon stimulated gene (ISG)
Duox2	Interferon stimulated gene (ISG)
Dusp5	Interferon stimulated gene (ISG)
Dynlt1	Interferon stimulated gene (ISG)
Ehd4	Interferon stimulated gene (ISG)
Eif2ak2	Interferon stimulated gene (ISG)
Eif3l	Interferon stimulated gene (ISG)
Elf1	Interferon stimulated gene (ISG)
Enpp1	Interferon stimulated gene (ISG)
Epas1	Interferon stimulated gene (ISG)
Erlin1	Interferon stimulated gene (ISG)
Etv6	Interferon stimulated gene (ISG)
Ext1	Interferon stimulated gene (ISG)
Fadd	Interferon stimulated gene (ISG)
Fam125b	Interferon stimulated gene (ISG)
Fam134b	Interferon stimulated gene (ISG)
Fam46a	Interferon stimulated gene (ISG)
Fam46c	Interferon stimulated gene (ISG)
Fam70a	Interferon stimulated gene (ISG)
Fbxo6	Interferon stimulated gene (ISG)
Fcgr1a	Interferon stimulated gene (ISG)
Ffar2	Interferon stimulated gene (ISG)
Fgr	Interferon stimulated gene (ISG)
Fkbp5	Interferon stimulated gene (ISG)
Flt1	Interferon stimulated gene (ISG)

Fndc3b	Interferon stimulated gene (ISG)
Fndc4	Interferon stimulated gene (ISG)
Fosl1	Interferon stimulated gene (ISG)
Fut4	Interferon stimulated gene (ISG)
Fv1	Interferon stimulated gene (ISG)
Fzd5	Interferon stimulated gene (ISG)
G6Pc	Interferon stimulated gene (ISG)
Gak	Interferon stimulated gene (ISG)
Galnt2	Interferon stimulated gene (ISG)
Gbp2	Interferon stimulated gene (ISG)
Gbp4	Interferon stimulated gene (ISG)
Gbp5	Interferon stimulated gene (ISG)
Gca	Interferon stimulated gene (ISG)
Gch1	Interferon stimulated gene (ISG)
Gem	Interferon stimulated gene (ISG)
Gja4	Interferon stimulated gene (ISG)
Gk	Interferon stimulated gene (ISG)
Glipr2	Interferon stimulated gene (ISG)
Glrx	Interferon stimulated gene (ISG)
Gmpr	Interferon stimulated gene (ISG)
Gpx2	Interferon stimulated gene (ISG)
Gtpbp2	Interferon stimulated gene (ISG)
Gzmb	Interferon stimulated gene (ISG)
Hbxip	Interferon stimulated gene (ISG)
Heg1	Interferon stimulated gene (ISG)
Herc6	Interferon stimulated gene (ISG)
Hesx1	Interferon stimulated gene (ISG)
Hk2	Interferon stimulated gene (ISG)
Hla-f	Interferon stimulated gene (ISG)
Hla-g	Interferon stimulated gene (ISG)
Hnrnpul1	Interferon stimulated gene (ISG)
Hpse	Interferon stimulated gene (ISG)
Hsh2d	Interferon stimulated gene (ISG)
Hyal1	Interferon stimulated gene (ISG)
Hyal2	Interferon stimulated gene (ISG)
Hyal3	Interferon stimulated gene (ISG)
Ido1	Interferon stimulated gene (ISG)
Ifi27l2	Interferon stimulated gene (ISG)
Ifi30	Interferon stimulated gene (ISG)
Ifi35	Interferon stimulated gene (ISG)
Ifi44	Interferon stimulated gene (ISG)
Ifi44l	Interferon stimulated gene (ISG)

Ifih1	Interferon stimulated gene (ISG)
Ifit1	Interferon stimulated gene (ISG)
Ifit2	Interferon stimulated gene (ISG)
Ifit3	Interferon stimulated gene (ISG)
Ifitm1	Interferon stimulated gene (ISG)
Ifitm2	Interferon stimulated gene (ISG)
Ifitm3	Interferon stimulated gene (ISG)
Ifne	Interferon stimulated gene (ISG)
Igfbp2	Interferon stimulated gene (ISG)
Ikbkb	Interferon stimulated gene (ISG)
Ikbke	Interferon stimulated gene (ISG)
Ikbkg	Interferon stimulated gene (ISG)
Il10	Interferon stimulated gene (ISG)
Il12B	Interferon stimulated gene (ISG)
Il12rb1	Interferon stimulated gene (ISG)
Il15	Interferon stimulated gene (ISG)
Il15ra	Interferon stimulated gene (ISG)
Il17rb	Interferon stimulated gene (ISG)
Il1r1	Interferon stimulated gene (ISG)
Il1rn	Interferon stimulated gene (ISG)
Il23a	Interferon stimulated gene (ISG)
Il23r	Interferon stimulated gene (ISG)
Il28ra	Interferon stimulated gene (ISG)
Il6	Interferon stimulated gene (ISG)
Il6st	Interferon stimulated gene (ISG)
Impa2	Interferon stimulated gene (ISG)
Irf1	Interferon stimulated gene (ISG)
Irf2	Interferon stimulated gene (ISG)
Irf3	Interferon stimulated gene (ISG)
Irf7	Interferon stimulated gene (ISG)
Irf9	Interferon stimulated gene (ISG)
Isg15	Interferon stimulated gene (ISG)
Isg20	Interferon stimulated gene (ISG)
Itch	Interferon stimulated gene (ISG)
Ivns1abp	Interferon stimulated gene (ISG)
Jak2	Interferon stimulated gene (ISG)
Jun	Interferon stimulated gene (ISG)
Junb	Interferon stimulated gene (ISG)
Lamp3	Interferon stimulated gene (ISG)
Lap3	Interferon stimulated gene (ISG)
Lcn2	Interferon stimulated gene (ISG)
Lepr	Interferon stimulated gene (ISG)

Lgals3	Interferon stimulated gene (ISG)
Lgals9	Interferon stimulated gene (ISG)
Lgmn	Interferon stimulated gene (ISG)
Lipa	Interferon stimulated gene (ISG)
Lmo2	Interferon stimulated gene (ISG)
Lta	Interferon stimulated gene (ISG)
Ly6e	Interferon stimulated gene (ISG)
Mab21l2	Interferon stimulated gene (ISG)
Mafb	Interferon stimulated gene (ISG)
Maff	Interferon stimulated gene (ISG)
Map3k14	Interferon stimulated gene (ISG)
Map3k5	Interferon stimulated gene (ISG)
Mapkapk2	Interferon stimulated gene (ISG)
Mastl	Interferon stimulated gene (ISG)
Mavs	Interferon stimulated gene (ISG)
Max	Interferon stimulated gene (ISG)
Mb21d1	Interferon stimulated gene (ISG)
Mcl1	Interferon stimulated gene (ISG)
Med14	Interferon stimulated gene (ISG)
Mfn1	Interferon stimulated gene (ISG)
Micb	Interferon stimulated gene (ISG)
Mkx	Interferon stimulated gene (ISG)
Mov10	Interferon stimulated gene (ISG)
Ms4a4a	Interferon stimulated gene (ISG)
Mst1r	Interferon stimulated gene (ISG)
Mt1h	Interferon stimulated gene (ISG)
Mthfd2l	Interferon stimulated gene (ISG)
Myd88	Interferon stimulated gene (ISG)
Myof	Interferon stimulated gene (ISG)
N4bp1	Interferon stimulated gene (ISG)
Nampt	Interferon stimulated gene (ISG)
Napa	Interferon stimulated gene (ISG)
Ncf1	Interferon stimulated gene (ISG)
Ncoa3	Interferon stimulated gene (ISG)
Ndc80	Interferon stimulated gene (ISG)
Nfil3	Interferon stimulated gene (ISG)
Nlrx1	Interferon stimulated gene (ISG)
Nmi	Interferon stimulated gene (ISG)
Nod2	Interferon stimulated gene (ISG)
Nos2	Interferon stimulated gene (ISG)
Npas2	Interferon stimulated gene (ISG)
Nt5c3	Interferon stimulated gene (ISG)

Nup50	Interferon stimulated gene (ISG)
Oas1	Interferon stimulated gene (ISG)
Oas1b	Interferon stimulated gene (ISG)
Oas2	Interferon stimulated gene (ISG)
Oas3	Interferon stimulated gene (ISG)
Oasl	Interferon stimulated gene (ISG)
Odc1	Interferon stimulated gene (ISG)
Ogfr	Interferon stimulated gene (ISG)
Optn	Interferon stimulated gene (ISG)
Otub1	Interferon stimulated gene (ISG)
Otub2	Interferon stimulated gene (ISG)
P2ry6	Interferon stimulated gene (ISG)
Pabpc4	Interferon stimulated gene (ISG)
Padi2	Interferon stimulated gene (ISG)
Pdgfrl	Interferon stimulated gene (ISG)
Pdia3	Interferon stimulated gene (ISG)
Pdk1	Interferon stimulated gene (ISG)
Pfdn6	Interferon stimulated gene (ISG)
Pfkfb3	Interferon stimulated gene (ISG)
Phf15	Interferon stimulated gene (ISG)
Pi4k2b	Interferon stimulated gene (ISG)
Pias1	Interferon stimulated gene (ISG)
Pim3	Interferon stimulated gene (ISG)
Pin1	Interferon stimulated gene (ISG)
Plekha4	Interferon stimulated gene (ISG)
Plin2	Interferon stimulated gene (ISG)
Plp1	Interferon stimulated gene (ISG)
Plscr1	Interferon stimulated gene (ISG)
Pml	Interferon stimulated gene (ISG)
Pmm2	Interferon stimulated gene (ISG)
Pnpt1	Interferon stimulated gene (ISG)
Pnrc1	Interferon stimulated gene (ISG)
Ppm1k	Interferon stimulated gene (ISG)
Prkd2	Interferon stimulated gene (ISG)
Prkra	Interferon stimulated gene (ISG)
Psmb5	Interferon stimulated gene (ISG)
Psmb6	Interferon stimulated gene (ISG)
Psmb8	Interferon stimulated gene (ISG)
Psmb9	Interferon stimulated gene (ISG)
Ptpn2	Interferon stimulated gene (ISG)
Ptpn6	Interferon stimulated gene (ISG)
Pus1	Interferon stimulated gene (ISG)

Pxk	Interferon stimulated gene (ISG)
Rab27a	Interferon stimulated gene (ISG)
Raf1	Interferon stimulated gene (ISG)
Rasgef1b	Interferon stimulated gene (ISG)
Rassf4	Interferon stimulated gene (ISG)
Rbck1	Interferon stimulated gene (ISG)
Rbm25	Interferon stimulated gene (ISG)
Rela	Interferon stimulated gene (ISG)
Rgs1	Interferon stimulated gene (ISG)
Ripk1	Interferon stimulated gene (ISG)
Rnase4	Interferon stimulated gene (ISG)
Rnasel	Interferon stimulated gene (ISG)
Rnf114	Interferon stimulated gene (ISG)
Rnf216	Interferon stimulated gene (ISG)
Rpl22	Interferon stimulated gene (ISG)
Rps15a	Interferon stimulated gene (ISG)
Rsad2	Interferon stimulated gene (ISG)
Rtp4	Interferon stimulated gene (ISG)
S100a8	Interferon stimulated gene (ISG)
Saa1	Interferon stimulated gene (ISG)
Samd4a	Interferon stimulated gene (ISG)
Samhd1	Interferon stimulated gene (ISG)
Sat1	Interferon stimulated gene (ISG)
Scarb2	Interferon stimulated gene (ISG)
Sco2	Interferon stimulated gene (ISG)
Sectm1	Interferon stimulated gene (ISG)
Serpinb9	Interferon stimulated gene (ISG)
Serpine1	Interferon stimulated gene (ISG)
Serping1	Interferon stimulated gene (ISG)
Sike1	Interferon stimulated gene (ISG)
Sirpa	Interferon stimulated gene (ISG)
Slc15a3	Interferon stimulated gene (ISG)
Slc16a1	Interferon stimulated gene (ISG)
Slc1a1	Interferon stimulated gene (ISG)
Slc25a28	Interferon stimulated gene (ISG)
Slc25a30	Interferon stimulated gene (ISG)
Slfn5	Interferon stimulated gene (ISG)
Smad3	Interferon stimulated gene (ISG)
Snn	Interferon stimulated gene (ISG)
Socs1	Interferon stimulated gene (ISG)
Socs2	Interferon stimulated gene (ISG)
Socs3	Interferon stimulated gene (ISG)

Sp110	Interferon stimulated gene (ISG)
Spaca3	Interferon stimulated gene (ISG)
Spn	Interferon stimulated gene (ISG)
Spsb1	Interferon stimulated gene (ISG)
Sptlc2	Interferon stimulated gene (ISG)
Ssbp3	Interferon stimulated gene (ISG)
Stap1	Interferon stimulated gene (ISG)
Stard5	Interferon stimulated gene (ISG)
Stat1	Interferon stimulated gene (ISG)
Stat2	Interferon stimulated gene (ISG)
Stat3	Interferon stimulated gene (ISG)
Steap4	Interferon stimulated gene (ISG)
Sun2	Interferon stimulated gene (ISG)
Tagap	Interferon stimulated gene (ISG)
Tank	Interferon stimulated gene (ISG)
Tap1	Interferon stimulated gene (ISG)
Tap2	Interferon stimulated gene (ISG)
Tapbp	Interferon stimulated gene (ISG)
Tbk1	Interferon stimulated gene (ISG)
Tbx3	Interferon stimulated gene (ISG)
Tcf7l2	Interferon stimulated gene (ISG)
Tdrd7	Interferon stimulated gene (ISG)
Tfec	Interferon stimulated gene (ISG)
Thbd	Interferon stimulated gene (ISG)
Ticam1	Interferon stimulated gene (ISG)
Timp1	Interferon stimulated gene (ISG)
Tlk2	Interferon stimulated gene (ISG)
Tlr3	Interferon stimulated gene (ISG)
Tlr7	Interferon stimulated gene (ISG)
Tlr8	Interferon stimulated gene (ISG)
Tmem140	Interferon stimulated gene (ISG)
Tmem173	Interferon stimulated gene (ISG)
Tmem51	Interferon stimulated gene (ISG)
Tnf	Interferon stimulated gene (ISG)
Tnfaip3	Interferon stimulated gene (ISG)
Tnfrsf10a	Interferon stimulated gene (ISG)
Tnfrsf9	Interferon stimulated gene (ISG)
Tnfsf10	Interferon stimulated gene (ISG)
Traf2	Interferon stimulated gene (ISG)
Traf3	Interferon stimulated gene (ISG)
Traf6	Interferon stimulated gene (ISG)
Trafd1	Interferon stimulated gene (ISG)

Trex1	Interferon stimulated gene (ISG)
Trim14	Interferon stimulated gene (ISG)
Trim21	Interferon stimulated gene (ISG)
Trim25	Interferon stimulated gene (ISG)
Trim38	Interferon stimulated gene (ISG)
Trim5	Interferon stimulated gene (ISG)
Trim56	Interferon stimulated gene (ISG)
Txnip	Interferon stimulated gene (ISG)
Tyk2	Interferon stimulated gene (ISG)
Tymp	Interferon stimulated gene (ISG)
Uba7	Interferon stimulated gene (ISG)
Ube2l6	Interferon stimulated gene (ISG)
Ulk4	Interferon stimulated gene (ISG)
Unc93b1	Interferon stimulated gene (ISG)
Upp2	Interferon stimulated gene (ISG)
Uri1	Interferon stimulated gene (ISG)
Usp18	Interferon stimulated gene (ISG)
Vamp5	Interferon stimulated gene (ISG)
Vav1	Interferon stimulated gene (ISG)
Vegfc	Interferon stimulated gene (ISG)
Vmp1	Interferon stimulated gene (ISG)
Wars	Interferon stimulated gene (ISG)
Whamm	Interferon stimulated gene (ISG)
Xaf1	Interferon stimulated gene (ISG)
Xcl1	Interferon stimulated gene (ISG)
Xpr1	Interferon stimulated gene (ISG)
Zbp1	Interferon stimulated gene (ISG)
Zc3hav1	Interferon stimulated gene (ISG)
Znf295	Interferon stimulated gene (ISG)
Znf385b	Interferon stimulated gene (ISG)
1110017F19Rik	Stemness gene
4931406C07Rik	Stemness gene
AK046388	Stemness gene
AK079675	Stemness gene
Acot1	Stemness gene
Aldoc	Stemness gene
B144;Lst1	Stemness gene
Basp1	Stemness gene
Bgn	Stemness gene
Car2	Stemness gene
Cd27	Stemness gene
Cd274	Stemness gene

Cd74	Stemness gene
Cd81	Stemness gene
Cish	Stemness gene
Clip3	Stemness gene
Dapp1	Stemness gene
Dkkl1	Stemness gene
Eltd1	Stemness gene
Gabarapl1	Stemness gene
Gcnt2	Stemness gene
Gimap1	Stemness gene
Gimap6	Stemness gene
Gm6251	Stemness gene
Gpr56	Stemness gene
H2-K1	Stemness gene
Hlf	Stemness gene
Hoxb2	Stemness gene
Ifitm1	Stemness gene
Ifitm2	Stemness gene
Ifitm3	Stemness gene
Krt18	Stemness gene
Ldhb	Stemness gene
Leprel2	Stemness gene
Lhcgr	Stemness gene
Lmo2	Stemness gene
Ly6a	Stemness gene
Malat1	Stemness gene
Mecom	Stemness gene
Mllt3	Stemness gene
Mpl	Stemness gene
Mycn	Stemness gene
Myct1	Stemness gene
Myl10	Stemness gene
Nfe2	Stemness gene
Oasl2	Stemness gene
Osbpl1a	Stemness gene
Pcp4l1	Stemness gene
Pde4b	Stemness gene
Pdzk1ip1	Stemness gene
Pglyrp2;tagL	Stemness gene
Pla2g16	Stemness gene
Pnrc1	Stemness gene
Procr	Stemness gene

Ptplad2	Stemness gene
Ptpn18	Stemness gene
Ptprcap	Stemness gene
Rbp1	Stemness gene
Rbpms;Rbpms2	Stemness gene
Rgs1	Stemness gene
Rtp4	Stemness gene
Shisa5	Stemness gene
Srgn	Stemness gene
Stxbp4	Stemness gene
Tbxas1	Stemness gene
Tmem176a	Stemness gene
Tmem176b	Stemness gene
Tnip3	Stemness gene
Txnip	Stemness gene
Ube2l6	Stemness gene
Wfdc2	Stemness gene
Zfand5	Stemness gene
Zfp831	Stemness gene
Aifm1	Necroptosis
Birc2	Necroptosis
Birc3	Necroptosis
Bok	Necroptosis
Casp2	Necroptosis
Casp6	Necroptosis
Casp8	Necroptosis
Cav1	Necroptosis
Cflar	Necroptosis
Cyld	Necroptosis
Dnm1l	Necroptosis
Fadd	Necroptosis
Fas	Necroptosis
Fasl	Necroptosis
Ipmk	Necroptosis
Itpk1	Necroptosis
Map3k7	Necroptosis
Mlkl	Necroptosis
Mutyh	Necroptosis
Nlrp6	Necroptosis
Parp1	Necroptosis
Peli1	Necroptosis
Pgam5	Necroptosis

Ppif	Necroptosis
Pygl	Necroptosis
Rbck1	Necroptosis
Ripk1	Necroptosis
Ripk3	Necroptosis
Rnf31	Necroptosis
Slc25a4	Necroptosis
Spata2	Necroptosis
Tlr3	Necroptosis
Tnf	Necroptosis
Tnfrsf23	Necroptosis
Trp53	Necroptosis
Trpm7	Necroptosis
Ybx3	Necroptosis
Zbp1	Necroptosis
Aim2	Pyroptosis
Casp1	Pyroptosis
Casp4	Pyroptosis
Casp6	Pyroptosis
Dhx9	Pyroptosis
Nlrc4	Pyroptosis
Naip2	Pyroptosis
Papss2	Monoccyte differenttiation
Ass1	Monoccyte differenttiation
Tcfec	Monoccyte differenttiation
Trem2	Monoccyte differenttiation
Rassf4	Monoccyte differenttiation
Ly6c2	Monoccyte differenttiation
Ms4a6c	Monoccyte differenttiation
F13a1	Monoccyte differenttiation
Ctss	Monoccyte differenttiation
Klf4	Monoccyte differenttiation
S100a4	Monoccyte differenttiation
Slpi	Monoccyte differenttiation
Prdx4	Monoccyte differenttiation
Hpse	Monoccyte differenttiation
Tifab	Monoccyte differenttiation
Csf1r	Monoccyte differenttiation
Ly86	Monoccyte differenttiation
Emb	Monoccyte differenttiation
Glipr1	Monoccyte differenttiation
Irf8	Monoccyte differenttiation

Elane	Monoccyte differenttiation
Ifitm1	Monoccyte differenttiation
Gpr56	Monoccyte differenttiation
Cd34	Monoccyte differenttiation
Eltd1	Monoccyte differenttiation
Serpina3f	Monoccyte differenttiation
Ifitm6	Neutrophil differentiation
Chi3l3	Neutrophil differentiation
S100a9	Neutrophil differentiation
Ngp	Neutrophil differentiation
Syne1	Neutrophil differentiation
S100a8	Neutrophil differentiation
Orm1	Neutrophil differentiation
Chi3l1	Neutrophil differentiation
Ltf	Neutrophil differentiation
Lrg1	Neutrophil differentiation
Pglyrp1	Neutrophil differentiation
Itgb2l	Neutrophil differentiation
Camp	Neutrophil differentiation
Cd177	Neutrophil differentiation
Lcn2	Neutrophil differentiation
Fcnb	Neutrophil differentiation
Mpo	Neutrophil differentiation
Elane	Neutrophil differentiation
Gstm1	Neutrophil differentiation
Ifitm1	Neutrophil differentiation
Gpr56	Neutrophil differentiation
Cd34	Neutrophil differentiation
Eltd1	Neutrophil differentiation
Serpina3f	Neutrophil differentiation
Prc1	cellcycle
Pcna	cellcycle
Nucks1	cellcycle
Nde1	cellcycle
Mki67	cellcycle
Mcm6	cellcycle
Mcm5	cellcycle
Lig1	cellcycle
Lbr	cellcycle
Kif22	cellcycle
Kif11	cellcycle
Incenp	cellcycle

Hn1	cellcycle
H3f3a	cellcycle
H2afx	cellcycle
Ezh2	cellcycle
Ect2	cellcycle
Dyrk1a	cellcycle
Dnajc9	cellcycle
Ctcf	cellcycle
Clspn	cellcycle
Ckap2l	cellcycle
Cit	cellcycle
Cenpm	cellcycle
Cenpf	cellcycle
Cenpe	cellcycle
Cenpa	cellcycle
Cdk1	cellcycle
Cdca8	cellcycle
Cdca3	cellcycle
Ccnb2	cellcycle
Ccnd2	cellcycle
Ccne1	cellcycle
Ccne2	cellcycle
Cdkn1b	cellcycle
Ccnb1	cellcycle
Ccna2	cellcycle
Ccnf	cellcycle
Ccnb2	cellcycle
Ccng1	cellcycle
Cdk4	cellcycle
Cdk6'	cellcycle
Nme2	Purine nuceleotide synthesis
Pnp	Purine nuceleotide synthesis
Impdh2	Purine nuceleotide synthesis
Ppat	Purine nuceleotide synthesis
Hprt	Purine nuceleotide synthesis
Aprt	Purine nuceleotide synthesis
Gda	Purine nuceleotide synthesis
Ampd2	Purine nuceleotide synthesis
Cebpe	Myeloid transcription factor
Calr	Myeloid transcription factor
Arid3a	Myeloid transcription factor
Gfi1	Myeloid transcription factor

Lmo4	Myeloid transcription factor
Cebpa	Myeloid transcription factor
Spi1	Myeloid transcription factor
Cux1	Myeloid transcription factor
Scand1	Myeloid transcription factor
Nfkbia	Myeloid transcription factor
Irf8	Myeloid transcription factor
Id2	Myeloid transcription factor
Chd3	Myeloid transcription factor
Cbfa2t3	Myeloid transcription factor
Etv6	Myeloid transcription factor
Stat3	Myeloid transcription factor
Pnrc1	Myeloid transcription factor
Pbx1	Myeloid transcription factor
Mef2c	Myeloid transcription factor
Fli1	Myeloid transcription factor
Elf1	Myeloid transcription factor
Lmo2	Myeloid transcription factor
Cited2	Myeloid transcription factor
Sox4	Myeloid transcription factor
Runx1	Myeloid transcription factor
Gata2	Myeloid transcription factor
Nfe2	Myeloid transcription factor
Myb	Myeloid transcription factor
Foxp1	Myeloid transcription factor
Zfpm1	Myeloid transcription factor
Hmgb3	Myeloid transcription factor
Klf1	Myeloid transcription factor
Gfi1b	Myeloid transcription factor
Tcf3	Myeloid transcription factor
Pa2g4	Myeloid transcription factor
Mbd2	Myeloid transcription factor
Gata1	Myeloid transcription factor
Phf10	Myeloid transcription factor
Phb2	Myeloid transcription factor
Gtf2f1	Myeloid transcription factor
Csda	Myeloid transcription factor
E2f4	Myeloid transcription factor
Cited4	Myeloid transcription factor
Ccne1	Myeloid transcription factor

6.1 List of abbreviations

Abbreviation	Definition
α	Alpha
β	Beta
γ	gamma
2KO	*Ifnar*$^{-/-}$*Ifngr*$^{-/-}$
5-FU	5-Fluorouracil
5KO	Ifnar$^{-/-}$Ifngr$^{-/-}$Tnfrsf1a$^{-/-}$Tnfrsf1b$^{-/-}$Il1r$^{-/-}$
AGM	Aorta-Gonad-Mesonephros
aHSC	Active hematopoetic stem cells
APCs	antigen-presenting cells
BCG	Bacille Calmette-Guérin
BM	bone marrow
BrdU	5-Bromo-3'-deoxyuridine
CFU	colony-forming unit
CLP	Common Lymphoid Precursor
CMP	common myeloid progenitors
DEGs	Differentially expressed genes
dHSCs	Dormant hematopoetic stem cells
FACs	Fluorescence-activated cell sorting
FC	foldchange
GM	Granulocytic monocytic
GMP	granulocyte-monocyte progenitors
GO	Gene Ontology
GSEA	Gene Set Enrichment Analysis
h	hours
HE	hemogenic endothelium
HSCs	Hematopoietic Stem Cells
HSPCs	Hematopoietic Stem and Progenitor Cell
i.v.	intravenous injection
Ifnar	interferon alpha receptor
Ifngr	interferon gamma receptor
IFNs	Interferons

IFNα	Interferon alpha
IFNγ	Interferon-gamma
IL	Interleukin
IL-6R	Interleukin 6 Receptor
IL1R	Interleukin 1 Receptor
IRF9	IFN-regulatory factor 9
ISG	Interferon-Stimulated Genes
ISREs	IFN-stimulated response elements
JAKS	Janus-activated kinases
KEGG	Kyoto Encyclopedia of Genes and Genomes
KO	knockout
Lin	Lineage
LK	Lineage-cKit+
LMPP	lymphoid-primed multipotent progenitors
LPS	Lipopolysaccharide
LS-K	Lin+ Sca-1- c-Kit+ cells
LSKs	Lin- c-Kit+ Sca-1+ cells
LSK SLAM	LSK CD150+ CD48-
LT	Long-term
M.tb	Mycobacterium tuberculosis
MEP	Megakaryocytic-erythroid progenitors
MSCs	Mesenchymal stromal cells
MFI	Median Fluorescence Intensity
Mk	Megakaryocytic
MPPs	Multipotent Progenitor
MSigDB	Molecular Signatures Database
Myel. Prog.	myeloid progenitor
NES	Normalized expresion score
NK	Natural Killer
OXPHOS	oxidative phosphorylation
PBS	Phosphate Buffered Saline
PB	Peripheral blood
PCA	Principal Component Analysis
PAMPs	pathogen-associated molecular patterns

pIC	Polyinosinic:polycytidylic acid
PPP	Pentose phosphate pathway
qPCR	quantitative real-time PCR
RIPK1	Receptor-Interacting Serine-Threonine Protein Kinase 1
PRR	Pattern recognition receptor
RNA	ribonucleic acid
RNA-seq	RNA sequencing
Sc	Single cell
Sca-1	stem cell antigen 1
SEM	Standard Error of Mean
SLAM	signaling lymphocyte activation molecule
s.c.	subcutaneous
STAT	signal transducer and activator transcription
TCA	tricarboxylic acid
TLR	Toll-Like Receptor
TLRs	toll-like receptors
TNFR	TNFα Receptor
TNFα	Tumor Necrosis Factor α
WT	wildtype

6.2 List of figures

6.3 List of tables

6.4 Presentation of work

6.4.1 Talks

SFB873 “Maintenance and Differentiation of Stem Cells in Development and Disease” Research in Progress Seminar Series.

- 24.06.2022, in Heidelberg, Germany. (Virtual)

DKFZ International PhD Program Retreat 2022

- 27.07- 29.07.2022, in Löwenstein, Germany

6.4.2 Poster presentation

SFB873 “Maintenance and Differentiation of Stem Cells in Development and Disease” – Young Scientist Retreat

- 02.04. – 03.04.2019, in St. Martin, Germany

European Hematology Association (EHA) 2022 Hybrid Congress.

- 09.06 - 12.06.2022, in Vienna, Austria.
- Awarded with GSCN travel grant

51st Annual Scientific Meeting International Society for Experimental Hematology (ISEH) 2022.

- 01.09 - 04.09.2022, In Edinburgh, Scotland. (Virtual)

DKFZ International PhD Program poster session 2022

- 18.11.2022, in Heidelberg, Germany.

6.4.3 Publications

Bouman BJ*, **Demerdash Y***, Sood S, Grünschläger F, Pilz F, Itani AR, Kuck A, Haas S, Haghverdi L, Essers MAG **2023**. Single-cell time series analysis reveals the dynamics of *in vivo* HSPC responses to inflammation. bioRxiv 2023.03.09.531881 * shared first authors.

Marot-Lassauzaie V, Bouman BJ, Donaghy FD, **Demerdash Y**, Essers MAG, Haghverdi L. Towards reliable quantification of cell state velocities. PLoS Comput Biol. **2022** Sep 28;18(9):e1010031. doi: 10.1371/journal.pcbi.1010031. PMID: 36170235; PMCID: PMC9550177.

Demel UM*, Lutz R*, Sujer S, **Demerdash Y,** Sood S, Grünschläger F, Kuck A, Werner P, Blaszkiewicz S, Uckelmann HJ, Haas S, Essers MAG. A complex proinflammatory cascade mediates the activation of HSCs upon LPS exposure in vivo. Blood Adv. **2022** Jun 14;6(11):3513-3528. doi: 10.1182/bloodadvances.2021006088. PMID: 35413096; PMCID: PMC9198917.

Demerdash Y, Kain B, Essers MAG, King KY. Yin and Yang: The dual effects of interferons on hematopoiesis. Exp Hematol. **2021** Apr;96:1-12. Doi: 10.1016/j.exphem.2021.02.002. Epub 2021 Feb 8. PMID: 33571568; PMCID: PMC8919039.

7 Contributions

This dissertation has been proofread and corrected by **Dr. Marieke Essers.**

All the projects described in this dissertation were conceptualized under the guidance of **Dr. Marieke Essers.**

Franziska Pilz and Andrea Kuck provided valuable technical support, encompassing tasks such as maintaining mice, conducting genotyping, titrating antibodies, and providing experimental assistance for the experiments. **Franziska Pilz** made a significant contribution to all experiments with mice and completed all necessary paperwork, including writing and submitting the animal protocols for all experiments included in this work.

Abdul Rahman Itani, a PhD student in our research group, provided experimental assistance and technical support for the experiments.

Important support in mouse husbandry and irradiation was provided by all caretakers of the **DKFZ mouse facility**.

The Flow Cytometry Core Facility at DKFZ (**Marcus Eich, Florian Blum, Klaus Hexel, Tobias Rubner and Steffen Schmitt)** provided technical support for the operation of the flow cytometer analyzers and sorters. **The Genomics and Proteomics Core Facility** at DKFZ generated all the high-throughput libraries and performed the sequencing. **The Omics IT and Data Management Core Facility (ODCF)** at the DKFZ handled and managed the data.

In the following sections, I will specify the precise contributions to the outcomes for each of the aims outlined in this dissertation.

Aim 1: Uncover the mechanisms and dynamics of the stress response of HSCs to IFNα

RNA isolation and qPCR experiment were performed by **Fransizka Pilz.** The time series bulk RNA sequencing experiment was performed jointly with **Dr. Shubhankar Sood and Franziska Pilz** from our group. The downstream bioinformatics analysis was performed by me with some guidance of **Dr. Adrien Jolly** from the lab of Prof. Dr. Thomas Höfer at the DKFZ.

Aim 2: Understanding the heterogeneity of hematopoietic stem and progenitor cells (HSPCs) response to IFNα.

This section of the thesis is based on a collaborative project between the groups of **Dr. Laleh Haghverdi** from Max Delbrück Center for Molecular Medicine (Max Delbrück Center) in Berlin and the lab of **Dr. Marieke Essers.** The outcomes presented in this section are largely drawn from a manuscript titled “Single-cell time series analysis reveals the dynamics of in vivo HSPC responses to inflammation“, currently available online as a preprint at BioRxiv (Bouman et al. 2023) and presently under review for publication.

The optimization experiments and ultimately the scRNAseq experiment that forms the basis of the manuscript was performed by myself and **Dr. Shubhankar sood**. The Single Cell Open Lab, with special thanks to **Dr. Jan-Philipp Mallm**, offered technical support for the library preparation.

The codes and methods derived from the bioinformatic analysis were performed by **Dr. Laleh Haghverdi and Brigitte Bouman**, with additional bioinformatics support for the hashtag analysis from **Florian Grünschlager** from the Haas Lab, HI-STEM, DKFZ. Data analysis based on these codes and methods was performed by myself together with **Brigitte Bouman.**

For the manuscript I have utilized specific segments of the text, as well as figures and their legends. I, together with **Brigitte Bouman** from Dr. Laleh Haghverdi’s lab, wrote the text of the manuscript. Based on our equal contribution to this manuscript, I and **Brigitte Bouman** are shared first co-authors on the manuscript.

Aim 3: Dissect the interplay of pro-inflammatory cytokines in the acute response of HSCs to stress

The data generated for the experiments discussed in this section are the result of the collaboration between myself and **Luisa Bast**, the MSc student I co-supervised with **Dr. Marieke Essers.**

Aim 4: Investigating the net impact of pro-inflammatory cytokine receptor signaling in hematopoiesis under homeostasis

Andrea Kuck and Franziska Pilz greatly assisted this project by helping with and performing several experiments independently.
Abdulrahman Itani helped with the transplantation experiment of the 5KO mice.

8 Acknowledgments

I feel immensely blessed and fortunate to have had the support of such an amazing group of individuals throughout this thesis journey. First and foremost, I would like to express my heartfelt gratitude to my supervisor, **Dr. Marieke Essers**. Your mentorship has been invaluable and instrumental in my development as a researcher. Thank you for enabling me to explore new scientific areas while acquiring the skills to complete my research project successfully. It has been a long and fulfilling journey, starting with an internship in your lab, continuing with my master's thesis, and now finishing with my PhD. I am deeply grateful for the opportunity to have had this journey with you, and I am thrilled to say that you will always be my home lab, where I learned how to conduct research with excellence. Thank you for always being approachable and willing to discuss anything with me.

I would like to thank my TAC members **Prof. Dr. F. Nina Papavasiliou**, **Dr. Michael Milsom**, and **Dr. Lars Velten**, who provided me with invaluable advice throughout my PhD journey. I am sincerely grateful for the time and effort you have spent supporting me.

I would like to extend a heartfelt thank you to **Abdulrahman Itani,** who has been my constant companion throughout my PhD journey. Words cannot express my gratitude for the help and support you have given me. Without you, my PhD experience would not have been the same. Thank you for always making me feel accompanied and supported. While I can not thank you for the endless supply of sweets in the lab (which led to a few extra kilos for me!), I must express my appreciation for the fantastic dinners you prepared and the delicious food you cooked. It was and always will be the best Lebanese food I have tasted.

Franzi, I would like to express my gratitude for the support and assistance you have provided me with since the beginning of my PhD. I have seen you grow personally and professionally during this time. I am extremely proud of your achievements. With the hard work, organization, and dedication you apply to everything you do, I am certain you will go far in life. Our conversations during prepping were always a highlight for

me. And let us not forget our fun Christmas cookie-baking; that memory will always stay with me. I will always remember the great times we spent together.

Luisa, you were my first and only student, and I was thrilled to be your supervisor. You are exceptionally kind, and I hope you will always remember the wonderful time we spent singing and dancing together at DKFZ. We spent countless hours together sorting, having stimulating conversations, and overcoming challenges together. I loved hearing about your family and hope you are living a happy life. Despite the difficulties of working during the pandemic, we made it together, and I am incredibly proud of what we achieved.

Andrea, I am truly impressed by your enthusiasm and passion for science. Your support for my experiments has been invaluable, and I would like to express my sincere gratitude for all you have done. Thank you so much.

Paula, you are an exceptional laboratory colleague and an ideal collaborator. Your presence brings a sense of calm to the work environment that is truly invaluable. I cannot express how much I appreciate your contributions.

I would like to thank both current and former members of the **Essers group** for their support and assistance throughout my PhD project. Thank you for all the enjoyable moments, including lunches, coffee breaks, and our creative activities. I truly appreciated the time spent with you both inside and outside of the lab.

I would like to thank **Dagmar** for her help with the many organizational issues. Without you, it would not have been possible for me to go on business trips and fill out all the various forms.

I would like to express my gratitude to **Florian Grünschläger** for his support in helping me and answering numerous questions regarding the single-cell analysis. I truly appreciate all the insightful conversations and scientific discussions we've had.

In addition, I would like to thank all the different people working in the **DKFZ core facilities**, including **the genomics and proteomics core facility.** Especially, I want to thank **Agnes from the Omics IT and data management core facility** for helping me with the single-cell data submission. Also, a big thank you to the **flow cytometry department**, including **Steffen, Flo, Klaus, Marcus, and Tobi**. I spent so many hours on the 7th floor, and you all were always there for me.

I want to express my gratitude to **Dr. Laleh Haghverdi** for her outstanding role as a co-supervisor in the single-cell project. Thank you for the valuable input and remarkable ideas that you have contributed to this project.

I would like to express my gratitude to my collaborator and friend, **Brigitte Boumann**. Thank you for joining the single-cell project and helping us to accelerate its progress with your invaluable input. Your hard work and dedication have been amazing, and I appreciate all you have done. Furthermore, I would like to thank you for the great times we have shared outside of work. We have had many fun moments exploring new business ideas and discussing women's empowerment. Trying new food together has also been an enjoyable experience. I am thankful for everything we have been able to accomplish together while still having fun and enjoying every moment.

I would like to express my gratitude to four special people whom I consider great mentors and amazing friends. Without them, my PhD journey would not have been the same. Firstly, I would like to thank **Lamia Bahnassawy**. you have been my go-to person for any problem that I've failed to find a solution for, whether professional or personal. You always provide me with the best advice. Although we don't see each other often, your friendship is extremely valuable to me. Thank you for always being there for me when I needed you and for your unwavering support and understanding. Secondly, I would like to express my gratitude to **Mohamed Hemid** for our amazing and stimulating scientific discussions. Thank you for all the valuable advice and guidance you gave me; you were never wrong. I also want to thank you for recommending great books and sharing the best homemade jam I've ever tasted. I truly appreciate all of it. I would like to extend a big thank you to **Menna El Serafy**. I can confidently say that I am where I am today because of you. You have been a role

model and an amazing person to look up to. Thank you for always being there for me whenever I needed your support. Lastly, I would like to express my deepest gratitude to **Ahmed Sadik.** Words cannot describe how much I appreciate everything you have done for me. You have always been there to lend a helping hand whenever I needed it, and you have gone above and beyond to assist me. Your knowledge is remarkable, and you are one of the smartest people I have ever met. You are truly one of a kind. I cannot thank you enough for all your support and the long hours we spent discussing science. I feel blessed to have had your unwavering support throughout my journey

I want to express my gratitude to my friends in Mannheim, who are like family to me. Specifically, I want to thank **Dalia Hosny, Sarah Fathallah, Aya El Seify, Khaled Soliman, Mohamed Ashry, Ibrahim Ashour, Iman Ashraf, Ahmed Hazem, Mohamed Ashraf, Hana Ateeba, Ahmed Taha, Nada Meligy, Mostafa Sharawy, and Shady Mamdouh** for all the wonderful times we've had together. Our time spent together was filled with laughter and joy, and it was truly the best time of my life. Thank you for being there.

I want to express my deep appreciation to **Iman Ashraf and Ahmed Hazem** for being such wonderful neighbors and friends. You have always been supportive and there for me whenever I needed help with technical issues in my apartment or navigating German bureaucracy. During the challenging times of the pandemic, you have been there for me, cooking and having fun together. I am grateful for our friendship.

I would also like to express my gratitude to **Mohamed Ashraf and Hana Ateeba**. **Mohamed**, thank you for always being there to support and assist me with German bureaucracy and financial consultations. Your help has been invaluable to me. **Hana**, thank you for being my companion during the thesis writing process. Your friendship has been greatly appreciated.

I would like to express my deepest gratitude to **Ahmed Taha**. Words cannot adequately convey how thankful I am for the exceptional support, advice, and motivation that you have given me throughout my journey. It has been wonderful to have you as a friend, and I cannot thank you enough for your support.

I want to express my gratitude to my friends in Germany, particularly my trio: **Nada Ragab, Dina El Harouni, and Iman Nafis.** I am immensely grateful for the countless hours we spent together during quarantine, chatting over Skype, having sleepovers,

enjoying movie nights, cooking, and essentially sharing every moment of 2020 together. This year has been one of the most difficult for me, and I can't imagine how I would have coped without your support. Thank you so much.

I would like to express my sincere gratitude to **Dina el Harouni**, who has been with me since day one. Dina, you have been an incredible PhD companion and a constant source of support for me. I am truly fortunate to have shared this journey with someone as remarkable and inspiring as you. Thank you for always being there when I needed you.

I would like to express my appreciation to **Shehab El Zohairy** for being an exceptional brother-in-law. I am grateful for your ability to generate unique and creative ideas and for introducing us to a variety of exciting activities.

I would like to express my gratitude to **Hadil Hamdi** for the immense support that you have provided me scientifically. We embarked on our scientific journey at the same time, and I am truly grateful for your presence and the wonderful friendship we share. I deeply appreciate the time you took to read my thesis, this means a lot to me.

I would like to express my heartfelt appreciation to **Nourhan Shafik** for being the most exceptional companion in writing my thesis. I am deeply thankful that you took the time to read some portions of my thesis.

I would like to thank my dear friends from back home – **Mirna Yacout, Yasmine Mostafa, Vivien Mohamed, Salma Hany, and Khaled Saeed**. You made my holidays back home the best I have ever had. The memories we created together, from our fun-filled trips to our long conversations and trying new food and activities, will forever be cherished. Thank you for your support, kindness, and presence in my life. I feel truly blessed to have such amazing friends like you.

I would like to extend a special thanks to **Mirna and Yasmine** for your support throughout my PhD journey. You have been there for me during my low moments, and I am truly grateful for your belief in me. Thank you, for always standing by me.

I want to express my gratitude to **Mai El-Hamd** for all of her support. No amount of words can truly convey how thankful I am to have you in my life.

I want to express my heartfelt gratitude to **Nada Dawish** and her small family for adopting me and becoming my substitute family in Germany. Since day 1, you have welcomed me into your home and made me feel like a part of your family. I cannot thank you enough for all the fun times we have had together, filled with laughter, jokes, and sleepovers. I cherish the memories we have created together, and I will always hold them close to my heart.

I am grateful to **Dalia Hosny** for always supporting me and making my life outside the lab more enjoyable. We have tried different sports together, and you have supported me in adopting new habits for a better life. your incredible personality and our conversations always bring joy to my life. Thank you for making my life so much more enjoyable outside of the lab.

Yomn Abdullah, I just want to take a moment to express my gratitude for your friendship. It's hard to believe we've only known each other for two years, as it feels like we've been lifelong friends. I am incredibly grateful for your support throughout the past two years of my PhD journey. I cannot express enough how invaluable your presence has been during this challenging time. Without you by my side, I honestly do not know how I would have managed. I consider myself extremely fortunate to have you as my friend, and I am deeply thankful for everything you did for me. Our lunch breaks and our conversations in the prayer room have meant the world to me. I cannot thank you enough for being such a wonderful friend. Even with the impending arrival of baby Joe, you still took the time to read my thesis, which I appreciate more than words can express. I love you so much, sister, and I can't wait to celebrate your defense.

Nada Ragab, I am at a loss for words to express how grateful I am for the last 5 years. You have shown me love, understanding, and support, and I am truly blessed to have you in my life. Your friendship has given me a new perspective on what it means to be a true friend. You are the epitome of strength and kindness, and I can not imagine what my journey would have been like without you. Your support in everything I do never fails to impress me, and you have been there for me in good times and bad. Thank you for being my haven where I can express all my feelings without fear of judgment. I

cannot thank you enough for all you have done for me. My journey would not have been the same without you.

I am immensely grateful **to my family** for their unwavering support and encouragement throughout my journey. Their constant love and care have been the driving force behind my success. I would like to express my deepest gratitude to my parents for their sacrifices and dedication in raising me to become the person I am today. **To my father**, I want to express my deepest appreciation for everything you have done for us. You have always been the rock of our family, and your kindness and generosity know no bounds. Your unwavering support and encouragement have been instrumental in helping me achieve my goals. **To my mother**, Thank you for always being there for me, and for allowing me to express myself freely. Your trust in my decisions and your openness to listen to whatever I tell you mean the world to me. Thank you again for being the amazing mother that you are, and for always being my rock. I love you more than words can express. **To my sister**, I owe you a debt of gratitude for always reminding me of my passion and goals and for being a constant source of inspiration and motivation. Despite missing every event for the past 7.5 years, I want you to know that your accomplishments have not gone unnoticed, and I am truly proud of you. **To my brother**, I dedicate this thesis to you as a symbol that hard work pays off, and that with determination and perseverance, you can overcome any obstacle and achieve your goals. I wish you all the best in this world, and I know that you will continue to make me proud.

Finally, I would like to thank **myself** for putting so much strength and hard work into completing this thesis. I'm proud of the person I have become despite all the emotional challenges and a rollercoaster journey. The pandemic made things even more challenging, but I learned a lot scientifically and personally.

9 Bibliography

Abramson, S., R. G. Miller, and R. A. Phillips. 1977. “The Identification in Adult Bone Marrow of Pluripotent and Restricted Stem Cells of the Myeloid and Lymphoid Systems.” Journal of Experimental Medicine. https://doi.org/10.1084/jem.145.6.1567.

Adolfsson, Jörgen, Robert Månsson, Natalija Buza-Vidas, Anne Hultquist, Karina Liuba, Christina T. Jensen, David Bryder, et al. 2005. “Identification of Flt3+ Lympho-Myeloid Stem Cells Lacking Erythro-Megakaryocytic Potential a Revised Road Map for Adult Blood Lineage Commitment.” Cell 121 (2): 295–306.

Ali MAE, Park CY. A new view of hematopoiesis during inflammation. Blood. 2020 Sep 3;136(10):1117-1118. doi: 10.1182/blood.2020006887. PMID: 32882015.

Ashton-Rickardt, Philip G. 2012. “An Emerging Role for Serine Protease Inhibitors in T Lymphocyte Immunity and Beyond.” *International Scholarly Research Notices* 2012 (November). https://doi.org/10.5402/2012/354365.

Baldridge MT, King KY, Boles NC, Weksberg DC, Goodell MA. Quiescent haematopoietic stem cells are activated by IFN-gamma in response to chronic infection. Nature. 2010 Jun 10;465(7299):793-7. doi: 10.1038/nature09135. PMID: 20535209; PMCID: PMC2935898.

Baldridge MT, King KY, Goodell MA. Inflammatory signals regulate hematopoietic stem cells. Trends Immunol. 2011 Feb;32(2):57-65. doi: 10.1016/j.it.2010.12.003. Epub 2011 Jan 11. PMID: 21233016; PMCID: PMC3042730.

Bar-Joseph, Ziv, Anthony Gitter, and Itamar Simon. 2012. “Studying and Modelling Dynamic Biological Processes Using Time-Series Gene Expression Data.” *Nature Reviews. Genetics* 13 (8): 552–64.

Bernitz, Jeffrey M., Huen Suk Kim, Ben MacArthur, Hans Sieburg, and Kateri Moore. 2016. “Hematopoietic Stem Cells Count and Remember Self-Renewal Divisions.” *Cell* 167 (5): 1296–1309.e10.

Bigas, Anna, and Lluis Espinosa. 2012. “Hematopoietic Stem Cells: To Be or Notch to Be.” *Blood*. https://doi.org/10.1182/blood-2011-10-355826.

Binder, D., J. Fehr, H. Hengartner, and R. M. Zinkernagel. 1997. “Virus-Induced Transient Bone Marrow Aplasia: Major Role of Interferon-Alpha/beta during Acute Infection with the Noncytopathic Lymphocytic Choriomeningitis Virus.” *The Journal of Experimental Medicine* 185 (3): 517–30.

Biswas, Lincoln, Junyu Chen, Jessica De Angelis, Amit Singh, Charlotte Owen-Woods, Zhangfan Ding, Joan Mane Pujol, et al. 2023. “Lymphatic Vessels in Bone Support Regeneration after Injury.” *Cell* 186 (2): 382–97.e24.

Bogeska R, Mikecin AM, Kaschutnig P, Fawaz M, Büchler-Schäff M, Le D, Ganuza M, Vollmer A, Paffenholz SV, Asada N, Rodriguez-Correa E, Frauhammer F, Buettner F, Ball M, Knoch J, Stäble S, Walter D, Petri A, Carreño-Gonzalez MJ, Wagner V, Brors B, Haas S, Lipka DB, Essers MAG, Weru V, Holland-Letz T, Mallm JP, Rippe K, Krämer S, Schlesner M, McKinney Freeman S, Florian MC, King KY, Frenette PS, Rieger MA, Milsom MD. “Inflammatory exposure drives long-lived impairment of hematopoietic stem cell self-renewal activity and accelerated aging”. Cell Stem Cell. 2022 Aug 4;29(8):1273-1284.e8. doi: 10.1016/j.stem.2022.06.012. Epub 2022 Jul 19. PMID: 35858618; PMCID: PMC9357150.

Borden, Ernest C., Ganes C. Sen, Gilles Uze, Robert H. Silverman, Richard M. Ransohoff, Graham R. Foster, and George R. Stark. 2007. “Interferons at Age 50: Past, Current and Future Impact on Biomedicine.” *Nature Reviews. Drug Discovery* 6 (12): 975–90.

Bouman, Brigitte Joanne, Yasmin Demerdash, Shubhankar Sood, Florian Grünschläger, Franziska Pilz, Abdul Rahman Itani, Andrea Kuck, Simon Haas, Laleh Haghverdi, and Marieke Alida Gertruda Essers. 2023. “Single-Cell Time Series Analysis Reveals the Dynamics Of*in vivo*HSPC Responses to Inflammation.” https://doi.org/10.1101/2023.03.09.531881.

Bowers, Emily, Anastasiya Slaughter, Paul S. Frenette, Rork Kuick, Oscar M. Pello, and Daniel Lucas. 2018. “Granulocyte-Derived TNFα Promotes Vascular and Hematopoietic Regeneration in the Bone Marrow.” *Nature Medicine* 24 (1): 95–102.

Bradley, J. R. 2008. “TNF-Mediated Inflammatory Disease.” *The Journal of Pathology* 214 (2): 149–60.

Broxmeyer, H. E., D. E. Williams, L. Lu, S. Cooper, S. L. Anderson, G. S. Beyer, R. Hoffman, and B. Y. Rubin. 1986. “The Suppressive Influences of Human Tumor Necrosis Factors on Bone Marrow Hematopoietic Progenitor Cells from Normal Donors and Patients with Leukemia: Synergism of Tumor Necrosis Factor and Interferon-Gamma.” *Journal of Immunology* 136 (12): 4487–95.

Bruijn, M. F. de, N. A. Speck, M. C. Peeters, and E. Dzierzak. 2000. “Definitive Hematopoietic Stem Cells First Develop within the Major Arterial Regions of the Mouse Embryo.” *The EMBO Journal* 19 (11): 2465–74.

Bruin, Alexander M. de, Sten F. Libregts, Marijke Valkhof, Louis Boon, Ivo P. Touw, and Martijn A. Nolte. 2012. “IFNγ Induces Monopoiesis and Inhibits Neutrophil Development during Inflammation.” *Blood* 119 (6): 1543–54.

Bryder, David, Derrick J. Rossi, and Irving L. Weissman. 2006. “Hematopoietic Stem Cells: The Paradigmatic Tissue-Specific Stem Cell.” *The American Journal of Pathology* 169 (2): 338–46.

Burrill, Devin R., and Pamela A. Silver. 2010. “Making Cellular Memories.” *Cell*. https://doi.org/10.1016/j.cell.2009.12.034.

Cabezas-Wallscheid, Nina, Florian Buettner, Pia Sommerkamp, Daniel Klimmeck, Luisa Ladel, Frederic B. Thalheimer, Daniel Pastor-Flores, et al. 2017. “Vitamin A-Retinoic Acid Signaling Regulates Hematopoietic Stem Cell Dormancy.” *Cell* 169 (5): 807–23.e19.

Caiado, Francisco, Eric M. Pietras, and Markus G. Manz. 2021. “Inflammation as a Regulator of Hematopoietic Stem Cell Function in Disease, Aging, and Clonal Selection.” *The Journal of Experimental Medicine* 218 (7). https://doi.org/10.1084/jem.20201541.

Caux, C., S. Saeland, C. Favre, V. Duvert, P. Mannoni, and J. Banchereau. 1990. “Tumor Necrosis Factor-Alpha Strongly Potentiates Interleukin-3 and Granulocyte-Macrophage Colony-Stimulating Factor-Induced Proliferation of Human CD34+ Hematopoietic Progenitor Cells.” *Blood* 75 (12): 2292–98.

Challen, Grant A., Nathan Boles, Karen Kuan-Yin Lin, and Margaret A. Goodell. 2009. “Mouse Hematopoietic Stem Cell Identification and Analysis.” *Cytometry. Part A: The Journal of the International Society for Analytical Cytology* 75 (1): 14–24.

Chan, David C. 2012. “Fusion and Fission: Interlinked Processes Critical for Mitochondrial Health.” *Annual Review of Genetics* 46 (August): 265–87.

Chen, Chong, Yu Liu, Yang Liu, and Pan Zheng. 2010. “Mammalian Target of Rapamycin Activation Underlies HSC Defects in Autoimmune Disease and Inflammation in Mice.” *The Journal of Clinical Investigation* 120 (11): 4091–4101.

Chiba, Yukino, Izuru Mizoguchi, Hideaki Hasegawa, Mio Ohashi, Naoko Orii, Taro Nagai, Miyaka Sugahara, et al. 2018. “Regulation of Myelopoiesis by Proinflammatory Cytokines in Infectious Diseases.” *Cellular and Molecular Life Sciences: CMLS* 75 (8): 1363–76.

Ciriza, Jesús, Heather Thompson, Raffi Petrosian, Jennifer O. Manilay, and Marcos E. García-Ojeda. 2013. “The Migration of Hematopoietic Progenitors from the Fetal Liver

to the Fetal Bone Marrow: Lessons Learned and Possible Clinical Applications." *Experimental Hematology*. https://doi.org/10.1016/j.exphem.2013.01.009.

Cirovic, Branko, L. Charlotte J. de Bree, Laszlo Groh, Bas A. Blok, Joyce Chan, Walter J. F. M. van der Velden, M. E. J. Bremmers, et al. 2020. "BCG Vaccination in Humans Elicits Trained Immunity via the Hematopoietic Progenitor Compartment." *Cell Host & Microbe* 28 (2): 322–34.e5.

Clapes, Thomas, Stylianos Lefkopoulos, and Eirini Trompouki. 2016. "Stress and Non-Stress Roles of Inflammatory Signals during HSC Emergence and Maintenance." *Frontiers in Immunology* 7 (November): 487.

Clark, B. R., C. Jamieson, and A. Keating. 1997. "Human Long-Term Bone Marrow Culture." *Methods in Molecular Biology* 75: 249–56.

Clevers, Hans. 2015. "STEM CELLS. What Is an Adult Stem Cell?" *Science* 350 (6266): 1319–20.

Cline, Melissa S., Michael Smoot, Ethan Cerami, Allan Kuchinsky, Nerius Landys, Chris Workman, Rowan Christmas, et al. 2007. "Integration of Biological Networks and Gene Expression Data Using Cytoscape." *Nature Protocols* 2 (10): 2366–82.

Collins A, Mitchell CA, Passegué E. "Inflammatory signaling regulates hematopoietic stem and progenitor cell development and homeostasis". J Exp Med. 2021 Jul 5;218(7):e20201545. doi: 10.1084/jem.20201545. Epub 2021 Jun 15. PMID: 34129018; PMCID: PMC8210624.

Conway, Jake R., Alexander Lex, and Nils Gehlenborg. 2017. "UpSetR: An R Package for the Visualization of Intersecting Sets and Their Properties." *Bioinformatics* 33 (18): 2938–40.

Czechowicz, Agnieszka, and Irving L. Weissman. 2011. "Purified Hematopoietic Stem Cell Transplantation: The next Generation of Blood and Immune Replacement." Hematology/oncology Clinics of North America 25 (1): 75–87.

Dann E, Henderson NC, Teichmann SA, Morgan MD, Marioni JC. "Differential abundance testing on single-cell data using k-nearest neighbor graphs". Nat Biotechnol. 2022 Feb;40(2):245-253. doi: 10.1038/s41587-021-01033-z. Epub 2021 Sep 30. PMID: 34594043.

Demel UM, Lutz R, Sujer S, Demerdash Y, Sood S, Grünschläger F, Kuck A, Werner P, Blaszkiewicz S, Uckelmann HJ, Haas S, Essers MAG. "A complex proinflammatory cascade mediates the activation of HSCs upon LPS exposure in vivo". Blood Adv.

2022 Jun 14;6(11):3513-3528. doi: 10.1182/bloodadvances.2021006088. PMID: 35413096; PMCID: PMC9198917.

Demerdash, Yasmin, Bailee Kain, Marieke A. G. Essers, and Katherine Y. King. 2021. “Yin and Yang: The Dual Effects of Interferons on Hematopoiesis.” *Experimental Hematology* 96 (April): 1–12.

DeVilbiss, Andrew W., Zhiyu Zhao, Misty S. Martin-Sandoval, Jessalyn M. Ubellacker, Alpaslan Tasdogan, Michalis Agathocleous, Thomas P. Mathews, and Sean J. Morrison. 2021. “Metabolomic Profiling of Rare Cell Populations Isolated by Flow Cytometry from Tissues.” *eLife* 10 (January). https://doi.org/10.7554/eLife.61980.

Douple, Evan B., Kiyohiko Mabuchi, Harry M. Cullings, Dale L. Preston, Kazunori Kodama, Yukiko Shimizu, Saeko Fujiwara, and Roy E. Shore. 2011. “Long-Term Radiation-Related Health Effects in a Unique Human Population: Lessons Learned from the Atomic Bomb Survivors of Hiroshima and Nagasaki.” *Disaster Medicine and Public Health Preparedness* 5 Suppl 1 (0 1): S122–33.

Dunn, Eleanor, John E. Sims, Martin J. H. Nicklin, and Luke A. J. O’Neill. 2001. “Annotating Genes with Potential Roles in the Immune System: Six New Members of the IL-1 Family.” *Trends in Immunology*. https://doi.org/10.1016/s1471-4906(01)02034-8.

Dybedal, I., D. Bryder, A. Fossum, L. S. Rusten, and S. E. Jacobsen. 2001. “Tumor Necrosis Factor (TNF)-Mediated Activation of the p55 TNF Receptor Negatively Regulates Maintenance of Cycling Reconstituting Human Hematopoietic Stem Cells.” *Blood* 98 (6): 1782–91.

Dykstra, Brad, David Kent, Michelle Bowie, Lindsay McCaffrey, Melisa Hamilton, Kristin Lyons, Shang-Jung Lee, Ryan Brinkman, and Connie Eaves. 2007. “Long-Term Propagation of Distinct Hematopoietic Differentiation Programs in Vivo.” *Cell Stem Cell* 1 (2): 218–29.

Ehninger, Armin, and Andreas Trumpp. 2011. “The Bone Marrow Stem Cell Niche Grows up: Mesenchymal Stem Cells and Macrophages Move in.” *The Journal of Experimental Medicine* 208 (3): 421–28.

El-Brolosy, Mohamed A., and Didier Y. R. Stainier. 2017. “Genetic Compensation: A Phenomenon in Search of Mechanisms.” *PLoS Genetics* 13 (7): e1006780.

Espín-Palazón, Raquel, David L. Stachura, Clyde A. Campbell, Diana García-Moreno, Natasha Del Cid, Albert D. Kim, Sergio Candel, José Meseguer, Victoriano Mulero, and David Traver. 2014. “Proinflammatory Signaling Regulates Hematopoietic Stem Cell Emergence.” *Cell* 159 (5): 1070–85.

Espín-Palazón, Raquel, and David Traver. 2016. “The NF-κB Family: Key Players during Embryonic Development and HSC Emergence.” *Experimental Hematology* 44 (7): 519–27.

Espin-Palazon, Raquel, Bart Weijts, Victor Mulero, and David Traver. 2018. “Proinflammatory Signals as Fuel for the Fire of Hematopoietic Stem Cell Emergence.” *Trends in Cell Biology*. https://doi.org/10.1016/j.tcb.2017.08.003.

Essers MA, Offner S, Blanco-Bose WE, Waibler Z, Kalinke U, Duchosal MA, Trumpp A. “IFNalpha activates dormant haematopoietic stem cells in vivo”. Nature. 2009 Apr 16;458(7240):904-8. doi: 10.1038/nature07815. Epub 2009 Feb 11. PMID: 19212321.

Filippi, Marie-Dominique. 2021. “Hematopoietic Stem Cell (HSC) Divisional Memory: The Journey of Mitochondrial Metabolism through HSC Division.” *Experimental Hematology* 96 (April): 27–34.

Flurkey, K., J. Mcurrer, and D. Harrison. 2007. “Mouse Models in Aging Research.” *The Mouse in Biomedical Research*. https://doi.org/10.1016/b978-012369454-6/50074-1.

Garlanda, Cecilia, Charles A. Dinarello, and Alberto Mantovani. 2013. “The Interleukin-1 Family: Back to the Future.” *Immunity*. https://doi.org/10.1016/j.immuni.2013.11.010.

Geiger, Hartmut, Gerald de Haan, and M. Carolina Florian. 2013. “The Ageing Haematopoietic Stem Cell Compartment.” *Nature Reviews. Immunology* 13 (5): 376–89.

Giladi A, Paul F, Herzog Y, Lubling Y, Weiner A, Yofe I, Jaitin D, Cabezas-Wallscheid N, Dress R, Ginhoux F, Trumpp A, Tanay A, Amit I. “Single-cell characterization of haematopoietic progenitors and their trajectories in homeostasis and perturbed haematopoiesis”. Nat Cell Biol. 2018 Jul;20(7):836-846. doi: 10.1038/s41556-018-0121-4. Epub 2018 Jun 18. PMID: 29915358.

Goedhart, Marieke, Anne S. Cornelissen, Carlijn Kuijk, Sulima Geerman, Marion Kleijer, Jaap D. van Buul, Stephan Huveneers, et al. 2018. “Interferon-Gamma Impairs Maintenance and Alters Hematopoietic Support of Bone Marrow Mesenchymal Stromal Cells.” *Stem Cells and Development* 27 (9): 579–89.

Göthert, Joachim R., Sonja E. Gustin, Mark A. Hall, Anthony R. Green, Berthold Göttgens, David J. Izon, and C. Glenn Begley. 2005. “In Vivo Fate-Tracing Studies Using the Scl Stem Cell Enhancer: Embryonic Hematopoietic Stem Cells Significantly Contribute to Adult Hematopoiesis.” *Blood* 105 (7): 2724–32.

Grover, Amit, Alejandra Sanjuan-Pla, Supat Thongjuea, Joana Carrelha, Alice Giustacchini, Adriana Gambardella, Iain Macaulay, et al. 2016. “Single-Cell RNA

Sequencing Reveals Molecular and Functional Platelet Bias of Aged Haematopoietic Stem Cells." *Nature Communications* 7 (March): 11075.

Haase, Christa, Karin Gustafsson, Shenglin Mei, Shu-Chi Yeh, Dmitry Richter, Jelena Milosevic, Raphaël Turcotte, et al. 2022. "Image-Seq: Spatially Resolved Single-Cell Sequencing Guided by in Situ and in Vivo Imaging." *Nature Methods* 19 (12): 1622–33.

Haas S, Hansson J, Klimmeck D, Loeffler D, Velten L, Uckelmann H, Wurzer S, Prendergast ÁM, Schnell A, Hexel K, Santarella-Mellwig R, Blaszkiewicz S, Kuck A, Geiger H, Milsom MD, Steinmetz LM, Schroeder T, Trumpp A, Krijgsveld J, Essers MA. "Inflammation-Induced Emergency Megakaryopoiesis Driven by Hematopoietic Stem Cell-like Megakaryocyte Progenitors". Cell Stem Cell. 2015 Oct 1;17(4):422-34. doi: 10.1016/j.stem.2015.07.007. Epub 2015 Aug 20. PMID: 26299573.

Haas, Simon, Andreas Trumpp, and Michael D. Milsom. 2018. "Causes and Consequences of Hematopoietic Stem Cell Heterogeneity." *Cell Stem Cell*. https://doi.org/10.1016/j.stem.2018.04.003.

Hadland, Brandon K., Stacey S. Huppert, Jyotshnabala Kanungo, Yingzi Xue, Rulang Jiang, Thomas Gridley, Ronald A. Conlon, Alec M. Cheng, Raphael Kopan, and Gregory D. Longmore. 2004. "A Requirement for Notch1 Distinguishes 2 Phases of Definitive Hematopoiesis during Development." *Blood* 104 (10): 3097–3105.

Hangoc, G., D. E. Williams, J. H. Falkenburg, and H. E. Broxmeyer. 1989. "Influence of IL-1 Alpha and -1 Beta on the Survival of Human Bone Marrow Cells Responding to Hematopoietic Colony-Stimulating Factors." *Journal of Immunology* 142 (12): 4329–34.

Harrison, D. E. 1980. "Competitive Repopulation: A New Assay for Long-Term Stem Cell Functional Capacity." *Blood* 55 (1): 77–81.

Hie, Brian, Bryan Bryson, and Bonnie Berger. 2019. "Efficient Integration of Heterogeneous Single-Cell Transcriptomes Using Scanorama." *Nature Biotechnology* 37 (6): 685–91.

Hirche, Christoph, Theresa Frenz, Simon F. Haas, Marius Döring, Katharina Borst, Pia-K Tegtmeyer, Ilija Brizic, et al. 2017. "Systemic Virus Infections Differentially Modulate Cell Cycle State and Functionality of Long-Term Hematopoietic Stem Cells In Vivo." *Cell Reports* 19 (11): 2345–56.

Huang, Tzu-Hsuan, Koteswara R. Chintalacharuvu, and Sherie L. Morrison. 2007. "Targeting IFN-α to B Cell Lymphoma by a Tumor-Specific Antibody Elicits Potent

Antitumor Activities." *The Journal of Immunology*. https://doi.org/10.4049/jimmunol.179.10.6881.

Hulett, H. R., Bonner, W. A., Barrett, J., & Herzenberg, L. A. (1969). "Cell Sorting: Automated Separation of Mammalian Cells as a Function of Intracellular Fluorescence". Science. https://doi.org/747

Hulsen, Tim, Jacob de Vlieg, and Wynand Alkema. 2008. "BioVenn - a Web Application for the Comparison and Visualization of Biological Lists Using Area-Proportional Venn Diagrams." *BMC Genomics* 9 (October): 488.

Hurwitz, Stephanie N., Seul K. Jung, and Peter Kurre. 2020. "Hematopoietic Stem and Progenitor Cell Signaling in the Niche." *Leukemia* 34 (12): 3136–48.

Ivashkiv, Lionel B., and Laura T. Donlin. 2014. "Regulation of Type I Interferon Responses." *Nature Reviews Immunology*. https://doi.org/10.1038/nri3581.

Jacobson, L. O., E. L. Simmons, E. K. Marks, and J. H. Eldredge. 1951. "Recovery from Radiation Injury." *Science* 113 (2940): 510–11.

Jovcic, G., Z. Ivanovic, L. Biljanovic-Paunovic, D. Bugarski, S. Stosic-Grujicic, and P. Milenkovic. 1996. "In Vivo Effects of Interleukin-1 Receptor Antagonist on Hematopoietic Bone Marrow Progenitor Cells in Normal Mice." *European Cytokine Network* 7 (1): 71–74.

Kanayama, Masashi, Yuta Izumi, Yasuharu Yamauchi, Shoko Kuroda, Takaei Shin, Shun Ishikawa, Taku Sato, Mihoko Kajita, and Toshiaki Ohteki. 2020. "CD86-Based Analysis Enables Observation of Bona Fide Hematopoietic Responses." *Blood* 136 (10): 1144–54.

Kanehisa, M., and S. Goto. 2000. "KEGG: Kyoto Encyclopedia of Genes and Genomes." *Nucleic Acids Research* 28 (1): 27–30.

Kanehisa, Minoru, Miho Furumichi, Yoko Sato, Masayuki Kawashima, and Mari Ishiguro-Watanabe. 2023. "KEGG for Taxonomy-Based Analysis of Pathways and Genomes." *Nucleic Acids Research* 51 (D1): D587–92.

Kaplan, Mariana J. 2011. "Neutrophils in the Pathogenesis and Manifestations of SLE." *Nature Reviews Rheumatology*. https://doi.org/10.1038/nrrheum.2011.132.

Karigane, Daiki, Hiroshi Kobayashi, Takayuki Morikawa, Yukako Ootomo, Mashito Sakai, Go Nagamatsu, Yoshiaki Kubota, et al. 2016. "p38α Activates Purine Metabolism to Initiate Hematopoietic Stem/Progenitor Cell Cycling in Response to Stress." *Cell Stem Cell* 19 (2): 192–204.

Karigane, Daiki, and Keiyo Takubo. 2017. “Metabolic Regulation of Hematopoietic and Leukemic Stem/progenitor Cells under Homeostatic and Stress Conditions.” *International Journal of Hematology* 106 (1): 18–26.

Kaschutnig, Paul, Ruzhica Bogeska, Dagmar Walter, Amelie Lier, Sina Huntscha, and Michael D. Milsom. 2015. “The Fanconi Anemia Pathway Is Required for Efficient Repair of Stress-Induced DNA Damage in Haematopoietic Stem Cells.” *Cell Cycle* 14 (17): 2734–42.

Kaufmann, Eva, Joaquin Sanz, Jonathan L. Dunn, Nargis Khan, Laura E. Mendonça, Alain Pacis, Fanny Tzelepis, et al. 2018. “BCG Educates Hematopoietic Stem Cells to Generate Protective Innate Immunity against Tuberculosis.” *Cell* 172 (1-2): 176–90.e19.

Khan N, Downey J, Sanz J, Kaufmann E, Blankenhaus B, Pacis A, Pernet E, Ahmed E, Cardoso S, Nijnik A, Mazer B, Sassetti C, Behr MA, Soares MP, Barreiro LB, Divangahi M. “M. tuberculosis Reprograms Hematopoietic Stem Cells to Limit Myelopoiesis and Impair Trained Immunity“. Cell. 2020 Oct 29;183(3):752-770.e22. doi: 10.1016/j.cell.2020.09.062. PMID: 33125891; PMCID: PMC7599081.

Kiel, Mark J., Omer H. Yilmaz, Toshihide Iwashita, Osman H. Yilmaz, Cox Terhorst, and Sean J. Morrison. 2005. “SLAM Family Receptors Distinguish Hematopoietic Stem and Progenitor Cells and Reveal Endothelial Niches for Stem Cells.” *Cell* 121 (7): 1109–21.

Kim, Peter Geon, Matthew C. Canver, Catherine Rhee, Samantha J. Ross, June V. Harriss, Ho-Chou Tu, Stuart H. Orkin, Haley O. Tucker, and George Q. Daley. 2016. “Interferon-α Signaling Promotes Embryonic HSC Maturation.” *Blood* 128 (2): 204–16.

King, Katherine Y., Megan T. Baldridge, David C. Weksberg, Stuart M. Chambers, Georgi L. Lukov, Shihua Wu, Nathan C. Boles, et al. 2011. “Irgm1 Protects Hematopoietic Stem Cells by Negative Regulation of IFN Signaling.” *Blood* 118 (6): 1525–33.

King KY, Goodell MA. “Inflammatory modulation of HSCs: viewing the HSC as a foundation for the immune response”. Nat Rev Immunol. 2011 Sep 9;11(10):685-92. doi: 10.1038/nri3062. PMID: 21904387; PMCID: PMC4154310.

Kleppe, Maria, Matthew H. Spitzer, Sheng Li, Corinne E. Hill, Lauren Dong, Efthymia Papalexi, Sofie De Groote, et al. 2018. “Jak1 Integrates Cytokine Sensing to Regulate Hematopoietic Stem Cell Function and Stress Hematopoiesis.” *Cell Stem Cell* 22 (2): 277.

Kwarteng, Edward O., and Krista M. Heinonen. 2016. “Competitive Transplants to Evaluate Hematopoietic Stem Cell Fitness.” *Journal of Visualized Experiments: JoVE*, no. 114 (August). https://doi.org/10.3791/54345.

Kwok, Immanuel, Etienne Becht, Yu Xia, Melissa Ng, Ye Chean Teh, Leonard Tan, Maximilien Evrard, et al. 2020. “Combinatorial Single-Cell Analyses of Granulocyte-Monocyte Progenitor Heterogeneity Reveals an Early Uni-Potent Neutrophil Progenitor.” *Immunity* 53 (2): 303–18.e5.

Lause, Jan, Philipp Berens, and Dmitry Kobak. 2021. “Analytic Pearson Residuals for Normalization of Single-Cell RNA-Seq UMI Data.” *Genome Biology* 22 (1): 258.

Laval, Bérengère de, Julien Maurizio, Prashanth K. Kandalla, Gabriel Brisou, Louise Simonnet, Caroline Huber, Gregory Gimenez, et al. 2020. “C/EBPβ-Dependent Epigenetic Memory Induces Trained Immunity in Hematopoietic Stem Cells.” *Cell Stem Cell* 26 (5): 793.

Lee, Amanda J., and Ali A. Ashkar. 2018. “The Dual Nature of Type I and Type II Interferons.” *Frontiers in Immunology* 9 (September): 2061.

Lê, Sébastien, Julie Josse, and François Husson. 2008. “**FactoMineR**: An*R*Package for Multivariate Analysis.” *Journal of Statistical Software*. https://doi.org/10.18637/jss.v025.i01.

Liberzon, A., A. Subramanian, R. Pinchback, H. Thorvaldsdottir, P. Tamayo, and J. P. Mesirov. 2011. “Molecular Signatures Database (MSigDB) 3.0.” *Bioinformatics*. https://doi.org/10.1093/bioinformatics/btr260.

Li, Lei, Susan M. Byrne, Nicole Rainville, Su Su, Edward Jachimowicz, Anne Aucher, Daniel M. Davis, Philip G. Ashton-Rickardt, and Don M. Wojchowski. 2014. “Brief Report: Serpin Spi2A as a Novel Modulator of Hematopoietic Progenitor Cell Formation.” *Stem Cells* 32 (9): 2550–56.

Linehan, Melissa M., Thayne H. Dickey, Emanuela S. Molinari, Megan E. Fitzgerald, Olga Potapova, Akiko Iwasaki, and Anna M. Pyle. 2018. “A Minimal RNA Ligand for Potent RIG-I Activation in Living Mice.” *Science Advances* 4 (2): e1701854.

Liu, Beiyun C., Joseph Sarhan, and Alexander Poltorak. 2018. “Host-Intrinsic Interferon Status in Infection and Immunity.” *Trends in Molecular Medicine* 24 (8): 658–68.

Li, Yan, Virginie Esain, Li Teng, Jian Xu, Wanda Kwan, Isaura M. Frost, Amanda D. Yzaguirre, et al. 2014. “Inflammatory Signaling Regulates Embryonic Hematopoietic Stem and Progenitor Cell Production.” *Genes & Development* 28 (23): 2597–2612.

Love, Michael I., Wolfgang Huber, and Simon Anders. 2014. “Moderated Estimation of Fold Change and Dispersion for RNA-Seq Data with DESeq2.” *Genome Biology* 15 (12): 550.

Macnair, Will, Revant Gupta, and Manfred Claassen. 2022. “Psupertime: Supervised Pseudotime Analysis for Time-Series Single-Cell RNA-Seq Data.” *Bioinformatics* 38 (Supplement_1): i290–98.

Mancini, Stéphane J. C., Dominique Bonnet, and César Nombela Arrieta. 2022. *Harnessing the Complexity of Normal and Pathological Hematopoietic Supportive Niches*. Frontiers Media SA.

Mann, Mati, Arnav Mehta, Carl G. de Boer, Monika S. Kowalczyk, Kevin Lee, Pearce Haldeman, Noga Rogel, et al. 2018. “Heterogeneous Responses of Hematopoietic Stem Cells to Inflammatory Stimuli Are Altered with Age.” *Cell Reports* 25 (11): 2992–3005.e5.

Manz MG, Boettcher S. “Emergency granulopoiesis.” Nat Rev Immunol. 2014 May;14(5):302-14. doi: 10.1038/nri3660. Epub 2014 Apr 22. PMID: 24751955.

Maryanovich, Maria, and Keisuke Ito. 2022. “CD36-Mediated Fatty Acid Oxidation in Hematopoietic Stem Cells Is a Novel Mechanism of Emergency Hematopoiesis in Response to Infection.” *Immunometabolism* 4 (2). https://doi.org/10.20900/immunometab20220008.

Matatall, Katie A., Mira Jeong, Siyi Chen, Deqiang Sun, Fengju Chen, Qianxing Mo, Marek Kimmel, and Katherine Y. King. 2016. “Chronic Infection Depletes Hematopoietic Stem Cells through Stress-Induced Terminal Differentiation.” *Cell Reports* 17 (10): 2584–95.

Matatall, Katie A., Ching-Chieh Shen, Grant A. Challen, and Katherine Y. King. 2014. “Type II Interferon Promotes Differentiation of Myeloid-Biased Hematopoietic Stem Cells.” *Stem Cells* 32 (11): 3023–30.

Matsuoka, S., Y. Ebihara, M. Xu, T. Ishii, D. Sugiyama, H. Yoshino, T. Ueda, et al. 2001. “CD34 Expression on Long-Term Repopulating Hematopoietic Stem Cells Changes during Developmental Stages.” *Blood* 97 (2): 419–25.

Merico, Daniele, Ruth Isserlin, Oliver Stueker, Andrew Emili, and Gary D. Bader. 2010. “Enrichment Map: A Network-Based Method for Gene-Set Enrichment Visualization and Interpretation.” *PloS One* 5 (11): e13984.

Mirantes, Cristina, Emmanuelle Passegué, and Eric M. Pietras. 2014. “Pro-Inflammatory Cytokines: Emerging Players Regulating HSC Function in Normal and Diseased Hematopoiesis.” *Experimental Cell Research* 329 (2): 248–54.

Mistry, Jayna J., Jamie A. Moore, Charlotte Hellmich, Aisha Jibril, Iain Macauley, Mar Moreno-Gonzalez, Federica Di Palma, Naiara Beraza, Kristian M. Bowles, and Stuart A. Rushworth. 2020. “Enhanced Free Fatty Acid Uptake Via CD36 Promotes a Metabolic Switch to B-Oxidation within Hematopoietic Stem Cells in Response to Acute Infection.” *Blood*. https://doi.org/10.1182/blood-2020-139454.

Moignard, Victoria, Iain C. Macaulay, Gemma Swiers, Florian Buettner, Judith Schütte, Fernando J. Calero-Nieto, Sarah Kinston, et al. 2013. “Characterization of Transcriptional Networks in Blood Stem and Progenitor Cells Using High-Throughput Single-Cell Gene Expression Analysis.” *Nature Cell Biology* 15 (4): 363–72.

Moorlag, Simone J. C. F. M., Nargis Khan, Boris Novakovic, Eva Kaufmann, Trees Jansen, Reinout van Crevel, Maziar Divangahi, and Mihai G. Netea. 2020. “β-Glucan Induces Protective Trained Immunity against Mycobacterium Tuberculosis Infection: A Key Role for IL-1.” Cell Reports 31 (7): 107634.

Morganti C, Cabezas-Wallscheid N, Ito K. “Metabolic Regulation of Hematopoietic Stem Cells”. Hemasphere. 2022 Jun 28;6(7):e740. doi: 10.1097/HS9.0000000000000740. PMID: 35785147; PMCID: PMC9242402.

Morita, Yohei, Hideo Ema, and Hiromitsu Nakauchi. 2010. “Heterogeneity and Hierarchy within the Most Primitive Hematopoietic Stem Cell Compartment.” *The Journal of Experimental Medicine* 207 (6): 1173–82.

Morrison, Sean J., and Allan C. Spradling. 2008. “Stem Cells and Niches: Mechanisms That Promote Stem Cell Maintenance throughout Life.” *Cell* 132 (4): 598–611.

Murry, Charles E., and Gordon Keller. 2008. “Differentiation of Embryonic Stem Cells to Clinically Relevant Populations: Lessons from Embryonic Development.” *Cell* 132 (4): 661–80.

Negrotto, S., C. J De Giusti, M. J. Lapponi, J. Etulain, L. Rivadeneyra, R. G. Pozner, R. M. Gomez, and M. Schattner. 2011. “Expression and Functionality of Type I Interferon Receptor in the Megakaryocytic Lineage.” *Journal of Thrombosis and Haemostasis: JTH* 9 (12): 2477–85.

Nestorowa, Sonia, Fiona K. Hamey, Blanca Pijuan Sala, Evangelia Diamanti, Mairi Shepherd, Elisa Laurenti, Nicola K. Wilson, David G. Kent, and Berthold Göttgens. 2016. “A Single-Cell Resolution Map of Mouse Hematopoietic Stem and Progenitor Cell Differentiation.” *Blood* 128 (8): e20–31.

Nestorowa, Sonia, Fiona K. Hamey, Blanca Pijuan Sala, Evangelia Diamanti, Mairi Shepherd, Elisa Laurenti, Nicola K. Wilson, David G. Kent, and Berthold Göttgens.

2016. “A Single-Cell Resolution Map of Mouse Hematopoietic Stem and Progenitor Cell Differentiation.” *Blood*. https://doi.org/10.1182/blood-2016-05-716480.

Netea, Mihai G., Jorge Domínguez-Andrés, Luis B. Barreiro, Triantafyllos Chavakis, Maziar Divangahi, Elaine Fuchs, Leo A. B. Joosten, et al. 2020. “Defining Trained Immunity and Its Role in Health and Disease.” *Nature Reviews. Immunology* 20 (6): 375–88.

Netea, Mihai G., Leo A. B. Joosten, Eicke Latz, Kingston H. G. Mills, Gioacchino Natoli, Hendrik G. Stunnenberg, Luke A. J. O’Neill, and Ramnik J. Xavier. 2016. “Trained Immunity: A Program of Innate Immune Memory in Health and Disease.” *Science* 352 (6284): aaf1098.

Ng, Ashley P., and Warren S. Alexander. 2017. “Haematopoietic Stem Cells: Past, Present and Future.” *Cell Death Discovery* 3 (February): 17002.

Nicholson, Lindsay B. 2016. “The Immune System.” *Essays in Biochemistry* 60 (3): 275–301.

Oguro, Hideyuki, Lei Ding, and Sean J. Morrison. 2013. “SLAM Family Markers Resolve Functionally Distinct Subpopulations of Hematopoietic Stem Cells and Multipotent Progenitors.” *Cell Stem Cell* 13 (1): 102–16.

Orelio, Claudia, Esther Haak, Marian Peeters, and Elaine Dzierzak. 2008. “Interleukin-1-Mediated Hematopoietic Cell Regulation in the Aorta-Gonad-Mesonephros Region of the Mouse Embryo.” *Blood* 112 (13): 4895–4904.

Palis, J., and M. C. Yoder. 2001. “Yolk-Sac Hematopoiesis: The First Blood Cells of Mouse and Man.” *Experimental Hematology* 29 (8): 927–36.

Papa, Luena, Mansour Djedaini, and Ronald Hoffman. 2019. “Mitochondrial Role in Stemness and Differentiation of Hematopoietic Stem Cells.” *Stem Cells International* 2019 (February): 4067162.

Parthibane, Velayoudame, Diwash Acharya, Sargur Madabushi Srideshikan, Jing Lin, Dru G. Myerscough, Thiruvaimozhi Abimannan, Nagampalli Vijaykrishna, et al. 2019. “Sptlc1 Is Essential for Myeloid Differentiation and Hematopoietic Homeostasis.” *Blood Advances* 3 (22): 3635–49.

Paucker, K., K. Cantell, and W. Henle. 1962. “Quantitative Studies on Viral Interference in Suspended L Cells. III. Effect of Interfering Viruses and Interferon on the Growth Rate of Cells.” *Virology* 17 (June): 324–34.

Paul, Franziska, Ya ’ara Arkin, Amir Giladi, Diego Adhemar Jaitin, Ephraim Kenigsberg, Hadas Keren-Shaul, Deborah Winter, et al. 2016. “Transcriptional Heterogeneity and Lineage Commitment in Myeloid Progenitors.” *Cell* 164 (1-2): 325.

Peterson, Vanessa M., Kelvin Xi Zhang, Namit Kumar, Jerelyn Wong, Lixia Li, Douglas C. Wilson, Renee Moore, Terrill K. McClanahan, Svetlana Sadekova, and Joel A. Klappenbach. 2017. “Multiplexed Quantification of Proteins and Transcripts in Single Cells.” *Nature Biotechnology*. https://doi.org/10.1038/nbt.3973.

Petropoulos, Sophie, Daniel Edsgärd, Björn Reinius, Qiaolin Deng, Sarita Pauliina Panula, Simone Codeluppi, Alvaro Plaza Reyes, Sten Linnarsson, Rickard Sandberg, and Fredrik Lanner. 2016. “Single-Cell RNA-Seq Reveals Lineage and X Chromosome Dynamics in Human Preimplantation Embryos.” *Cell*. https://doi.org/10.1016/j.cell.2016.08.009.

Petukhov, Viktor, Rosalind J. Xu, Ruslan A. Soldatov, Paolo Cadinu, Konstantin Khodosevich, Jeffrey R. Moffitt, and Peter V. Kharchenko. 2022. “Cell Segmentation in Imaging-Based Spatial Transcriptomics.” *Nature Biotechnology* 40 (3): 345–54.

Pietras, Eric M. 2017. “Inflammation: A Key Regulator of Hematopoietic Stem Cell Fate in Health and Disease.” *Blood* 130 (15): 1693–98.

Pietras EM, Lakshminarasimhan R, Techner JM, Fong S, Flach J, Binnewies M, Passegué E. “Re-entry into quiescence protects hematopoietic stem cells from the killing effect of chronic exposure to type I interferons”. J Exp Med. 2014 Feb 10;211(2):245-62. doi: 10.1084/jem.20131043. Epub 2014 Feb 3. PMID: 24493802; PMCID: PMC3920566.

Pietras EM, Mirantes-Barbeito C, Fong S, Loeffler D, Kovtonyuk LV, Zhang S, Lakshminarasimhan R, Chin CP, Techner JM, Will B, Nerlov C, Steidl U, Manz MG, Schroeder T, Passegué E. “Chronic interleukin-1 exposure drives hematopoietic stem cells towards precocious myeloid differentiation at the expense of self-renewal”. Nat Cell Biol. 2016 Jun;18(6):607-18. doi: 10.1038/ncb3346. Epub 2016 Apr 25. PMID: 27111842; PMCID: PMC4884136.

Platanias, Leonidas C. 2005. “Mechanisms of Type-I- and Type-II-Interferon-Mediated Signalling.” *Nature Reviews. Immunology* 5 (5): 375–86.

Post, Yorick, and Hans Clevers. 2019. “Defining Adult Stem Cell Function at Its Simplest: The Ability to Replace Lost Cells through Mitosis.” *Cell Stem Cell* 25 (2): 174–83.

Prendergast, Áine M., Andrea Kuck, Mieke van Essen, Simon Haas, Sandra Blaszkiewicz, and Marieke A. G. Essers. 2017. “IFNα-Mediated Remodeling of Endothelial Cells in the Bone Marrow Niche.” *Haematologica* 102 (3): 445–53.

Pronk, Cornelis J. H., Ole Petter Veiby, David Bryder, and Sten Eirik W. Jacobsen. 2011. “Tumor Necrosis Factor Restricts Hematopoietic Stem Cell Activity in Mice:

Involvement of Two Distinct Receptors." *The Journal of Experimental Medicine* 208 (8): 1563–70.

Purton, Louise E., and David T. Scadden. 2007. "Limiting Factors in Murine Hematopoietic Stem Cell Assays." *Cell Stem Cell*. https://doi.org/10.1016/j.stem.2007.08.016.

Qiu, Jiajing, Dmitri Papatsenko, Xiaohong Niu, Christoph Schaniel, and Kateri Moore. 2014. "Divisional History and Hematopoietic Stem Cell Function during Homeostasis." *Stem Cell Reports* 2 (4): 473–90.

Ramkumar, Charusheila, Rachel M. Gerstein, and Hong Zhang. 2013. "Serial Transplantation of Bone Marrow to Test Self-Renewal Capacity of Hematopoietic Stem Cells in Vivo." *Methods in Molecular Biology* 976: 17–24.

Randall, T. D., and I. L. Weissman. 1997. "Phenotypic and Functional Changes Induced at the Clonal Level in Hematopoietic Stem Cells after 5-Fluorouracil Treatment." *Blood* 89 (10): 3596–3606.

Rebel, Vivienne I., Sheila Hartnett, Geoffrey R. Hill, Suzan B. Lazo-Kallanian, James L. M. Ferrara, and Colin A. Sieff. 1999. "Essential Role for the P55 Tumor Necrosis Factor Receptor in Regulating Hematopoiesis at a Stem Cell Level." *Journal of Experimental Medicine*. https://doi.org/10.1084/jem.190.10.1493.

Redig, Amanda J., Antonella Sassano, Beata Majchrzak-Kita, Efstratios Katsoulidis, Hui Liu, Jessica K. Altman, Eleanor N. Fish, Amittha Wickrema, and Leonidas C. Platanias. 2009. "Activation of Protein Kinase C{eta} by Type I Interferons." *The Journal of Biological Chemistry* 284 (16): 10301–14.

Rezzoug, Francine, Yiming Huang, Michael K. Tanner, Marcin Wysoczynski, Carrie L. Schanie, Paula M. Chilton, Mariusz Z. Ratajczak, Isabelle J. Fugier-Vivier, and Suzanne T. Ildstad. 2008. "TNF-Alpha Is Critical to Facilitate Hemopoietic Stem Cell Engraftment and Function." *Journal of Immunology* 180 (1): 49–57.

Rodriguez-Fraticelli, Alejo E., Caleb Weinreb, Shou-Wen Wang, Rosa P. Migueles, Maja Jankovic, Marc Usart, Allon M. Klein, Sally Lowell, and Fernando D. Camargo. 2020. "Single-Cell Lineage Tracing Unveils a Role for TCF15 in Haematopoiesis." *Nature* 583 (7817): 585–89.

Rönnblom, Lars, and Dag Leonard. 2019. "Interferon Pathway in SLE: One Key to Unlocking the Mystery of the Disease." *Lupus Science & Medicine* 6 (1): e000270.

Saeed, Sadia, Jessica Quintin, Hindrik H. D. Kerstens, Nagesha A. Rao, Ali Aghajanirefah, Filomena Matarese, Shih-Chin Cheng, et al. 2014. "Epigenetic Programming of

Monocyte-to-Macrophage Differentiation and Trained Innate Immunity." *Science* 345 (6204): 1251086.

Saelens, Wouter, Robrecht Cannoodt, Helena Todorov, and Yvan Saeys. 2019. "A Comparison of Single-Cell Trajectory Inference Methods." *Nature Biotechnology* 37 (5): 547–54.

Sato, Taku, Nobuyuki Onai, Hiroki Yoshihara, Fumio Arai, Toshio Suda, and Toshiaki Ohteki. 2009. "Interferon Regulatory Factor-2 Protects Quiescent Hematopoietic Stem Cells from Type I Interferon-Dependent Exhaustion." *Nature Medicine* 15 (6): 696–700.

Sawamiphak, Suphansa, Zacharias Kontarakis, and Didier Y. R. Stainier. 2014. "Interferon Gamma Signaling Positively Regulates Hematopoietic Stem Cell Emergence." *Developmental Cell* 31 (5): 640–53.

Schaper, Fred, and Stefan Rose-John. 2015. "Interleukin-6: Biology, Signaling and Strategies of Blockade." *Cytokine & Growth Factor Reviews* 26 (5): 475–87.

Scheller, Jürgen, Athena Chalaris, Dirk Schmidt-Arras, and Stefan Rose-John. 2011. "The pro- and Anti-Inflammatory Properties of the Cytokine Interleukin-6." *Biochimica et Biophysica Acta* 1813 (5): 878–88.

Schürch, Christian M., Carsten Riether, and Adrian F. Ochsenbein. 2014. "Cytotoxic CD8+ T Cells Stimulate Hematopoietic Progenitors by Promoting Cytokine Release from Bone Marrow Mesenchymal Stromal Cells." *Cell Stem Cell* 14 (4): 460–72.

Seita, Jun, and Irving L. Weissman. 2010. "Hematopoietic Stem Cell: Self-renewal versus Differentiation." *WIREs Systems Biology and Medicine*. https://doi.org/10.1002/wsbm.86.

Shao, Li, Rui Xue, Xiaoyan Lu, Jie Liao, Xin Shao, and Xiaohui Fan. 2021. "Identify Differential Genes and Cell Subclusters from Time-Series scRNA-Seq Data Using scTITANS." *Computational and Structural Biotechnology Journal* 19 (July): 4132–41.

Shemin, David, and D. Rittenberg. 1946. "THE LIFE SPAN OF THE HUMAN RED BLOOD CELL." *Journal of Biological Chemistry*. https://doi.org/10.1016/s0021-9258(17)35201-8.

Shlomovitz, Inbar, Sefi Zargrian, and Motti Gerlic. 2017. "Mechanisms of RIPK3-Induced Inflammation." *Immunology and Cell Biology* 95 (2): 166–72.

Sieburg, Hans B., Rebecca H. Cho, and Christa E. Müller-Sieburg. 2002. "Limiting Dilution Analysis for Estimating the Frequency of Hematopoietic Stem Cells: Uncertainty and Significance." *Experimental Hematology* 30 (12): 1436–43.

Stoeckius, Marlon, Christoph Hafemeister, William Stephenson, Brian Houck-Loomis, Pratip K. Chattopadhyay, Harold Swerdlow, Rahul Satija, and Peter Smibert. 2017. "Simultaneous Epitope and Transcriptome Measurement in Single Cells." *Nature Methods* 14 (9): 865–68.

Subramanian, Aravind, Pablo Tamayo, Vamsi K. Mootha, Sayan Mukherjee, Benjamin L. Ebert, Michael A. Gillette, Amanda Paulovich, et al. 2005. "Gene Set Enrichment Analysis: A Knowledge-Based Approach for Interpreting Genome-Wide Expression Profiles." *Proceedings of the National Academy of Sciences of the United States of America* 102 (43): 15545–50.

Suda, Toshio, Keiyo Takubo, and Gregg L. Semenza. 2011. "Metabolic Regulation of Hematopoietic Stem Cells in the Hypoxic Niche." *Cell Stem Cell*. https://doi.org/10.1016/j.stem.2011.09.010.

Takeuchi, Osamu, Jill Fisher, Heikyung Suh, Hisashi Harada, Barbara A. Malynn, and Stanley J. Korsmeyer. 2005. "Essential Role of BAX,BAK in B Cell Homeostasis and Prevention of Autoimmune Disease." *Proceedings of the National Academy of Sciences of the United States of America* 102 (32): 11272–77.

Takizawa, Hitoshi, Steffen Boettcher, and Markus G. Manz. 2012. "Demand-Adapted Regulation of Early Hematopoiesis in Infection and Inflammation." *Blood* 119 (13): 2991–3002.

Taoudi, Samir, Christèle Gonneau, Kate Moore, Julie M. Sheridan, C. Clare Blackburn, Erin Taylor, and Alexander Medvinsky. 2008. "Extensive Hematopoietic Stem Cell Generation in the AGM Region via Maturation of VE-cadherin+CD45+ Pre-Definitive HSCs." *Cell Stem Cell* 3 (1): 99–108.

Taswell, C. 1981. "Limiting Dilution Assays for the Determination of Immunocompetent Cell Frequencies. I. Data Analysis." *Journal of Immunology* 126 (4): 1614–19.

Taylor, Milton W. 2014. "Interferons." *Viruses and Man: A History of Interactions*. https://doi.org/10.1007/978-3-319-07758-1_7.

Traag, V. A., L. Waltman, and N. J. van Eck. 2019. "From Louvain to Leiden: Guaranteeing Well-Connected Communities." *Scientific Reports* 9 (1): 5233.

Tran, Thinh N., and Gary D. Bader. 2020. "Tempora: Cell Trajectory Inference Using Time-Series Single-Cell RNA Sequencing Data." *PLoS Computational Biology* 16 (9): e1008205.

Treutlein, Barbara, Qian Yi Lee, J. Gray Camp, Moritz Mall, Winston Koh, Seyed Ali Mohammad Shariati, Sopheak Sim, et al. 2016. “Dissecting Direct Reprogramming from Fibroblast to Neuron Using Single-Cell RNA-Seq.” *Nature* 534 (7607): 391–95.

Trumpp, Andreas, Marieke Essers, and Anne Wilson. 2010. “Awakening Dormant Haematopoietic Stem Cells.” *Nature Reviews. Immunology* 10 (3): 201–9.

Ueda, Yoshihiro, Derek W. Cain, Masayuki Kuraoka, Motonari Kondo, and Garnett Kelsoe. 2009. “IL-1R Type I-Dependent Hemopoietic Stem Cell Proliferation Is Necessary for Inflammatory Granulopoiesis and Reactive Neutrophilia.” *Journal of Immunology* 182 (10): 6477–84.

Velten, Lars, Simon F. Haas, Simon Raffel, Sandra Blaszkiewicz, Saiful Islam, Bianca P. Hennig, Christoph Hirche, et al. 2017. “Human Haematopoietic Stem Cell Lineage Commitment Is a Continuous Process.” *Nature Cell Biology* 19 (4): 271–81.

Verma, Amit, Dilip K. Deb, Antonella Sassano, Shahab Uddin, John Varga, Amittha Wickrema, and Leonidas C. Platanias. 2002. “Activation of the p38 Mitogen-Activated Protein Kinase Mediates the Suppressive Effects of Type I Interferons and Transforming Growth Factor-Beta on Normal Hematopoiesis.” *The Journal of Biological Chemistry* 277 (10): 7726–35.

Vogel, Mona, Bettina Moehrle, Andreas Brown, Karina Eiwen, Vadim Sakk, and Hartmut Geiger. 2019. “HPRT and Purine Salvaging Are Critical for Hematopoietic Stem Cell Function.” *Stem Cells*. https://doi.org/10.1002/stem.3087.

Walter, Dagmar, Amelie Lier, Anja Geiselhart, Frederic B. Thalheimer, Sina Huntscha, Mirko C. Sobotta, Bettina Moehrle, et al. 2015. “Exit from Dormancy Provokes DNA-Damage-Induced Attrition in Haematopoietic Stem Cells.” *Nature* 520 (7548): 549–52.

Watcham, Sam, Iwo Kucinski, and Berthold Gottgens. 2019. “New Insights into Hematopoietic Differentiation Landscapes from Single-Cell RNA Sequencing.” *Blood* 133 (13): 1415–26.

Wath, Richard C. van der, Anne Wilson, Elisa Laurenti, Andreas Trumpp, and Pietro Liò. 2009. “Estimating Dormant and Active Hematopoietic Stem Cell Kinetics through Extensive Modeling of Bromodeoxyuridine Label-Retaining Cell Dynamics.” *PloS One* 4 (9): e6972.

Weber, Axel, Peter Wasiliew, and Michael Kracht. 2010. “Interleukin-1 (IL-1) Pathway.” *Science Signaling*. https://doi.org/10.1126/scisignal.3105cm1.

Weissman, Irving L., and Judith A. Shizuru. 2008. “The Origins of the Identification and Isolation of Hematopoietic Stem Cells, and Their Capability to Induce Donor-Specific Transplantation Tolerance and Treat Autoimmune Diseases.” *Blood* 112 (9): 3543–53.

Wilson A, Laurenti E, Oser G, van der Wath RC, Blanco-Bose W, Jaworski M, Offner S, Dunant CF, Eshkind L, Bockamp E, Lió P, Macdonald HR, Trumpp A. “Hematopoietic stem cells reversibly switch from dormancy to self-renewal during homeostasis and repair”. Cell. 2008 Dec 12;135(6):1118-29. doi: 10.1016/j.cell.2008.10.048. Erratum in: Cell. 2009 Jul 10;138(1):209. PMID: 19062086.

Winkler, Ingrid G., Jean Hendy, Paul Coughlin, Anita Horvath, and Jean-Pierre Lévesque. 2005. “Serine Protease Inhibitors serpina1 and serpina3 Are down-Regulated in Bone Marrow during Hematopoietic Progenitor Mobilization.” *The Journal of Experimental Medicine* 201 (7): 1077–88.

Woolthuis, Carolien M., and Christopher Y. Park. 2016. “Hematopoietic Stem/progenitor Cell Commitment to the Megakaryocyte Lineage.” *Blood* 127 (10): 1242–48.

Yamamoto R, Morita Y, Ooehara J, Hamanaka S, Onodera M, Rudolph KL, Ema H, Nakauchi H. “Clonal analysis unveils self-renewing lineage-restricted progenitors generated directly from hematopoietic stem cells”. Cell. 2013 Aug 29;154(5):1112-1126. doi: 10.1016/j.cell.2013.08.007. PMID: 23993099.

Yamashita M, Passegué E. “TNF-α Coordinates Hematopoietic Stem Cell Survival and Myeloid Regeneration”. Cell Stem Cell. 2019 Sep 5;25(3):357-372.e7. doi: 10.1016/j.stem.2019.05.019. Epub 2019 Jun 20. PMID: 31230859; PMCID: PMC6733032.

Yang, Yibin, Arthur L. Shaffer 3rd, N. C. Tolga Emre, Michele Ceribelli, Meili Zhang, George Wright, Wenming Xiao, et al. 2012. “Exploiting Synthetic Lethality for the Therapy of ABC Diffuse Large B Cell Lymphoma.” *Cancer Cell* 21 (6): 723–37.

Yoshida, K., T. Taga, M. Saito, S. Suematsu, A. Kumanogoh, T. Tanaka, H. Fujiwara, et al. 1996. “Targeted Disruption of gp130, a Common Signal Transducer for the Interleukin 6 Family of Cytokines, Leads to Myocardial and Hematological Disorders.” *Proceedings of the National Academy of Sciences of the United States of America* 93 (1): 407–11.

Yu, Guangchuang, Li-Gen Wang, Yanyan Han, and Qing-Yu He. 2012. “clusterProfiler: An R Package for Comparing Biological Themes among Gene Clusters.” *Omics: A Journal of Integrative Biology* 16 (5): 284–87.

Zakrzewski, Wojciech, Maciej Dobrzyński, Maria Szymonowicz, and Zbigniew Rybak. 2019. “Stem Cells: Past, Present, and Future.” *Stem Cell Research & Therapy* 10 (1): 68.

Zhang, Huiyuan, Hoainam Nguyen-Jackson, Athanasia D. Panopoulos, Haiyan S. Li, Peter J. Murray, and Stephanie S. Watowich. 2010. “STAT3 Controls Myeloid Progenitor Growth during Emergency Granulopoiesis.” *Blood* 116 (14): 2462–71.

Zhang, Y., A. Harada, H. Bluethmann, J. B. Wang, S. Nakao, N. Mukaida, and K. Matsushima. 1995. “Tumor Necrosis Factor (TNF) Is a Physiologic Regulator of Hematopoietic Progenitor Cells: Increase of Early Hematopoietic Progenitor Cells in TNF Receptor p55-Deficient Mice in Vivo and Potent Inhibition of Progenitor Cell Proliferation by TNF Alpha in Vitro.” *Blood* 86 (8): 2930–37.

Zhao, Jimmy L., and David Baltimore. 2015. “Regulation of Stress-Induced Hematopoiesis.” *Current Opinion in Hematology*. https://doi.org/10.1097/moh.0000000000000149.

Zhao, Jimmy L., Chao Ma, Ryan M. O’Connell, Arnav Mehta, Race DiLoreto, James R. Heath, and David Baltimore. 2014. “Conversion of Danger Signals into Cytokine Signals by Hematopoietic Stem and Progenitor Cells for Regulation of Stress-Induced Hematopoiesis.” *Cell Stem Cell* 14 (4): 445–59.